Stanford University Petroleum Research Institute
Stanford, California 94305

ANALYSIS OF UNIT MOBILITY RATIO WELL-TO-WELL TRACER FLOW TO DETERMINE RESERVOIR HETEROGENEITY

SUPRI TR-36

By

Maghsood Abbaszadeh-Dehghani and William E. Brigham

Work Performed for the Department of Energy
Under Contract No. DE-AC03-81SF11564

December 1982

DISCLAIMER

"This report was prepared as an account of work sponsored by an agency of the United States Government. Neither the United States Government nor any agency thereof, nor any of their employees, makes any warranty, express or implied, or assumes any legal liability of responsibility for the accuracy, completeness, or usefulness of any information, apparatus, product, or process disclosed, or represents that its use would not infringe privately owned rights. Reference herein to any specific commercial product, process, or service by trade name, trademark, manufacturer, or otherwise, does not necessarily constitute or imply its endorsement, recommendation, or favoring by the United States Government or any agency thereof. The views and opinions of authors expressed herein do not necessarily state or reflect those of the United States Government of any agency thereof."

TABLE OF CONTENTS

	Page
LIST OF TABLES	v
LIST OF FIGURES	vi
ABSTRACT	ix
ACKNOWLEDGEMENTS	x
1. INTRODUCTION	1
2. LITERATURE REVIEW	2
2.1 QUALITATIVE INTERPRETATION OF TRACER DATA	2
2.2 MECHANISM OF TACER FLOW	3
2.2.1 Convection	4
2.2.2 Hydrodynamic Dispersion	4
2.2.2.1 Linear Flow	4
2.2.2.2 Non-Linear Flow	9
2.3 QUANTITATIVE ANALYSIS OF TRACER FLOW	11
2.3.1 Petroleum Reservoirs	11
2.3.2 Underground Aquifers	13
2.3.3 Geothermal Reservoirs	14
2.4 SUMMARY	15
3. METHOD OF SOLUTION	16
3.1 PATTERN PERFORMANCE	16
3.1.1 Steady Multi-Well Flow Theory	16
3.1.2 Pattern Breakthrough Curves	18
3.1.3 Correlation of Pattern Breakthrough Curves	20
3.1.4 Pattern Breakthrough Curves for Non-Unit Mobility Ratio	26
3.2 TRACER FLOW IN HOMOGENEOUS SYSTEMS	32
3.2.1 Mixing Theory	33
3.2.2 Tracer Production Curves	36
3.2.3 Correlation of Tracer Production Curves	48
3.3 TRACER FLOW IN HETEROGENEOUS SYSTEMS	55
3.3.1 Concept of Multi-Layered Modeling	55
3.3.2 Tracer Production Curves from Layered Systems	57
3.3.3 Optimization Technique	62

4. FIELD EXAMPLE 68
4.1 HISTORY AND DESIGN OF THE TEST 68
4.2 ANALYSIS OF TRACER RESULTS 74
5. CONCLUSIONS 83
6. RECOMMENDATIONS FOR FUTURE WORK 85
NOMENCLATURE 86
REFERENCES 91
APPENDICES 96
Appendix A: DERIVATION OF EQUATIONS FOR PATTERN BREAKTHROUGH CURVES FOR MOBILITY RATIO OF ONE 96
A.1 STAGGERED LINE DRIVE 98
A.2 FIVE-SPOT 106
A.3 DIRECT LINE DRIVE 107
A.4 INVERTED SEVEN-SPOT 112
A.5 RELATING DERIVATIVES OF THE STREAM FUNCTIONS TO THE STREAM FUNCTIONS 120
A.5.1 Staggered Line Drive 120
A.5.2 Direct Line Drive 122
Appendix B: DERIVATION OF EQUATIONS FOR PATTERN RECOVERY CURVES AT VARIOUS MOBILITY RATIOS 125
Appendix C: EVALUATION OF THE LINE INTEGRAL IN MIXING EQUATIONS 136
C.1 STAGGERED LINE DRIVE 136
C.2 FIVE-SPOT 140
C.3 DIRECT LINE DRIVE 141
Appendix D: COMPUTER PROGRAMS 146
D.1 PROGRAM TO ANALYZE A TRACER ELUTION CURVE 146
D.2 PROGRAM TO COMPUTE PATTERN BREAKTHROUGH CURVES OF A DEVELOPED INVERTED SEVEN-SPOT FOR UNIT MOBILITY RATIO.. 177
D.3 PROGRAM TO COMPUTE PATTERN BREAKTHROUGH CURVE OF A DEVELOPED FIVE-SPOT AT AN ARBITRARY MOBILITY RATIO 182

LIST OF TABLES

Table		Page
3.1	Values of Breakthrough and Areal Sweep Efficiency Curves for a Developed Five-Spot, Mobility Ratio = 1	25
3.2	Values of Breakthrough and Areal Sweep Efficiency Curves for a Developed Inverted Seven-Spot, Mobility Ratio 1	26
3.3	Values of Breakthrough and Areal Sweep Efficiency Curves for Developed Direct Line Drive Patterns, Mobility Ratio = 1	27
3.4	Values of Breakthrough and Areal Sweep Efficiency Curves for Developed Staggered Line Drive Patterns, Mobility Ratio = 1	28
3.5	Values of Breakthrough and Areal Sweep Efficiency Curves for a Developed Five-Spot Pattern at Various Mobility Ratios	29
3.6	Breakthrough Areal Sweep Efficiencies Extracted from the Higgins and Leighton's Match to the Data Reported by Douglas et al. (1959)	32
3.7	Correction Factors on Tracer Peak Concentration and a/u for Staggered Line Drive and Direct Line Drive at Various d/a Ratios	52
3.8	Assumed and Computed Parameters of the Layers for the Theoretical Staggered Line Drive, Example 1	59
3.9	Assumed and Computed Parameters of the Layers for the Theoretical Staggered Line Drive, Example 2	61
3.10	Computed Parameters of the Layers Using the Optimization Technique with Various Number of Layers, Example 2	67
4.1	Computed Layer Parameters for Field Test, Well D, Using the Optimization Routine with Different Number of Layers	77
4.2	Computed Permeabilities and Thicknesses of Layers for Field Test, Well D, with Different Number of Layers	78
4.3	Computed Layer Parameters for Field Test, Well A, Using the Optimization Routine with Different Number of Layers	81
4.4	Computed Permeability and Thicknesses of Layers for Field Test, Well A, with Different Number of Layers	81
4.5	Computed Parameters of Layers for Well A with Ten Layers and Drainage Area of 40,800 ft^2	82

LIST OF FIGURES

Figure		Page
2.1	Effect of Rate and Type of Porous Medium on Mixing Coefficients (Brigham et al., 1961)	7
2.2	Longitudinal and Lateral Mixing Coefficients for Various Sands (after Blackwell, 1962)	7
2.3	Match to Produced Tracer Concentration for Well A, Reported by Smith and Brigham, after Baldwin (1966)	13
3.1	Front Location and Breakthrough Curve in a Displacement of Two Fluids which Do Not Mix	17
3.2	Convection Effects on the Breakthrough of a Slug of Fluid B	17
3.3	Pattern Breakthrough Curves for Developed Systems, Mobility Ratio = 1	19
3.4	Areal Sweep Efficiency Curves for Developed Patterns, Mobility Ratio = 1	21
3.5	Correlation of Developed pattern Breakthrough Curves, Mobility Ratio = 1	22
3.6	Comparison of the Experimental Data from Various Developed Patterns and the Correlated Pattern Breakthrough Curve, Mobility Ratio = 1	22
3.7	Comparison of Correlated Pattern Breakthrough Curve and Developed Five-Spot Data, Mobility Ratio = 1	23
3.8	Correlation of Areal Sweep Efficiency Curves of Developed Patterns, Mobility Ratio = 1	24
3.9	Correlation of Displacing Fluid Cut vs Dimensionless Areal Sweep Efficiency, Developed Pattern and Mobility Ratio = 1	24
3.10	Areal Sweep Efficiency Curves for a Developed Five-Spot Pattern at Various Mobility Ratios (Assuming Streamlines are Independent of Mobility Ratio)	30
3.11	Breakthrough Curves for a Developed Five-Spot Pattern at Various Mobility Ratios (Assuming Streamlines are Independent of Mobility Ratio)	30
3.12	Comparison of Laboratory Data and Computer Performance Calculations for a Developed Five-Spot Pattern (Higgins and Leighton, 1962)	31
3.13	Fractional Flow Curves Constructed from the Data Supplied by Douglas et al. (1959)	31
3.14	A General Flow Passage	35
3.15	A Developed Staggered Line Drive with Tracer Concentration Profile in a Streamtube	37
3.16	Approximate Location of a Tracer Slug in a Streamtube	39

3.17	Element Considered in Computing Tracer Production Curves for the Staggered Line Drive Pattern.....	44
3.18	Element Considered in Computing Tracer Production Curves for the Direct Line Drive.....	46
3.19	Dimensionless Tracer Concentrations versus Pore Volumes Injected, Staggered Line Drive, d/a = 1.5.....	46
3.20	Dimensionless Tracer Concentrations versus Pore Volumes Injected, Developed Five-Spot.....	47
3.21	Dimensionless Tracer Concentrations versus Pore Voumes Injected, Developed Direct Line Drive, d/a = 1.....	47
3.22	Tracer Production Curves for Different Developed and Homogeneous Patterns a/a = 500.....	48
3.23	Plot of Dimensionless Maximum Tracer Concentrations versus Peclet Number for Homogeneous Developed Patterns.....	49
3.24	Plot of Dimensionless Peak Pore Volume Locations versus Peclet Number for Homogeneous Developed Patterns.....	49
3.25	Correction Factors on Peak Concentrations.....	50
3.26	Correction Factors on a/a to Calculate Peak Locations.....	51
3.27	Normalized Tracer Production Curves for a Homogeneous Developed Five-Spot.....	54
3.28	Correlation of Tracer Production Curves for Homogeneous Developed Patterns.....	54
3.29	Outcrops of Sandstone Reservoirs (after Zeito, 1965).....	56
3.30	Tracer Response from a Four-Layered Developed Staggered Line Drive, d/a = 1, First Example.....	60
3.31	Match Obtained Using the Deconvolution Routine and Tracer Correction Factors.....	61
3.32	Tracer Response from a Four-Layered Developed Staggered Line Drive, d/a = 1, and the Match Obtained Using the Deconvolution Routine, Second Example.....	62
3.33	Match Using the Optimization Routine with Four Layers, Second Example.....	65
3.34	Match Using the Optimization Routine with Three Layers, Second Example.....	66
3.35	Match Using the Optimization Routine with Five Layers, Second Example.....	66
4.1	Isopach Map of Loco Waterflood Pilot Area (after Martin et al., 1968).....	68
4.2	Pattern Configuration and Reservoir Data for the Field Test.....	69
4.3	Isotherms of Average Sand Temperature During Hot Water Injection (after Martin et al., 1968).....	72
4.4	Tracer Elution Curves for Field Test (Smith and Brigham, 1965)..	73

4.5	Qualitative Streamlines for Well D of the Pilot	74
4.6	Analysis of Tracer Data for Well D with Five Layers	75
4.7	Analysis of Tracer Data for Well D with Seven Layers	76
4.8	Analysis of Tracer Data for Well D with Nine Layers	76
4.9	Analysis of Tracer Data for Well D with Ten Layers	77
4.10	Analysis of Tracer Data for Well A with Five Layers	79
4.11	Analysis of Tracer Data for Well A with Seven Layers	80
4.12	Analysis of Tracer Data for Well A with Ten Layers	80
A-1	A Developed Staggered Line Drive. in Z-Plane	98
A-2	W-Plane Showing the Transformation	99
A-3	Well Locations for a Developed Staggered Line Drive in the W-Plane	100
A-4	Coordinate System for a Developed Staggered Line Drive	102
A-5	A Developed Direct Line Drive in Z-Plane	107
A-6	Coordinate System for a Developed Direct Line Drive	109
A-7	Coordinate System for an Inverted Developed Seven-Spot	114
B-1	Front Location in a Developed Five-Spot Pattern at an Arbitrary Mobility Ratio	126
C-1	Dimensions for a Staggered Line Drive Considered in the Analysis of Mixing Line Integral	136
c-2	Variation of Mixing Line Integral with Tracer Front Location for Various Streamlines of a Staggered Line Drive. d/a = 1	139
c-3	Dimensions of a Developed Direct Line Drive Considered in the Analysis of Mixing Line Integral	141

ABSTRACT

This study has been carried out in two related sections. In the first section, exact analytic equations have been derived to define breakthrough curves (displacing fluid cut versus pore volumes injected, or area swept versus pore volume injected) for different developed flooding well patterns for unit mobility ratio. In the derivation of equations, it was assumed that the displacements were piston-like with no capillary and gravity effects. The analytic solutions are various forms of elliptic integrals which differ depending on the geometry of the pattern. The exact elliptic integral solutions for the breakthrough curves have been correlated into a single curve by defining a correlating parameter, we have called the dimensionless pore volume. Since breakthrough curves for the patterns considered in this study (five-spot, inverted seven-spot, direct line drive, and staggered line drive) all correlate into a single curve, it is concluded that the breakthrough curves for any other repeating patterns should also lie reasonably near this same correlating curve.

The first section also includes an extension of an analytical definition of pattern breakthrough curves for mobility ratio other than one. In the derivations, it was assumed that the streamlines of a pattern did not change with mobility ratio. The results of the analysis showed that the breakthrough areal sweep efficiencies at various mobility ratios were nearly independent of mobility ratios, while the post breakthrough data were different for each mobility ratio.

The second part discusses flow of a tracer slug in various patterns. In each system, the longitudinal mixing of the tracer slug in a general streamtube of the pattern has been formulated mathematically. A line integral along a streamtube was derived which represents the length of the mixed zone. When this line integral was substituted into the mixing equation, an expression for the concentration of tracer at any location within a streamtube resulted. Furthermore, these expressions integrated over all the streamlines produced a set of equations describing tracer production curves from homogeneous repeated patterns. The study shows that the effluent tracer concentration depends upon the pattern geometry and size, and the dispersion constant of the formation.

Tracer production curves for the different patterns considered have also been correlated into a set of curves depending on a/α, (a = distance between like wells, α = dispersion constant). The correlation was achieved by deriving two sets of correction factors, one for tracer peak concentration, and another for a/α ratio. As a result of this correlation, a tracer response from any repeated homogeneous pattern can be estimated from the response of an equivalent five-spot system by utilizing the correction factors.

A computer program based on a non-linear optimization technique was developed which decomposes a detected tracer breakthrough profile from a multilayered system into responses from individual layers. The program computes porosity-thickness and fractional permeability-thickness for each layer. The algorithm

utilizes the equations of the five-spot pattern in conjunction with the developed correction factors. A five-spot field example which has been successfully decomposed into eeveral layers is shown to illustrate the use of this research.

ACKNOWLEDGEMENTS

Financial support during the course of this work was provided by the Department of Energy through the Stanford University Petroleum Research Institute, under Contract No. DE-AC03-81SF11564.

1. INTRODUCTION

Reservoir heterogeneities play an important role in oil recovery by improved recovery techniques. In any fluid injection operation, high permeability streaks divert substantial quantities of the injected fluid. This unequal distribution of the injected fluid greatly reduces the volumetric sweep efficiency of the reservoir and, hence, lowers the efficiency of the displacement processes. Therefore, detection of high permeability zones and channels would be helpful in the understanding, design, operation, and interpretation of injection projects.

A means to follow fluid movement in a reservoir would be an important tool in determining the characteristics of a formation directly. Radioactive and chemical tracers provide the capability to achieve this purpose. Information on reservoir heterogeneity supplied by flow of tracers in a reservoir is invaluable in the design of assisted recovery operations and also useful in reservoir simulation studies. This information, whether qualitative or quantitative, is generally extracted from tracer breakthrough profiles detected at the production wells. Often, tracer breakthrough profiles are a summation of tracer responses from several layers which constitute the formation. In practice, the number of the layers is unknown and only a tracer breakthrough curve from a stratified system is available. This is a classic inversion problem. To analyze tracer breakthrough profiles, results must be deconvoluted into the constituent layer responses. From the constructed layer responses, it would be possible to compute important parameters for the layers such as permeability, porosity, and thickness.

Several works (Brigham and Smith, 1965; Baldwin, 1966; and Yuen ~~et al.~~ 1979) have been published on tracer flow which have attempted to obtain quantitative information about the nature of reservoirs. Each of these had limitations which led to incorrectly defined reservoir parameters and also each of these methods considered only fully developed five-spot patterns and unit mobility ratio.

This study draws from these earlier works and was initiated to develop an analysis for tracer tests which could be used for any repeated pattern within the limitation of mobility ratio of one. To do this a mathematical description of tracer breakthrough curves for any developed homogeneous pattern is required. For the breakthrough curves to be precise, the analysis must include a rigorous treatment of the mixing of tracer in the patterns. Also, a correlation of these tracer production curves into a single curve (or a single set of curves) could simplify the analysis. Finally, a method which could analyze tracer elution curves from stratified reservoirs without adopting lengthy trial and error procedures could reduce the needed time for an analysis. With these points in mind, a new tracer analysis method has been developed.

2. LITERATURE REVIEW

In the past several decades, both radioactive and chemical tracers have been used as effective tools for evaluation of various subterranean formations such as petroleum and geothermal reservoirs and underground aquifers. The tracer tests conducted are usually of two types: 1) well-to-well (interwell) tests in which a tracer is injected in an injection well and detected continuously at a production well; or 2) single well tests in which the tracer is injected into a well and is allowed to react with the formation fluid before being produced from the same well. In this study, only the well-to-well tracer flow tests are considered.

This chapter has been divided into four main parts. In the first, literature related to qualitative interpretation of tracer tests is presented. The second part discusses the mechanism of tracer flow in porous media. In this part, dispersion (mixing) in linear and non-linear flow geometries is covered at length. Quantitative analysis of tracer test data from various underground reservoirs is presented in the third part. The last part provides a summary to this chapter.

2.1 QUALITATIVE INTERPRETATION OF TRACER DATA

The results of interwell tracer tests usually have been interpreted on a qualitative basis. Therefore, only general ideas about the characteristics of the formation have been extracted from the tracer tests. Strum and Johnson (1951) verified the occurrence of crevices and joint-plane partings in the Pennsylvanian Bradford Third Sand formation by qualitatively studying the results of several tracer tests conducted in this sand. Three different tracers were used: brine, fluorescein and a surface active compound. The results verified the existence of directional permeabilities which had already been measured from core samples. Based on this finding, subsequent waterflood well patterns were designed to improve the swept volumes.

Carpenter et al. (1952) used boron in the form of Borax and boric acid as a water soluble tracer to find the main features of three oil-bearing formations. They concluded that in two of the formations, several channels were present instead of a single "pipe-line" channel, and the third formation did not have channels or by-passing zones. Their conclusions were based upon the concentration levels of boron detected at the producers, and the elapsed time between the injection of the tracer and its appearance at the producing wells.

A comprehensive list of information obtainable from tracer tests was presented by Wagner (1977), who studied the results of twenty tracer programs conducted in reservoirs undergoing waterfloods, gas drives and water-solvent injection operations. His list included the following items:

1) Volumetric sweep—The volume of fluid injected at an injection well to breakthrough of the tracer at an offset producer is indicative of the volumetric sweep-efficiency between that pair of wells. A small breakthrough sweep efficiency indicates the existence of a fracture or a thin, high permeability streak between the two wells.

2) Identification of offending injectors--With different tracers injected into a formation, a comparison of arrival times of tracers at the production wells can determine the injectors responsible for early breakthrough in specific producers. Remedial treatment of the injectors would normally be necessary.

3) Directional flow trends—When different tracers are injected into regular patterns, the existing directional flow trends are identified by early tracer breakthrough at the producers located along the preferential flow direction.

4) Delineation of flow barriers— Lack of response to an injected tracer at a production well indicates the existence of a barrier or a sealing fault between the pair of wells.

5) Relative velocities of injected fluids— When different fluids tagged with different: tracers are injected simultaneously or sequentially in the same well, the individual arrival time of the tracers at the producers can be used to measure the relative velocities of the injected fluids. This information is useful in determining the appropriate fluid to use for mobility control to achieve a more uniform sweep in tertiary oil recovery operations.

6) Evaluation of sweep improvement treatments— The success or effectiveness of sweep efficiency treatments can be evaluated by comparing the breakthrough times of tracers before and after the treatment.

As an implementation of Wagner's work, D'Hooge et al. (1981) simultaneously injected four radioactive tracers (carbon-14, cobalt-57, cobalt-60 and tritium) into the West Sumatra formation (Pennsylvanian age sandstone) to track the movements of the injected fluids. A qualitative interpretation of tracer concentration arrival curves at different production wells provided valuable information on the direction of flow, reservoir discontinuities, and probable areas of poor sweep efficiency. These investigators, however, did not analyze the tracer elution curves in detail to obtain quantitative information about formation heterogeneity.

2.2 MECHANISM OF TRACER FLOW

To perform detailed quantitative analysis on interwell tracer breakthrough curves, one must have a thorough knowledge of the mechanism of tracer movement in the formation. In general, the transport of tracer material in a porous medium is subject to two phenomena--convection and hydrodynamic dispersion (Bear, 1972).

2.2.1 Convection

Convection is used here to describe bulk movement of fluids as governed by Darcy's law. This flow results from potential gradients imposed on the system. In a reservoir, the potential differences are established either by density differences between the flowing fluids, or by production and injection wells drilled into a formation. Convection depends mainly on the well arrangements and operating conditions, such as flow rates of the wells. A comprehensive survey of the work done on convection for different well patterns was provided by Craig (1971).

2.2.2 Hydrodynamic Dispersion

Hydrodynamic dispersion is composed of two parts — molecular diffusion and mechanical dispersion. Molecular diffusion results from component concentration gradients established between two miscible fluids, and is independent of flow velocity. Mechanical dispersion, on the other hand, is the result of movement of individual fluid particles in tortuous pore channels of a porous medium. On a microscopic level, dispersion results from variations in velocity of tracer material as it flows through the separating and rejoining pore passages. In two dimensional flow, a distinction has been made between mechanical dispersion occurring in the direction of flow (longitudinal dispersion), and that occurring in a direction perpendicular to the mean flow (transverse dispersion).

As a consequence of hydrodynamic dispersion, tracer material gradually spreads and occupies an increasing portion of the flow domain beyond the region it would occupy according to fluid convection alone. The amount of spreading (or mixing) depends on the dispersivity of the porous medium and the geometry of the flow system. Considerable work, both theoretical and experimental, has been done to study the phenomenon of dispersion (mixing) in porous media for various flow geometries.

2.2.2.1 Linear Flow

Aronofsky and Heller (1957) presented a mathematical analysis of mixing (dispersion) that occurs between two miscible fluids as one fluid displaces the other linearly through a porous medium. They solved the following continuity equation for the fluid concentration:

$$K \frac{\partial^2 C}{\partial x^2} - v \frac{\partial C}{\partial x} = \frac{\partial C}{\partial t} \qquad (2\text{-}1)$$

$$C(0,t) = C_o$$

$$C(x,0) = 0$$

$$C(\infty,t) = 0$$

Where,

C = concentration of displacing fluid, mass fraction

K = effective mixing coefficient

v = microscopic velocity, $q/A\phi$

The Aronofsky–Heller solution is:

$$\frac{C(x,t)}{C_o} = \frac{1}{2}\left[\operatorname{erfc}\left(\frac{x - vt}{2\sqrt{Kt}}\right) + e^{\frac{vx}{K}} \operatorname{erfc}\left(\frac{x + vt}{2\sqrt{Kt}}\right)\right] \qquad (2\text{-}2)$$

The authors showed that the second term in the brackets was quite small except at small values of x or large values of K.

Aronofsky and Heller used this solution to analyze data from miscible flow experiments that were available in the literature. They were able to match the data reported by von Rosenburg (1956), as well as data provided by Koch and Slobod (1957). From the analysis of von Rosenburg's data, they discovered that the effective mixing coefficient, K, was a function of fluid velocity. Furthermore, the K–values computed from von Rosenburg's data when graphed against flow rate on log–log graph paper resulted in a straight line with a slope equal to 1.2. From this observation, Aronofsky and Heller concluded that the effective mixing coefficient was proportional to flow velocity to the power 1.2.

Ogata and Banks (1961) independently solved the one–dimensional convective diffusivity equation (Eq. 2–1) with the same boundary conditions considered by Aronofsky and Heller, and obtained a solution identical in form to Eq. 2–2. Ogata and Banks showed that the concentration profiles corresponding to Eq. 2–2 solution were not symmetrical about the plane of x = vt for small values of vx/K. For vx/K > 500, a maximum error of 3% was introduced by neglecting the second term in Eq. 2–2, and the corresponding concentration profiles became symmetric about the x = vt plane. In ordinary experiments, errors of the order of magnitude of experimental errors are introduced if a symmetrical solution is assumed instead of the actual asymmetrical one. This implies that the second term can be neglected for all practical purposes.

Raimondi ~~et al.~~ (1959) found that mixing between miscible fluids was controlled by two parameters: coefficient of molecular diffusion, and a constant determined by structure of the porous medium. They concluded that the effective mixing coefficient was given by $K = D' + av$. In this relationship, D' is the apparent coefficient of molecular diffusion within the porous medium. It is less than the actual molecular diffusion coefficient by product of formation resistivity factor and porosity. The term a is a constant which depends on the structure, pore size and grain size distribution of the porous medium. For consolidated Berea sandstone cores, the experimental values of a were between 0.15 and 0.25 cm. For packings of uniform size particles, a was equal to $\varepsilon^2 d_p$, where d_p is the average grain diameter and ε^2 is a characteristic constant of the packs which was found to be equal to 0.68 for uniform spheres. The experiments showed that molecular diffusion was the dominating factor at low flow rates, and became negligible at high flow rates.

Handy (1959) designed an experiment to study the effects of molecular diffusion on the mixing-zone size for miscible displacements. He added methanol and sucrose as double tracers to the displacing fluid. Methanol has a higher molecular diffusion coefficient than sucrose. The methanol and sucrose concentration profiles detected at the outlet end of the linear core showed no appreciable differences at two displacement rates: 0.5 ft/day and 16.5 ft/day. This indicated that molecular diffusion was not an important factor in the mixing of displacing and displaced fluids in the frontal regions.

A thorough experimental investigation of hydrodynamic dispersion in linear miscible displacements was carried out by Brigham ~~et al.~~ (1961). They studied the effects of fluid velocity, distance travelled, bead size (type of porous medium), viscosity ratio of the fluids and pack diameter on the amount of hydrodynamic dispersion which they called length of mixed zone. Their conclusion was that mixing phenomenon in displacements with favorable viscosity ratio could be explained by:

$$\frac{C(x,t)}{C_o} = \frac{1}{2}\,\mathrm{erfc}\left(\frac{x - vt}{2\sqrt{Kt}}\right) \qquad (2\text{-}3)$$

with an effective mixing coefficient of:

$$K = \frac{D}{F\phi} + \alpha\, v^{1.2} \qquad (2\text{-}4)$$

The first term on the right hand side of Eq. 2-4 is the apparent molecular diffusion, which is equal to the ratio of the molecular diffusion constant: divided by the product of the formation resistivity factor and porosity of the system. The second term is the mechanical dispersion. Constant a, known as the dispersion constant, depends on the nature of porous medium as well as the viscosity ratio of the fluids. For consolidated cores, values of *a* were found to be 10 to 100 times greater than the values of *a* for unconsolidated cores. This implied that substantial mixing had occurred in consolidated cores compared to the packed beds. The authors also discovered that the effect of molecular diffusion on mixing was negligible except at very low velocities. Their Fig. 5 is reproduced here as Fig. 2.1, and illustrates these points clearly. Brigham et al., however, did not present the effects of lateral (transverse) dispersion on mixing.

Blackwell (1962) studied both longitudinal and transverse dispersion in sand-packed columns. He found that mixing in both directions was dominated by molecular diffusion at low rates, and by mechanical dispersion at high rates. However, mass transport by molecular diffusion was more important for transverse mixing than for longitudinal mixing. At sufficiently high rates, transverse mixing coefficients were found to be smaller by a factor of about 24 compared to those in the flow direction for both 20-30 mesh Ottawa sand and 40-400 mesh silica sand. Figure 7 of their paper is reproduced here as Fig. 2.2, and shows the mixing coefficients for various packs.

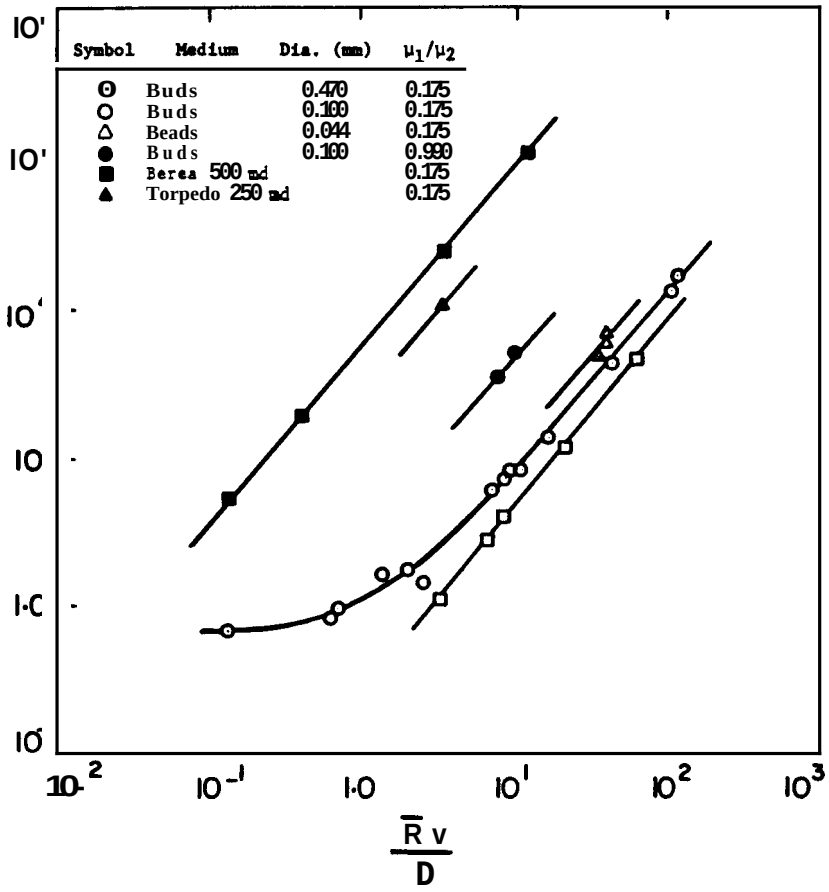

Fig. 2.1: EFFECT OF RATE AND TYPE OF POROUS MEDIUM ON MIXING COEFFICIENT (Brigham et al., 1961)

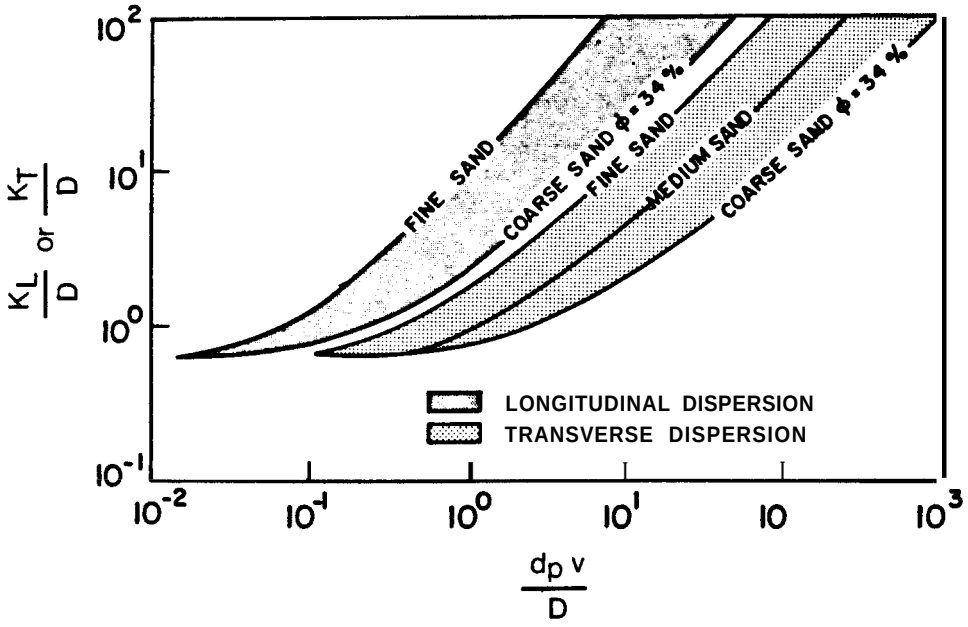

Fig. 2.2: LONGITUDINAL AND LATERAL MIXING COEFFICIENTS FOR VARIOUS SANDS (after Blackwell, 1962)

Harleman and Rumer's (1963) experimental work showed that the longitudinal mixing coefficient was $K_L = \alpha_L v^{1.2}$, while the transverse mixing coefficient was $K_T = a_T v^{0.7}$. The velocity, v, is the microscopic average velocity along the main flow direction. The ratio of the dispersion constants α_L/α_T was 18.3. This was in good agreement with the value of 24 reported by Blackwell. Although molecular diffusion was not reported in this study, the authors speculated that the effects of molecular diffusion would be minimal.

Besides the diffusion model (error function type solutions) describing mixing phenomenon, other models have also been presented to predict mixing in a porous medium. The simplest one is the mixing cell, or stirred-tank model, presented by Aris and Amundson (1957). In this model, the porous medium is viewed as a series of cells or tanks connected to each other by tubes having no volumes. Complete mixing is assumed within each cell, resulting in a uniform composition in each cell. For a small number of such cells in series, the calculated concentration profile is asymmetrical. However, for larger numbers of cells, the concentration profile approaches the symmetrical normal distribution curve computed from a diffusion model.

In some linear miscible flow experiments, especially those run with short cores, a "talling" in the effluent concentration profile is observed and the effluent profile is asymmetric. The degree of asymmetry is more pronounced in consolidated porous media than in laboratory packed columns. Usually, the deviation is not serious and the diffusivity equations provide a good approximation to actual observations. However, several investigators have attempted to explain the asymmetrical concentration profiles quantitatively. Deans (1963) considered the porous medium as a series of normal pores with frequent dead-end passages, or stagnant zones distributed throughout the system. These stagnant pockets store fluids, thereby elongate the mixing zone, and give a tall to the concentration profile. To describe this phenomenon mathematically, Deans modified the mixing cell model to include mass transfer from the flowing stream into the stagnant volumes. As a result, he produced a capacitance model which has three parameters: number of mixing cells (equivalent to dispersion coefficient); amount of stagnant volume (1-f), f being the flowing volume as a fraction of total pore volume; and a rate constant for the mass transfer into the stagnant volumes. Because of the existence of three degrees of freedom (three constants), the capacitance model fits experimental data better than does a diffusion model which contains only one constant (the dispersion coefficient, K).

Coats and Smith (1964) augmented the diffusion equation with Deans' modified mixing-cell model and produced a differential capacitance model. They used the new model to match their data obtained from displacement of calcium choloride solution by a sodium chloride solution in linear cores. The cores were both consolidated and unconsolidated, and between 8 and 9 inches long. The effluent concentration profiles from the consolidated cores exhibited considerable asymmetry, while the unconsolidated cores yielded nearly symmetrical profiles. Coats and Smith demonstrated that the differential capacitance model matched the data significantly better than a simple diffusion model. This behavior was rationalized on the basis that the capacitance model attributed a certain amount of mixing to dead end pore volume effects, while the dispersion model considered only part of the mixing generated in the experiments. The degree of contribution of capacitance effects could be estimated from a dimensionless group defined as $a = K_m L/v$,

(K_m = mass transfer rate, L = length of the system and v = velocity). For their laboratory experiments, "a" was a small number which indicated a significant contribution to the mixing by capacitance effects. However, for field cases, where "a" is a large number (small v and large L), the capacitance effects would be virtually absent and mixing would be controlled almost entirely by a dispersion mechanism. Thus, danger arises from attributing the total mixing observed in short laboratory cores to the dispersion mechanism alone, and subsquently extrapolating the results to field scale. An easy alternative would be to use longer cores in the experiments designed to study dispersion characteristics of a specific porous medium. Because it is often impossible to retrieve long cores from a formation, the results of experiments conducted with short cores should be interpreted with special considerations.

A specific study of mixing in short linear cores was performed by Brigham (1974). For such systems, the boundary conditions used in solving the convective diffusivity equation (Eq. 2-1), greatly affected the resultant solutions. However, by differentiating between the in-situ concentration and the flowing concentration, and allowing for this difference at the boundary conditions as well, Brigham showed that the results computed from various forms of solutions to the diffusivity equation were nearly identical. The solution given by Aronofsky and Heller and Ogata and Banks (Eq. 2-2) was found to generate values for concentrations which were in good agreement with other solutions. The dead-end-pore models (capacitance and differential capacitance models) were found to have been based on the in-situ concentrations, while Coats and Smith had used them to match the flowing concentration data. Although Coats and Smith obtained good matches to their experimental data, the parameters computed from the differential capacitance model would not properly represent the behavior of the same porous medium with longer lengths. Brigham adjusted Coats and Smith's solution (Eq. 28 in their paper) to consider the difference between flowing and in-situ concentrations. He showed that with the new solution, the behavior of large systems might be computed correctly by parameters obtained from small cores (Fig. 6 in Brigham's paper). Brigham concluded that for large systems, the corrected capacitance model behaves like the ordinary diffusion model with a somewhat greater effective dispersion constant, and that the simple error function solution (Eq. 2-3) to the diffusivity equation yields satisfactory results.

2.2.2.2 Non-linear Flow

The preceeding considers mixing or dispersion in linear systems where the flow is uniform and the average velocity is constant. For other geometries, fluid velocity is a function of position, and correspondingly, the mixing coefficient varies from point to point. Therefore, any study of mixing in systems that do not exhibit uniform flow must consider the dependence of dispersion on velocity. The varing dispersion coefficient makes it very difficult, if not impossible, to derive analytic equations to describe mixing in non-uniform flow fields. Even for a simple geometry, such as a diverging radial flow, the exact analytic solution to the convective diffusivity equation has not been obtained in a usable form, according to Bear (1972). However, several approximate solutions are available which describe mixing in radial flow systems with good accuracy. Raimondi et al. (1959) derived an approximate solution based on the assumption that the influence of dispersion becomes small in comparison to local convection as the displacing fluid (or tracer) moves away from the source (injection well). Raimondi's solution is:

$$\frac{C(r,t)}{C_o} = \frac{1}{2}\,\mathrm{erfc}\left(\frac{0.5r^2 - Qt}{\sqrt{\frac{4}{3}\alpha r^3 + \frac{D'}{Q} r^4}}\right) \tag{2-5}$$

where,

$Q = q/2\pi\phi h$

q = injection rate

α = dispersion constant

D' = apparent molecular diffusion coefficient

In this solution, the initial condition $C(r,0) = 0$ is not satisfied. This implies that the approximate solution assumes a finite amount of tracer mass present initially in the porous medium. Although this error is large in the immediate vicinity of the injection well, it is virtually negligible at larger distances from the injection well.

Another appraximate solution for dispersion in a radially diverging flow was obtained by Lau ~~et al.~~ (1959). The approach was based on the assumption that the growth of the length of the mixed zone in a radial miscible displacement was a linear sum of two effects: one due to distance travelled (longitudinal dispersion), and the other due to the geometry of flow (divergence of stream-lines). The distance effects were obtained from the mixing equation for a linear system. The geometry effects were derived from consideration of material balance, noting that the volume of the dispersed zone had to remain constant at a given point regardless of the geometry of the system. The solution presented by Lau et al. is:

$$\frac{C}{C_o} = \frac{1}{2}\,\mathrm{erfc}\left(\frac{r - \bar{r}}{\sqrt{\frac{4}{3}\alpha\bar{r}}}\right) \tag{2-6}$$

where $\bar{r}$ is the average radius of the displacing fluid. Raimondi's solution (Eq. 2-5), also reduces to this equation by using the material balance relationship, $Qt = 0.5\,\bar{r}^2$, neglecting the molecular diffusion term and assuming that $r + \bar{r} \approx 2\bar{r}$ in Eq. 2-5. For systems in which the size of mixed zone is small, these assumptions are realistic.

Lau ~~et al.~~ (1959) and Bentsen and Nielsen (1965) verified the applicability of Eq. 2-6 experimentaly. Bentsen and Nielsen conducted their experiments in a homogeneous slab of circular consolidated Berea sandstone which had a radius of 91.4 cm and a thickness of 1.9 cm. The viscosity of the displacing fluid was higher than the viscosity of the displaced fluid to avoid viscous fingering. The concentrations were measured in-situ using the dielectric constants of the fluids at each radius.

An extension of Lau ~~et al.~~'s method was made by Baldwin (1966) to describe mixing in convergent radial flow. Baldwin was primarily interested in computing the tracer effluent concentration profile from a developed five-spot pattern for a batch of tracer injected into the system. He divided the five-spot flow domain into a series of radially divergent-convergent flow tubes and

computed the tracer concentrations entering the production well from each flow tube. By this method, he matched the experimentally determined tracer breakthrough curves reasonably well.

Gelhar and Collins (1971) developed a general approximate analytic solution for longitudinal dispersion in steady flows with variations in velocity along streamlines. Their solution contains two integrals related to velocity. When this general solution was applied to a radial flow, it generated the same approximate solution as proposed by Raimondi et al. (1959). A comparison of results computed from Raimondi-type solutions with those obtained from numerical simulation of a radial miscible flow was made to determine the accuracy of the approximate solution. The comparison indicated that Raimondi's solution would yield good results after the front had travelled a distance on the order of 100 times the dispersivity of the porous medium ($\bar{r}/\alpha > 100$). In reservoirs, this condition is easily met because the overall scale of the flow is much larger than the dispersivity of the formation. This illustrates the fact that in field applications the approximate solutions usually generate acceptable results. Although the solution given by Gelhar and Collins is a general one, for complicated velocity fields it becomes difficult to evaluate the velocity integrals. Therefore, more simple approximate solutions would be more desirable for practical applications.

Brigham (1973) derived simple equations to describe mixing in systems in which the width of the flow passage varied linearly with the distance travelled. Although this might impose some restrictions on the applicability of his equations, Brigham showed that by breaking the flow system into segments in which width was a linear function of distance, and by repeated use of his solution, mixing could be computed for a variety of geometries. Despite the fact that this method contains several approximations, it has a definite advantage over numerical schemes and other complex solutions. The method is simple, fast and produces reliable results.

The preceeding survey on hydrodynamic dispersion reveals the following facts. Molecular diffusion and transverse dispersion play negligible roles in the amount of mixing in miscible displacements. An equation similar to Eq. 26 can adequately describe mixing in linear and non-linear flow geometries for practical purposes.

2.3 QUANTITATIVE ANALYSIS OF TRACER DATA

The rest of this section will focus on works which have dealt with quantitative analysis of tracer breakthrough profiles from petroleum and geothermal reservoirs and underground aquifers.

2.3.1 Petroleum Reservoirs

Perhaps Wallick and Jenkins (1954) were the earliest investigators who tried to extract quantitative information about the characteristics of a formation from tracer output data. They developed a theoretical method to compute the results of a short-time tracer test. In this, a pulse of tracer material was injected under steady state flow conditions into one well and was detected at a second well. In the analysis, the reservoir was assumed to be homogeneous and infinitely large. The dispersion of tracer in the formation was ignored,

meaning that the tracer material did not mix with fluids ahead or behind it. The theoretical computation of tracer concentration profiles at the production well was then achieved by computing the tracer travel times on various streamlines of this isolated source-sink system. Therefore, only convection was considered. Wallick and Jenkins applied their method to analyze the results of a field tracer test in which helium was injected with air into a reservoir undergoing in-situ combustion. The computed concentration profile was in qualitative agreement with the observed data, and the average permeability and porosity values computed for the formation were reasonably close to those determined from core data.

Brigham and Smith (1965) performed a detailed quantitative analysis on tracer elution curves for developed five-spot patterns. First, they derived an equation to compute the tracer response curves for a homogeneous developed five-spot pattern for a slug of tracer injected into the system. The derivation of this equation was accomplished by combining the tracer dispersion effects with the areal sweep effects for this particular pattern. The dispersion effects were evaluated by approximating the flow field as radial flow to the production well and using the simple mixing equation (Eq. 2-6) for radial flow systems. This approximation, however, introduced errors in the computation of dispersion effects. Brigham and Smith extended the theoretical analysis to developed five-spot patterns with vertical variations in the permeability. They modeled this type of reservoir as a stack of non-communicating homogeneous layers. The overall tracer breakthrough curve from this composite model was computed by volumetrically adding the tracer arrival curves from individual layers. The model was applied to analyze tracer breakthrough curves from a field test conducted in a five-spot pattern. The computed tracer curves had the same trends as the field data. To arrive at these matched curves, Brigham and Smith used three layers, and had to vary the permeability and thickness of the layers by a trial and error procedure. This process was time consuming.

Baldwin (1966) also analyzed the field tracer data reported by Brigham and Smith. He modeled the reservoir with twenty homogeneous, non-communicating layers with permeability of layers ranging from 34 to 4200 md as determined from core data. Based on his equations for radially convergent-divergent flow, he calculated a tracer response curve from this layer-cake model. Figure 8 of his paper is reproduced here as Fig. 2.3 to illustrate the results. The match is good for the early portion of data, but it deviates from the later data appreciably. Since the major portion of tracer flow is in the high permeable zones, the low permeability values used by Baldwin are not important. In reality, Baldwin's match is with fewer than 20 layers.

Yuen et al. (1979) revised Brigham and Smith's analytical solution to include the effect of diverging-converging flow on dispersion. Based on the revised solution, a computer program was developed which would decompose an overall tracer curve from a multilayer developed five-spot pattern into the constituting layer responses, and compute ϕh and $kh/\Sigma kh$ of the layers. The algorithm could handle four layers. As input, peak data (concentration and volume) of tracer breakthrough curves from the layers were required. Yuen et al. demonstrated that peak locations in the overall tracer efflux curve did not correspond exactly to peak locations in the individual layer responses. Therefore, the peak data for the layers had to be determined by a trial-and-error procedure.

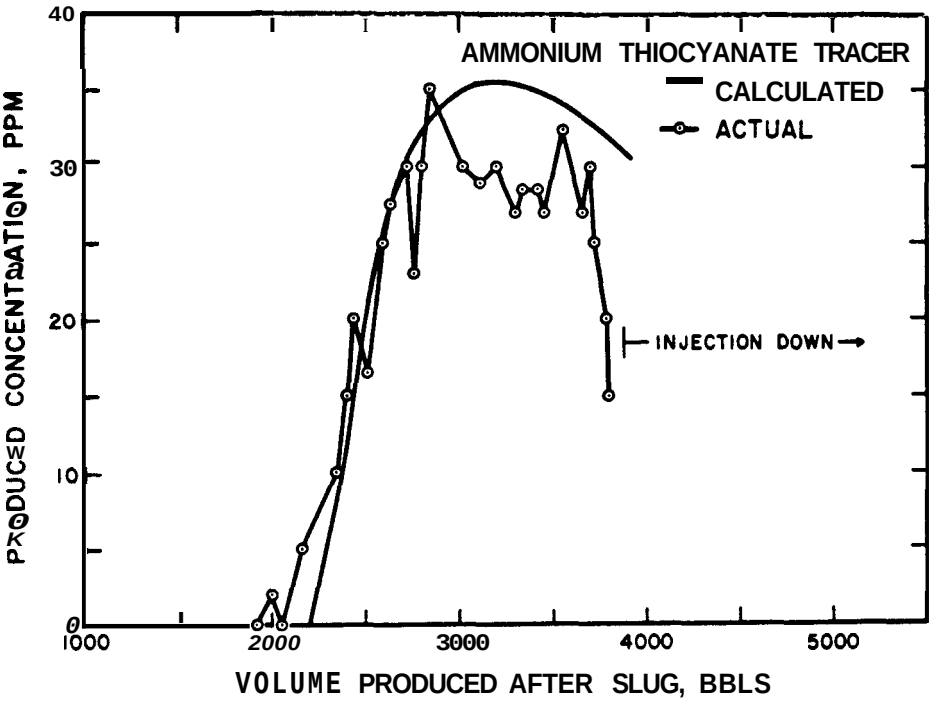

Fig. 2.3: MATCH TO PRODUCED TRACER CONCENTRATION FOR WELL A, REPORTED BY SMITH AND BRIGHAM, AFTER BALDWIN (1966)

Yuen et al's work was modified by Brown and Brigham (1981) to handle larger number of layers. This modified algorithm was used to analyze one of the tracer breakthrough curves reported by Brigham and Smith (1965). Several matches were obtained with different numbers of layers, the best match being with ten layers. The method is useful but cumbersome as it requires many trials to obtain the optimum match for any chosen number of layers.

2.3.2 Underground Aquifers

Besides petroleum engineers, hydrologists have also been interested in defining aquifers in adequate detail. Halevy and Nir (1962) introduced a pulse of radioactive Co^{60} in the form of $K_3Co(CN)_6$ into a fairly homogeneous aquifer and continously recorded activity of the water at a pumped well located 250 meters from the input well. This test differed from usual inter-well tracer tests because the injected batch of tracer was not displaced by a chase fluid. Instead, the tracer flowed towards the pumped well as a result of regional pressure gradients established by the pumping action. Since the flow field was essentially radial, it was assumed that produced tracer peak concentration occurred after pumping a volume equal to the cylindrical pore volume between the observation well and the pumped well. Porosity of the aquifer was subsequently calculated from this peak tracer volume. This was feasible because formation thickness had already been determined from geological data. Halevy and Nir neglected dispersion of tracer. This simplification detracted from the accuracy of their results.

A similar test was conducted by Mercado and Halevy (1966) in a shallow stratified aquifer. The same radioactive material was injected through a dually completed observation well. The tracer arrival curve indicated that the aquifer was composed of four distinct layers. The permeability-thickness product of layers and average porosity of the formation were computed from an analysis based on the method illustrated by Halevy and Nir (1962). Tracer dispersion effects as well as interaction of tracer response curves from individual layers were neglected. These assumptions are unrealistic, and therefore reduce the accuracy of the results.

Zaghi (1977) extended Wallick and Jenkins' (1954) work for a case of nine doublets (nine injectors and nine producers) unequally spaced in a direct line-drive fashion. He assumed that the tracer dispersion was negligible and as a result, the tracer had sharp interfaces with the contacted fluids ahead and behind. He developed a computer program to calculate the breakthrough curves both for the leading and the trailing edges of the tracer slug at the production wells. The effluent tracer concentration curve at each production well was then the difference of these two breakthrough curves at that well. Although this analysis correctly included the convective effects in the transport of tracer material, a neglect of the tracer mixing effects did not generate accurate tracer concentration curves at the wells.

Ivanovich and Smith (1978) included dispersion effects in analyzing tracer data from a pilot investigation of an underground aquifer. The procedure for the test was the same as the one reported by Halevy and Nir except the tracer used was Br^{82}. The tracer concentration profile detected at the pumped well indicated that at least two different responses had been superimposed on each other. A statistical model was used to fit the observed field data with two one-dimensional dispersion equations. As a result of the analysis, the layers had different dispersion constants, permeabilities, porosities and average linear velocities. The velocities were considered to be along the line joining the input and the pumped wells.

The main drawback in this analysis was the use of an unidirectional dispersion equation in the statistical model. For a radial drawdown, such as this one, the streamlines are not linear and the actual amount of dispersion caused by non-uniform velocity field is different from that predicted by one-dimensional models.

2.3.3 Geothermal Reservoirs

Geologic characteristics of geothermal reservoirs can also be revealed through detailed analysis of tracer tests conducted in geothermal formations. Unlike petroleum reservoirs, most geothermal reservoirs are highly fractured and the fractures are connected to each other forming a network of channels (Horne, 1981). Short circuiting and early appearance of injected material at the production wells are common. A response from an injected pulse of tracer is generally detected in a matter of hours and the response curve usually has a single peak with a long tail. Although methods developed to analyze geothermal tracer data are somewhat different from those of sedimentary formations, the basic ideas are the same.

Tester et al. (1979) concluded that a tracer response curve from a hydraulically fractured granitic geothermal reservoir was also a combination of several responses, each arriving from a subzone of the formation. A field test was conducted with a pair of injection and production wells using Br^{82} and I^{131} as radioactive tracers. Tester et al. proposed a mathematical model in which the reservoir was assumed to be composed of several porous zones, each zone being homogeneous but different in characteristics from others. In this model, a two-dimensional convective diffusivity equation, with dispersion coefficients being proportional to fluid velocity in each direction, was solved to compute the tracer response profile from a homogeneous layer. The analysis of tracer field data was performed basically by curve fitting the observed field data with those computed from the model. The curve fitting process automatically generated the parameters of the zones.

Horne and Rodriguez (1981) derived an analytic expression to describe the flow of tracers in a single fractured system. Based on Taylor's (1953) classic work of convective dispersion in pipe flow, they obtained an effective longitudinal dispersion coefficient for tracer flow in a fracture. Horne and Rodriguez matched a tracer response curve from a geothermal field with their model and computed the width and length of the fracture directly. Although the match did not include the tail end of the data, it was postulated that a multiple fracture model similar to Tester's (1979) multizone or Brigham and Smith' (1965) multilayer model could be developed which would match all the data closely.

2.4 SUMMARY

From the preceding literature survey, it becomes evident that flow of tracers in any formation--whether it be a petroleum, a geothermal or an underground aquifer--can reveal detailed information about the reservoir which may otherwise be unattainable. This information can generally be obtained from a detailed mathematical analysis of a tracer breakthrough curve. In most of the analyses, the convective diffusivity equation has been solved in some geometry to include dispersion of a tracer and some flow pattern has been assumed to take into consideration the areal movement of the tracer. The accuracy of the methods depends on how well dispersion is defined and whether the assumed flowlines are close to the true streamlines. However, in most of the previous works, either dispersion has not been formulated correctly (even sometimes neglected) or the flow field has been approximated by too simple and unrealistic flow geometries.

Methods developed to analyze complex tracer breakthrough curves have only been for bounded (repeated) five-spot patterns. These methods generally require a direct and lengthy interaction with the computer in order to generate a good match to the tracer production data from five-spot patterns. In these methods, dispersion of tracer has not been formulated accurately. No studies of tracer breakthrough curves for other patterns have been reported. It was the purpose of thls study to develop a method which would adequately analyze tracer breakthrough curves not only for developed five-spot patterns but also for other common developed flooding patterns. It was also the goal of this research that the analysis technique be free of cumbersome trial-and-error procedures.

3. METHOD OF SOLUTION

This section provides a mathematical analysis of tracer flow in several bounded flooding patterns for a mobility ratio of unity. The section is divided into three main parts. In the first, analytic equations are derived to define the performance of the flooding patterns for immiscible displacements with unit mobility ratio. In this part, an attempt has also been made to extend the analytical analysis for mobility ratios other than one. The second part covers the flow of a tracer slug in homogeneous reservoirs. Tracer dispersion effects are mathematically superimposed on the immiscible pattern breakthrough curves to generate tracer production curves. The analytically defined tracer production curves are correlated into a single set of curves which represents tracer flow in various patterns. The last part of this section studies tracer breakthrough curves from non-communicating, stratified reservoirs. A technique developed to analyze tracer response curves for these systems is presented.

3.1 PATTERN PERFORMANCE

The areal movement of displacement fluids is the prime feature in the recovery performance of a pattern. In general, this is characterized by a pattern breakthrough curve, or areal sweep efficiency curve. This section illustrates the analytical derivation and correlation of these curves for a variety of repeated flooding patterns.

3.1.1 Steadv Multi-Well Flow Theorv

As was discussed in the literature review, the transport of tracer solutions in any flow system is subject to convection and dispersion. Convection represents the gross movement of fluids in the system. Its effects are obtained from displacements in which sharp fronts between the fluids are preserved. To illustrate this point, consider a five-spot pattern initially filled with fluid A. Fluid B is injected into the pattern continuously to displace fluid A with a sharp front. Figure 3.1a shows the location of fluid B in the system after injecting a definite volume of the fluid. The breakthrough curve describing the fraction of fluid B in the producing stream at a production well is given in Fig. 3.1b. As this figure shows, there is no production of B until breakthrough, after which production of B rises steeply and approaches 100% asymptotically. This situation corresponds to the fill-up of the entire pattern by fluid B. The shape of the curve in Fig. 3.1b is a function of two parameters: the geometry of the pattern, and the mobility ratio of the fluids.

Consider another case in which a slug of fluid B is injected into the same pattern and then followed by fluid A as shown in Fig. 3.2a. Because sharp fronts are assumed between B/A and A/B, the breakthrough curve for A displacing B is identical in shape to the curve in Fig. 3.1b except that it lags

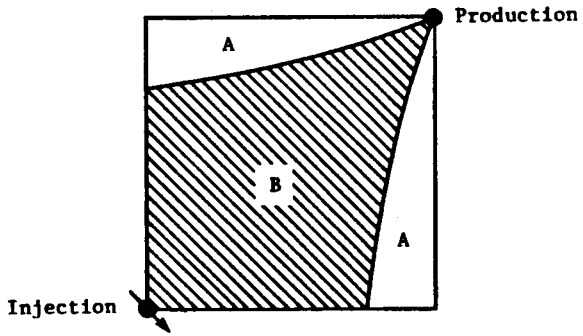

Fig 3.1a Front Locati n

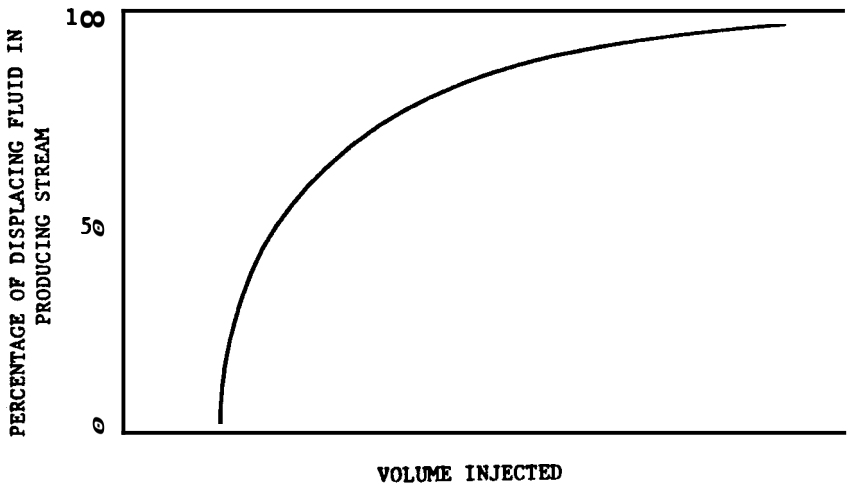

Fig. 3.1b Breakthrough Curve

Fig 3.1: FRONT LOCATION AND BREAKTHROUGH CURVE IN A DISPLACEMENT OF TWO FLUIDS WHICH DO NOT MIX

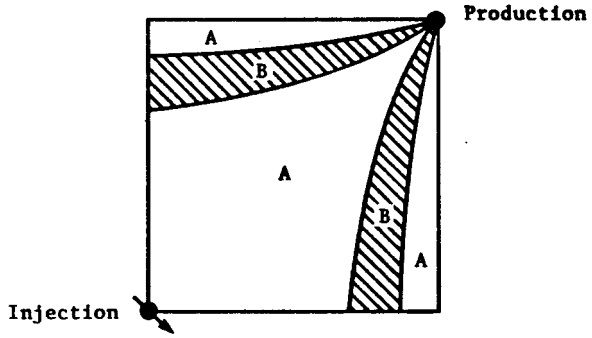

Fig. 3.2b Front Locations

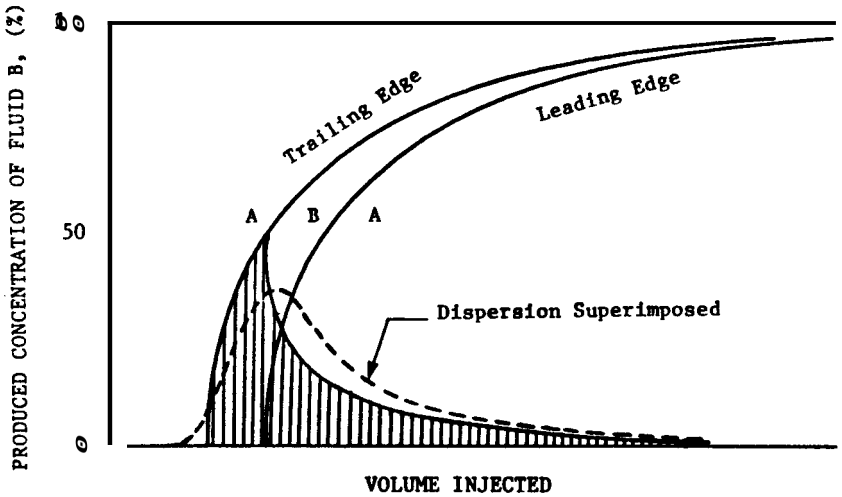

Fig. 3.2b Breakthrough Curves

Fig. 3.2: CONVECTION EFFECTS ON THE BREAKTHROUGH OF A SLUG OF FLUID B

by an amount equal to the volume of slug B. Figure 3.2b shows the theoretical breakthrough curves for B displacing A and for A displacing B. The breakthrough curve for fluid B is then the difference of these two curves. This is illustrated as a shaded profile in Fig. 3.2b. The peak concentration (or fraction) of B produced from this system is considerably less than the concentration flowing in the reservoir which is 100 percent. The dilution of B is the result of convection or areal sweep effects. For the case where B is miscible with A, dispersion effects are imposed on the shaded curve, hence, causing further dilution. The broken-line profile in the same figure shows the breakthrough curve for fluid B from this pattern with dispersion effects. To conserve a material balance, the areas under these two curves must be equal.

In early phases of this research, it was speculated that any theoretical description of tracer flow in patterns must be related to the pattern breakthrough curves such as the one shown in Fig. 3.1b. Therefore, an attempt was made to describe the pattern breakthrough curves analytically for several common, bounded, flooding patterns at a mobility ratio of unity.

3.1.2 Pattern Breakthrounh Curves

Any mathematical description of fluid movement in a flow system requires a knowledge of a potential field for that system. For single-phase steady flow, the potential field can usually be obtained either from a solution of the Laplace equation with appropriate boundary conditions, or by application of the superposition principle as indicated by Muskat (1949) and Prats et al. (1955). Generally, it is simpler to solve the problem in a complex plane and derive an expression for the complex potential of the geometry. This expression can be decomposed into a real part and an imaginary part. The real part is the equation for the potential distribution (proportional to pressures), and the imaginary part is the stream function. Morel-Seytoux (1966) provides the complex potentials for a variety of flooding patterns. Although he does not give the pressure and stream functions for all patterns, they can be generally derived from the complex potentials.

Since stream functions are available or can be constructed for a variety of flow patterns, it is feasible to describe the displacement of two fluids in different patterns mathematically. The displacements are assumed to be of unit mobility ratio and piston-like. Fluids are assumed incompressible and gravity and capillary effects are neglected. The following general procedure is used to derive the analytic expressions for the breakthrough curve (displacing fluid cut versus pore volumes injected) of any pattern:

1) Compute the time required for a particle to travel from the injection well to a production well on a general streamline of a pattern. This is the breakthrough time for that streamline.

2) Multiply the breakthrough time by the injection rate and divide by the pattern area to obtain the pore volumes injected at breakthrough of that streamline.

3) Compute the angle at which the considered streamline enters the production well or leaves the injection well. Divide this angle by the total angle subject to flow at either the production or injection well to obtain the displacing fluid cut at the producing stream. This calculation is correct because for mobility ratio of one, the total flow rate of each fluid is proportional to the total angle from which each fluid enters the production well. The calculated cut corresponds to the pore volume determined in item 2.

The mathematical formulation of breakthrough curves for four bounded homogeneous patterns--staggered line drive, five-spot, direct line drive and inverted seven-spot--are given in Appendices A.1, A.2, A.3, A.4, respectively. Figure 3.3 shows breakthrough curves for these four patterns. Staggered line drive and direct line drive patterns have different breakthrough curves depending on their d/a ratios. The ratio d/a represents the ratio of the distance between the unlike wells (an injector and a producer) to the distance between like wells (two injectors or two producers).

These results are useful in computing oil recovery from displacement processes wherein the assumption of unit mobility ratio can be justified. However, for such calculations; areal sweep efficiency versus pore volume of displacing

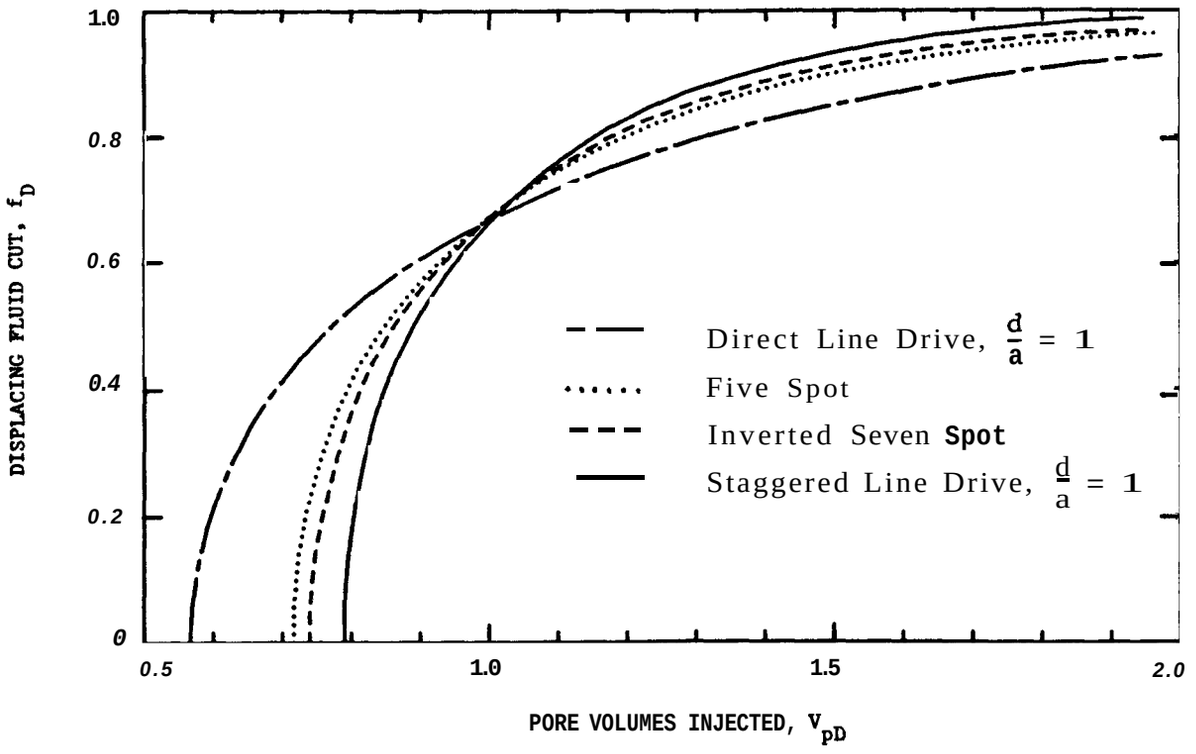

Fig. 3.3: PATTERN BREAKTHROUGH CURVES FOR DEVELOPED SYSTEMS, MOBILITY RATIO = 1

fluid injected would be more useful. Areal sweep efficiency may be computed from the following (Craig, 1971):

$$E_A = \int_0^{V_{pD}} (1 - f_D)\, dV_{pD}$$

$$= V_{pDbt} + \int_{V_{pDbt}}^{V_{pD}} (1 - f_D)\, dV_{pD} \qquad (3\text{-}1)$$

where,

E_A = areal sweep efficiency

f_D = displacing fluid cut in the production stream

V_{pDbt} = breakthrough pore volume or breakthrough areal sweep efficiency

V_{pD} = displacing pore volume corresponding to cut, f_D

This integral corresponds to the area above the curves in Fig. 3.3. It is alternatively given by:

$$E_A = (1 - f_D)\, V_{pD} + \int_0^{f_D} V_{pD}\, df_D \qquad (3\text{-}2)$$

The integrand is a function of f_D and the functional relationships are given in Appendix A for various patterns. The results of integration are shown in Fig. 3.4.

3.1.3 Correlation of Pattern Breakthroueh Curves

For patterns other than those included in this study, the same derivations must be performed to obtain a breakthrough curve similar to the curves in Fig. 3.3. However, it would be desirable to relate all pattern breakthrough curves and find a general correlation which would be applicable for all patterns. Previously, Morgan (1977) in continuation of Morales' (1975) work concluded that the breakthrough curves for different patterns could possibly be correlated into a single curve for each mobility ratio of displacement. The parameter that was used in the correlation was a dimensionless quantity defined as:

$$PV_D = \frac{V_{pD} - V_{pDbt}}{1 - V_{pDbt}} \qquad (3\text{-}3)$$

The PV_D term will be referred to as dimensionless pore volume in this study.

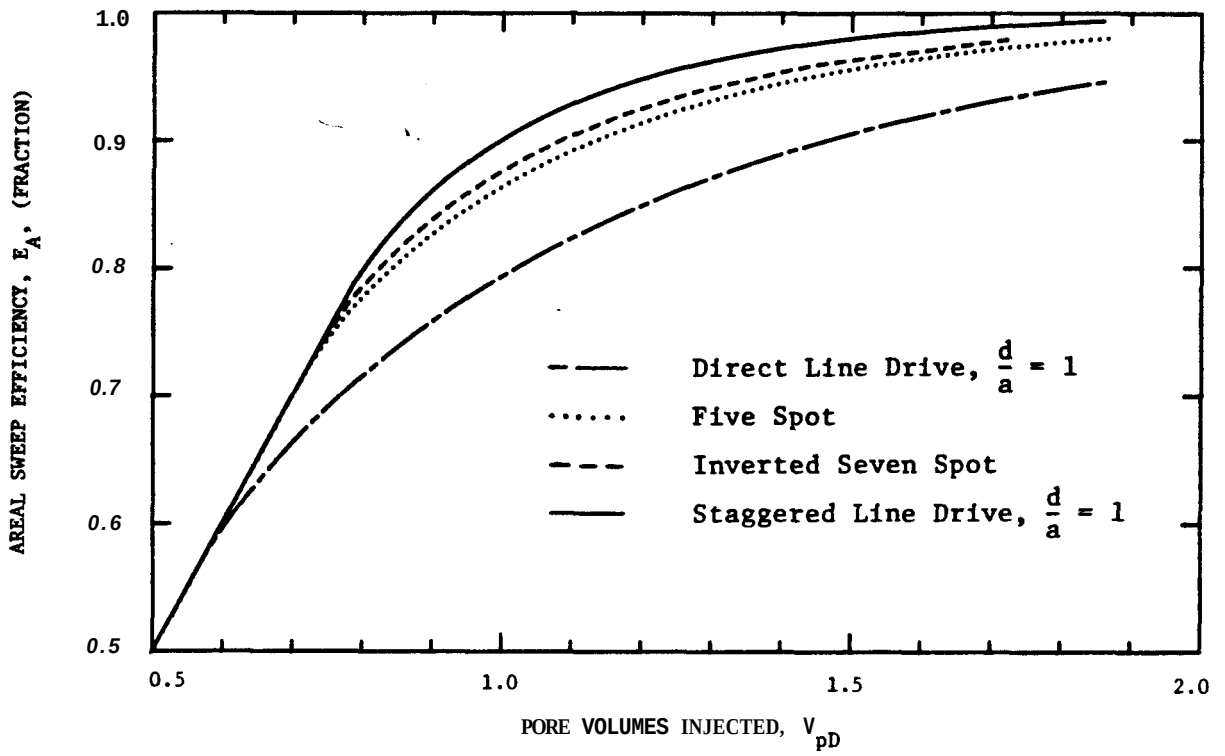

Fig. 3.4: AREAL SWEEP EFFICIENCY CURVES FOR DEVELOPED PATTERNS, MOBILITY RATIO = 1

Since Morgan was working with limited experimental data, he could not confirm the accuracy of the correlation, although it appeared to be reasonably accurate. In this study, however, it is demonstrated that by using the dimensionless parameter defined by Eq. 3-3, all the analytically defined pattern breakthrough curves collapse into virtually a single curve as shown in Fig. 3.5. Staggered line drive and direct line drive patterns with various d/a ratios are all included in this single correlation. A simple equation for the curve in Fig. 3.5 is obtained by a non-linear curve-fitting method, as follows:

$$f_D = 1 - 0.5 \left[e^{10(PV_n)^{0.530}} + e^{15(PV_n)^{0.792}} \right] \qquad (3\text{-}4)$$

Equation 3-4 yields a maximum error of 2% in f_D for all the curves, except for very early parts of the curves where the error is large.

A comparison of the experimentally-measured data with the analytically computed and correlated curve is illustrated in Fig. 3.6. The data for the five-spot, direct line drive and the staggered line drive have been taken from Dyes et al. (1954). The data for the inverted seven-spot pattern are from Guckert (1961). Figure 3.7 shows a comparison of results for a repeated five-spot pattern where several investigators have reported either numerical or experimental data for the performance of this pattern (Fay and Prats, 1951;

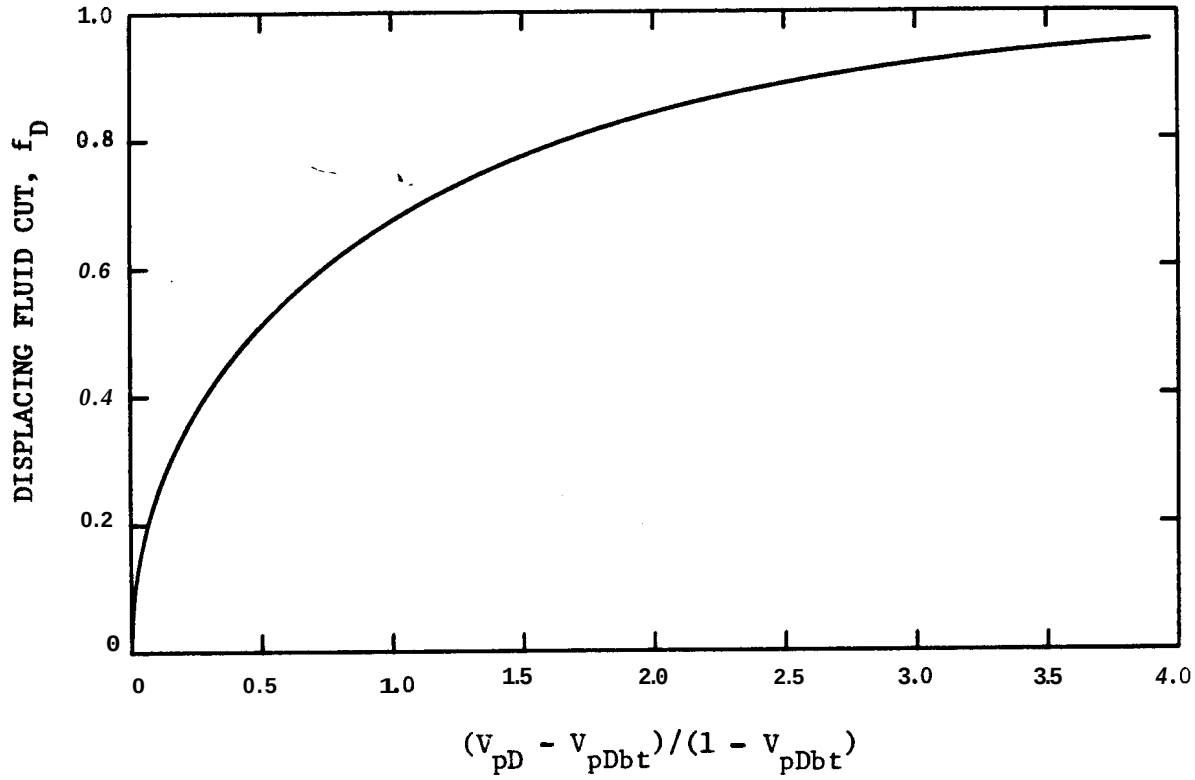

Fig. 3.5: CORRELATION OF DEVELOPED PATTERN BREAKTHROUGH CURVES, MOBILITY RATIO = 1

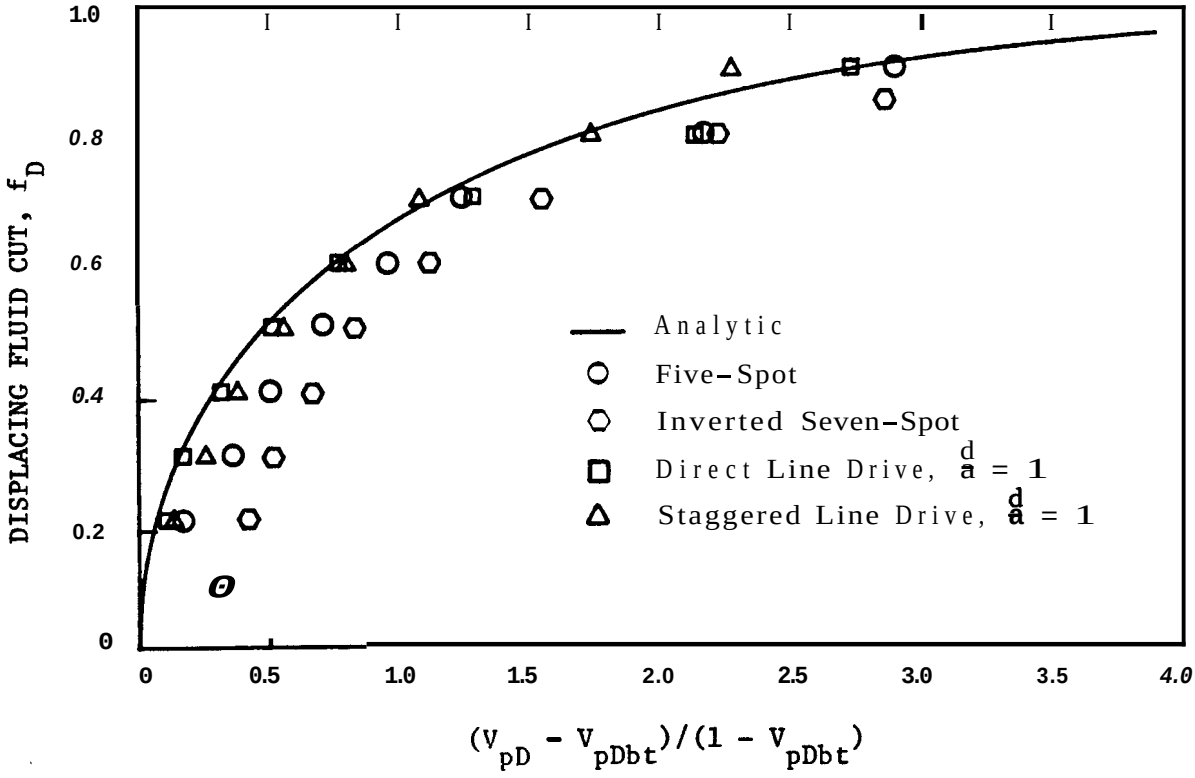

Fig. 3.6: COMPARISON OF THE EXPERIMENTAL DATA FROM VARIOUS DEVELOPED PATTERNS AND THE CORRELATED PATTERN BREAKTHROUGH CURVE, MOBILITY RATIO = 1

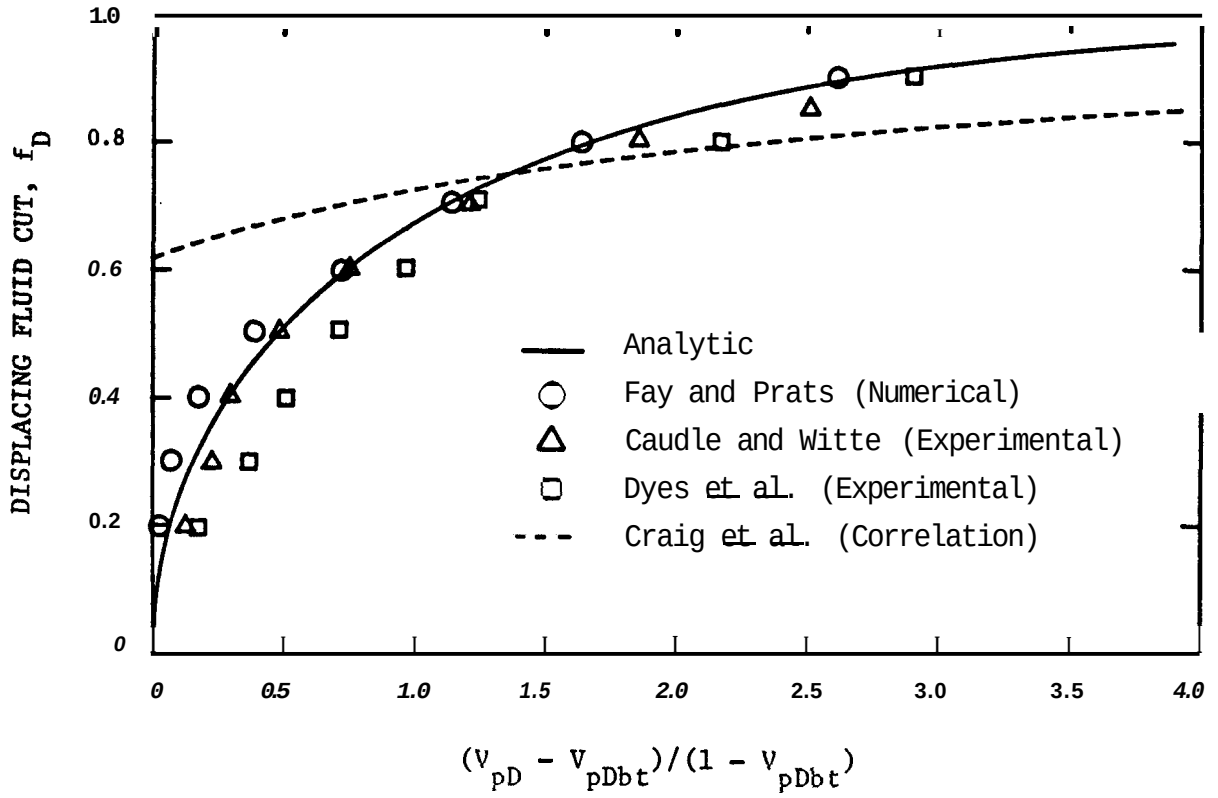

Fig, 3.7 : COMPARISON OF THE CORRELATED PATTERN BREAKTHROUGH CURVE AND DEVELOPED FIVE-SPOT DATA, MOBILITY RATIO = 1

Dyes et al., 1954; and Caudle and Witte, 1959). The dashed curve in this figure has been obtained by differentiating the equation for the areal sweep efficiencies reported by Craig et. al. (1955). It is believed that the deviations of data from the analytic curve are due to smearing of the displacement fronts by capillary forces (immiscible displacements) or mixing (miscible displacements). Experimental errors also contribute to the deviations.

The curves in Fig. 3.4 can also be correlated into a single curve. This requires defining another parameter, called dimensionless areal sweep efficiency, as follows:

$$E_{AD} = \frac{E_A - E_{Abt}}{1 - E_{Abt}} \tag{3-5}$$

where:

E_{Abt} = breakthrough areal sweep efficiency = V_{pDbt}

The correlation is shown in Fig. 3.8. The equation for this curve obtained by a non-linear curve-fitting routine is:

$$E_{AD} = 1 - e^{-0.7413(PV_D)^{0.9273}} \tag{3-6}$$

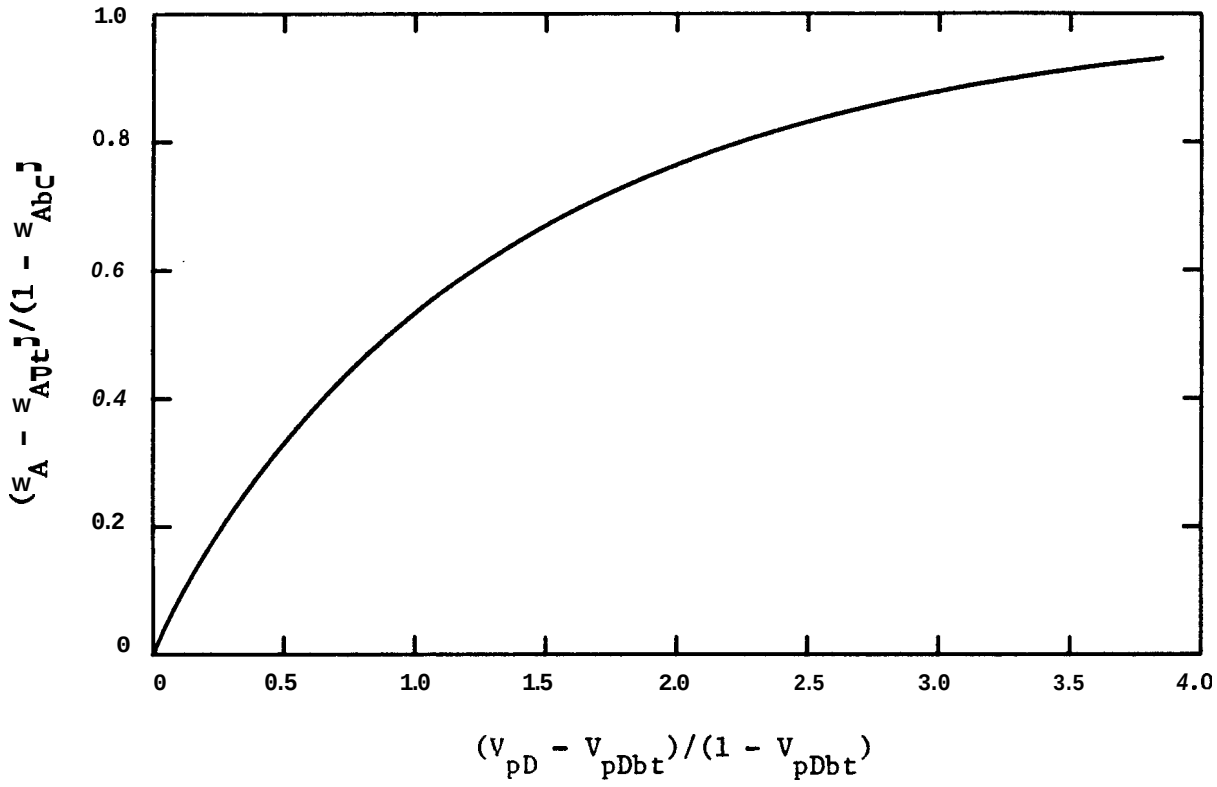

Fig. 3.8: CORRELATION OF AREAL SWEEP EFFICIENCY CURVES OF DEVELOPED PATTERNS, MOBILITY RATIO = 1

A correlation of f_D and E_{AD} is provided in Fig. 3.9 to complete the set of correlations. Also shown in this figure is the correlation originally reported by Morgan (1977). Tables 3.1 through 3.4 give the numerical values of the dimensionless pore volumes and the dimensionless areal sweep efficiencies for different patterns. Comparison of these values for the various patterns shows the accuracy of the correlations.

The fact that the breakthrough curves and areal sweep curves for all the patterns studied could be condensed into single curves is important for rapid calculation of recoveries by flooding.

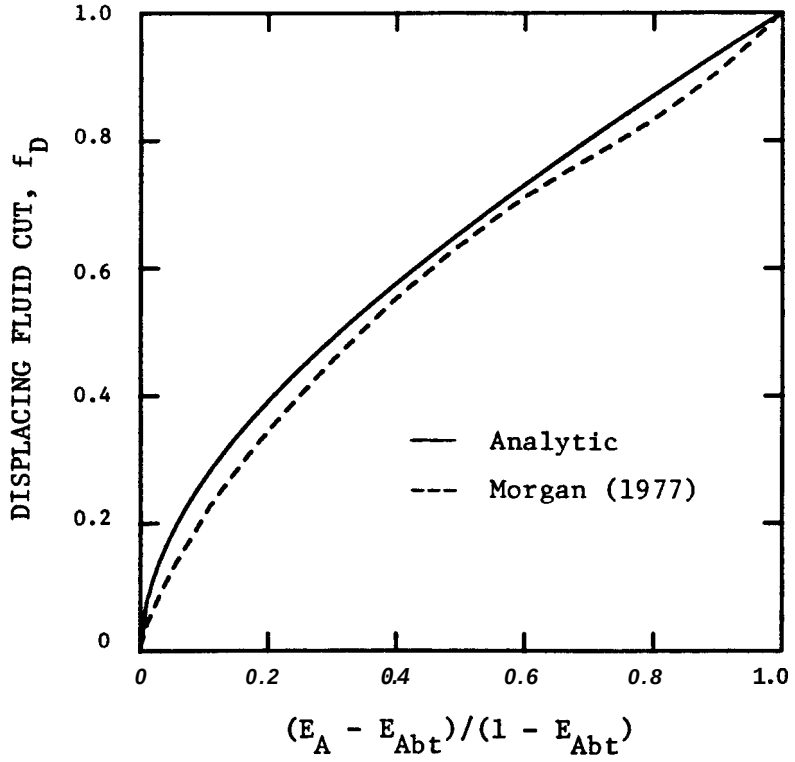

Fig. 3.9: CORRELATION OF DISPLACING FLUID CUT VS DIMENSIONLESS AREAL SWEEP EFFICIENCY, DEVELOPED PATTERNS AND MOBILITY RATIO = 1

From these results, one could expect that the generalized curves of Figs. 3.5 and 3.8 or 3.9 would be valid for any balanced patterns. Thus, one of the correlated curves could be used as a basis for post-breakthrough calculation of recovery versus volume injected for floods without resorting to complex modeling calculations.

Table 3.1

VALUES OF BREAKTHROUGH AND AREAL SWEEP EFFICIENCY CURVES FOR A DEVELOPED FIVE-SPOT, MOBILITY RATIO = 1

f_D	V_{pD}	PV_D	E_A	E_{AD}
0.00	0.71777	0.00000	0.71777	0.00000
0.05	0.71887	0.00391	0.71884	0.00378
0.10	0.72222	0.01576	0.72192	0.01471
0.15	0.72786	0.03573	0.72684	0.03215
0.20	0.73589	0.06419	0.73346	0.05559
0.25	0.74645	0.10164	0.74164	0.08457
0.30	0.75976	0.14880	0.75128	0.11872
0.35	0.77608	0.20661	0.76228	0.15700
0.40	0.79576	0.27634	0.77456	0.20123
0.45	0.81926	0.35961	0.78806	0.24905
0.50	0.84720	0.45860	0.80270	0.30094
0.55	0.88038	0.57617	0.81844	0.35671
0.60	0.91993	0.71630	0.83522	0.41616
0.65	0.96742	0.88456	0.85299	0.47912
0.70	1.02514	1.08908	0.87170	0.54542
0.75	1.09666	1.34248	0.89130	0.61486
0.80	1.18789	1.66572	0.91173	0.68724
0.85	1.30986	2.09791	0.93291	0.76230
0.90	1.48714	2.72604	0.95475	0.83968
0.95	1.79710	3.82430	0.97709	0.91883

Table 3.2

VALUE OF BREAKTHROUGH AND AREAL SWEEP EFFICIENCY CURVES FOR A DEVELOPED INVERTED SEVEM-SPOT, MOBILITY RATIO = 1

f_D	V_{pD}	PV_D	E_A	E_{AD}
0.00	0.74368	0.00000	0.74368	0.00000
0.05	0.74470	0.00390	0.74458	0.00350
0.10	0.74778	0.01592	0.74703	0.01305
0.15	0.75297	0.03616	0.75156	0.03072
0.20	0.76036	0.06499	0.75760	0.05447
0.25	0.77007	0.10290	0.76517	0.08382
0.30	0.78230	0.15061	0.77403	0.11838
0.35	0.79728	0.20905	0.78412	0.15775
0.40	0.81532	0.27942	0.79538	0.20168
0.45	0.83683	0.36337	0.80774	0.24990
0.50	0.86237	0.46299	0.82112	0.30214
0.55	0.89265	0.58116	0.83549	0.35818
0.60	0.92869	0.72175	0.85077	0.41781
0.65	0.97187	0.89025	0.86694	0.48087
0.70	1.02426	1.09467	0.88392	0.54713
0.75	1.08905	1.34744	0.90168	0.61642
0.80	1.17153	1.66927	0.92014	0.68843
0.85	1.28162	2.72209	0.93925	0.76301
0.90	1.44137	2.72209	0.95894	0.83981
0.95	1.72088	3.81263	0.97908	0.91838

3.1.4 Pattern Breakthrough Curves for Non-Unit Mobility Ratio

Displacement of fluids with unequal mobilities differs from single phase flow (mobility ratio equal to one) for two reasons. First, the overall resistivity to fluid flow depends on the location of displacement interface. This implies that for a constant flow rate displacement, the pressure drop between an injection well and a production well varies continually as the displacement front advances towards the production well. For a favorable mobility ratio ($M < 1$), the pressure drop increases while for an unfavorable mobility ratio ($M > 1$) it decreases. Second, potential distributions in the displaced region

Table 3.3

VALUES OF BREAKTHROUGH AND AREAL SWEEP EFFICIENCY CURVES FOR DEVELOPED DIRECT LINE-DRIVE PATTERNS, MOBILITY RATIO = 1

	d/a = 1				d/a = 1.5				d/a = 2			
f_D	V_{pD}	PV_D	E_A	E_A	V	P_D	[illegible]	E_{AD}	V_{pD}	PV_D	E_A	E_{AD}
0.00	0.3495	0.00000	0.5495	0.00000	0.1045	0.00000	0.7043	0.00000	0.77939	0.00000	0.77939	0.00000
0.05	0.57124	0.00390	0.9118	0.00377	0.7047	0.00000	0.70759	0.00425	0.78037	0.00005	0.7805	0.00030
0.10	0.5731	0.01547	0.9157	0.01543	0.71153	0.01755	0.71115	0.01505	0.7333	0.01786	0.78307	0.01567
0.15	0.5807	0.0337	0.5833	0.03200	0.7150	0.03995	0.71590	0.03593	0.7555	0.0039	0.7571	0.03535
0.20	0.59711	0.0601	0.59 2	0.05353	0.7357	0.9151	0.7355	0.0592	0.79335	0.9125	0.7931	0.0527
0.25	0.61329	0.1015	0.6594	0.0855	0.73955	0.11307	0.73398	0.09511	0.8035	0.11515	0.80035	0.0930
0.30	0.9377	0.1591	0.6077	0.11897	0.75578	0.1359	0.75091	0.1318	0.8510	0.1639	0.8570	0.1325
0.35	0.65902	0.7055	0.3119	0.15857	0.7335	0.7553	0.75751	0.1725	0.83010	0.2987	0.8151	0.1756
0.40	0.6895	0.7395	0.6591	0.20293	0.79558	0.3033	0.77135	0.2313	0.85681	0.3057	0.8 57	0.2299
0.45	0.7251	0.3539	0.67 2	0.5197	0.8215	0.39 2	0.7539	0.7257	0.8533	0.39 0	0.83390	0.2 8
0.50	0.77030	0.4535	0.70 3	0.3053	0.85235	0.49 7	0.8023	0.3150	0.8595	0.49984	0.8320	0.3293
0.55	0.8259	0.3785	0.7583	0.9305	0.8553	0.6025	0.8192	0.385	0.9157	0.6257	0.8587	0.3785
0.60	0.8598	0.7317	0.5230	0.4255	0.9302	0.7555	0.8358	0.4591	0.9583	0.7351	0.7835	0.4585
0.65	0.9397	0.9055	0.4028	0.4895	0.9305	0.9 5	0.8530	0.5 5	0.9897	0.9350	0.89237	0.5121
0.70	1.0 1	1 1155	0.8 58	0 5571	1.0057	1 1317	0.9157	0.3752	1.03071	1 1921	0.9058	0.3779
0.75	1 1610	1.9157	0.83999	0.6282	1 1123	1.3 557	0.89559	0.6555	1.0811	1.3578	0.9179	0.9555
0.80	1 3006	1.6985	0.8125	0.9309	1 2051	1.6917	0.91595	0.71379	1 1517	1.6951	0.9370	0.7155
0.85	1 5507	2 1251	0.9312	0.7793	1 3237	2 1011	0.9357	0.7535	1 2 5	2.0390	0.9533	0.7890
0.90	1 7353	2 3159	0.9333	0.8975	1 5950	2.6505	0.9357	0.85575	1 3955	2.9155	0.9555	0.8351
0.95	2 1937	3 7321	0.9757	0.9 9	1 7555	3 5753	0.9757	0.9 73	1 3955	3.9123	0.9509	0.9279

Table 3.4

VALUES OF BREAKTHROUGH AND AREAL SWEEP EFFICIENCY CURVES FOR DEVELOPED STAGGERED-LINE-DRIVE PATTERNS, MOBILITY RATIO = 1

	d/a = 1				d/a = 1.5				d/a = 2			
f_D	V_{pD}	PV_D	E_A	E_{AD}	V_{pD}	PV_D	E_A	E_{AD}	V_{pD}	PV_D	E_A	E_{AD}
0.00	0.78888	0.00000	0.78888	0.00000	0.83339	0.00000	0.85339	0.00000	0.88971	0.00000	0.88971	0.00000
0.05	0.78975	0.00029	0.78972	0.00415	0.85404	0.00442	0.8[illegible]02	0.00229	0.89020	0.00445	0.890[illegible]	0.00230
0.10	0.79228	0.01172	0.79[illegible]	0.01608	0.85[illegible]0	0.01[illegible]0	0.85583	0.01662	0.89168	0.01[illegible]8	0.89132	0.01668
0.15	0.79707	0.03829	0.79625	0.03508	0.85930	0.04027	0.83871	0.03362	0.89416	0.02021	0.89372	0.03636
0.20	0.80360	0.069 9	0.80162	0.06052	0.86397	0.0[illegible]21[illegible]	0.86255	0.06228	0.89769	0.07238	0.89662	0.06270
0.25	0.81213	0.1[illegible]20	0.80825	0.09189	0.[illegible]008	0.11382	0.86728	0.09275	0.90230	0.11420	0.90019	0.09506
0.30	0.82287	0.[illegible]6116	0.81601	0.12865	0.[illegible]77[illegible]	0.16592	0.[illegible]7[illegible]2	0.13[illegible]9	0.90806	0.[illegible]66[illegible]5	0.[illegible]0[illegible]36	0.13290
0.35	0.83593	0.2[illegible]302	0.82[illegible]81	0.17[illegible]5	0.88701	0.22927	0.[illegible]790[illegible]	0.0[illegible]319	0.91507	0.22990	0.90903	0.17571
0.40	0.85157	0.29709	0.83458	0.21659	0.89809	0.30487	0.88600	0.22239	0.[illegible]2[illegible]2	0.30570	0.9[illegible]30	0.22300
0.45	0.87010	0.38[illegible]83	0.[illegible]52[illegible]2	0.26699	0.91101	0.39[illegible]11	0.89331	0.26[illegible]36	0.93328	0.39[illegible]8	0.91996	0.27[illegible]3[illegible]
0.50	0.[illegible]9192	0.48818	0.83666	0.32117	0.92652	0.49882	0.90136	0.32[illegible]5[illegible]	0.9[illegible]	0.49992	0.92609	0.32931
0.55	0.92158	0.60969	0.86883	0.37881	0.93450	0.62[illegible]3	0.9[illegible]09	0.38670	0.93388	0.62263	0.93205	0.38751
0.60	0.9[illegible]78[illegible]	0.75290	0.[illegible]8[illegible]6	0.43957	0.96360	0.76331	0.[illegible]1[illegible]	0.[illegible]4175	0.[illegible]1[illegible]25	0.76655	0.93918	0.44858
0.63	0.98369	0.92275	0.89508	0.50310	0.99030	0.93[illegible]	0.92 36	0.31130	0.99299	0.93601	0.96019	0.51216
0.70	1.02672	1.[illegible]265[illegible]	0.90900	0.56921	1.0[illegible]23	1.13[illegible]	0.[illegible]3800	0.57713	1.01535	1.13919	0.93305	0.37791
0.75	1.[illegible]794	1.[illegible]552	0.92[illegible]	0.63[illegible]6	1.03663	1.38[illegible]8	0.96792	0.66[illegible]8	1.02[illegible]5	1.38[illegible]2	0.96090	0.6[illegible]9
0.80	1.15[illegible]0	1.68860	0.93[illegible]	0.70[illegible]3	1.[illegible]172	1.69382	0.93[illegible]	0.7139	1.[illegible]65[illegible]	1.69[illegible]	0.96 5[illegible]	0.7[illegible]39
0.85	1.23251	2.[illegible]111	0.95339	0.77925	1.16115	2.093	0.[illegible]689	0.78[illegible]1	1.12020	2.09888	0.97628	0.78490
0.90	1.3573[illegible]	2.692[illegible]	0.96871	0.85211	1.24601	2.[illegible]302	0.[illegible]885	0.85576	1.1[illegible]91	2.[illegible]69	0.98613	0.8563[illegible]
0.95	1.573[illegible]	3.714[illegible]1	0.[illegible]8[illegible]3[illegible]	0.92583	1.39233	3.67604	0.98940	0.92[illegible]3	1.29[illegible]3	3.[illegible]20	0.[illegible]9205	0.92790

and the non-invaded zone continuously change with the movement of the displacement front. As a result of these variable pressure fields, streamlines deviate from those of a single fluid flow. The amount and nature of deviation depends on the location of the interface.

If the shift of streamlines from those corresponding to a single fluid flow is assumed to be minor, calculations can be made to predict recovery performance of patterns for different mobility ratios. Appendix B presents the derivation of equations for recovery performance of a developed five-spot pattern for various mobility ratios. The derivation is based on fixed streamlines and piston-like displacements. Table 3.5 and Figs. 3.10 and 3.11 show the results. As these figures illustrate, the breakthrough areal sweep efficiencies calculated using these assumptions are nearly independent of mobility ratio. This conclusion has also been reached by Morel-Seytoux (1965), whose mathematical approach is different from the one taken in this study. The independence of areal sweep efficiencies for different mobility ratios is in direct conflict with experimental data which show that breakthrough areal sweep efficiencies are functions of mobility ratio (Dyes et al., 1954). Therefore, the assumption of no streamline change with mobility ratio is unrealistic and calculations of piston-like displacements based on this assumption generate erroneous results.

One of the methods that has been extensively used in approximate calculation of waterflood and gas flood performances is Higgins and Leighton's (1962) streamtube method. This method is based on the assumption that streamlines are independent of mobility ratio and that Buckley-Leverett theory can be applied to calculate the fluid displacement in streamtubes comprising the flow system. The principle justification of the method was the good agreement between the recovery values computed from their method and the laboratory data reported by Douglas et al. (1959) for a repeated five-spot waterflood in a

Table 3.5

VALUES OF BREAKTHROUGH AND AREAL SWEEP EFFICIENCY CURVES FOR A DEVELOPED FIVE-SPOT PATTERN AT VARIOUS MOBILITY RATIOS

M = 0.5			M = 1			M = 3		
f_D	V_{pD}	E_A	f_D	V_{pD}	E_A	f_D	V_{pD}	E_A
0.0000	0.7232	0.7232	0.00	0.7178	0.7178	0.0000	0.7093	0.7093
0.1646	0.7403	0.7305	0.10	0.7222	0.7219	0.1690	0.7142	0.7137
0.3437	0.7946	0.7787	0.20	0.7359	0.7335	0.3164	0.7305	0.7257
0.4399	0.0396	0.0063	0.30	0.7590	0.7513	0.4433	0.7611	0.7442
0.5410	0.9017	0.0301	0.40	0.7950	0.7746	0.5537	0.0106	0.7602
0.6473	0.9890	0.0734	0.50	0.0472	0.8027	0.6505	0.0063	0.7973
0.7591	1.1204	0.9133	0.60	0.9199	0.0352	0.7361	1.0002	0.0300
0.0767	1.3551	0.9556	0.70	1.0251	0.0717	0.8123	1.1752	0.0603
0.9253	1.5300	0.9732	0.80	1.1079	0.9117	0.8809	1.4619	0.9094
0.9749	1.9093	0.9910	0.90	1.4071	0.9548	0.9430	2.0190	0.9537

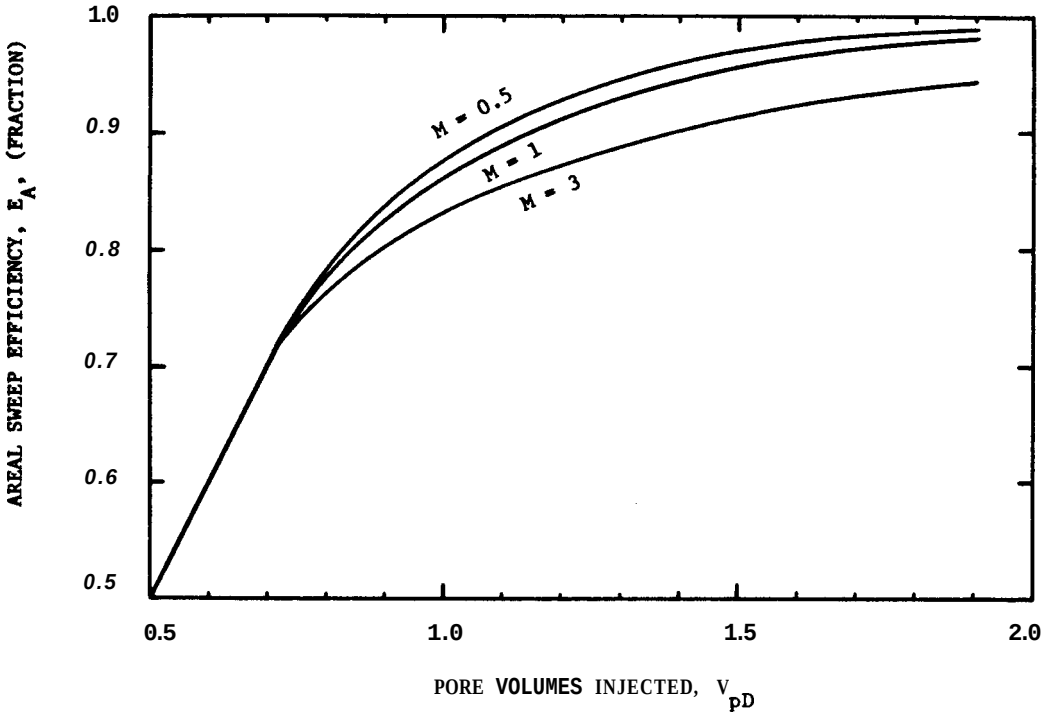

Fig. 3.10: AREAL SWEEP EFFICIENCY CURVES FOR A DEVELOPED FIVE-SPOT PATTERN AT VARIOUS MOBILITY RATIOS (ASSUMING STREAMLINES ARE INDEPENDENT OF MOBILITY RATIO)

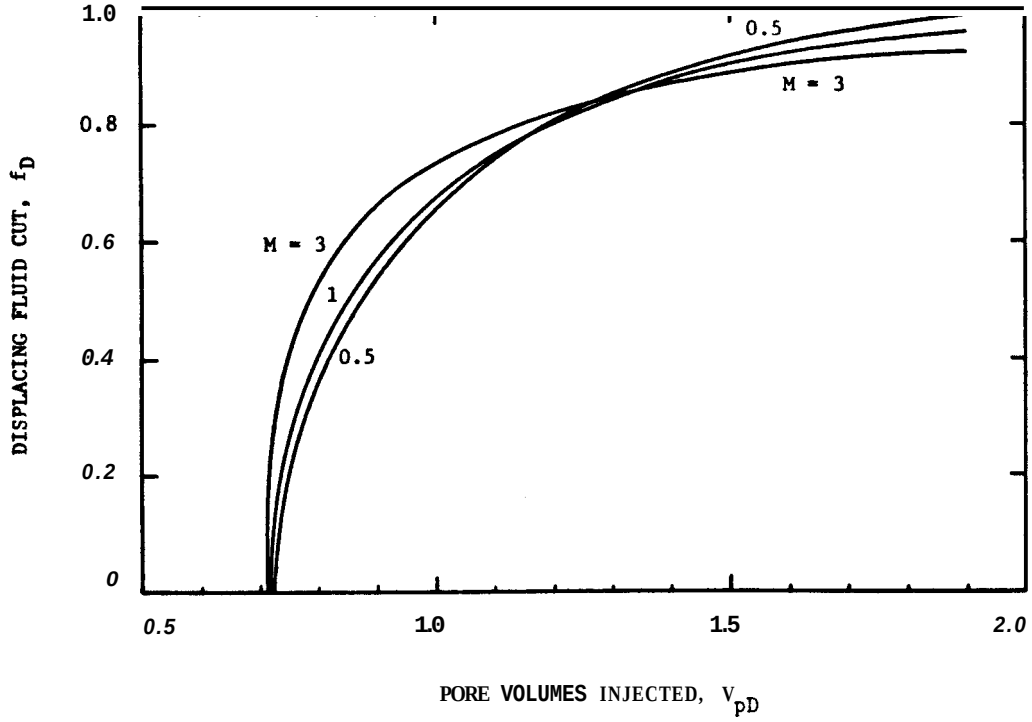

Fig. 3.11: BREAKTHROUGH CURVES FOR A DEVELOPED FIVE-SPOT PATTERN AT VARIOUS MOBILITY RATIOS (ASSUMING STREAMLINES ARE INDEPENDENT OF MOBILITY RATIO)

sand model. Figure 3.12, which is a reproduction of Fig. 1 in Higgins and Leighton's paper, shows the closeness of the agreement.

Since waterflooding is a Buckley–Leverett type displacement process, the pore volumes of oil produced in Fig 3.12 are equal to the product of areal sweep efficiencies and displacement efficiencies. Displacement efficiency is defined as the difference between average water saturation behind the front and irreducible water saturation. At breakthrough, values of displacement efficiencies can be obtained from the fractional flow curves generated from relative permeability data and oil-water viscosity ratios. Figure 3.13 shows the fractional flow curves constructed for the four oil–water viscosity ratios used in the Higgins and Leighton paper.

From the fractional flow curves and the recovery data in Fig. 3.12, the breakthrough areal sweep efficiency for each displacement is calculated by dividing the computed breakthrough oil recovery value by the corresponding breakthrough displacement efficiency. Table 3.6 presents the results. As this table shows, the computed breakthrough areal sweep efficiencies for viscosity ratios of 0.083 and 8.08 are practically the same and close to that for unit mobility ratio, while the sweep values corresponding to higher viscosity ratios are even higher and are thus in error. This discrepancy seems to be due to the low breakthrough displacement efficiencies obtained from the fractional flow curves. Although a good reason for this discrepancy could not be found, the invalidity of Buckley–Leverett theory at high mobility ratios might be a factor.

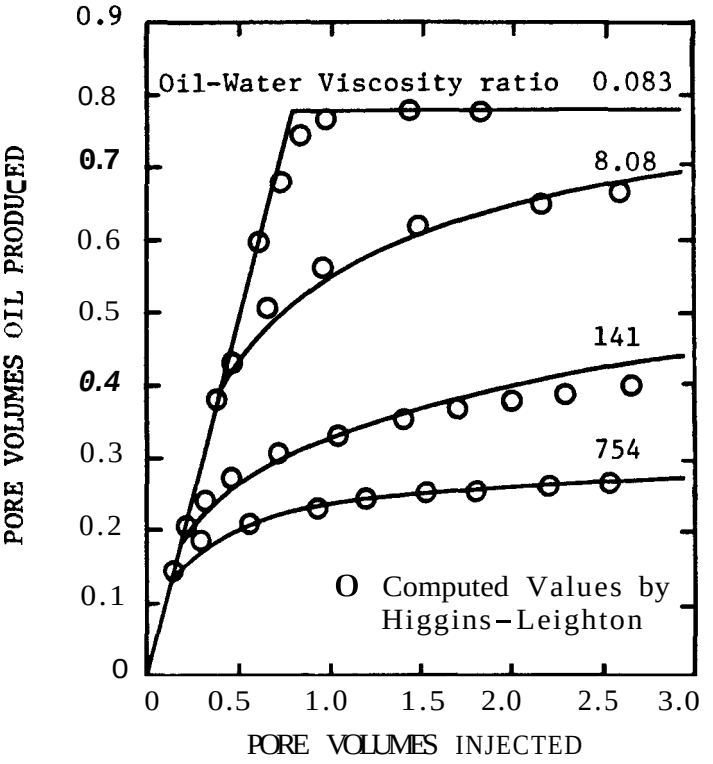

Fig. 3.12: COMPARISON OF LABORATORY DATA AND COMPUTER PERFORMANCE CALCULATIONS FOR A DEVELOPED FIVE-SPOT PATTERN (Higgins and Leighton, 1962)

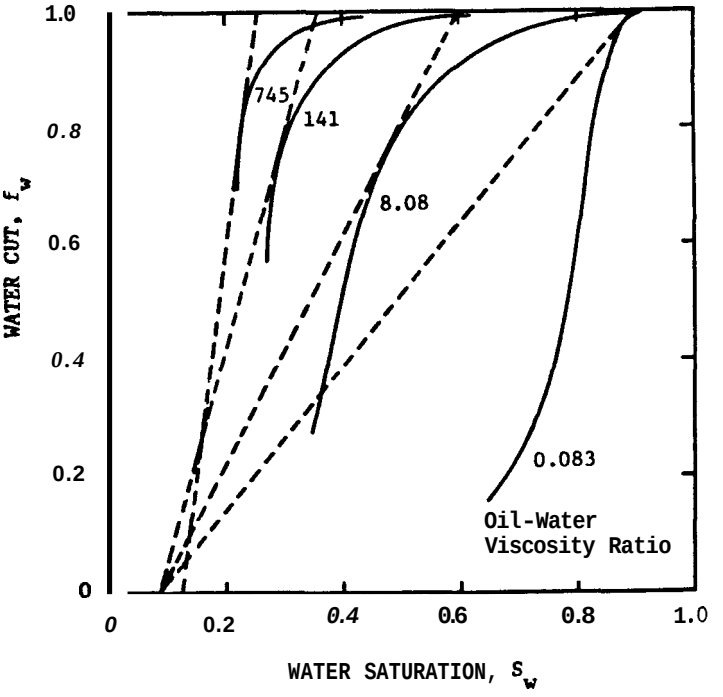

Fig. 3.13: FRACTIONAL FLOW CURVES CONSTRUCTED FROM THE DATA SUPPLIED BY DOUGLAS ET AL. (1959)

Table 3.6

BREAKTHROUGH AREAL SWEEP EFFICIENCIES EXTRACTED FROM HIGGINS AND LEIGHTON MATCH TO DATA REPORTED BY DOUGLAS ET AL. (1959)

Oil-water viscosity ratio	0.083	8.080	141	754
Irreducible water saturation	0.125	0.087	0.087	0.087
Average water saturation behind front	0.895	0.600	0.340	0.245
Breakthrough displacement efficiency	0.770	0.513	0.253	0.158
Pore volume oil produced at breakthrough	0.600	0.380	0.210	0.140
Breakthrough areal sweep efficiency	0.770	0.740	0.830	0.880

Wu (1964) investigated the accuracy of the Higgins and Leighton method both at breakthrough and after breakthrough. He conducted several displacement experiments on a quadrant of a five-spot sand model in which water displaced oil at different viscosity ratios. The same computer program developed by Higgins and Leighton was used to match the experimental recovery data. Fractional flow curves needed for the program were prepared from the pre-determined relative permeability curves on a linear core with the same sand. From the analysis, Wu concluded that: 1) breakthrough areal sweep efficiencies computed by the streamtube method at various mobility ratios were not different from each other, in contrast to his experimental observations that confirmed a strong variation of areal sweep efficiencies with mobility ratio; and 2) post-breakthrough oil recoveries computed from the streamtube program closely approximated the experimental data. No reasons for this were given.

Despite the fact that Higgins and Leighton's method generates nearly identical values for breakthrough areal sweep efficiencies at all mobility ratios, the method appears to adequately describe recovery performance of Buckley-Leverett-type displacements. The main reason for this seems to be that the effect of displacement efficiency on recovery calculations is more important than the effect of areal sweep. On the other hand, in piston-like displacements, such as miscible displacements in which the displacement efficiency is 100 percent, calculation of pattern breakthrough curves based on fixed streamlines will not generate accurate results. Because of this conclusion, the computation of tracer flow in this study was only performed for unit mobility ratio.

3.2 TRACER FLOW IN HOMOGENEOUS SYSTEMS

Besides pattern sweep efficiency (areal effects), mixing due to dispersion influences breakthrough history of a tracer from a pattern. A mathematical description of mixing in a general flow passage is provided in the first part of this section. The second part utilizes this mixing equation to derive

expressions for tracer production curves from various systems. Lastly, a technique is presented which correlates tracer production curves into a single set of curves.

3.2.1 Mixing Theory

When one fluid miscibly displaces another fluid in a porous medium, a transition zone (mixed region) is formed between them at the region of contact. The establishment of the mixed zone is due to a phenomenon known as hydrodynamic dispersion. In general, hydrodynamic dispersion consists of two parts: mechanical dispersion and molecular diffusion. Mechanical dispersion results from the movement of individual fluid particles which travel at variable velocities through tortuous pore channels of the porous medium. This random fluid movement in irregular flow paths spreads the displacing fluid into the displaced fluid, thereby generating a blended region between them. The amount of spreading depends on the dispersive capability of the porous medium. The property of porous medium that is a measure of its capacity to cause mechanical dispersion is called dispersivity. In general, dispersivity is considered to have two components: one in the direction of mean flow (longitudinal dispersion) and one perpendicular to the direction of mean flow (transverse dispersion). For practical purposes, however, transverse dispersion has a small effect on the amount of mixing between fluids compared to longitudinal dispersion, as was illustrated by Blackwell (1962), Harleman and Rumer (1963), and Sauty (1980).

The second component of hydrodynamic dispersion--namely, molecular diffusion--occurs on a macroscopic level as a consequence of net concentration gradients across surfaces perpendicular to the average flow direction. It is caused by the random movement of the differing molecules. This molecular diffusion contributes to the growth of the mixed region as well. However, it has been verified that the effect of molecular diffusion on mixing is negligible unless the displacement takes place at low velocities (Raimondi et al., 1959; Handy, 1959; Brigham et al., 1961; and Blackwell, 1962). Therefore, in most practical miscible fluid flow through porous media, longitudinal mechanical dispersion is the major factor in creating a mixed zone between the fluids.

The concentration of each fluid in the mixed zone can be computed as a function of position if the flow geometry and the dispersivity of porous medium are known. For stable miscible displacements (in the absence of viscous fingering), equations in closed form are available which describe concentration of the fluids. These equations have been derived for non-adsorbing, non-decaying and non-reactive miscible fluids. Aronofsky and Heller (1957) and Ogata and Banks (1961) present exact solutions for linear displacements (Eq. 2-2), while Ogata (1958) gives an exact equation for a diverging radial flow. Ogata's solution involves a very difficult integral. However, these exact solutions can be reduced to more simple forms, provided that the physical dimensions of the flow systems are larger than the dispersion constant of a porous medium, and that the molecular diffusion effects are negligible. The dimensionless group which characterizes this condition is known as the Peclet number. It is defined as the ratio of the displacement front position to the dispersion constant of the porous medium. For a linear

uniform displacement with a Peclet number of $\bar{x}/\alpha > 100$ (Sauty, 1980), the resulting equation is:

$$\frac{C}{C_o} = \frac{1}{2}\,\mathrm{erfc}\left(\frac{x - \bar{x}}{\sqrt{4\alpha\bar{x}}}\right) \tag{3-7}$$

where:

C = concentration at location x

C_o = initial concentration of displacing fluid

$\bar{x}$ = front location corresponding to $C = 0.5\ C_o$

a = longitudinal dispersion constant, length unit, same as x

erfc = complementary error function = 1 - erf

The corresponding approximate equation for radial flow is given by Lau ~~et al.~~ (1959) and Raimondi ~~et al.~~ (1959). The solution is accurate when the Peclet number is greater than 100 ($\bar{r}/a > 100$), as was shown by Gelhar and Collins (1971) and Sauty (1980):

$$\frac{C}{C_o} = \frac{1}{2}\,\mathrm{erfc}\left(\frac{r - \bar{r}}{\sqrt{\frac{4}{3}\alpha\bar{r}}}\right) \tag{3-8}$$

For most field applications, the condition of Peclet number greater than 100 is usually achieved because of the distances involved. Therefore, the following equation can be viewed as a general defining equation to describe mixing in different flow geometries with practical accuracy (Brigham, 1973):

$$\frac{C}{C_o} = \frac{1}{2}\,\mathrm{erfc}\left(\frac{s - \bar{s}}{\sqrt{2\sigma^2}}\right) \tag{3-9}$$

where:

s = location corresponding to concentration C

$\bar{s}$ = location of the front corresponding to $C = 0.5C_o$

σ = measure of the length of the mixed zone computed at $\bar{s}$. This corresponds to the standard deviation term in statistics. For linear flow, $\sigma^2 = 2\alpha\bar{x}$ and for radial flow, $\sigma^2 = 2\alpha\bar{r}/3$, as are deduced by comparing Eqs. 3-7 and 3-8 with Eq. 3-9, respectively.

If σ is known for a system, Eq. 3-9 can be used to compute the concentration of the displacing fluid at various points in the system. Hence, it is only necessary to derive an expression for σ in a general flow geometry. This can be accomplished by noting that in an arbitrary flow passage, such as Fig. 3.14, the growth of the length of the mixed zone is affected by two factors as the fluid moves from point A to point B:

1) The movement of fluid through porous media (the longer the distance travelled, the longer the mixed zone); and

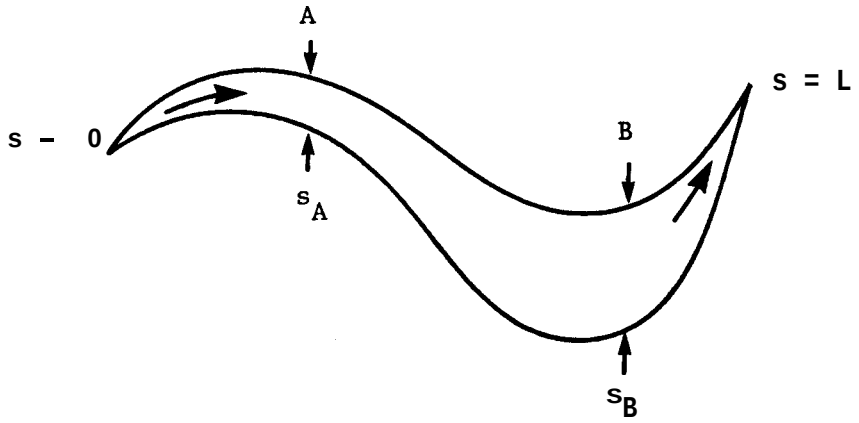

Fig. 3.14: A GENERAL FLOW PASSAGE

2) The change of geometry of the flow path (the wider the passage, the narrower the mixed zone).

Therefore, the total change in a is (Lau et al., 1959; Baldwin, 1966; and Brigham, 1973):

$$da = d\sigma_s + d\sigma_g \tag{3-10}$$

where, $d\sigma_s$ is the change due to movement along path s and da_g is the change due to the geometry of the passage. Equation 3-10 is similar to the superposition principle in which independently computed effects are added to each other to produce a combined effect.

In computing either of the changes in a, the other must be treated as a constant. In this manner, $d\sigma_s$ is computed from the mixing equation for a linear system for which $\sigma^2 = 2\alpha s$. Differentiating this expression:

$$d\sigma_s = \frac{a\, ds}{\sigma} \tag{3-11}$$

The geometry effects are obtained by noting that the volume of the mixed zone at any location must remain constant, regardless of the shape of the system at that position. Since the, mixed zone is usually small compared to the flow path, then σw = constant, where w is the width of the flow channel at that position. Differentiating this relationship:

$$w\, da_g + \sigma\, dw = 0 \tag{3-12}$$

then:

$$d\sigma_g = -\sigma \frac{dw}{w} \tag{3-13}$$

Since the width of the passage is inversely proportional to the velocity of fluid at that point, Eq. 3–13 in terms of velocity becomes:

$$d\sigma_g = \frac{\sigma\, dv}{v} \tag{3-14}$$

Substituting Eqs. 3–11 and 3–14 in Eq. 3–10, one gets:

$$d\sigma = \frac{a\, ds}{\sigma} + \frac{\sigma\, dv}{v} \tag{3-15}$$

Multiply both sides by $2\sigma/v^2$ and rearrange:

$$\frac{2\sigma\, d\sigma}{v^2} - \frac{2\sigma^2\, dv}{v^3} = \frac{2a\, ds}{v^2} \tag{3-16}$$

Or:

$$d\left(\frac{\sigma^2}{v^2}\right) = 2\alpha\, \frac{ds}{v} \tag{3-17}$$

Integrating between point A and point B:

$$\frac{\sigma_B^2}{v_B^2} - \frac{\sigma_A^2}{v_A^2} = 2\alpha \int_{s_A}^{s_B} \frac{ds}{v^2(s)} \tag{3-18}$$

If there is no mixing at the entry initially, then $\sigma_A = 0$ at $s = 0$ and:

$$\sigma^2 = 2\alpha\, v^2(\bar{s}) \int_0^{\bar{s}} \frac{ds}{v^2(s)} \tag{3-19}$$

This is the general equation for σ which is applicable for flow passages of any geometry. For example, in radial flow in which $ds = dr$, $v(s) = q/2\pi r$, and $v(\bar{s}) = q/2\pi\bar{r}$, it follows that $\sigma^2 = 2\alpha\bar{r}/3$. For spherical flow, $ds = dr$, $v(s) = q/4\pi r^2$, $v(\bar{s}) = q/4\pi\bar{r}^2$, the expression for σ^2 becomes $\sigma^2 = 2\alpha\bar{r}/5$. This is the same relationship as Gelhar and Collins (1971) reported, if $\bar{r} + \bar{r} = 2\bar{r}$ is used in their equation.

3.2.2 Tracer Production Curves

In this section, equations are derived which predict tracer breakthrough curves from several homogeneous flooding patterns for a slug of tracer injected into the patterns. In the development of the equations, the following assumptions are made:

1) Originally, there is only one mobile fluid in the system.

2) Tracer material is miscible with the fluids both ahead and behind.

3) Tracer slug has the same mobility as the displaced and the displacing fluids (unit mobility ratio displacements).

4) Tracer does not adsorb on the formation rock nor does it react with either the formation fluid or the formation matrix.

5) Dispersion of tracer can be described by the general approximate mixing equation (Eqs. 3-9 and 3-19).

6) Tracer slug size is small compared to the volume of the pattern.

7) A steady-state flow condition is established prior to and during tracer injection.

The flow of different fluids with the same mobility is essentially equivalent to a single-phase flow. Because in single-phase steady-state flow only one pressure field is imposed on the entire system, the streamlines and the isopotential lines for the system are unaffected by the location of the displacement fronts. Such flow systems can be divided into several unvarying streamtubes and fluid flow in each can be studied. As an example, consider a repeated flooding pattern such as a staggered line drive (as shown in Fig. 3.15). Assume that a slug of tracer with an initial concentration C_o is

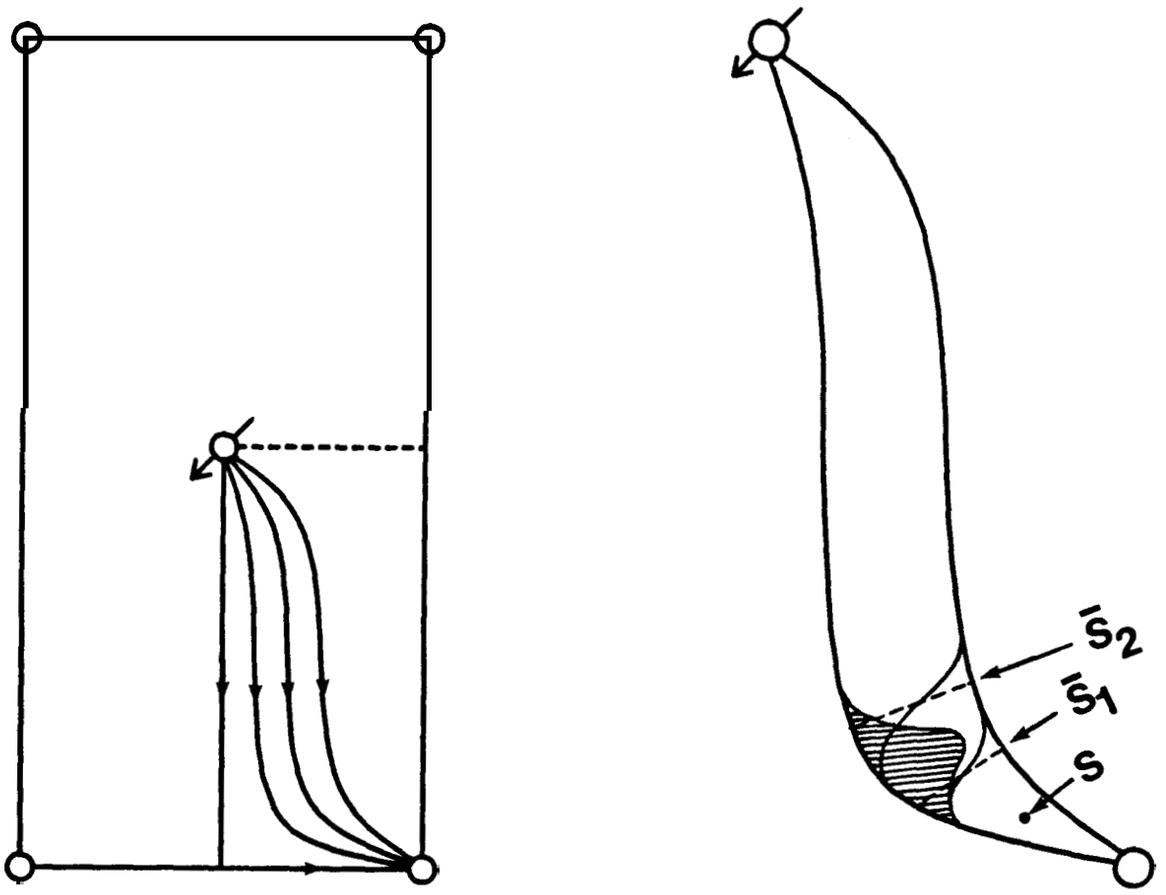

Fig. 3.15: A STAGGERED LINE DRIVE PATTERN WITH TRACER CONCENTRATION PROFILE IN A STREAMTUBE

injected into the pattern, followed by a chase fluid to displace it through the formation. The tracer slug will be distributed among the streamtubes that comprise the pattern volume. In any streamtube, mixing will occur at both the leading edge and the trailing edge of the slug, hence diluting the tracer slug as it moves down the tube. The amount of mixing occurring at each edge can be computed by assuming that the tracer slug behaves as though it was continuous at that edge. Mathematically, the mixings at the edges are given by Eq. 3-9 with σ defined by Eq. 3-19. At any point in the streamtube, the sum of three concentrations--tracer concentration, chase fluid concentration, and formation fluid concentration--is equal to the initial tracer concentration, C_o. Thus:

$$C = C_o - C_b - C_a \tag{3-20}$$

where:

C = concentration of tracer

C_a = concentration of fluid ahead of the slug (formation fluid)

C_b = concentration of fluid behind the slug (chase fluid)

From mixing equations, the concentration of fluid ahead of the slug is defined as:

$$\frac{C_a}{C_o} = 1 - \frac{1}{2}\,\mathrm{erfc}\left(\frac{s - \bar{s}_1}{\sqrt{2\,\sigma_1^2}}\right) \tag{3-21}$$

and behind the slug:

$$\frac{C_b}{C_o} = \frac{1}{2}\,\mathrm{erfc}\left(\frac{s - \bar{s}_2}{\sqrt{2\,\sigma_2^2}}\right) \tag{3-22}$$

Combining Eqs. 3-20, 3-21 and 3-22, the concentration profile of the tracer slug is expressed by:

$$\frac{C}{C_o} = \frac{1}{2}\,\mathrm{erfc}\left(\frac{s - \bar{s}_1}{\sqrt{2\,\sigma_1^2}}\right) - \frac{1}{2}\,\mathrm{erfc}\left(\frac{s - \bar{s}_2}{\sqrt{2\,\sigma_2^2}}\right) \tag{3-23}$$

where:

s = location corresponding to concentration C

$\bar{s}_1$ = location of the front at the leading edge

$\bar{s}_2$ = location of the front at the trailing edge

σ_1 = standard deviation computed at the leading edge

σ_2 = standard deviation computed at the trailing edge

Since adsorption and reaction (or decay) of the tracer material are assumed negligible, the volume of tracer slug within the streamtube remains constant at any time during the injection process. However, the undiluted width of tracer is a function of position; hence, the width is a function of the width of the streamtube at that location. The undiluted width of tracer is defined as:

$$\Delta s = \bar{s}_1 - \bar{s}_2 \tag{3-24}$$

If the tracer slug is small compared to the size of the streamtube (which is usually the case), then Eq. 3-23 may be written as:

$$\frac{C}{C_o} = \lim_{\Delta s \to 0} \left[F\left(s - \frac{\Delta s}{2}\right) - F\left(s + \frac{\Delta s}{2}\right) \right] = -\Delta s \frac{dF}{ds} \tag{3-25}$$

where,

$$F(s) = \frac{1}{2} \operatorname{erfc}\left(\frac{s - \bar{s}}{\sqrt{2\sigma^2}} \right) \tag{3-26}$$

Therefore,

$$\frac{C}{C_o} = \frac{\Delta s}{\sqrt{2\pi\sigma^2}} \exp\left[-\frac{(s - \bar{s})^2}{2\sigma^2} \right] \tag{3-27}$$

Equation 3-27 implies that maximum tracer concentration in a streamtube occurs at point $\bar{s}$. For small slug size, $\bar{s}$ can be viewed as the front location in an immiscible displacement of the original formation fluid by the chase fluid alone. The σ is computed at $\bar{s}$ and it is given by Eq. 3-19.

The computation of tracer concentrations from Eq. 3-27 requires calculations involving distances along the streamtubes. However, it is more convenient to replace the distance terms with their equivalent volumetric terms in Eq. 3-27. This conversion process is accomplished by approximating the actual location of the tracer slug in the streamtube by a rectangle as shown in Fig. 3.16. The approximation is justified since the slug size is small.

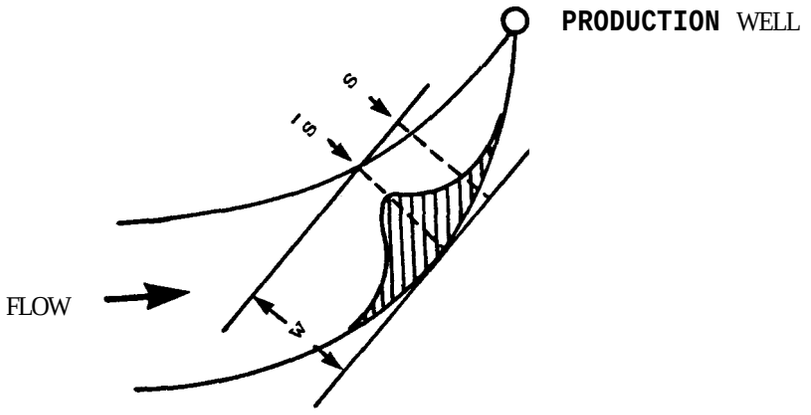

Fig. 3.16: APPROXIMATE LOCATION OF A TRACER SLUG IN A STREAMTUBE

From Fig. 3.16, the equation relating the distance terms to volumes is:

$$(s - \bar{s})wh\,\phi S_w = V - \bar{V} \tag{3-28}$$

where,

w = width of the streamtube at volumetric location $\bar{s}$

h = thickness of the streamtube

ϕ = porosity

S_w = displaced fluid saturation in the system

V = displaceable pore volume of streamtube up to location s

$\bar{V}$ = displaceable pore volume of streamtube up to location $\bar{s}$

The width of the streamtube at $\bar{s}$ is related to the velocity of fluid at that point by:

$$w = \frac{q}{v\phi h S_w} \tag{3-29}$$

where,

v = microscopic velocity, darcy velocity divided by porosity

q = injection rate into the streamtube

Substituting Eq. 3-29 into Eq. 3-28:

$$s - \bar{s} = \frac{V}{4}(V - \bar{V}) \tag{3-30}$$

Similarly, the undiluted width of tracer, Δs, is related to the volume of the tracer slug injected into the streamtube, V_{tr}. This is:

$$\Delta s = \frac{v}{q} V_{tr} \tag{3-31}$$

Substitution of Eqs. 3-19, 3-30 and 3-31 into Eq. 3-27 and further simplification results in:

$$\frac{C}{C_o} = \frac{V_{tr}}{2q\sqrt{\pi\alpha I}} \exp\left[-\frac{(V - \bar{V})^2}{4\alpha q^2 I}\right] \tag{3-32}$$

where,

$$I = \int_0^{\bar{s}} \frac{ds}{v^2(s)} \tag{3-33}$$

Equation 3–32 defines the tracer concentration at any location within the streamtube in terms of volumes. At the production well, the concentration of tracer is computed by substituting the total displaceable pore volume of the streamtube for V. For this case, at any time, t:

$$V - \bar{V} = q(t_{bt} - t) \qquad (3-34)$$

where t_{bt} is the breakthrough time of the injected fluid in the streamtube. The times, t_{bt} and t, may be obtained from material balance considerations as follows:

$$t = \frac{V_p}{q_t} \qquad (3-35)$$

$$t_{bt} = \frac{V_{pbt}}{q_t} \qquad (3-36)$$

where,

V_p = total volume of chase fluid injected into the pattern at time t

V_{pbt} = volume of chase fluid necessary to inject into the pattern in order to get breakthrough from the streamtube under study

q_t = total injection rate into the pattern

Therefore,

$$V - \bar{V} = \frac{q}{q_t}(V_{pbt} - V_p) \qquad (3-37)$$

In terms of pattern displaceable pore volumes, Eq. 3–37 reduces to:

$$V - \bar{V} = \frac{A\phi h S_w q}{q_t}(V_{pDbt} - V_{pD}) \qquad (3-38)$$

where,

V_{pDbt} = displaceable pore volumes injected into the pattern at breakthrough of the streamtube under study = $V_{pbt}/A\phi h S_w$

V_{pD} = displaceable pore volumes injected into the pattern = $V_p/A\phi h S_w$

A = area of the pattern

Similarly, the amount of tracer injected into a streamtube is proportional to flow rate in the tube. This means that:

$$V_{tr} = \frac{q}{q_t} V_{Tr} \qquad (3\text{-}39)$$

where V_{Tr} is the total volume of tracer injected into the pattern. Tracer volume in a streamtube can also be expressed in terms of displaceable pore volume of the pattern:

$$V_{tr} = \frac{q}{q_t} A\phi h S_w F_r \qquad (3\text{-}40)$$

where,

$$F_r = \frac{V_{Tr}}{A\phi h S_w} \qquad (3\text{-}41)$$

F_r is the tracer slug volume injected into the pattern expressed as a fraction of the displaceable pore volume of the pattern.

Since the flow around wellbores is essentially radial, the potentials in the immediate vicinity of a wellbore can be expressed by $4 = c_1 \ln(r) + c_2$ where c_1 and c_2 are constants. In general, the values of these constants can be determined from the flow rate and the potential value at a wellbore. Because absolute values of potentials and flow rates do not affect the nature of tracer flow, for mathematical convenience, the constants c_1 and c_2 are chosen to be equal to one and zero, respectively. Therefore, $4 = \ln(r)$ and consequently, the streamlines are defined in accordance with this latter potential equation as shown in Appendix A. From Darcy's Law:

$$q_t = \frac{k}{\mu} \; 2\pi r h \left(\frac{\partial \Phi}{\partial r}\right)_{r = r_w} = 2\pi h \frac{k}{\mu} \qquad (3\text{-}42)$$

Using this expression for q_t in Eqs. *3-40* and *3-39* and substituting the subsequent expressions into Eq. *3-32,* the following result is obtained:

$$\frac{C(\psi)}{C_o} = \frac{\mu\phi S_w A F_r}{4\pi k\sqrt{\pi\alpha I(\psi)}} \exp\left[-\frac{\mu^2\phi^2 S_w^2 A^2 \left(V_{pDbt}(\psi) - V_{pD}\right)^2}{16\pi^2 k^2 \alpha I(\psi)}\right] \qquad (3\text{-}43)$$

This is a general equation which describes tracer concentration in any particular streamtube, (ψ), at a production well for any repeated pattern. Equations for specific patterns can be deduced from this equation if expressions for the I integral (Eq. *3-33)* for these patterns are available. Derivation of expressions for the I integral for the developed staggered line drive, five-spot and direct line drive patterns has been provided in Appendices C.1, C.2 and *C.3,* respectively. With the aid of these appendices, the following equations which define tracer concentration in a general streamtube, ($), of these specific patterns are obtained.

Staggered Line Drive: Staggered line drive systems differ from each other by their d/a ratios, where d is the distance between unlike wells (injector-producer), and a is the distance between like wells (two injectors or two producers). From Appendix C.1 and Fig. C-1, the following relationships are obtained:

$$A = 2\ da \tag{3-44}$$

$$\frac{K'(m)}{2K(m)} \quad \frac{d}{a} - \tag{3-45}$$

and,

$$I(\psi) = \left(\frac{\mu\phi S_w}{k}\right)^2 \frac{ad^2}{4\ K(m)\ K'^2(m)}\ Y(\psi) \tag{3-46}$$

Substitute Eqs. 3-44, 3-45, 3-46 in Eq. 3-43, and rearrange:

$$\frac{C(\psi)}{C_o} = \frac{\sqrt{K(m)}\ K'(m)\sqrt{\frac{a}{\alpha}}\ F_r}{\pi\sqrt{\pi Y(\psi)}} \cdot \exp\left[-\frac{K(m)\ K'^2(m)\ \frac{a}{\alpha}\left(V_{pDbt}(\psi)\right) - V_{pD}\right)^2}{\pi^2 Y(\psi)}\right] \tag{3-37}$$

The term $V_{pDbt}(\psi)$ defines the pattern breakthrough curve and is given by Eq. A-35 in Appendix A.1 with η term in that equation related to the streamline ψ. The term $Y(\psi)$ is obtained from Eq. C-21 in Appendix C.1.

Five-Spot: The five-spot is a special case of a staggered line drive pattern when d/a = 1/2. For the five-spot:

$$K(m) = K'(m) = 1.8540747$$

Equation 3-47 simplifies to:

$$\frac{C(\psi)}{C_o} = \frac{0.453384}{\sqrt{Y(\psi)}}\sqrt{\frac{a}{\alpha}}\ F_r \cdot \exp\left|-\frac{0.645776}{Y(\psi)}\ \frac{a}{\alpha}\left(V_{pDbt}(\psi) - V_{pD}\right)^2\right| \tag{3-48}$$

For this pattern, $V_{pDbt}(\psi)$ and $Y(\psi)$ are given by Eqs. A-49 and C-23, respectively.

Direct Line Drive: Direct line drive systems are also characterized by their d/a ratios. From Appendix C.3:

$$A = 2\ da \tag{3-44}$$

$$\frac{K'(m)}{2K(m)} = \frac{d}{a} \tag{3-45}$$

and,

$$I(\psi) = \left(\frac{\mu\phi S_w}{k}\right)^2 \frac{ad^2}{4\ K(m)\ K'^2(m)}\ Y(\psi) \tag{3-46}$$

Therefore:

$$\frac{C(\psi)}{C_o} = \frac{\sqrt{K(m)}\ K'(m)\sqrt{\frac{a}{\alpha}}\ F_r}{\pi\ \sqrt{\pi Y(\psi)}} \cdot \exp\left[-\frac{K(m)\ K'^2(m)\ \frac{a}{\alpha}\left(V_{pDbt}(\psi) - V_{pD}\right)^2}{\pi^2 Y(\psi)}\right] \tag{3-47}$$

The $V_{pDbt}(\psi)$ term is given by Eq. *A-73* and $Y(\psi)$ is given by Eq. C–58.

Note that for these patterns, exactly the same form of equation describes tracer concentrations in a streamtube at the production well. Only the $Y(\psi)$ term which is related to tracer dispersion, and V_{pDbt}, which represents the convection of tracer, are different. Therefore, it is speculated that other patterns will also have the same form as Eq. *3-47* but with different expressions for the Y and V_{pDbt} terms.

For any pore volume of displacing fluid, V_{pD}, injected into a pattern, there is tracer flow from all the streamtubes to the production well. Therefore, the output tracer concentration from the production well of a homogeneous pattern is the sum of concentrations from the streamtubes. At the limit, the summation reduces to an integral and the streamtubes become streamlines. The following presents evaluation of tracer production curves from the patterns considered in this study.

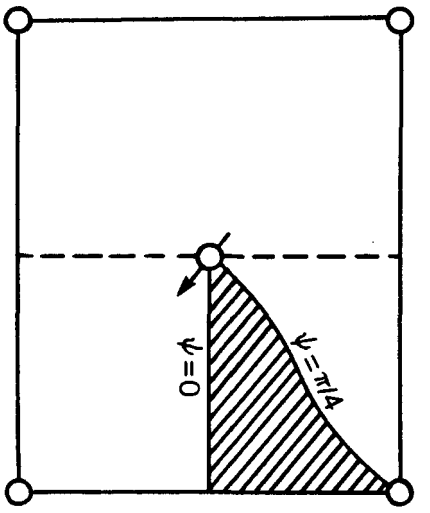

Fig. 3.17: ELEMENT CONSIDERED IN COMPUTING TRACER PRODUCTION CURVES FOR THE STAGGERED LINE DRIVE PATTERN

Staggered Line Drive: Due to symmetry, only 1/8 of a staggered line drive pattern is considered, as shown in Fig. *3.17*.

Effluent tracer concentration, $\bar{C}$, from this system is then given by:

$$\frac{\bar{C}}{C_o} = \frac{\int_0^{\pi/4} q\ \frac{C(\psi)}{C_o}\ d\psi}{\frac{q_t}{8}} \tag{3-49}$$

Because of unit mobility ratio displacement, flow rates in the streamtubes are constant and equal *to* each other. At the limit, when the streamtubes approach the streamlines:

$$q_t = 2\,\pi q \tag{3-50}$$

Substitution for $C(\psi)/C_o$ from Eq. *3-47* and q_t from Eq. *3-50* and simplification yields:

$$\bar{C}_D = \frac{4\sqrt{K(m)}\;K'(m)}{\pi^2\sqrt{\pi}} \int_0^{\pi/4} \frac{\exp\left[-\frac{K(m)\;K'^2(m)}{\pi^2\;Y(\psi)}\,\frac{a}{\alpha}\left(V_{pDbt}(\psi) - V_{pD}\right)^2\right]}{\sqrt{Y(\psi)}}\,d\psi \tag{3-51}$$

where $\bar{C}_D$ is a dimensionless quantity defined as:

$$\bar{C}_D = \frac{\bar{C}}{C_o F_r \sqrt{\frac{a}{\alpha}}} \tag{3-52}$$

Five-Spot: For this pattern, Eq. *3-51* with $K(m) = K'(m) = 1.854074$ reduces to:

$$\bar{C}_D = 0.577266 \int_0^{\pi/4} \frac{\exp\left[\frac{0.645776}{Y(\psi)}\,\frac{a}{\alpha}\left(V_{pDbt}(\psi) - V_{pD}\right)^2\right]}{\sqrt{Y(\psi)}}\,d\psi \tag{3-53}$$

The term $\bar{C}_D$ is defined by Eq. *3-52.*

Direct Line Drive: For a direct line drive, *1/4* of the pattern must be considered, as shown in Fig. *3.18.*

For this system, the effluent concentration integral is:

$$\frac{\bar{C}}{C_o} = \frac{\int_0^{\pi/2} q\,\frac{C(\psi)}{C_o}\,d\psi}{\frac{q_t}{4}} \tag{3-54}$$

where $C(\psi)/C_o$ is given by Eq. *3-47* and q_t by Eq. *3-50.* Therefore:

$$\bar{C}_D = \frac{2\sqrt{K(m)}\;K'(m)}{\pi^2\sqrt{\pi}} \int_0^{\pi/2} \frac{\exp\left[-\frac{K(m)\;K'2(m)}{\pi^2 Y(\psi)}\,\frac{a}{\alpha}\left(V_{pDbt}(\psi) - V_{pD}\right)^2\right]}{\sqrt{Y(\psi)}}\,d\psi \tag{3-55}$$

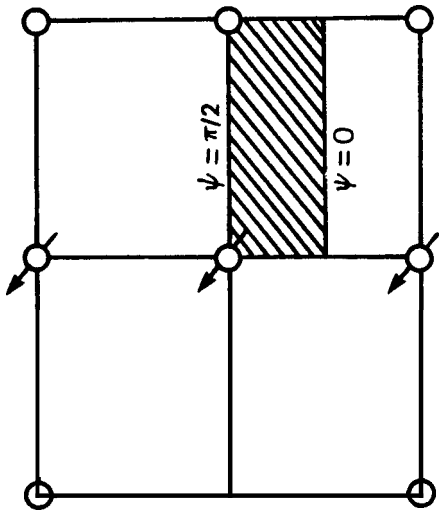

is due to the larger amount of mixing that occurs for small values of Peclet numbers. Another characteristic of these curves is that they all exhibit tracer production at values less than 0.85. This number is

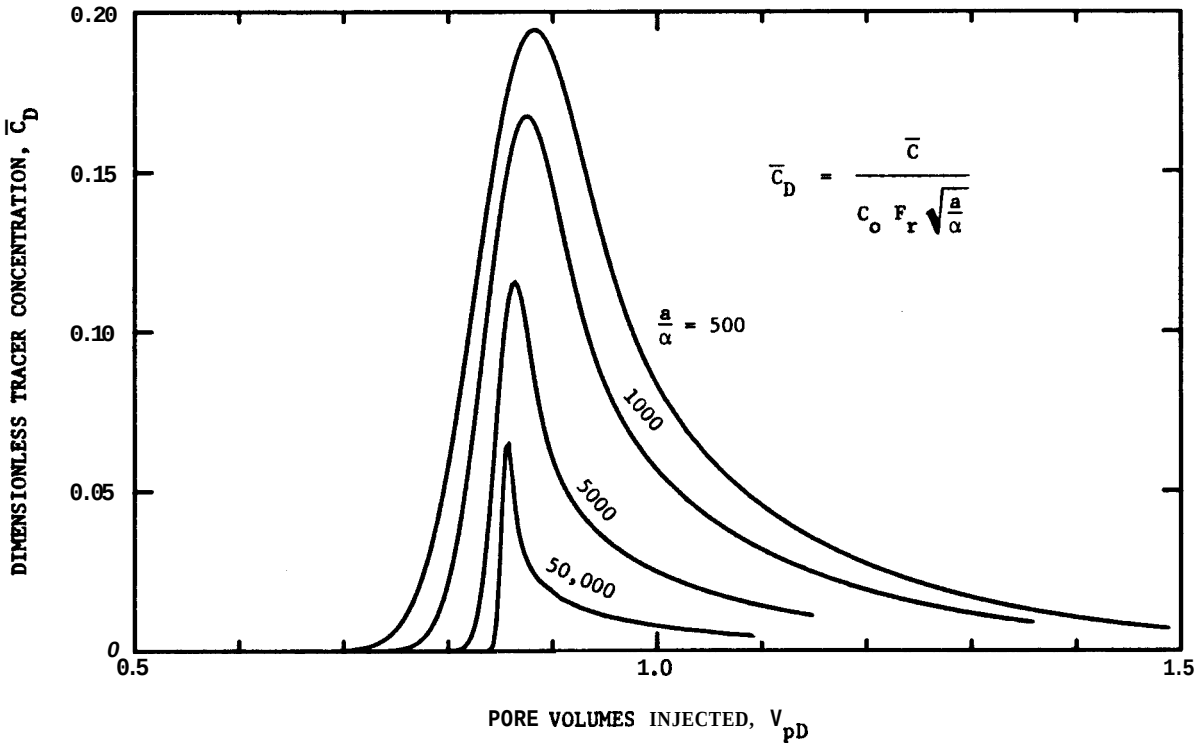

Fig. 3.19: DIMENSIONLESS TRACER CONCENTRATIONS VS PORE VOLUMES INJECTED, DEVELOPED STAGGERED LINE DRIVE, d/a = 1.5

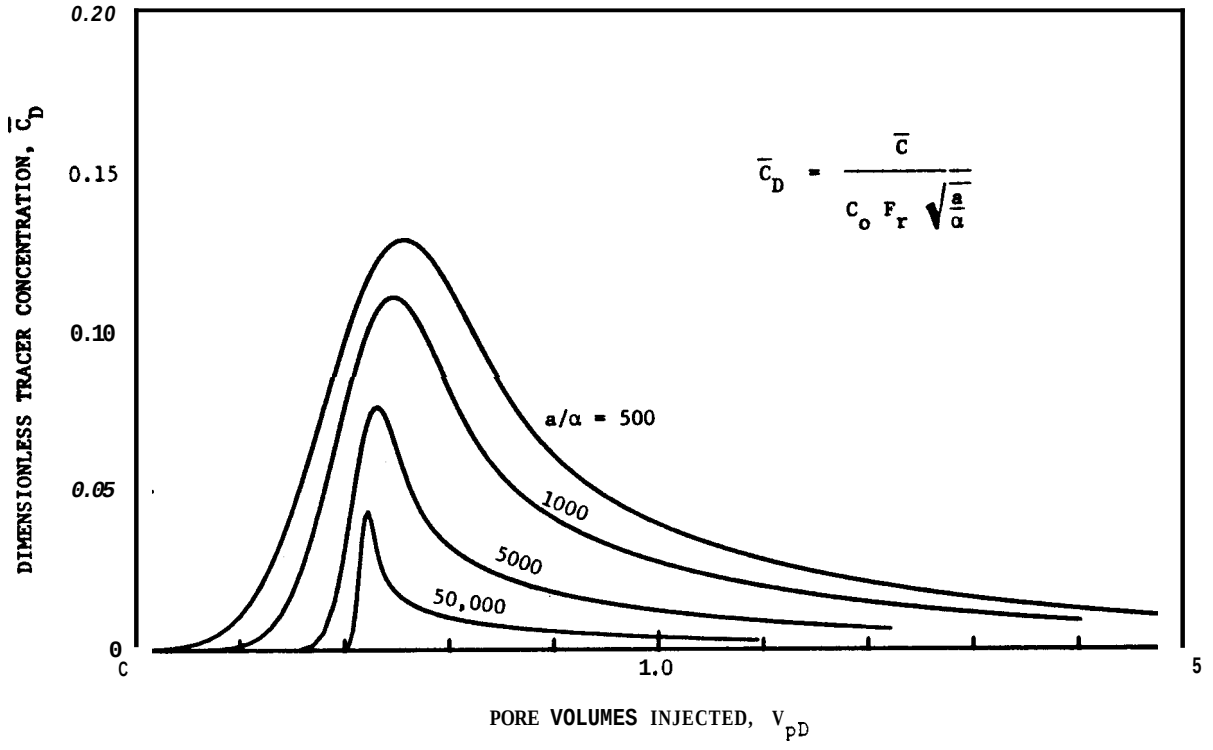

Fig. 3.20: DIMENSIONLESS TRACER CONCENTRATIONS VS PORE VOLUMES INJECTED, DEVELOPED FIVE-SPOT

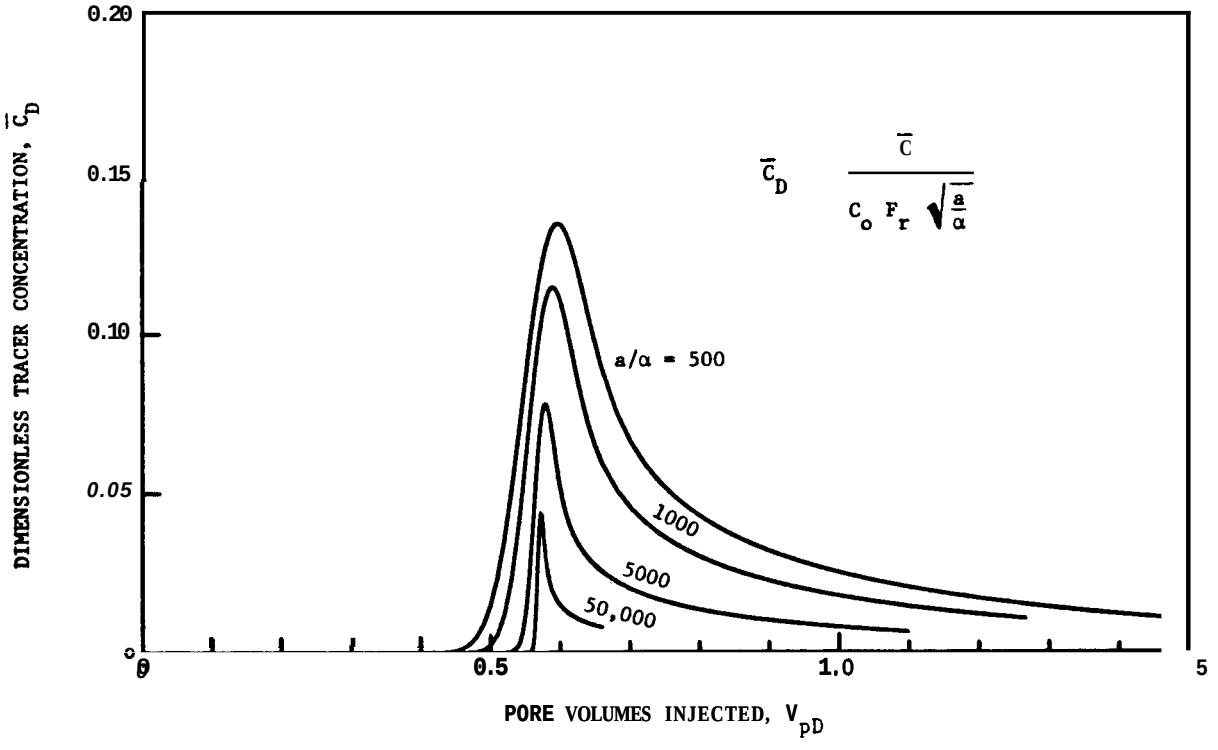

Fig. 3.21: DIMENSIONLESS TRACER CONCENTRATIONS VS PORE VOLUMES INJECTED, DIRECT LINE DRIVE, d/a = 1

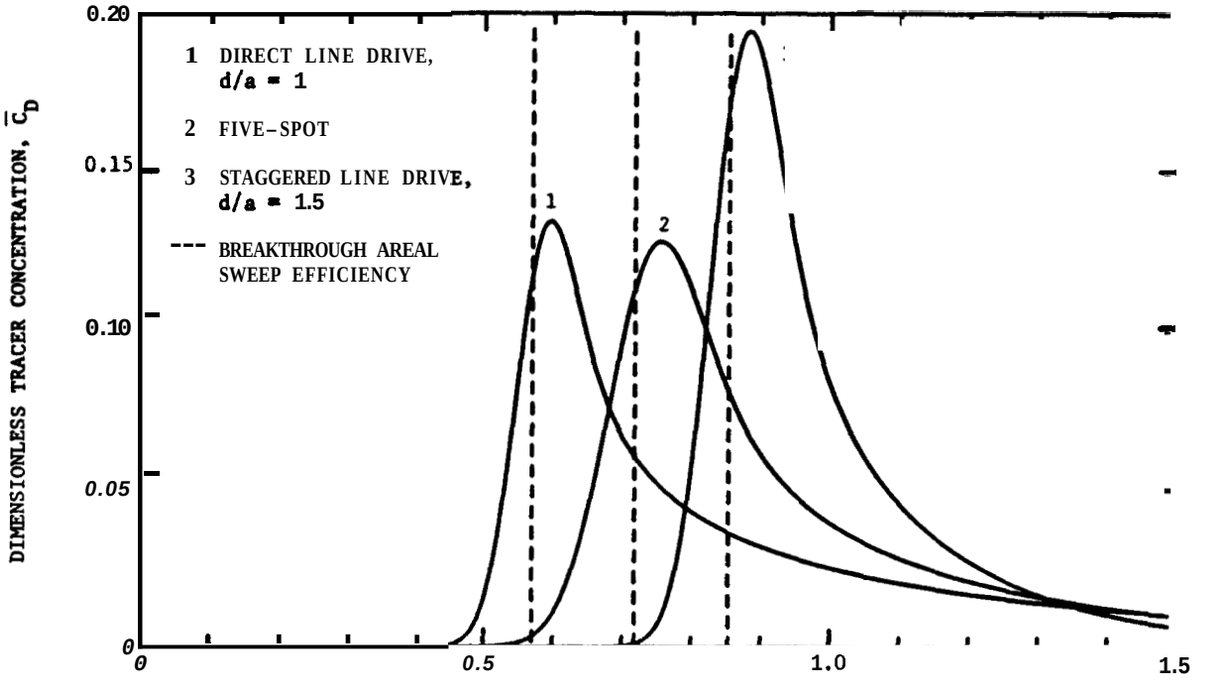

Fig. 3.22: TRACER PRODUCTION CURVES FOR DIFFERENT DEVELOPED AND HOMOGENEOUS PATTERNS, a/α = 500

the same general characteristics. A comparison of tracer production curves from these three patterns for a/a = 500 is illustrated in Fig. 3.22. Again, tracer production occurs before the theoretical breakthrough areal sweep efficiency of the patterns; the curves spread as the result of dispersion.

3.2.3 Correlation of Tracer Production Curves

In the previous section, it was shown that the tracer production curve from a pattern was a function of Peclet number, a/α. Therefore, for each pattern, a set of tracer response curves was obtained with a/α as a parameter. In this section, the sets of tracer profiles from various patterns are correlated into a single set of curves (a/α being the parameter) which represents the tracer production curves from repeated homogeneous patterns.

The following approach was taken to accomplish the correlation. The peak data (maximum tracer concentrations and corresponding pore volumes) of tracer production curves for different systems were plotted versus a/α. Figure 3.23 is the graph of dimensionless maximum concentration, and Fig. 3.24 is the graph of peak dimensionless volume location where the maximum tracer concentration occurs. The ordinate of the latter figure is the same dimensionless volume parameter that was used to correlate the pattern breakthrough curves in Section 3.1.3. In both of the figures, the data for every system yield a straight line on log-log paper. A vertical shift of lines in Fig. 3.23 and a horizontal shift of lines in Fig. 3.24 correlated the respective sets of lines into a single line for each figure. The five-spot system was chosen as a reference for correlation in both of the figures. The amount of shift of

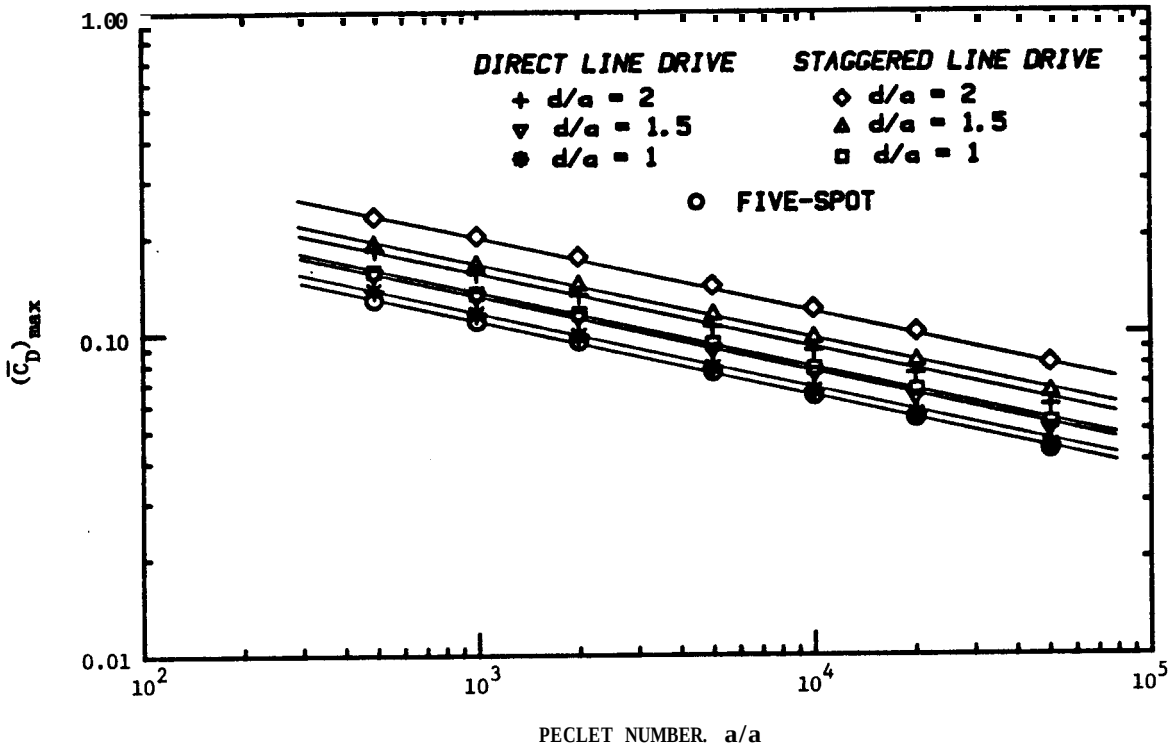

Fig. 3.23: PLOT OF DIMENSIONLESS MAXIMUM TRACER CONCENTRATIONS VS PECLET NUMBER FOR HOMOGENEOUS DEVELOPED PATTERNS

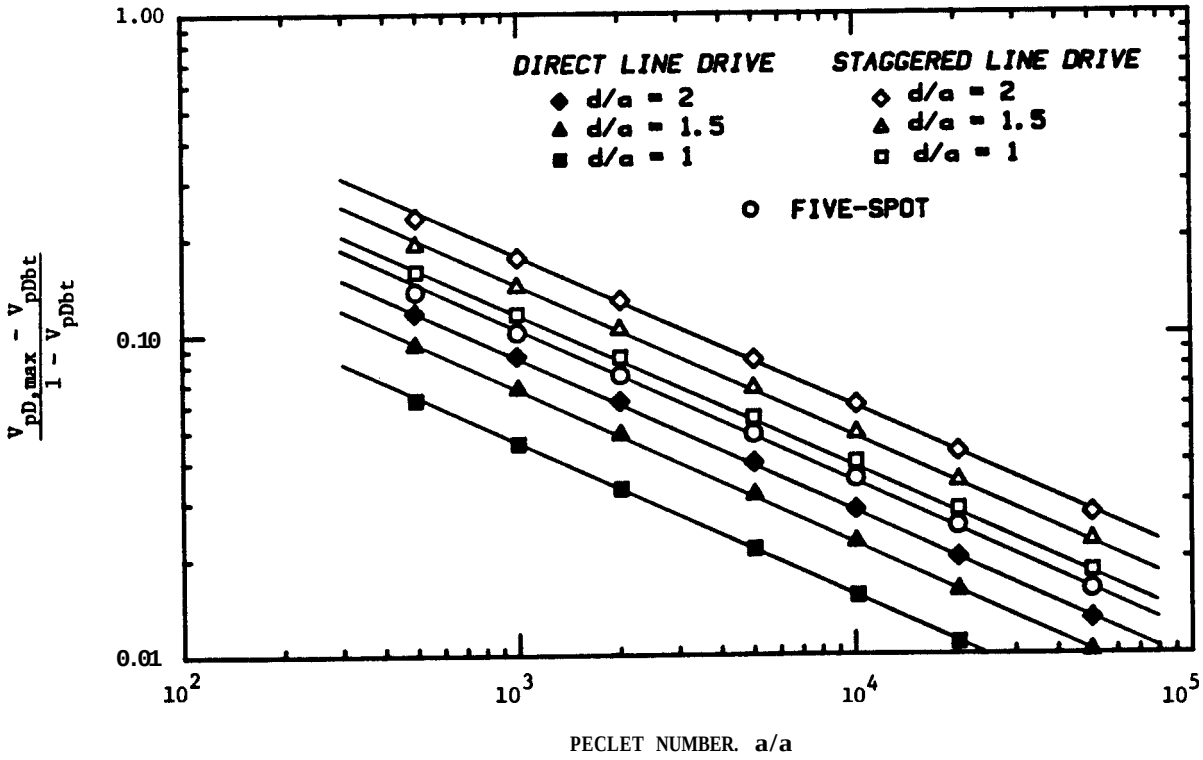

Fig. 3.24: PLOT OF DIMENSIONLESS PEAK PORE VOLUME LOCATION VS PECLET NUMBER FOR HOMOGENEOUS DEVELOPED PATTERNS

these lines with respect to the five-spot lines produced two sets of correction factors: one for maximum tracer concentration, and the other one for a/a to calculate the peak, location. The correction factors, which are in the form of multipliers, are shown in Figs. 3.25 and 3.26. The tabulated values of these correction factors are provided in Table 3.7. If the correction factors from these two figures are applied to the peak data of a tracer breakthrough curve from a five-spot system, they produce the peak data for the pattern

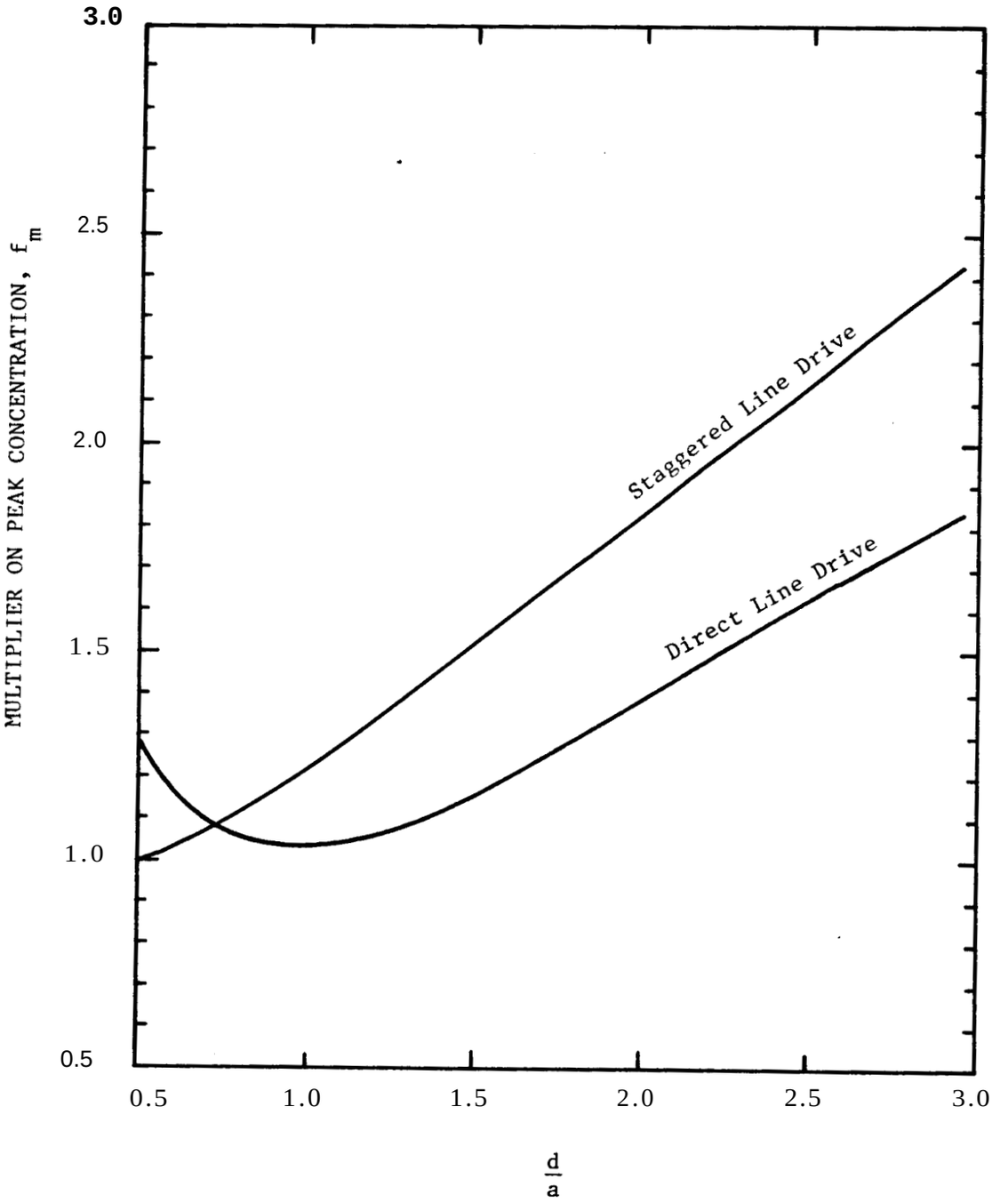

Fig. 3.25: CORRECTION FACTORS ON PEAK CONCENTRATIONS

corresponding to the selected correction factors. The following relationships may be used for the conversion:

$$\left(\bar{C}_{D,max}\right)_{pattern} = f_m \left(\bar{C}_{D,max}\right)_{5\text{-}spot} \tag{3-56}$$

where, f_m is the correction factor on the peak concentration (Fig. 3.25).

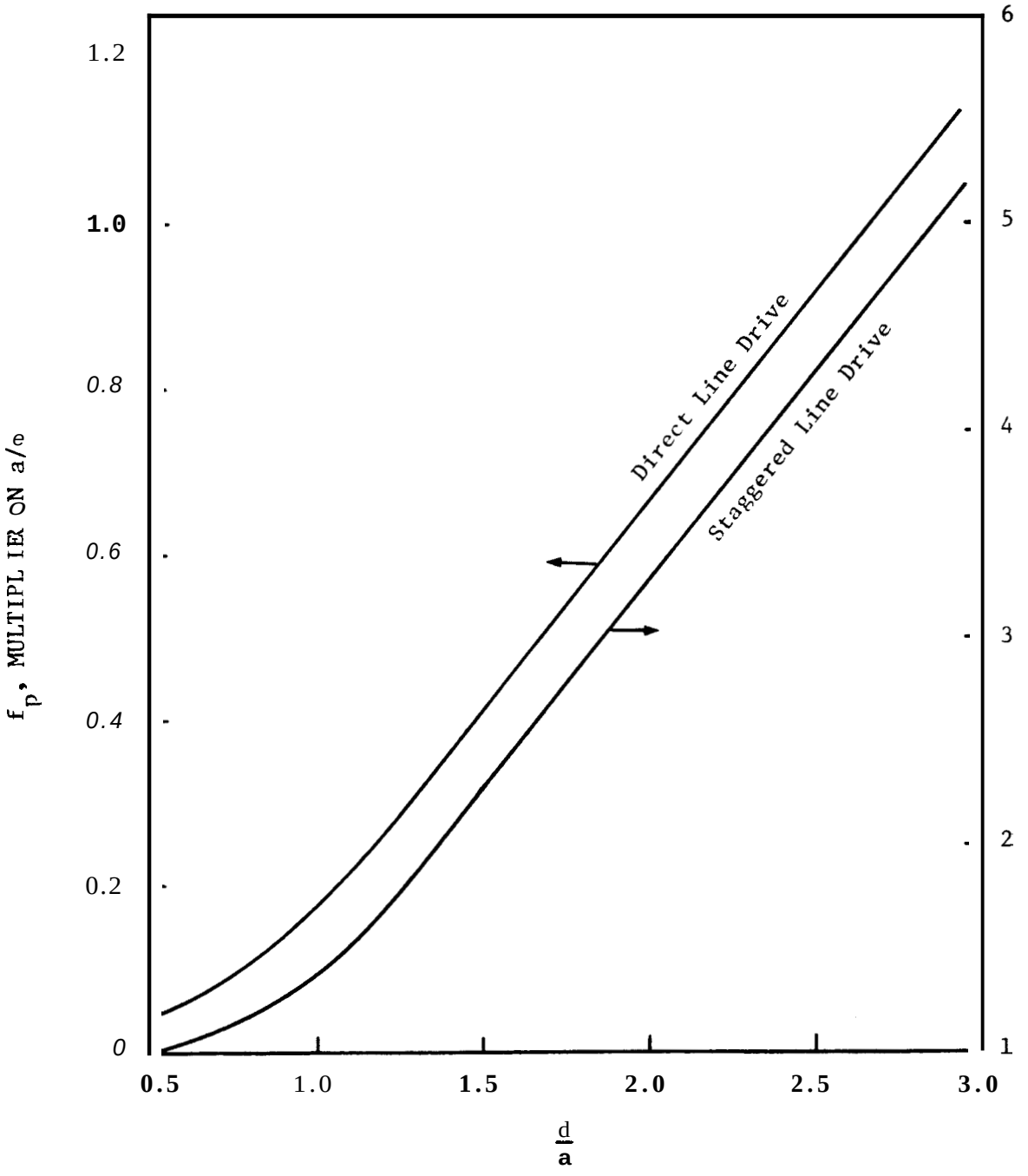

Fig. 3.26: CORRECTION FACTORS ON a/a TO CALCULATE PEAK LOCATIONS

Table 3.7

CORRECTION FACTORS ON TRACER PEAK CONCENTRATION AND a/a FOR STAGGERED LINE DRIVE AND DIRECT LINE DRIVE AT VARIOUS d/a RATIOS

$\frac{d}{a}$	STAGGERED LINE DRIVE		DIRECT LINE DRIVE	
	f_p	f_m	f_p	f_m
0.50	1.00	1.00	0.036	1.28
0.75	1.13	1.09	0.092	1.06
1.00	1.36	1.22	0.173	1.03
1.25	1.76	1.37	0.280	1.07
1.50	2.26	1.52	0.410	1.17
1.75	2.76	1.68	0.536	1.27
2.00	3.26	1.83	0.665	1.39
2.25	3.78	1.99	0.790	1.50
2.50	4.28	2.14	0.915	1.62
2.75	4.79	2.30	1.040	1.74
3.00	5.30	2.46	1.165	1.85
3.25	5.81	2.63	1.294	1.95
3.50	6.12	2.78	1.420	2.06

Substituting for $\bar{C}_D$ from Eq. 3-52 and simplifying:

$$\left(C_{max}\right)_{pattern} = f_m \left(C_{max}\right)_{5\text{-spot}} \cdot \frac{\left(\sqrt{\frac{a}{\alpha}}\right)_{pattern}}{\left(\sqrt{\frac{a}{\alpha}}\right)_{5\text{-spot}}} \qquad (3\text{-}57)$$

The correction factor on Peclet number, f_p (Fig. 3.26), relates a/a values:

$$\left(\frac{a}{\alpha}\right)_{pattern} = f_p \left(\frac{a}{\alpha}\right)_{5\text{-spot}} \qquad (3\text{-}58)$$

Finally:

$$\left(C_{max}\right)_{pattern} = f_m \sqrt{f_p} \left(C_{max}\right)_{5\text{-spot}} \tag{3-59}$$

Pore volumes corresponding to peak concentrations are also convertible, because maximum concentrations occur at the same dimensionless pore volumes, i.e.:

$$\left(\frac{V_{pD,max} - V_{pDbt}}{1 - V_{pDbt}}\right)_{pattern} = \left(\frac{V_{pD,max} - V_{pDbt}}{1 - V_{pDbt}}\right)_{5\text{-spot}} \tag{3-60}$$

Or, equivalently:

$$\left(V_{pD,max}\right)_{pattern} = \left(\frac{V_{pD,max} - V_{pDbt}}{- V_{pDbt}}\right)_{5\text{-spot}} \cdot \left(1 - V_{pDbt}\right)_{pattern} + \left(V_{pDbt}\right)_{pattern} \tag{3-61}$$

where, V_{pDbt} is the areal sweep efficiency expressed as a fraction.

Having been able to correlate one point from each curve--namely, the maximum point of the tracer breakthrough profile from various systems--the analysis was extended to correlate the tracer breakthrough curves over their entire concentration versus volume range. To do this, first, the tracer breakthrough profiles of systems were normalized by dividing the concentration values by the maximum concentrations for each curve. An example of this for a developed five-spot system is shown in Fig. 3.27. Second, the correction factors on a/a in Fig. 3.26 were utilized to correlate the normalized curves of different patterns into one curve. To accomplish this, the volume coordinate used on the abscissa was the same dimensionless pore volume function that was found useful in the correlation of pattern breakthrough curves discussed in Section 3.1.3. Figure 3.28 shows a particular correlation obtained when comparing a five-spot with a/a = 700 to the equivalent direct line drive (d/a = 1, a/a = 120), and the equivalent staggered line drive (d/a = 2, a/a = 2280). The values of a/a for the latter two patterns were computed using Eq. 3-58 with f_p = 0.17 and f_p = 3.26, respectively, obtained from Fig. 3.25. The correlation is excellent in the vicinity of the peak. At smaller and larger pore volumes, it is somewhat poor, but still adequate as will be seen later. Due to the low concentrations at each end of the correlation, the relative errors by the correlation are small at the volume extremes.

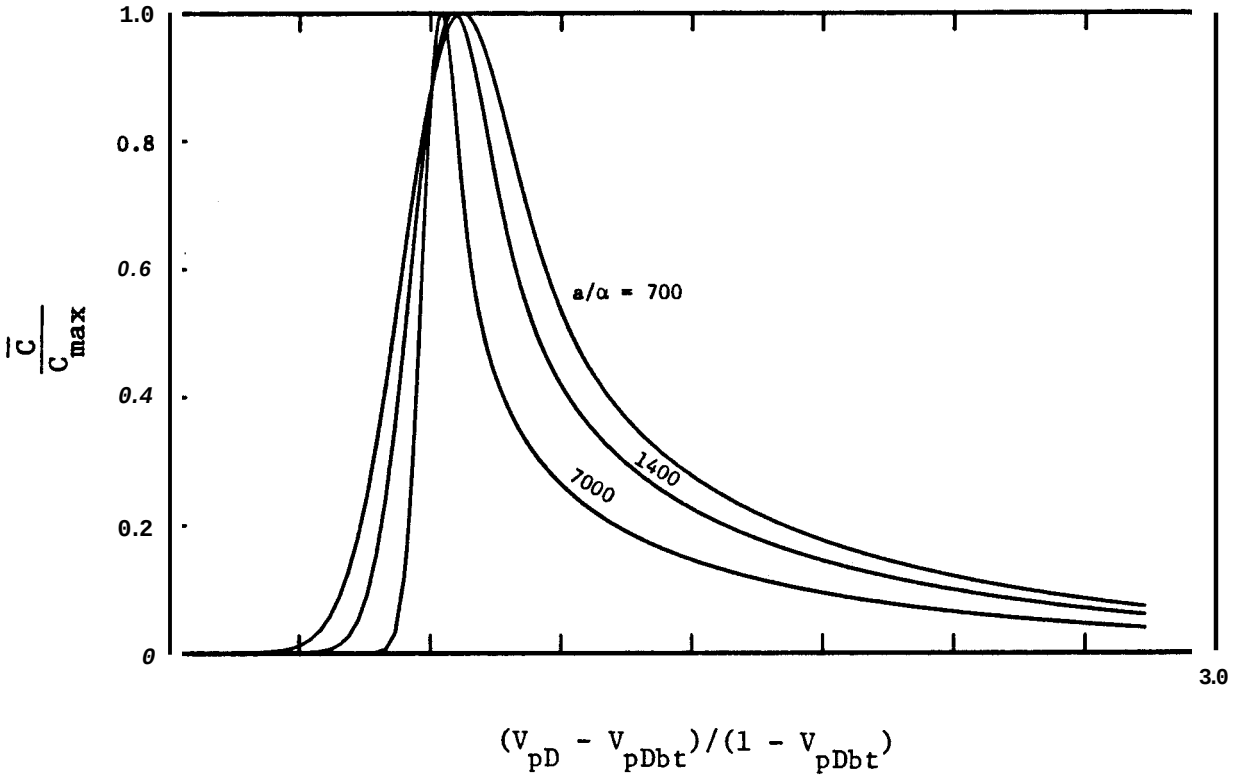

Fig. 3.27: NORMALIZED TRACER PRODUCTION CURVES FOR A HOMOGENEOUS DEVELOPED FIVE-SPOT

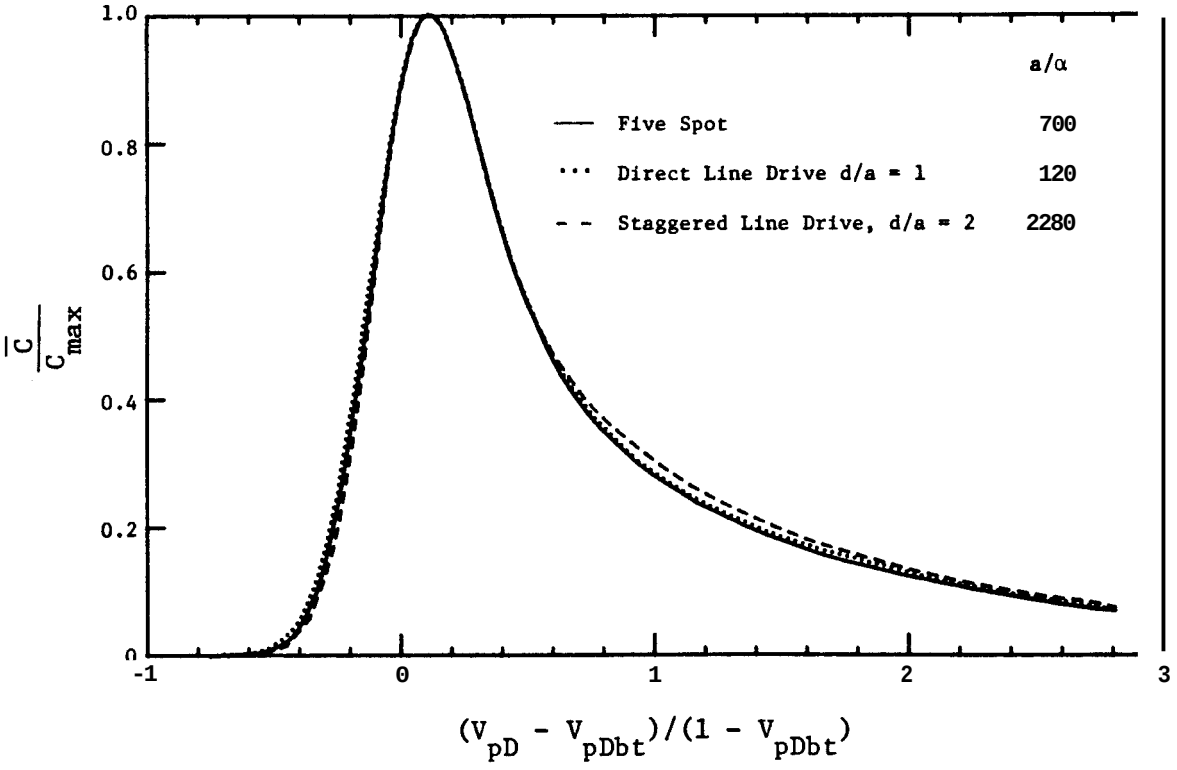

Fig. 3.28: CORRELATION OF TRACER PRODUCTION CURVES FOR HOMOGENEOUS DEVELOPED PATTERNS

For any value of a/α and for different geometries, the actual curves can be related to a five-spot system by using the parameters in the coordinates of Fig. 3.28, and the correction factors on Fig. 3.25 and 3.26 as follows:

$$\left(\frac{\bar{c}}{c_{max}}\right)_{pattern} = \left(\frac{\bar{c}}{c_{max}}\right)_{5-spot} \tag{3-62}$$

Substitute for maximum concentrations from Eq. 3-59:

$$\bar{c}_{pattern} = f_m \sqrt{f_p}\ \bar{c}_{5-spot} \tag{3-63}$$

The pore volumes at which the concentrations in Eq. 3-63 occur are obtained from the dimensionless pore volume abscissa coordinate of Fig. 3.28. The relationship is similar to Eq. 3-61 and subsequently is given by:

$$\left(V_{pD}\right)_{pattern} = \left(\frac{V_{pD} - V_{pDbt}}{1 - V_{pDbt}}\right)_{5-spot} \cdot \left(1 - V_{pDbt}\right)_{pattern} + \left(V_{pDbt}\right)_{pattern} \tag{3-64}$$

By using Eq. 3-58, different patterns can be correlated into an equivalent five-spot pattern; thereafter, breakthrough curves can be computed from the five-spot tracer breakthrough profile through Eqs. 3-63 and 3-64 only.

3.3 TRACER FLOW IN HETEROGENEOUS SYTEMS

This section focuses on the mathematical description of tracer movement in non-uniform reservoirs. The non-uniformity of a reservoir is represented with a stratified model.

3.3.1 Concept of Multilayered Modeling

Reservoirs often are sedimentary deposits laid down in a body of water over a long period of time. After deposition, they undergo further physical and chemical changes. As a result of the non-uniform nature of deposition and secondary alteration, heterogeneities develop within the reservoirs. The severity of the heterogeneity depends on the lithology and the external forces acting upon the system. In general, sandstone reservoirs tend to be more uniform than limestone or carbonate reservoirs. Levorsen (1956) details sedimentary basins including the origin of heterogeneities in each basin. Hutchinson (1959) presents an excellent review on reservoir inhomogeneity.

Since the sediments are deposited areally, it is expected that some lateral uniformity exists over wide ranges of a reservoir. However, a variation is anticipated in the vertical direction due to differences in the depositional

time and environment. This scheme of deposition indicates that the sediments are generally laid down in layers which are fairly uniform in lateral direction but differ with elevation. For many sandstone reservoirs, this type of heterogeneity is a fair representation of the reservoir. The fact that the permeabilities measured in the vertical direction are frequently a small fraction of the horizontal penneabilities emphasizes the validity of this representation. Figures 3.29a and b show outcrops of sandstone reservoirs. These pictures illustrate that formations are often composed of layers. In some cases, thin layers of shale or silt are deposited between the sand layers and prevent interlayer fluid transport. However, in other cases there is no barrier between the layers and hence, unrestricted or partially restricted cross-flow occurs between the layers. Sometimes, cross-bedding, pinching out and local non-uniformities within the layers distort the homogeneity and the continuity of the layers.

Despite physical limitations, reservoirs can often be simulated as though they are composed of parallel layers with no interlayer communication. Based on this model, several reservoir engineering calculations can be made. Dykstra and Parsons (1950) presented a method for calculating reservoir vertical coverage in waterflooding operations using this concept. Their method has been found to match the results of many waterflood operations. Elkins and Skov (1962) matched the performance of two gas-condensate cycling projects and an enriched gas-drive project with a multi-strata model. Fitch and Griffith (1964) also matched the performance of an LPG slug miscible drive in an isolated five-spot pilot test by using a stratified model with no cross-flow

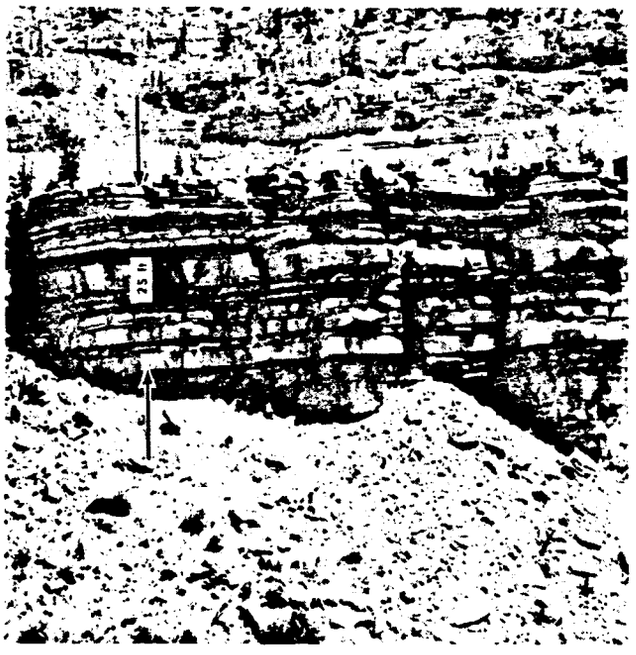

Fig. 3.29a Marine Sandstone Deposit with Thin Subunits of Sand

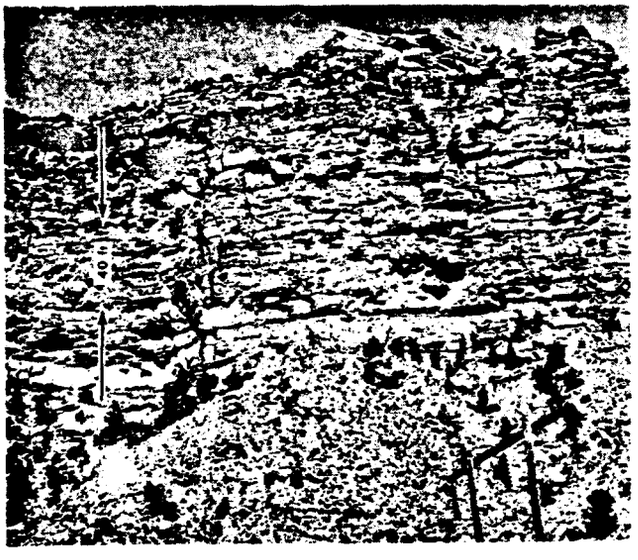

Fig. 3.29b Channel Sandstone Deposit Exhibiting Highly Irregular Bedding

Fig. 3.29: OUTCROPS OF SANDSTONE RESERVOIRS (after Zeito, 1965)

between the layers. The strata description for the pilot was obtained from core data. Based on a stratified model, Hearn (1971) developed theoretical pseudo-relative-permeability curves for a reservoir which included vertical permeability variation. The pseudo-relative-permeability curves converted the stratified reservoir into a mathematically-equivalent, two-dimensional homogeneous system with pseudo properties. This model was shown to match the performance of a waterflooding operation conducted in a carbonate reservoir. There was vertical communication among the layers of this reservoir.

Cross-flow between the layers occurs as a result of the establishment of a vertical pressure gradient between the layers. One or more of three forces may cause vertical pressure gradients to develop. These are gravity, capillary and viscous forces. In miscible displacements, vertical dispersion also contributes to the amount of cross-flow. In a miscible displacement of fluids with equal densities, there are no gravity and capillary forces. If the fluids also have the same viscosity (mobility ratio equal to one), no viscous forces will be present across the layers. A miscible displacement in which these forces are absent will theoretically produce similar results in a stratified system with no barrier between the layers, and in a system in which impermeable layers prevent cross-flow. However, the systems which exhibit cross-flow can also be modeled by a hypothetical system with no cross-flow. This was illustrated by Fitch and Griffith (1964), who matched the results of a miscible test by a stratified model with no cross-flow. The test was conducted in laboratory layered-prototypes without barriers between the layers at a mobility ratio of about twenty. The success of stratified reservoir models in matching performance of miscible and immiscible displacements indicates that this concept of modeling is often reasonable.

Similarly, the flow of tracers in heterogeneous reservoirs can be modeled by a stratified system. Since the tracer material is miscible with both the displacing and displaced fluids, and has the same density and viscosity as these fluids, cross-flow can occur only as a result of lateral dispersion. However, the effects of lateral dispersion are much smaller than longitudinal dispersion, as has been discussed earlier. Therefore, for practical purposes, the results of tracer flow in a stratified reservoir, with or without barriers between the layers, would be similar.

3.3.2 Tracer Production Curves from Layered Systems

To compute tracer response curves from layered systems, the following assumptions are made:

1) The individual layers are homogeneous (uniform porosity and permeability throughout each layer);
2) There is no cross flow between the layers;
3) The dispersion constant, *a*, is the same for each layer;
4) Water saturation is constant and is the same in each layer; and
5) The mobility ratio of the displacement is equal to unity.

The justification of the third assumption stems from two facts: 1) for the formations with the same sedimentary deposit origins, dispersion constants do not vary appreciably within the same producing zones of formations; and 2) tracer breakthrough 'curvet do not depend strongly on dispersion constants. This can be seen from either Fig. 3.19 or 3.23. The fifth assumption is valid for the tracer tests run in gas reservoirs or watered-out reservoirs (prior to tertiary operations) wherein the fluid flowing ahead of the tracer slug is essentially water, and the chase fluid is also water. In secondary recovery waterflooding in reservoirs with high connate-water saturation, the fluid bank ahead of the tracer slug will be mainly water. Hence, the assumption of unit mobility ratio would be applicable. In almost all gas cycling projects, the assumption of unit mobility ratio is valid.

In a layered system, the overall tracer output curve is a combination of responses from the constituent layers. The individual layer responses are predictable and correlatable by the analysis discussed in the previous sections. However, the tracer arrival time at the production well and the tracer concentration contributed from each layer are functions of the porosity, permeability and thickness of each layer. Because of the unit-mobility ratio assumption, any material injected into a multilayered system is distributed among the layers in proportion to conductances, kh. If V_T is the total volume (in barrels) of displacing fluid injected, then the pore volume injected into layer j is:

$$(V_{pD})_j = \frac{(kh)_j}{\Sigma kh} \frac{5.615\ V_T}{A(\phi h)_j S_w} = \frac{k_j}{\phi_j\ Ckh} \frac{5.615\ V_T}{A\ S_w} \tag{3-65}$$

At the producing wellbore, the tracer concentration is the volumetric sum of tracer concentrations from the layers. This is given by:

$$\bar{C} = \sum_{j=1}^{n} \frac{(kh)_j}{\Sigma kh}\ \bar{C}_j \tag{3-66}$$

where:

n = number of layers

$\bar{C}_j$ = tracer concentration flowing from layer j into the wellbore, computed at pore volume $(V_{pD})_j$

From Eq. 3-52 for layer j:

$$\bar{C}_j = C_o \sqrt{\frac{a}{\alpha}}\ F_{rj}\ \bar{C}_{Dj} \tag{3-67}$$

where F_{rj} is the tracer slug size injected into layer j in terms of fraction of the pore volume of layer j. It is thus given by:

$$j_{rj} = \frac{(kh)_j}{Ckh} \frac{V_{Tr}}{A\ (\phi h)_j\ S_w} = \frac{k_j}{\phi_j\ Ckh} \frac{V_{Tr}}{A\ S_w} \tag{3-68}$$

and $\bar{C}_{Dj}$ is the dimensionless concentration from layer j calculated at $V_{pD} = (V_{pD})_j$. This dimensionless concentration is given by one of the Eqs. 3-51, 3-53 or 3-55, depending on the type of pattern. If thickness, porosity and permeability of the layers are known, the tracer concentration profiles for various patterns can be constructed. Conversely, the decomposition of a tracer production curve from a multilayered system into the constituent layer responses can yield the layer parameters. Yuen et al. (1979) presented a method for the decomposition of overall tracer response curves from developed five-spot systems.

To study the flow of tracer in layered systems, a hypothetical four-layered staggered line drive with d/a = 1 was considered. The area of the system was 90,000 ft^2, the Peclet number was a/a = 2000, and the total tracer injected into the system was 10 ft^3. Also, the system was considered to be of unit thickness with a porosity of 0.25 and an initial water saturation of 60 percent. Table 3.8 shows the assumed parameters of the layers. The calculated tracer response from this system is presented in Fig. 3.30. There are four distinct peaks in this figure which are widely separated from each other. A computer algorithm, based on the Yuen et al.'s (1979) method, was prepared which would deconvolve the overall tracer profile into the constituent layer responses, and thus evaluate the porosity thickness and fractional permeability thickness products of the individual layers from the input peak data (concentration and volume). The computer program would then regenerate the entire tracer production profile based on the computed layer parameters. This program will be referred to as "deconvolution routine" in this study. Table 3.8 shows the computed results using the deconvolution routine based on exact equations for a staggered line drive system. The corresponding computed tracer curve was close to the original profile.

Table 3.8

ASSUMED AND COMPUTED PARAMETERS OF THE LAYERS FOR THE THEORETICAL STAGGERED LINE DRIVE, EXAMPLE 1

LAYER	ASSUMED PARAMETERS		COMPUTED PARAMETERS USING EQUATIONS FOR STAGGERED LINE DRIVE, d/a = 1		COMPUTED PARAMETERS USING EQUATIONS OF EQUIVALENT 5-SPOT SYSTEM	
	ϕh	$\frac{kh}{\Sigma kh}$	ϕh	$\frac{kh}{\Sigma kh}$	ϕh	$\frac{kh}{\Sigma kh}$
1	0.2850	0.2	0.2800	0.19750	0.27830	0.19630
2	1.0134	0.4	1.00601	0.39824	1.00197	0.39664
3	1.1403	0.3	1.13376	0.29921	1.13944	0.30071
4	0.5068	0.1	0.51094	0.101 13	0.52816	0.10454
SUM	2.9455	1.0	2.9307 1	0.99608	2.94787	0.99819

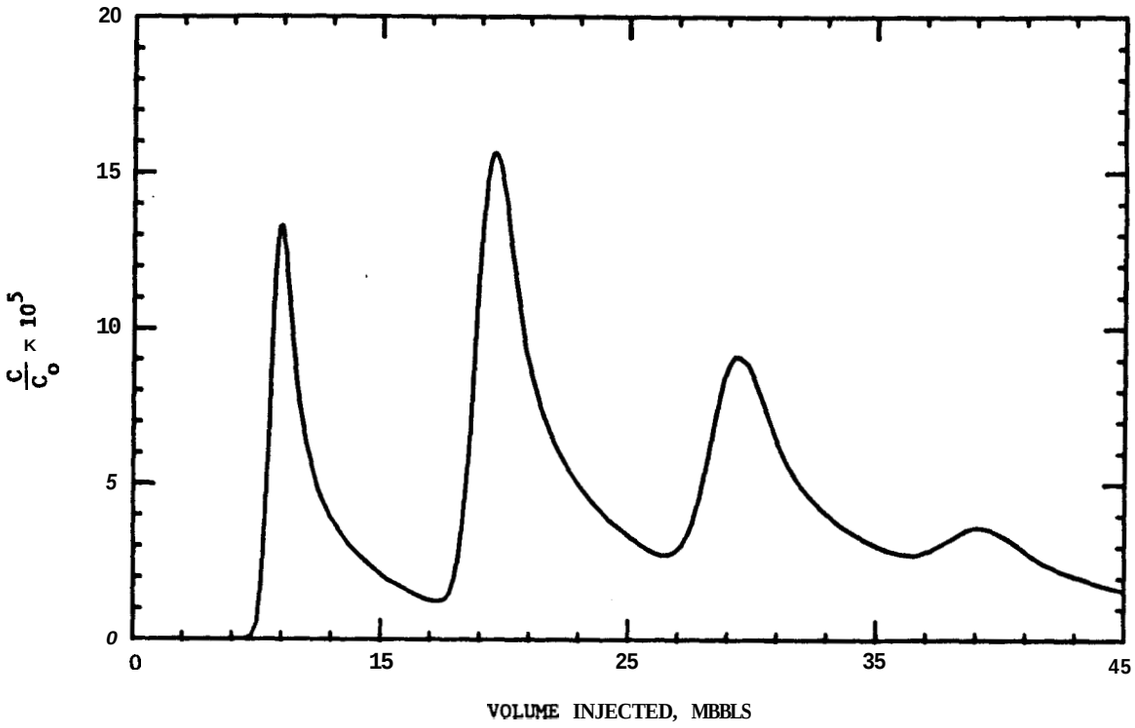

Fig. 3.30: TRACER RESPONSE FROM A FOUR-LAYERED STAGGERED LINE DRIVE, d/a = 1, "FIRST EXAMPLE"

The correlating technique developed for tracer production curves was applied to this multilayered system. The staggered line drive was converted into an equivalent five-spot using Eq. 3-58 with f_p = 1.36 obtained from Fig. 3.26. This changed the value of a/a from 2000 to 1470. Next, the deconvolution routine was modified to combine tracer concentration equations for the five-spot system with the correlating Eqs. 3-63 and 3-64. This modified version of the deconvolution routine was used, with appropriate multipliers and break-through areal sweep efficiencies, to decompose the original tracer curve in Fig. 3.30. The regenerated profile based on the correlation is seen in Fig 3.31. The match is good with only slight divergence in the vicinity of the local minima. This divergence was expected because the original correlation was not perfect at larger and smaller values of pore volumes. The parameters of the layers computed by the program are shown in Table 3.8. The calculated values of ϕh and kh are close to the values used to generate the data.

In the second hypothetical example, the same four-layer staggered line drive system was considered. This time the parameters of the layers were changed to obtain peaks near each other. Table 3.9 presents the selected parameters of the layers. The tracer response from this system is shown in Fig. 3.32. As before, the deconvolution routine was used with the input observed peak data to generate a match to this curve. The resulting match, shown in Fig. 3.32, is not a satisfactory one. Yuen et al. (1979) have illustrated that when peaks are near each other, the observed peak locations do not correspond to the exact peak locations from the individual layer responses. The individual

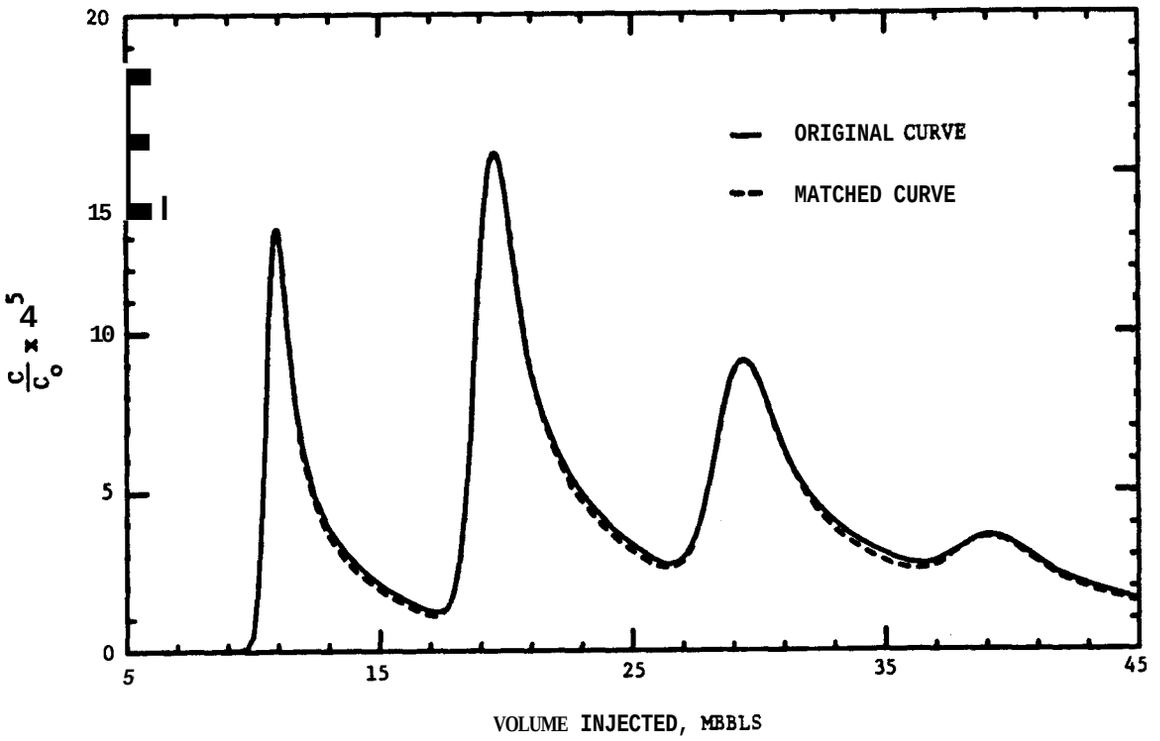

Fig. 3.31: MATCH OBTAINED USING THE DECONVOLUTION ROUTINE AND TRACER CORRELATION PARAMETERS

Table 3.9

ASSUMED AND COMPUTED PARAMETERS OF THE LAYERS FOR THE THEORETICAL STAGGERED LINE DRIVE, EXAMPLE 2*

LAYER	ASSUMED PARAMETERS				COMPUTED PARAMETERS USING OPTIMIZATION TECHNIQUE			
	ϕh	$\frac{kh}{Ckh}$	h, ft	k, md	ϕh	$\frac{kh}{Ckh}$	h, ft	k, md
1	0.315	0.15	1.26	119.05	0.314996	0.149998	1.26	119.05
2	1.000	0.40	4.00	100.00	0.999957	0.399984	4.00	100.00
3	0.6875	0.25	2.75	90.91	0.687447	0.249983	2.75	90.91
4	0.6000	0.20	2.4	83.33	0.600065	0.200024	2.40	83.33
SUM	2.6025	1.00			2.602466	0.999989		

* The k and h values in this table have been computed for ϕ = .25 and Ckh = 1000 md-ft.

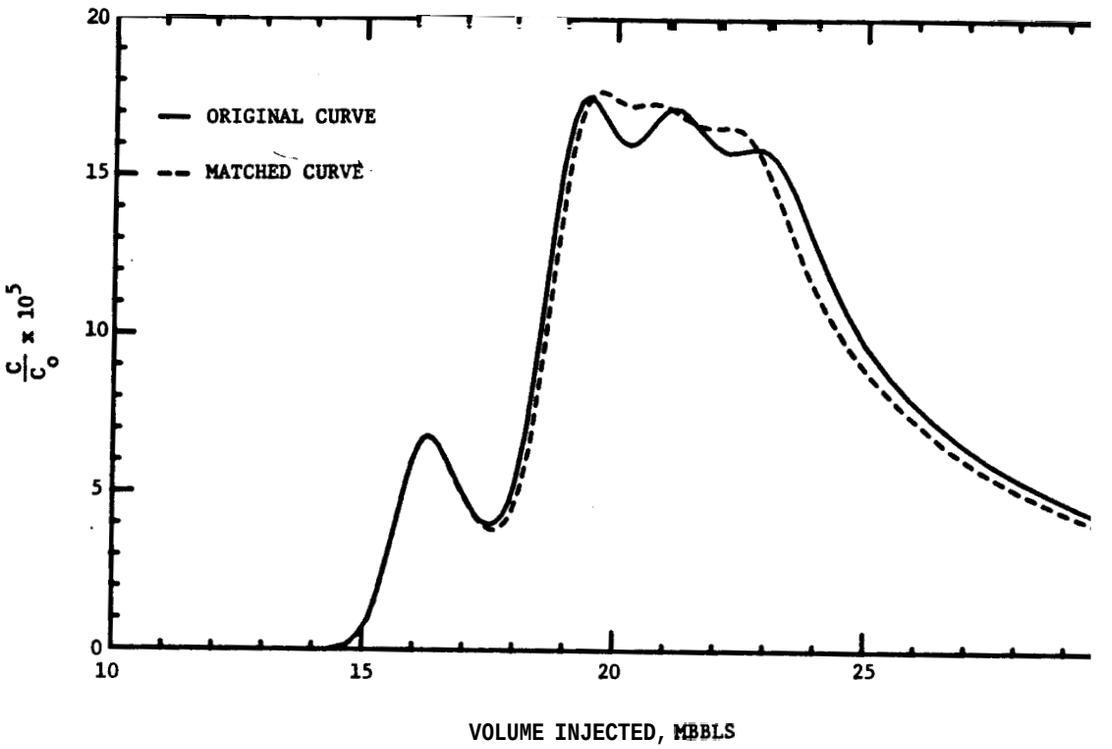

Fig. 3.32: TRACER RESPONSE FROM A FOUR-LAYER DEVELOPED STAGGERED LINE DRIVE (d/a = 1) AND THE MATCH OBTAINED USING THE DECONVOLUTION ROUTINE, "SECOND EXAMPLE"

tracer response curves interfere with each other and, hence, shift the location of the observed peaks from their corresponding layer peaks. Brown and Brigham **(1981)** have shown a method of handling this shift using a trial-and-error procedure for each peak. This usually requires many trials to achieve a desirable match and can be tedious for large systems. In this study, an attempt has been made to overcome this problem.

4.3.3 Optimization Technique

Non-linear optimization (or multiple regression analysis) is a powerful technique in fitting data by a set of variables. This procedure is also known **as** a non-linear least-squares method for curve fitting. The idea is to minimize the objective function F:

$$F = \sum_{i=1}^{N} (C_i^* - \bar{C}_i)^2 \qquad (3\text{-}69)$$

where:

C_i^* = observed concentration at sample point i

$\bar{C}_i$ = overall concentration computed at sample point i

N = number of data points or number of observed concentrations

i = an observation point

For a multilayer system, the injected tracer and displacing fluid will be divided into layers proportional to the kh of each layer. If $(V_T)_i$ is the total volume (in barrels) injected at the time point i is observed, the pore volumes injected into-layer j at this time from Eq. 3-65 are:

$$\left(V_{pD}\right)_{j,i} = \frac{k_j}{\phi_j \; \Sigma kh} \cdot \frac{5.615 \left(V_T\right)_i}{A \; S_w} \tag{3-70}$$

The overall tracer concentration being produced at the time of observation point i is the sum of tracer concentrations being supplied by each layer. This concept is considered in Eq. 3-66 and is given by:

$$\bar{C}_i = \sum_{j=1}^{n} \frac{(kh)_j}{\Sigma kh} \; \bar{C}_{j,i} \tag{3-71}$$

where $\bar{C}_{j,i}$ is the concentration flowing to the wellbore from layer j at the time and injection volume associated with point i. This concentration is computed from Eq. 3-67 as follows:

$$\bar{C}_{j,i} = C_o \sqrt{\frac{a}{\alpha}} \; F_{rj} \left(\bar{C}_D\right)_{j,i} \tag{3-72}$$

where F_{rj} is given by Eq. 3-68 and $(\bar{C}_D)_{j,i}$, dimensionless concentration in layer j, is calculated at $V_{pD} = (V_{pD})_{j,i}$ in the equation for tracer production curves from homogeneous patterns.

From Eqs. 3-51, or 3-53, or 3-55 (for the pattern of interest), and Eqs. 3-68 and 3-70 through 3-72, it can be concluded that $\bar{C}_i$ is only a function of $k_j/(\phi_j \Sigma kh)$, $(kh)_j/\Sigma kh$, $(V_T)_i$, and the number of layers. The functional form is:

$$\bar{C}_i = \sum_{j=1}^{n} \frac{k_j}{\phi_j \; \Sigma kh} \; \frac{(kh)_j}{\Sigma kh} \; \Gamma\left(\frac{k_j}{\phi_j \; \Sigma kh}, \left(V_T\right)_i\right) \tag{3-73}$$

where Γ is a function given by combining Eqs. 3-51, or 3-53, or 3-55 (for the patterns) with Eq. 3-70 and 3-72. Denoting:

$$\frac{k_j}{\phi_j \; \Sigma kh} = Z_j \tag{3-74}$$

and,

$$\frac{k_j}{\phi_j \; \Sigma kh} \; \frac{(kh)_j}{\Sigma kh} = X_j \tag{3-75}$$

Equation 3-73 becomes :

$$\bar{C}_i = \sum_{j=1}^{n} X_j \; \Gamma\left[Z_j \, , \left(V_T\right)_i\right] \tag{3-76}$$

The subroutine VARPRO at the Stanford Center for Information Technology (CIT) can minimize the function F given in Eq. 3-69 when $\bar{C}_i$ is in the form of Eq. 3-76. This subroutine requires initial estimates on non-linear parameters, Z_j, with no requirements on initial estimates for linear parameters, X_j. In the case of interest here, the initial estimates on Z_j can be obtained easily from Eq. 3-70 by assuming that the observed location of peaks in the tracer breakthrough curve correspond to the location of peaks from individual layer responses. This is given by the following equation:

$$\left(Z_j\right)_{est} = \frac{A \; S_w}{5.615 \left(V_{T,max}\right)_j} \; V_{pD,max} \tag{3-77}$$

where :

$\left(V_{T,max}\right)_j$ = volume corresponding to the jth peak in the observed tracer profile, bbls

$V_{pD,max}$ = pore volume corresponding to the peak location in tracer response from a homogeneous system. This can be obtained from Fig. 3.24 combined with breakthrough areal sweep efficiency equations provided in Appendix A for different patterns

A computer program has been developed which utilizes the subroutine VARPRO to perform the optimization. The input data for this program are as follows: N data points from the overall tracer profile, number of layers expected (n) where n is smaller than N, and n location volumes corresponding to peaks in the observed tracer breakthrough curve. The program computes n non-linear parameters and n linear parameters with the least possible errors. From these parameters, ϕh and $kh/\Sigma kh$ of each layer are computed as follows:

$$\frac{(kh)_j}{Ckh} \; \frac{X_j}{Z_j} \tag{3-78}$$

$$(\phi h)_j = \frac{X_j}{Z_j^2} \tag{3-79}$$

Based on the above computed parameters, the program regenerates the entire tracer breakthrough curve.

The tracer profile in Fig. 3.32 was analyzed using this optimization technique. Twenty data points and four layers were chosen. The result of this optimization is shown in Fig. 3.33. There is virtually no difference between the original profile and the matched curve. The important point here is that

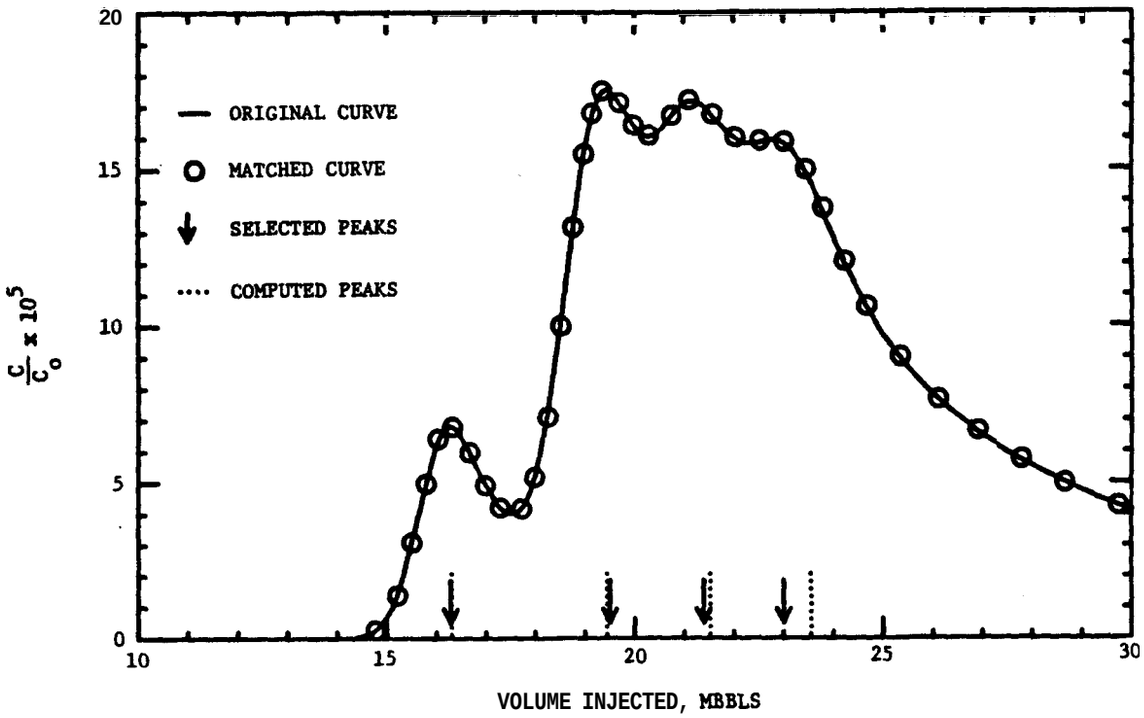

Fig. 3.33: MATCH OBTAINED USING THE OPTIMIZATION ROUTINE WITH FOUR LAYERS, "SECOND EXAMPLE"

Fig. 3.33 was obtained in one run, and no trial runs were necessary. Table **3.9** shows the numerical values of the parameters of the layers computed by the program. The results are virtually identical to the input data. If the layers are assumed to have the same porosity, and if average conductance of the system is known, the thicknesses and permeabilities of the layers can **be** computed. Table **3.9** also shows the computed permeability and thickness of the layers for uniform porosity of **0.25** and Ckh of 1000 md–ft.

To study the effect of assuming a smaller number of layers or a greater number of layers on the analysis, the profile in Fig. **3.32** was optimized using three and five layers. The results are shown **in** Figs. **3.34** and **3.35,** respectively. Both figures have the same area under the curve for the algorithm maintains a material balance. For the five–layer case, the program produced two peak locations that were very close to each other **(19,394** bbls and **19,399** bbls), implying that the two layers belonging to the peaks are actually only one layer and, therefore, the system **is** composed of four layers. Figure **3.34** shows that with three layers the analysis did not produce a good match. This indicates that more layers are required for a better match. Table 3.10 illustrates the results of the optimization with three and five layers. Also shown in this table are the computed values of permeabilities and thicknesses for equal values of porosity in the layers. Since two of the layers **in** Table **3.10** have virtually the same permeability, it is concluded that the system is actually composed of only four layers. Again, the results **of** this analysis are virtually identical with the input data.

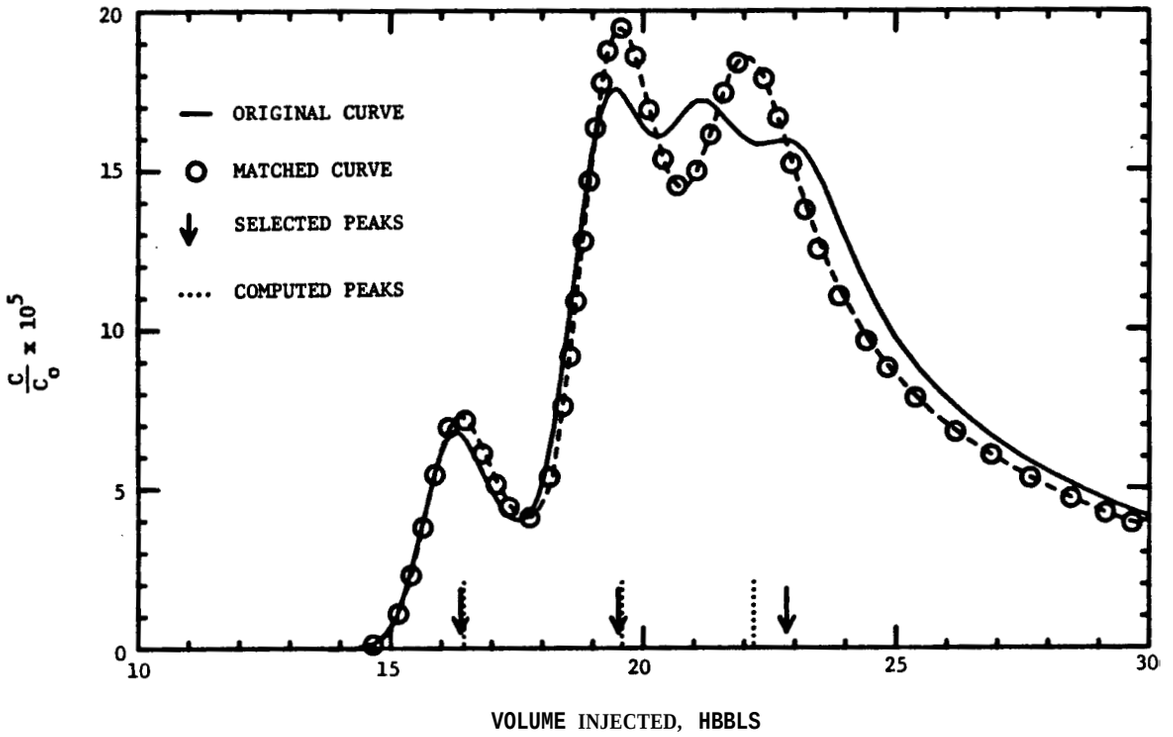

Fig. *3.34:* MATCH OBTAINED USING THE OPTIMIZATION ROUTINE WITH THREE LAYERS, "SECOND EXAMPLE"

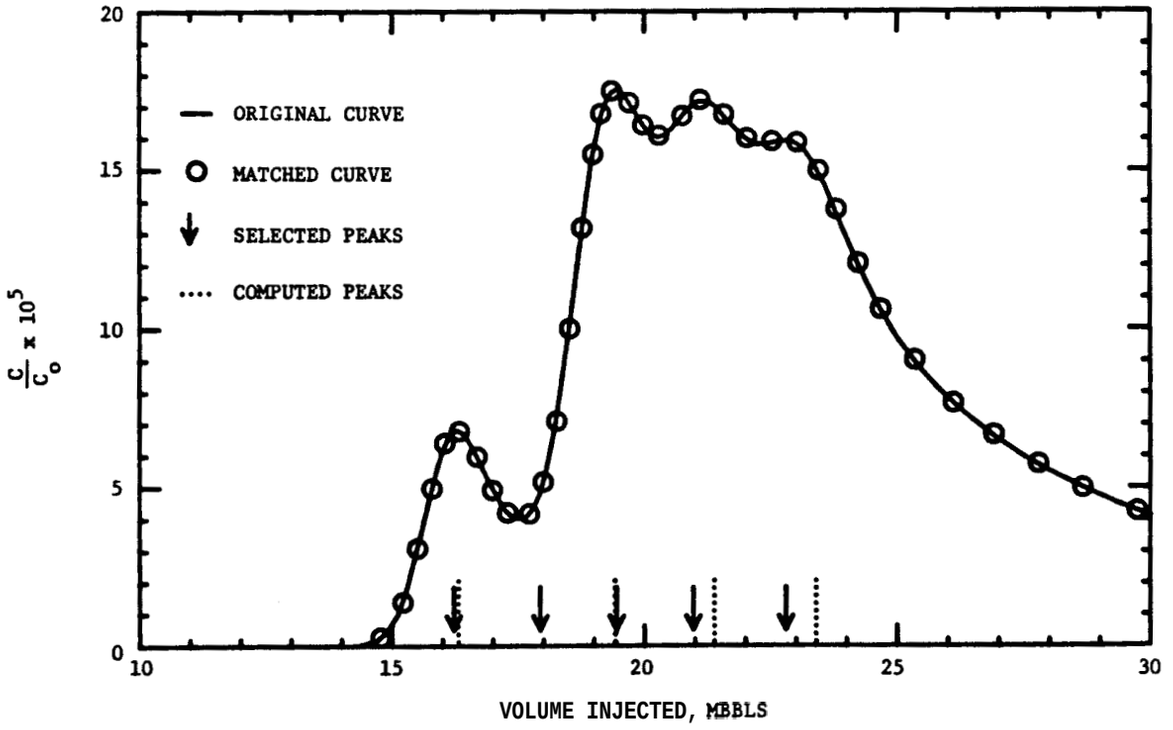

Fig. 3.35: MATCH OBTAINED USING THE OPTIMIZATION ROUTINE WITH FIVE LAYERS, "SECOND EXAMPLE"

Table 3.10

COMPUTED PARAMETERS OF THE LAYERS USING THE OPTIMIZATION TECHNIQUE WITH VARIOUS NUMBER OF LAYERS, EXAMPLE 2*

LAYER	COMPUTED PARAMETERS WITH THREE LAYERS				COMPUTED PARAMETERS WITH FIVE LAYERS			
	ϕh	kh Ckh	h, ft	k, md	ϕh	kh Ckh	h, ft	k, md
1	0.33817	0.16064	1.35	118.76	0.31499	0.15000	1.26	119.05
2	1.17024	0.46375	4.68	681.02	0.62362	0.24942	2.49	99.99
3	0.94361	0.32965	3.77	87.34	0.37630	0.15055	1.51	100.01
4					0.68738	0.24996	2.75	90.91
5					0.60014	0.20005	2.40	83.33
SUM	3.45202	0.95404	9.80		2.60243	0.99998	10.00	

* The k and h values in this table have been computed for ϕ = .25 and Ckh = 1000 md-ft.

The optimization computer program developed in this study generated excellent matches to theoretical tracer curves from multilayered patterns. The match obtained with fewer than the actual number of layers was not good, while that obtained with an excessive number of layers was excellent. The program also produced the correct number of layers whenever more layers were used than should have been. This proved that the program was capable of analyzing theoretical tracer curves. However, it remains to test the practical use of the method on field tracer response curves.

4. FIELD EXAMPLE

After successful analysis of tracer responses from hypothetically constructed multi-layered systems, the study was directed to the analysis of field data. The following example was taken from the paper by Brigham and Smith (1965).

4.1 HISTORY AND DESIGN OF THE TEST

The system considered was an unbalanced, inverted five-spot pilot pattern located in the Loco Field in Oklahoma. The reservoir had been under waterflooding since early 1950. In 1959, hot water injection began. The pilot location was selected in an area that had been depleted beyond the economic limit by conventional waterflooding. Beside the pilot injection well, seven other injectors had been also operating in the vicinity of the pilot area as shown in Fig. 4.1. Martin et al. (1968) present the geological data on the structure of the reservoir and the pilot area in particular.

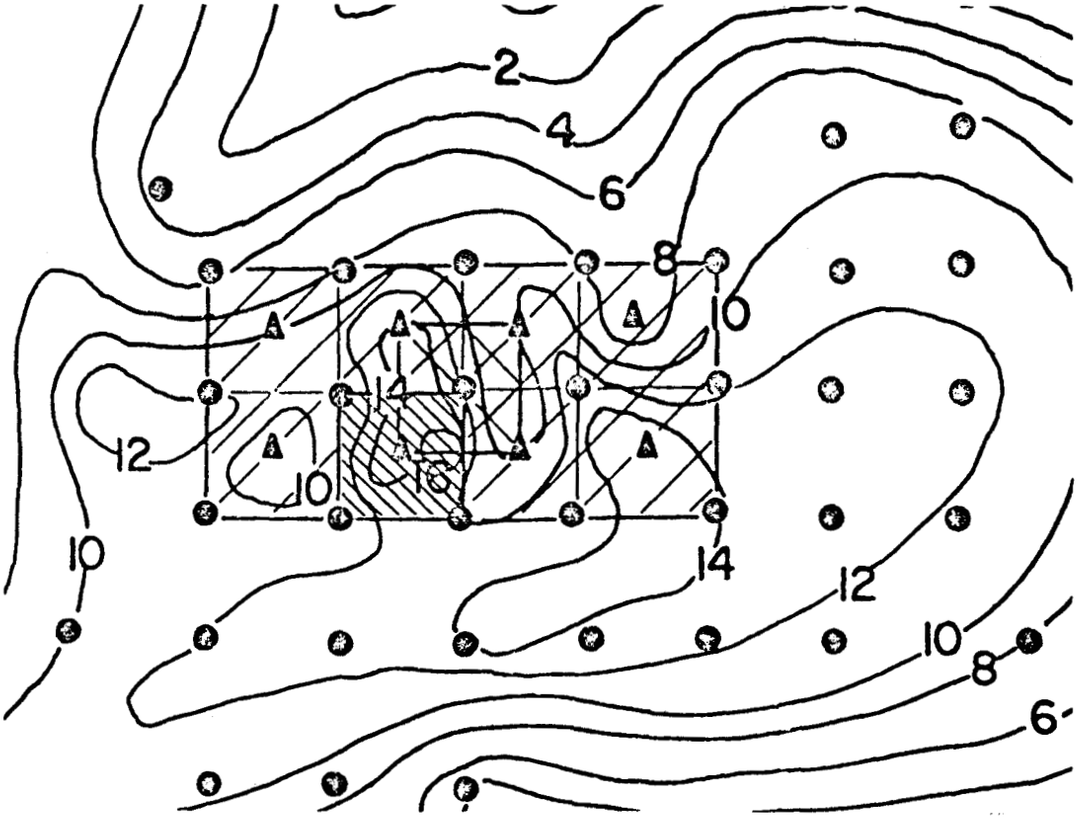

Fig. 4.1 : ISOPACH MAP OF LOCO WATERFLOOD PILOT AREA (After Martin et al., 1968)

A tracer program was initiated in 1962 to measure travel times and breakthrough characteristics for this pilot. Prior to the test, the injection and production rates were stable and remained constant during most of the test. Flow rates and information regarding the pattern and reservoir are shown on Fig. 4.2. Because of operating problems, the injection pump was shut down on the 18th day of the project through the 21st day. Water injection was then resumed at 600 BWPD, equal to the injection rate prior to the shut down. Total production rate from the four wells was 800 BWPD, implying that the production wells produced 200 BYPD from outside of the pattern area. This amount was not enough to balance the pattern completely. For an isolated five-spot pattern to act as though it is confined, it is necessary that the production rate from each well be equal to the injection rate.

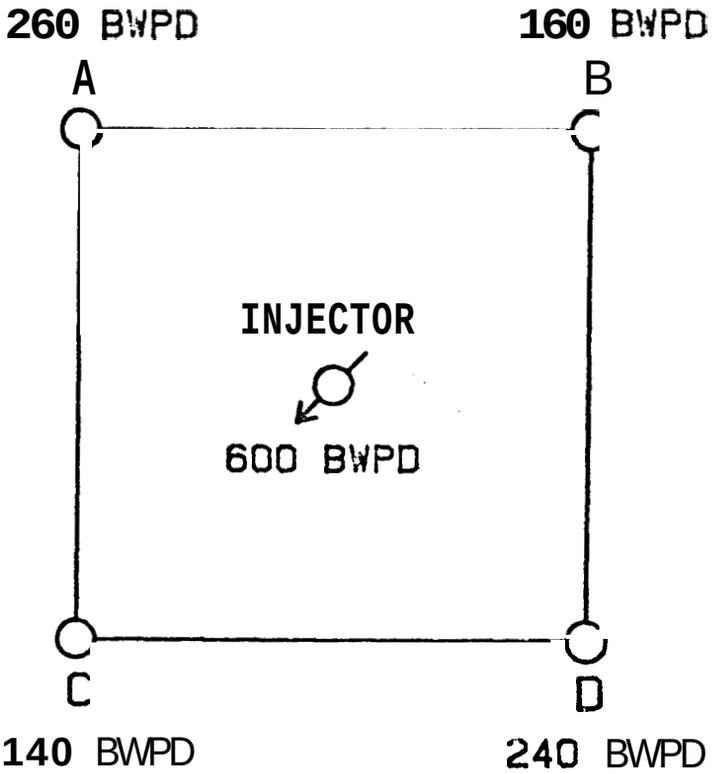

PATTERN AREA	=	2.5 acres
DISTANCE BETWEEN PRODUCERS, a	=	330 ft
TOTAL TRACER INJECTED	=	200 lbs
NET PAY THICKNESS	=	12 ft
AVERAGE PERMEABILITY	=	1500 md
AVERAGE POROSITY	=	0.26
AVERAGE WATER SATURATION	=	0.55
MIXING CONSTANT, α	=	0.05 ft

Fig. 4.2: PATTERN CONFIGURATION AND RESERVOIR DATA FOR THE FIELD TEST

Two hundred pounds of ammonium thiocyanate and 150 pounds of potassium iodide were dissolved in approximately ten barrels of water and injected into the formation as tracers. The volume of tracers used was chosen on the following basis. Analytical measuring techniques imposed a requirement of a minimum 25 ppm peak concentration to define the tracer breakthrough curves adequately. This required peak concentration was doubled as a safety factor. Hence, the test was designed for a 50 ppm peak concentration. For design purposes, the pattern was assumed to be a homogeneous, developed five-spot with h = 12 ft, ϕ = 0.26 and k = 1500 md. The dispersion constant, α, measured from laboratory miscible displacements on linear cores from the formation was found to be equal to 0.05 ft. Equation 23 in the paper by Brigham and Smith (1965)

showed that the amount of tracer required was about 150 pounds. To compensate for dilution caused by flow from outside the pattern, this amount was increased by 800/600 which resulted in 200 pounds of tracer requirement. Since laboratory analysis for iodide was more precise, the dilution effects for this tracer were neglected, and only 150 pounds of potassium iodide were used. The four producing wells were sampled every three hours for nine days, every four hours for eight days, every six hours for six days, and daily for twelve days to define tracer breakthrough curves adequately. Detailed information on the sampling procedure is provided in Smith and Brigham (1965).

The amount of tracer required to result in a 50 ppm peak concentration from a homogeneous, developed five-spot pattern was also calculated using the analysis developed in this study. The result was different from Brigham and Smith's designed value of 150 pounds. This was expected since Brigham and Smith had not formulated the tracer dispersion effects correctly. From Eqs. 3-41 and 3-52:

$$\bar{C}_{D,\,max} = \frac{\bar{C}_{max}}{C_o\, F_r \sqrt{\frac{a}{\alpha}}} \tag{4-1}$$

$$F_r = \frac{V_{Tr}}{A\, \phi h S_w} \tag{4-2}$$

Mass of tracer is related to volume by:

$$m_T = C_o\, V_{Tr}\, \rho_T \tag{4-3}$$

where,

m_T = mass of tracer, pounds

V_{Tr} = volume of tracer solution

C_o = initial tracer concentration, mass fraction

ρ_T = density of tracer solution ≈ density of water

From Eqs. 4-1, 4-2, and 4-3, the expression for m_T is:

$$m_T = \frac{\bar{C}_{max}\, \rho_T\, A\, \phi h S_w}{\bar{C}_{D,\,max} \sqrt{\frac{a}{\alpha}}} \tag{4-4}$$

For A = 2.5 acres, the value of a is equal to 330-ft and hence, a/a = 330/0.05 = 6600. From Fig. 3.23 for this 5-spot pattern, $C_{D,\ max}$ = 0.07. Therefore,

$$m_T = \frac{(50 \times 10^{-6})(62.4)(2.5 \times 43560)(0.26)(12)(0.55)}{0.07\sqrt{6600}} = 103 \text{ pounds}$$

The time to appearance of the peak for the assumed homogeneous pilot is computed from Fig. 3.24 for a/a = 6600 as follows:

$$\frac{V_{pD,\ max} - V_{pDbt}}{1 - V_{pDbt}} = 0.043$$

For a developed five-spot pattern, V_{pDbt} = 0.7178. Therefore,

$$V_{pD,\ max} = 0.73$$

The volume of fluid injected into the system at the peak:

$$V_{max} = A\ \phi h S_w\ V_{pD,\ max}$$

$$= (2.5 \times 43560)(0.26)(12)(0.55)(0.73)/5.615 = 24{,}300 \text{ bbls}$$

Time to the peak:

$$t_{ph} = \frac{V_{max}}{\text{injection rate}} = \frac{24300}{600} = 40.5 \text{ days}$$

If the system is stratified and the permeability of the most permeable layer is known, the time at which this layer reaches a peak is estimated from:

$$t_{PP} = t_{ph}\left(\frac{k_h}{k_p}\right) \qquad (4\text{-}5)$$

where,

t_{pp} = time to peak of the most permeable layer

t_{ph} = time to peak of the homogeneous system

k_p = permeability of the high permeable layer

k_h = permeability of the homogeneous system

The core data from the wells located in the pilot area had revealed a possibility of a thin, high-permeability streak with permeability of 5000 md. Therefore,

$$t_{PP} = 40.5 \left(\frac{1500}{5000}\right) = 12 \text{ days}$$

The time of 12 days can be viewed as an approximate time for tracer breakthrough from this pilot.

At the completion of the tracer test, there were unequal amounts of tracer flow from Wells A, C and D, with absolutely no tracer production from Well B during the test period. This implied that there was limited communication between the injector and Well B. This fact is substantiated further by a study of wellhead temperatures of the wells during the hot water injection period in which the temperature of Well B remained near 65°F. Figure 4.3 shows the isotherms of average sand temperature for the pilot. This figure was taken from Martin et al. (1968).

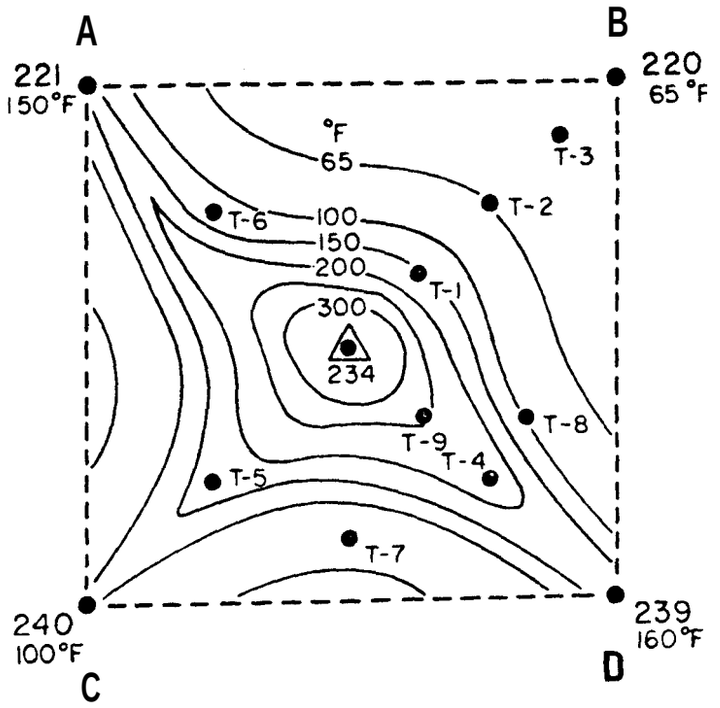

Fig. 4.3: ISOTHERMS OF AVERAGE SAND TEMPERATURE DURING HOT WATER INJECTION (after Martin et al., 1968)

The tracer elution curves for potassium iodide and ammonium thiocyanate were similar for each well, but not exactly the same. These are shown in Fig. 4.4. By integrating the areas under these curves, Smith and Brigham (1965) concluded that 40 percent of ammonium thiocyanate and 44 percent of potassium iodide were recovered from the three producing wells. This observation suggested that either there was little adsorption of the tracers in the formation or the adsorption of each tracer was nearly identical. The former alternative is the more likely. Furthermore, there is an uncertainty in the iodide data due to presence of background iodide concentration in both the injected and the formation water. Because of this uncertainty, only thiocyanate data is considered in this study. Since the injection was down for about four days near the end of the test, only early portions of the tracer breakthrough curves from Wells A and D are analyzed in detail, For this period, Well C did not exhibit substantial tracer production as is illustrated in Fig. 4.4b.

Fig. 4.4a

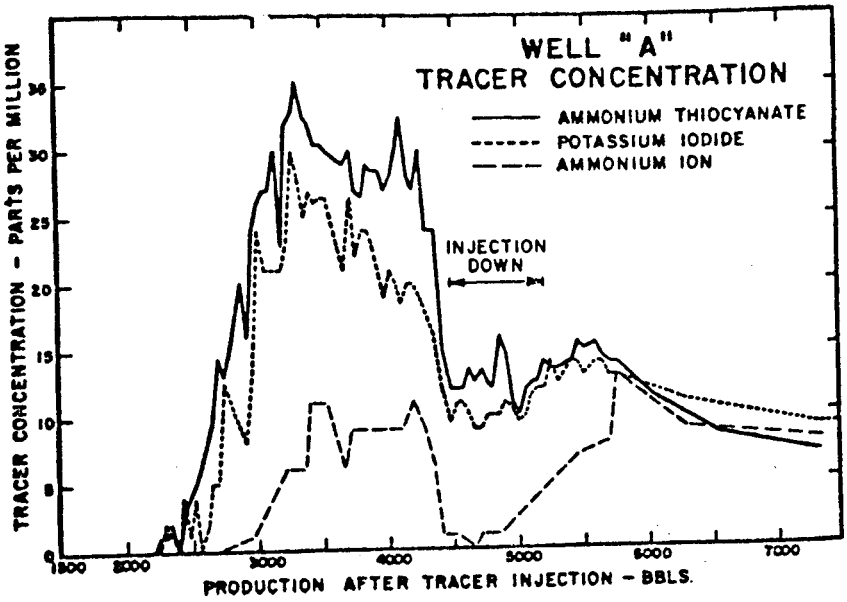

Fig. 4.4b

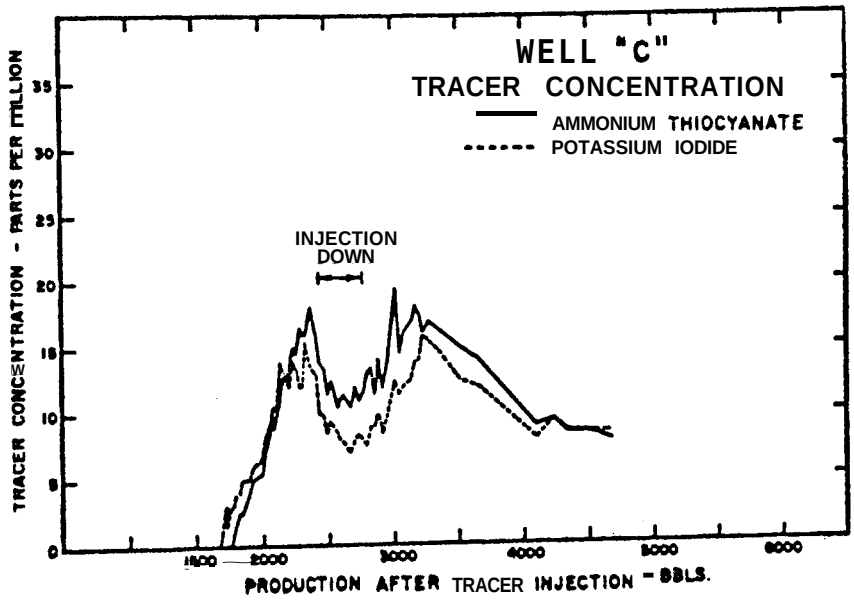

Fig. 4.4c

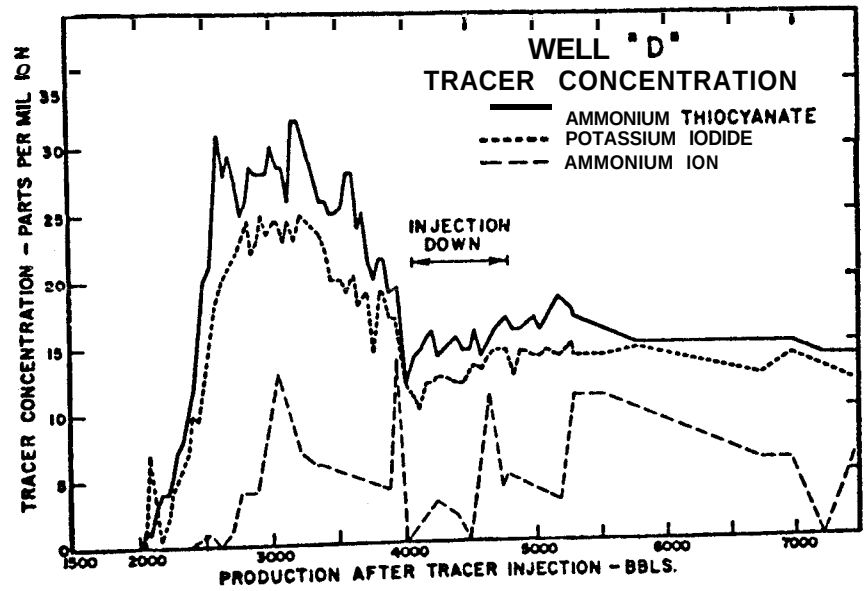

Fig. *4.4:* TRACER ELUTION **CURVES** FOR FIELD TEST (Smith **and** Brigham, 1965)

4.2 ANALYSIS OF TRACER RESULTS

The theoretical model to analyze tracer breakthrough curves developed in this study is based on developed patterns where a complete balance between the amount of injection and production is established. In this pilot pattern, however, the offset wells produced at unequal rates resulting in unequal distribution of injected fluids towards the producing wells. Furthermore, none of the wells received 1/4 of the produced fluid from the central injector. This indicated that the injected material could have taken low velocity routes along streamlines extending beyond the bounds of the five-spot. Figure 4.5 shows qualitatively the streamlines for Well D of the pilot. The area drained by the well does not correspond to one quarter of the five-spot pattern.

The theoretical model can be used to analyze this unbalanced pattern if assumptions regarding the flow lines and the amount of fluid injected into each drainage area can be made. Because the main portion of tracer flow is through the shortest streamtubes, tracer concentrations from the extended streamtubes are small due to dilution by the time fluids reach a production well. This indicates that approximation of the flow lines of the unbounded five-spot pattern by those of a developed one is reasonable.

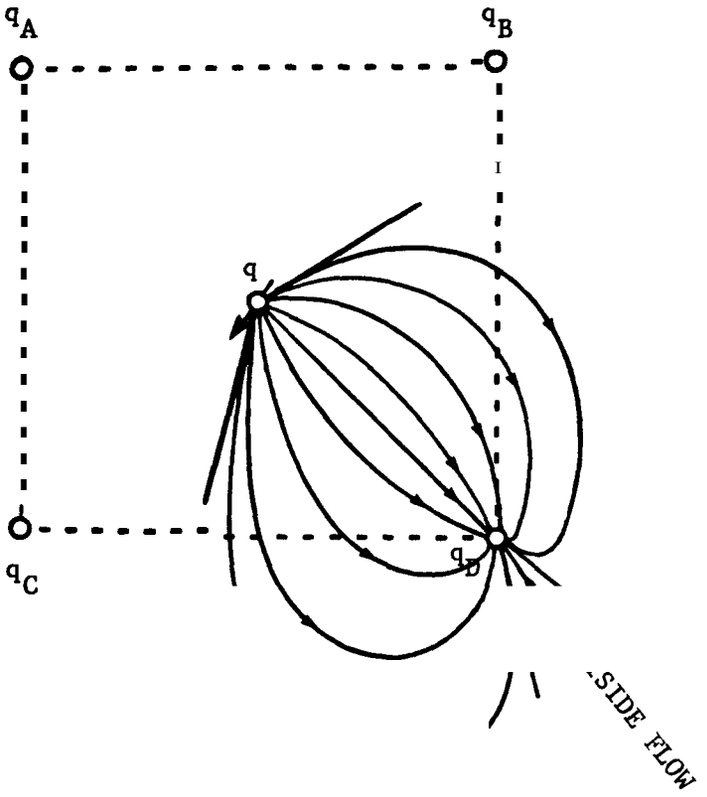

Fig. 4.5: QUALITATIVE STREAMLINES FOR WELL D OF THE PILOT

Distribution of injected fluids among the four producers was calculated by the following procedure. Since Well C did not produce tracer, it was assumed that only 50 BWPD was moving towards this well. This assumption can be justified from a heat balance on Fig. 4.3 from Martin et al. (1968). The remaining 550 BWPD was divided among the other three wells according to the production rates: Well A--225 BWPD, Well C--120 BWPD, and Well D--205 BWPD. The injected tracer was distributed among the drainage areas at a quantity proportional to the assumed rates flowing towards the wells. For example, for Well A the amount of tracer was equal to (225 BWPD) x (200 lbs)/(600 BWPD) = 75 pounds. The area drained by each well however, was assumed to be one quarter of the pattern area (27,225 ft^2). Although this assumption introduces some error in the computation of absolute values of the layer parameters, the relative values (to each other) of layer parameters will remain virtually unchanged as will be demonstrated later.

As a result of flow from outside the pattern, the tracer concentrations had been diluted and the corresponding produced volumes had been increased. Therefore, in the analysis of tracer data, the effect of flow from outside of the pattern on the produced tracer concentration curves was considered. For Well D, the observed concentrations were multiplied by 240/205, and the volumes were divided by 240/205. For Well A, this factor was 260/225.

The optimization routine was used to analyze the tracer production curve from Well D. Thirty four data points from the tracer curve were inputed into the routine. Figure 4.6 shows the match when only five layers were used. The input peak-volumes and the final peak-volumes computed by the routine are

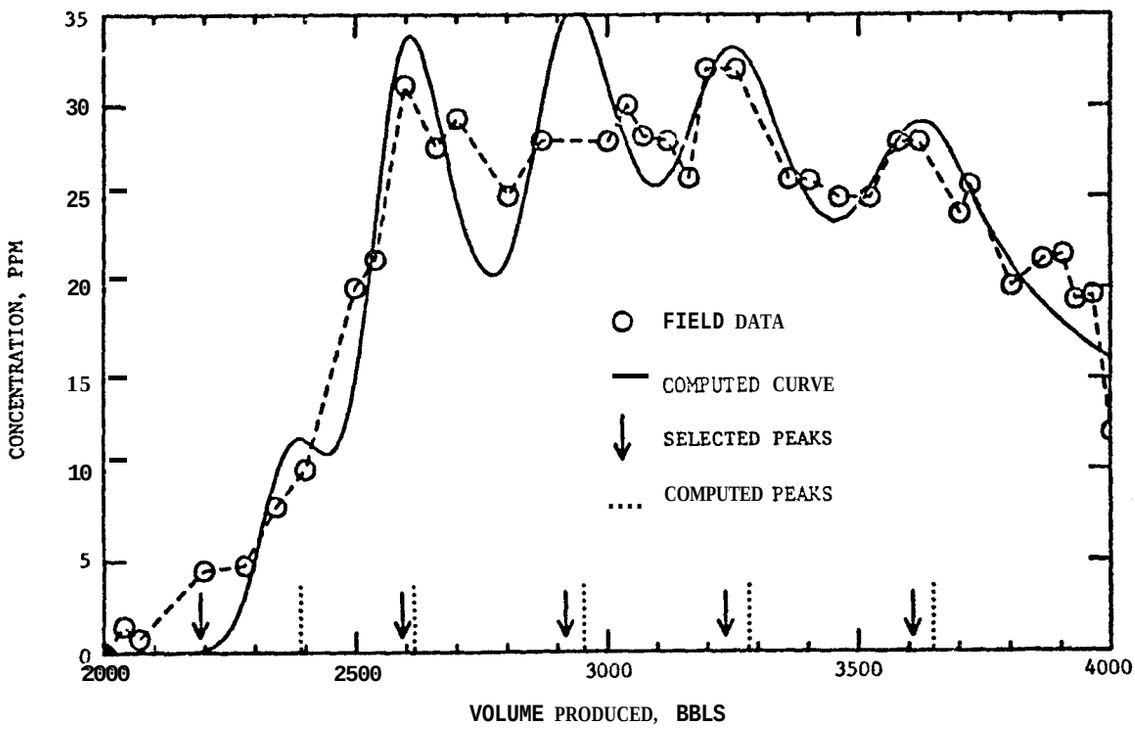

Fig. 4.6: ANALYSIS OF TRACER DATA FOR WELL D WITH FIVE LAYERS

shown on this figure. The shape of the computed curve shows that more layers should improve the match. Figure 4.7 illustrates the new match using seven layers. For this analysis, the peak volumes were chosen at the computed locations in Fig. 4.6 and the additional two peaks were selected at 3050 bbls and 2200 bbls. The match with seven layers shows an improvement over the match with five layers. The analysis was continued with nine and ten layers, each time utilizing the computed peak-locations from the previous match and adding additional peaks in the positions where the greatest divergence was observed between the field data and the match. Figures 4.8 and 4.9 are the matches with nine and ten layers, respectively. The later portion of the field data could not be matched very well as shown in these figures. This is believed to be due to inaccuracy of the field data close to the shut-down time. Table 4.1 shows the results of the analysis with differing numbers of

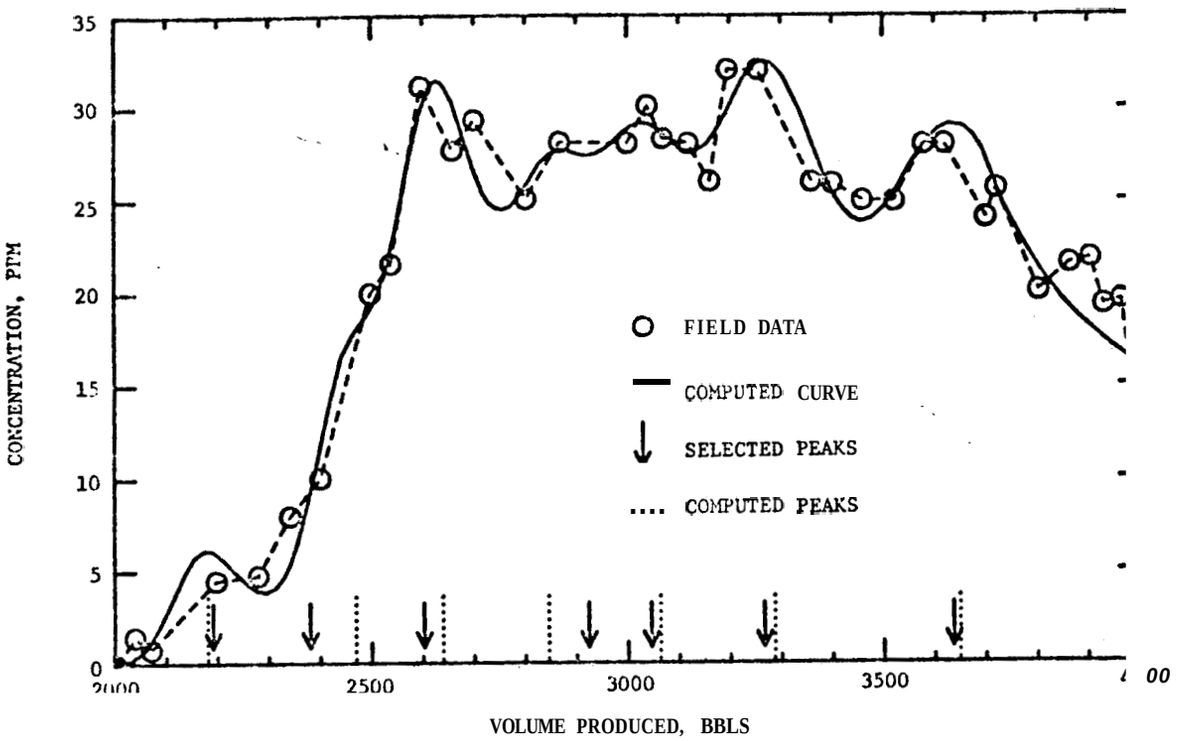

Fig. 4.7: ANALYSIS OF TRACER DATA FOR WELL D WITH SEVEN LAYERS

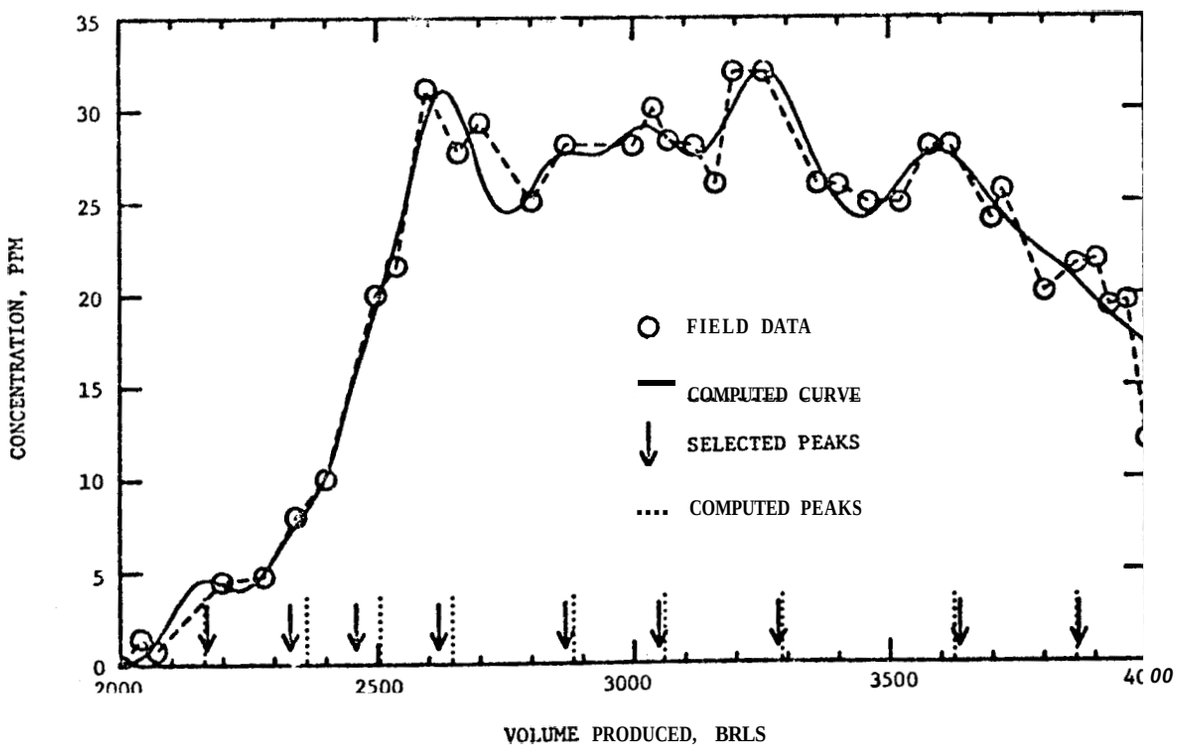

Fig. 4.8: ANALYSIS OF TRACER DATA FOR WELL D WITH NINE LAYERS

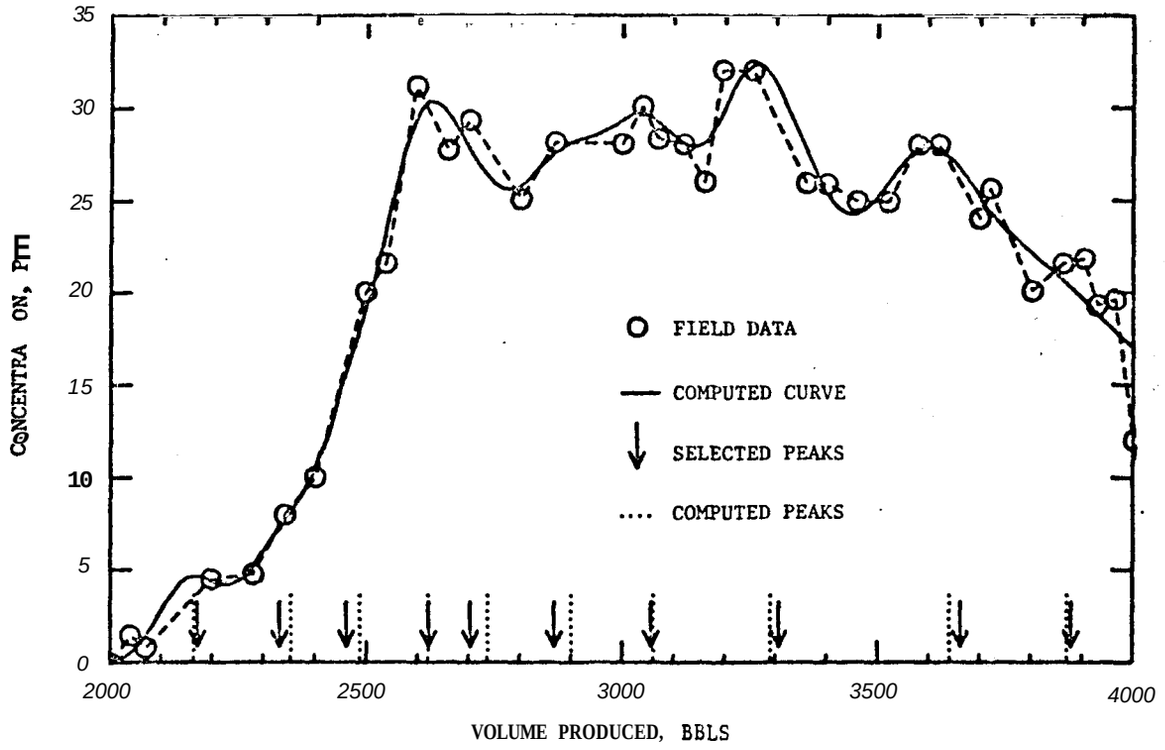

Fig. *4.9:* **ANALYSIS** OF TRACER **DATA** FOR **WELL** D WITH TEN **LAYERS**

Table *4.1*

COMPUTED LAYER PARAMETERS FOR FIELD **TEST,** WELL D, USING THE OPTIMIZATION ROUTINE **WITH** DIFFERENT NUMBER OF **LAYERS**

LAYER	FIVE LAYERS		SEVEN LAYERS		NINE LAYERS		TEN LAYERS	
	ϕh	$\frac{kh}{\Sigma kh}$	ϕh	$\frac{kh}{\Sigma kh}$	ϕh	$\frac{kh}{\Sigma kh}$	ϕh	$\frac{kh}{\Sigma kh}$
1	0.035312	0.033734	0.015658	0.016360	0.011562	0.012167	0.011410	0.012009
2	0.106529	0.092838	0.047419	0.043769	0.015575	0.015031	0.013782	0.013344
3	0.106198	0.082195	0.084410	0.072963	0.041926	0.038131	0.034880	0.031938
4	0.094516	0.066012	0.052945	0.041998	0.078987	0.068042	0.070605	0.061395
5	0.088629	0.055505	0.058256	0.043471	0.052492	0.041585	0.026728	0.022284
6			0.087285	0.060604	0.057068	0.042590	0.047820	0.037617
7			0.087122	0.054503	0.084869	0.058990	0.053306	0.039756
8					0.075888	0.047784	0.084649	0.058840
9					0.021086	0.012465	0.075661	0.047642
10							0.021079	0.012466
SUM	0.431180	0.330280	0.433100	0.333670	0.439450	0.337060	0.439920	0.337290

Table 4.2

COMPUTED PERMEABILITIES AND THICKNESSES OF LAYERS FOR FIELD TEST, WELL D, WITH DIFFERENT NUMBER OF LAYERS*

LAYER	FIVE LAYERS		SEVEN LAYERS		NINE LAYERS		TEN LAYERS	
	h,ft	k,md	h,ft	k,md	h,ft	k,md	h,ft	k,md
1	0.1358	4471	0.0602	4890	0.0445	4925	0.0439	4926
2	0.4097	4078	0.1824	4320	0.0599	4516	0.0530	4531
3	0.4085	3622	0.3248	4044	0.1613	4257	0.1342	4285
4	0.3635	3267	0.2036	3712	0.3038	4032	0.2716	4070
5	0.3409	2931	0.2036	3843	0.2019	3708	0.1028	3902
6			0.3357	3249	0.2195	3493	0.1839	3682
7			0.3351	2928	0.3264	3253	0.2050	3490
8					0.2919	2947	0.3256	3253
9					0.0811	2767	0.2910	2947
10							0.0810	2768

*The k and h values in this table have been computed for ϕ = .26 and Ckh = 18000 md-ft.

layers. In all the cases, the sum of ϕh and the sum of $kh/\Sigma kh$ are almost the same. This is due to conservation of mass by material balance. If layers are assumed to have the same porosity and if an average value for kh of the system is known, the individual permeability and thickness of each layer can also be computed. Table 4.2 presents the computed permeability and thickness of the layers for an average porosity of 0.26, and average permeability thickness product of 18,000 md-ft.

In order to improve the match as much as possible, an attempt was made to optimize the data by using more than ten layers. Each time this was tried, the routine failed to converge. This was found to be due to failure in a built-in matrix manipulation in the VARPRO routine. It appears that the data cannot be matched with more than ten layers. In any case, the match with ten layers, being the final match for Well D, is a satisfactory one. It is worth mentioning that it rook only a small number of iterations in the optimization routine to arrive at these matches with different number of layers. Usually, the number of iterations decreased with an increase in the number of layers.

For example, the match with ten layers was generated with only three iterations. It was also found that the initial estimates required by the routine (input peak volumes) sometimes were important in determining convergences. This was more important with a higher number of layers.

The tracer breakthrough curve for Well A was also matched with ten layers using the optimization routine. For this example, forty-four data points were chosen from the tracer breakthrough curve. Figures 4.10, 4.11 and 4.12 show the matches with five, seven, and ten layers, respectively. Again, the quality of the matches between 4,000 and 4,500 bbls is caused by the inaccurate field data near or during the shut-down period. Table 4.3 shows ϕh and $kh/\Sigma kh$ for the layers, as determined by the program. For a uniform porosity of 0.26 for the entire system and average kh of 18,000 md, the calculated permeabilities and thicknesses of the layers are given in Table 4.4. Comparisons of Tables 4.1 and 4.3 or Tables 4.2 and 4.4 show that the ten layers for each quadrant are somewhat: different for each quadrant. The differences in the formation characteristics calculated are due to independent modeling of each quadrant of the pattern. In other words, the behavior of Well D corresponds to behavior of a well in a ten-layer stratified formation with the parameters given in Table 4.1, while for Well A, the behavior will be predicted by another ten layer formation with parameters of Table 4.3.

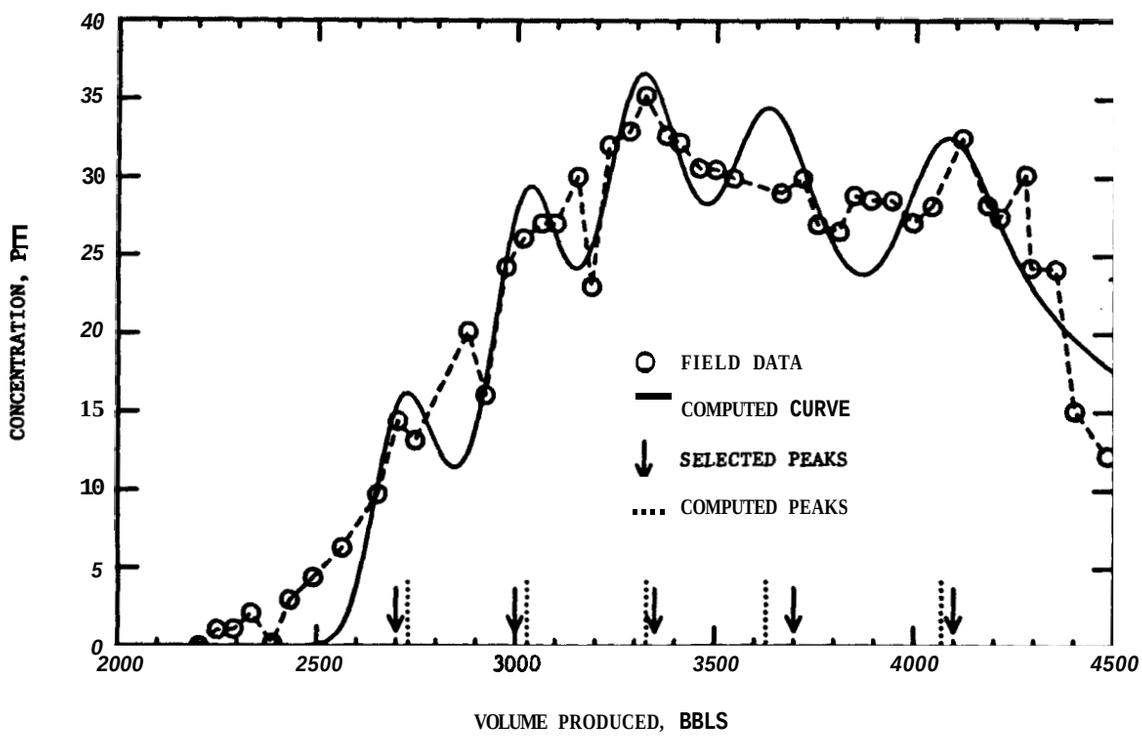

Fig. 4.10: ANALYSIS OF TRACER DATA FOR WELL A WITH FIVE LAYERS

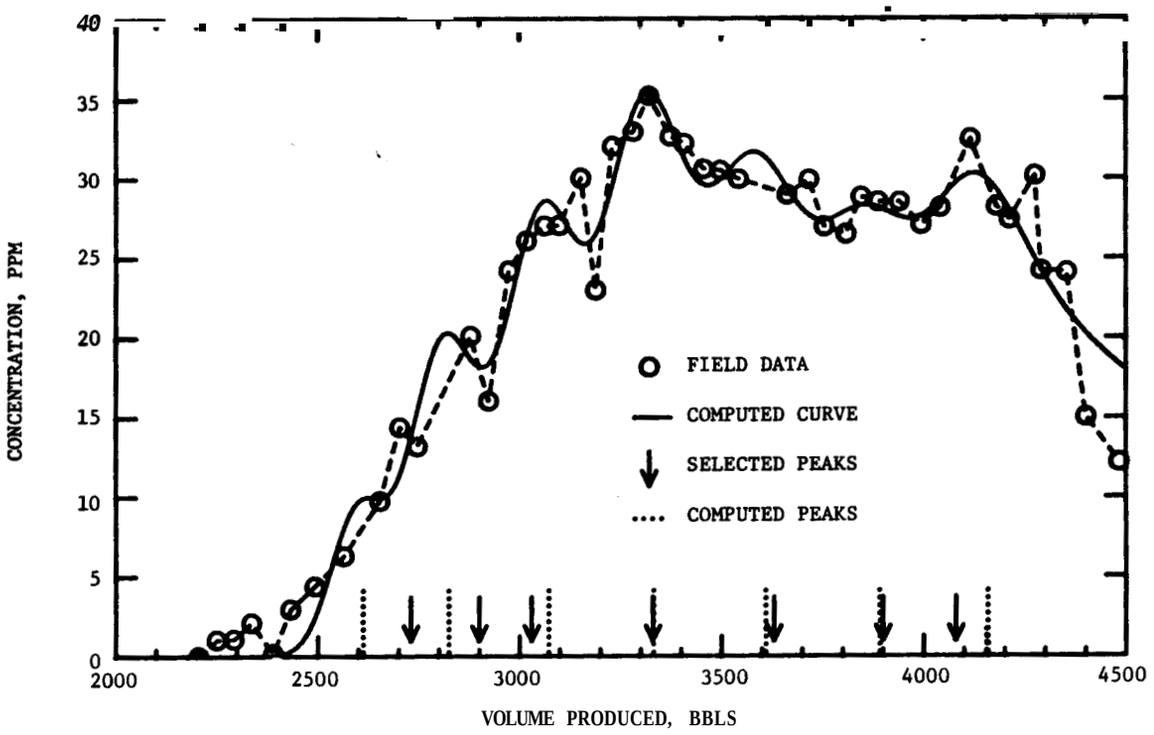

Fig. 4.11: ANALYSIS OF TRACER DATA FOR WELL A WITH SEVEN LAYERS

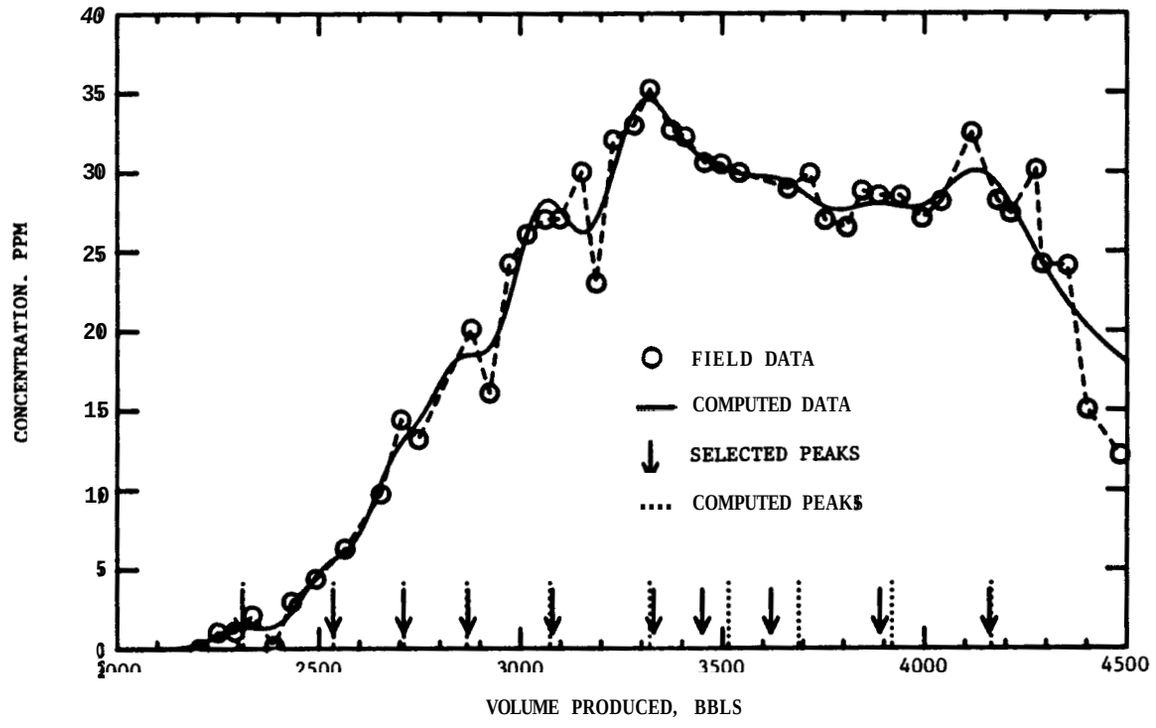

Fig. 4.12: ANALYSIS OF TRACER DATA FOR WELL A WITH TEN LAYERS

Table 4.3

COMPUTED LAYER PARAMETERS FOR FIELD TEST, **WELL A,** USING THE OPTIMIZATION ROUTINE WITH DIFFERENT NUMBER OF LAYERS

LAYER	FIVE LAYERS		SEVEN LAYERS		TEN LAYERS	
	ϕh	$\frac{kh}{\Sigma kh}$	ϕh	$\frac{kh}{\Sigma kh}$	ϕh	$\frac{kh}{\Sigma kh}$
1	0.059200	0.048826	0.032384	0.027887	0.003501	0.003406
2	0.106992	0.079197	0.062602	0.049838	0.014466	0.012830
3	0.127590	0.086185	0.088567	0.064821	0.033026	0.027410
4	0.108782	0.067011	0.114285	0.077143	0.044046	0.035187
5	0.133239	0.073089	0.080341	0.050052	0.085634	0.062662
6			0.066540	0.038455	0.104723	0.070947
7			0.101029	0.054634	0.045561	0.029158
8					0.055029	0.033550
9					0.061547	0.035315
10					0.096968	0.052357
SUM	0.535732	0.354308	0.545748	0.36283	0.545301	0.362822

Table 4.4

COMPUTED PERMEABILITIES AND THICKNESSES OF **LAYERS FOR** FIELD *TEST,* **WELL A,** WITH DIFFERENT NUMBER OF LAYERS

LAYER	FIVE LAYERS		SEVEN LAYERS		TEN LAYERS	
	h,ft	k,md	h,ft	k,md	h,ft	k,md
1	0.2277	3860	0.1246	4030	0.0135	4553
2	0.4115	3464	0.2408	3726	0.0556	4151
3	0.4905	3163	0.3406	3425	0.1270	3884
4	0.4184	2883	0.4396	3159	0.1725	3672
5	0.5125	2567	0.3090	2916	0.3294	3425
6			0.2559	2704	0.4028	3171
7			0.3886	2530	0.1752	2995
8					0.2117	2853
9					0.2367	2685
10					0.3730	2527

To investigate the effect of drainage areas on the analysis, the tracer data of Well A was recalculated using an estimated drained area of 40,800 ft^2 rather than 27,225 ft^2 as used before. This value was computed by dividing the pattern area into segments proportional to the amounts of fluids moving towards the wells, as has been suggested by Deppe (1961). The match based on this drainage area and ten layers was virtually identical to Fig. 4.12. Table 4.5 presents the parameters of the layers computed from this match. The permeability values all are greater than those in Table 4.3 by a factor of 40,800/27,225 = 15 (ratio of the assumed drainage areas); however, the relative values of permeabilities in Tables 4.2 and 4.5 are identical.

In summary, the tracer interpretation method developed in this study can provide valuable detailed information on reservoir characterization. Although the method is for developed patterns, its application to an unbounded, unbalanced five-spot pattern was illustrated in this section. The approximations made in analyzing the field data produced errors on the computed values of reservoir parameters, However, a method similar to the one presented in this study can be developed to incorporate the actual flow field of the pilot pattern with the tracer mixing equations, and thereby generate more precise results.

Table 4.5

COMPUTED PARAMETERS OF LAYERS FOR WELL A WITH TEN LAYERS AND DRAINAGE AREA OF 40,800 FT^2

LAYER	ϕh	$kh/\Sigma kh$	h,ft	k,md
1	0.002336	0.003406	0.0090	6824
2	0.009530	0.012830	0.0371	6220
3	0.022038	0.027410	0.0848	5821
4	0.029925	0.035187	0.1151	5503
5	0.057142	0.062662	0.2198	5132
6	0.069879	0.070947	0.2688	4752
7	0.030402	0.029158	0.1169	4488
8	0.036720	0.033550	0.1412	4276
9	0.041069	0.035315	0.1580	4024
10	0.064705	0.052357	0.2489	3788
SUM	0.363869	0.362822		

5. CONCLUSIONS

1, Equations were derived which describe the concentration of a tracer slug in a general streamtube for any flow system with mobility ratio of one. In the derivation of these equations, the mixing coefficient was assumed to be proportional to fluid velocity which was a function of location in the streamtube. The proportionality constant is the longitudinal dispersion constant of the porous medium. Transverse dispersion and molecular diffusion were assumed to be negligible.

2. By integrating individual streamtube-tracer concentration expressions over several developed patterns, analytic expressions were obtained which define the tracer breakthrough curves for each of these homogeneous developed patterns.

3. The study shows that the tracer breakthrough curves from a homogeneous system depend upon the geometry, pattern size, and dispersion constant of the formation rock.

4. In the derivation of equations for effluent tracer concentrations from patterns, it was also necessary to derive expressions for pattern breakthrough curves from developed patterns. Exact analytical equations were obtained in the form of elliptic integrals which describe several pattern breakthrough curves for a mobility ratio of unity. Results for different patterns were reduced into a single curve by defining a simple correlating parameter, which we have called the dimensionless pore volume. Because the breakthrough curves for various developed patterns considered in this study correlate as a single curve, it is concluded that the breakthrough curve for <u>any</u> repeating pattern should also lie on this same correlation.

5. An attempt was made to define analytically pattern breakthrough curves for mobility ratios other than one. It was assumed that the streamlines were independent of mobility ratio. For a developed five-spot, the analysis generated nearly identical values for breakthrough areal sweep efficiencies at any mobility ratio. This result is in direct conflict with experimental observations. Hence, the assumption of no streamline change with mobility ratio is.unrealistic.

6. Tracer breakthrough curves from several patterns were also correlated as a single set of curves using the Peclet number, a/α, as a parameter. The correlation was achieved by obtaining two sets of correction factors--one for a/a to determine peak-locations, and another for peak concentration. These correction factors convert all the patterns studied into equivalent five-spot systems.

7, A computer program was developed which analyzes tracer breakthrough Curves from stratified reservoirs, and computes porosity thicknesses and fractional permeability thicknesses of the layers, The algorithm utilizes a non-linear least-squares routine as an optimization technique to minimize

the differences between observed tracer data and computed concentrations and, hence, generates an optimum match for a given number of layers. Also incorporated in the algorithm are the correction factors developed in correlation of the tracer curves. As input, the program requires the estimated number of layers, volume of the produced fluid corresponding to each peak, and the type of pattern.

8. Tracer breakthrough curves from a field test on a five-spot pilot have been matched closely using this optimization program with ten layers. This example showed that tracer data furnish information about the high permeability zones of the reservoir.

9. The method developed in this study can also be used in design of well-to-well tracer tests. The amount of tracer required and tracer breakthrough times may be computed from the method presented herein.

6. RECOMMENDATIONS FOR FUTURE WORK

The method presented in this study considers only developed patterns. Because streamlines of a system with any well arrangement for unit mobility ratio are computable, the method can be extended to include analysis of tracer response curves from isolated and irregular patterns. Therefore, the tracer curves from the field example can be analyzed using actual flow lines of the system. Comparison of the results with those computed in this study would illustrate the accuracy of approximating an open system by a developed pattern.

Further work is necessary to compute tracer flow in systems where a contrast between the mobility of tracer solution and the mobilities of formation fluid and chase fluid exists. Because the pattern breakthrough curves at mobility ratios other than one could not be generated accurately by the streamtube procedure, it appears that numerical schemes should be adopted to compute tracer breakthrough curves. However, numerical dispersion associated with these schemes will likely mask the effects of physical tracer dispersion. One possible solution would be to incorporate the tracer mixing equations illustrated in this study with numerically pre-determined front locations to generate tracer concentration profiles. Viscous fingering associated with unstable displacement would further complicate the analysis.

Finally, tracer adsorption, reaction, and partitioning effects should be incorporated in the development of rigorous tracer interpretation techniques to generate precise results. Before these variables can be incorporated into mathematical models, more laboratory work is necessary to increase the understanding of how each affects tracer flow.

NOMENCLATURE

A = area, ft^2

a = distance between like wells, L

C_o = initial tracer concentration, mass fraction

C_a = formation fluid concentration in the tracer dispersed zone, mass fraction

C_b = chase fluid concentration in the trace dispersed zone, mass fraction

C, $C(\theta)$ = tracer concentration in a streamtube, mass fraction

C_{max} = maximum tracer concentration in the tracer breakthrough curve from a homogeneous pattern, mass fraction

$\overline{C}$ = effluent tracer concentration from a homogenenous or a stratified pattern, mass fraction

C_D = dimensionless tracer Concentration from a homogeneous pattern

$\overline{C}_{Dj}$ = dimensionless tracer concentration from layer j

$(\overline{C}_D)_{j,i}$ = dimensionless tracer concentration from layer j at sample point i

$\overline{C}_{D,\ max}$ = dimensionless maximum tracer concentration from a homogeneous pattern

$\overline{C}_j$ = effluent tracer concentration from layer j, mass fraction

$\overline{C}_{j,i}$ = effluent tracer concentration from layer j at sample point i, mass fraction

$\overline{C}_i$ = effluent tracer concentration from a multi-layered system, computed at sample point i, mass fraction

C_i^* = effluent tracer concentration from a multi-layered system observed at sample point i, mass fraction

D = molecular diffusion coefficient, L^2/T

D' = apparent molecular diffusion coefficient, L^2/T

d = distance between unlike wells, L

d_p = average grain size diameter, L

$d\sigma$ = differential change in standard deviation term used in mixing equation

E_A = areal sweep efficiency, fraction of pattern area

E_{Abt} = breakthrough areal sweep efficiency, fraction of pattern area

E_{AD} = dimensionless areal sweep efficiency, a correlating parameter

erfc (x) = complementary error function = 1 − erf (x)

$$\text{erf}(x) = \frac{2}{\sqrt{\pi}} \int_0^x e^{-\xi^2}\, d\xi$$

F = formation resistivity factor, dimensionless

f_D = displaclng fluid cut in the production stream, fraction

f = flowing volume of porous medium in the capacitance model, fraction of total pore volume

1 − f = stagnant or dead-end-pore volume, fraction of total pore volume

f_m = multiplier on peak concentration for tracer breakthrough curves from homogeneous systems

f_p = multiplier on a/a to convert patterns into equivalent developed five-spot

F_r = tracer slug size injected into a homogeneous pattern in terms of fraction of pattern displaceable pore volume, dimensionless

F_{rj} = tracer slug size injected into layer j in terms of fraction of layer displaceable pore volume, dimensionless

$F(\nu,\kappa)$ = incomplete elliptic integral of the first kind

$$= \int_0^{\nu} \frac{d\xi}{\sqrt{1 - \kappa^2 \sin^2 \xi}} = \int_0^{y} \frac{dt}{\sqrt{(1 - t^2)(1 - \kappa^2 t^2)}}$$

where $y = \sin \nu$

h = thickness, ft

h_j = thickness of layer j

I, $I(\psi)$ = mixing line integral for streamline ψ

k = permeability, md

k_j = permeability of layer j, md

k_h = permeability of a homogeneous pattern, md

k_p = permeability of the most permeable layer, md

K = effective mixing coefficient, L^2/T

K_L = effective longitudinal mixing coefficient, L^2/T

K_m = mass transfer coefficience in the capacitance model, $L^{2/T}$

K_T = effective transverse mixing coefficient, L^2/T

K(m), K'(m) = complementary and incomplementary complete elliptic integrals of the first kind

m, m_1 = parameters of the Jacobian elliptic functions and elliptic integrals, $m + m_1 = 1$

m_T = mass of tracer injected to a pattern, lbs

N = number of data points used in the optimization routine

n = number of layers in the multilayered model

p = pressure

PV_D = dimensionless pore volume, a correlating parameter

q = flow rate in the sfreamtube, L^3/T

q_t = total injection rate into a homogeneous pattern, L^3/T

R = average grain diameter, L

r = radius, L

$\bar{r}$ = front location in radial flow, L

S_w = water saturation, fraction of pore volume

s = dfstance along the etreamline, L

s_A, s_B = distances along a streamline up to points A and B on the streamline, L

$\bar{s}$, $\bar{s}_1$, $\bar{s}_2$ = front locations in the streamtubes, L

sn, cn, dn = elementary Jacobian elliptic functions

t = injection time, T

t_{bt} = breakthrough time of a streamline, T

t_{ph} = injection time necessary to reach the peak in tracer breakthrough curve from a homogeneous pattern, T

t_{pp} = time to peak of the most permeable layer, T

v = microscopic (pore) velocity, darcy velocity divided by porosity, L/T

v_x = microscopic velocity component in the x direction, L/T

v_Y = microscopic velocity component in the y direction, L/T

V = displaceable pore volume of a streamtube, L^3

$\bar{V}$ = displaceable pore volume of a streamtube up to tracer front location in the tube, L^3

$(V_{T,max})_j$ = volume corresponding to the jth peak in an observed (field) tracer profile, bbls

V_{max} = volume of chase fluid injected into a homogeneous pattern corresponding to the peak location in tracer response, L^3

V_p = total volume of chase fluid injected into a homogeneous pattern, L^3

V_{pbt} = total volume of chase fluid injected into a homogeneous pattern at a breakthrough of a streamline, L^3

$V_{pDbt}(\psi)$ = displaceable pore volume of displacing fluid injected at breakthrough of a streamline, $, dimensionless

V_{pDbt} = breakthrough pore volume or breakthrough areal sweep efficiency of a pattern, dimensionless

V_{pD} = displaceable pore volume injected into a homogeneous pattern, dimensionless

$(V_{pD})_j$ = displaceable pore volume injected into layer j, dimensionless

$(V_{pD})_{j,i}$ = displaceable pore volumes injected into layer j at sample point i, dimensionless

$V_{pD,max}$ = displaceable pore volume corresponding to the peak location in tracer response from homogeneous system, dimensionless

V_T = total volume injected into a pattern, bbls

$(V_T)_i$ = total volume injected into the pattern at sample point i, bbls

$(V_{T,max})_j$ = volume at the jth peak in the observed tracer profile, bbls

V_{Tr} = total volume of tracer slug injected into either homogeneous or layered pattern, ft^3

V_{tr} = tracer volume injected into a streamtube, ft^3

w = width of a streamtube, L

x = distance in a linear flow, L

$\bar{x}$ = front location in a linear displacement, L

X_j = j^{th} linear parameter in the optimization program

Y, $Y(\psi)$ = the integral in the equation of line integral

z_j = j^{th} non-linear parameter in the optimization program

$(z_j)_{est}$ = initial estimate of non-linear parameters

α = hydrodynamic dispersion constant, L

α_L = longitudinal dispersion constant, L

α_T = transverse dispersion coefficient, L

ε^2 = characteristic constant of the laboratory core packs

As = undiluted width of tracer in a streamtube, L

ϕ = porosity, fraction

ϕ_j = porosity of layer j, fraction

ρ_T = density of tracer solution, lb/ft^3

μ = viscosity, cp

σ, σ_1, 42 = standard deviation, measure of the length of mixed zone, L

ψ = stream function or value of a streamline

Φ = potential function

κ = modulus of an incomplete elliptic integral, where modulus is equal to the square root of parameter

Ω = complex potential

ν = argument of an incomplete elliptic integral

υ = strength of a source or a sink

REFERENCES

Abramowitz,' M., and Stegun, I. A.: "Handbook of Mathematical Functions," Dover Publications, Inc., New York (1972).

Aris, R., and Amundson, N. R.: "Some Remarks on Longitudinal Mixing or Diffusion in Fixed Beds," AIChE Jour. (1957), 3, 280.

Aronofsky, J. S., and Heller, J, P.: "A Diffusion Model to Explain Mixing of Flowing Miscible Fluids in Porous Media," Trans. AIME (1957), 210, 345–349.

Baldwin, D. E., Jr.: "Prediction of Tracer Performance in a Five–Spot Pattern," J. Pet. Tech. (April 1966), 513-517.

Bear, J.: "Dynamics of Fluids in Porous Media," Elsevier, New York (1972).

Bentsen, R. G., and Nielsen, R. F,: "A Study of Plane, Radial Miscible Displacement in a Consolidated Porous Medium," Soc. Pet. Eng. J. (March 1965), 1-5.

Blackwell, R. J.: "Laboratory Studies of Microscopic Dispersion Phenomena," Soc. Pet. Eng. J. (March 1962), 1–8.

Brigham, W. E., Reed, P. W., and Dew, J. N: "Experiments on Mixing During Miscible Displacements in Porous Media," Soc. Pet. Eng. J. (March 1961), 1-8.

Brigham, W. E., and Smith, D. H: "Prediction of Tracer Behavior in Five–Spots," Paper SPE 1130, presented at the 40th Annual Fall Meeting of SPE–AIME, Denver, Colorado, Oct. 1965.

Brigham, W. E.: "Mixing Equations in Various Geometries," SPE Paper 4585, presented at the 48th Annual Fall Meeting of SPE–AIME, Las Vegas, Nevada, Sept. 30–Oct. 3, 1973.

Brigham, W. E.: "Mixing Equations in Short Laboratory Cores," Soc. Per. Eng. J. (Feb. 1974), 91–99.

Brown, S L., and Brigham, W. E: "Further Results Determining Permeability and Thickness for Multilayer Five–Spot Tracer Test," SUPRI-TR-17 (DOE/ET/1205-17), Feb. 1981.

Byrd, P. F., and Friedman, M. D.: "Handbook of Elliptic Integrals for Scientists," Lange, Maxwell and Springer, Ltd., London (1954).

Carpenter, P. G., Morgan, T. D., and Parsons, E. D: "Use of Boron Compounds as Water Flood Tracers," Prod. Monthly (1952), 16, No. 12, 12–19.

Caudle, B. H., and Witte, M. D.: "Production Potential Changes During Sweep-Out in a Five-Spot System," Trans. AIME (1959), 216, 446.

Coats, K. H, and Smith, B. D.: "Dead-End Pore Volumes and Dispersion in Porous Media," Soc. Pet. Eng. J. (March 1964), 73-84.

Craig; F.: . "Reservoir Engineering Aspects of Waterflooding," SPE Monograph No. 3, (1971), Dallas, Texas.

Craig, F. F., Jr., Geffen, T. M., and Morse, R. A.: "Oil Recovery Performance of Pattern Gas or Water Injection Operations from Model Tests," Trans. AIME (1955), 204, 7-15.

Deans, H. A: "A Mathematical Model for Dispersion in the Direction of Flow in Porous Media," Trans. AIME (1963), 228, 49-52.

Deppe, J. C.: "Injection Rate - The Effect of Mobility Ratio, Area Swept and Pattern", Soc. Pet. Eng. J. (June 1961), 81-91.

D'Hooge, J. A., Sheely, C. Q, and Williams, B. J.: "Interwell Tracers--An Effective Reservoir Evaluation Tool: West Sumatra Field Results," J. Pet. Tech. (May 1981), 779-782.

Douglas, J., Jr, Peaceman, D. W., and Rachford, H. H.: "A Method for Calculating Multi-Dimensional Immiscible Displacement," Trans. AIME (1959), 216, 297-308.

Dyes, A. B., Caudle, B. H., and Erickson, R. A: "Oil Production after Breakthrough as Influenced by Mobility Ratio," J. Pet. Tech., (April 1954), 27-32.

Dykstra, H, and Parsons, R. L.: "The Prediction of Waterflood Performance with Variation in Permeability Profile," Prod. Monthly, (1950), 14, 9-12.

Elkins, L. F., and Skov, A. M.: "Some Field Observations of Heterogenekty of Reservoir and Its Effects on Oil Displacement Efficiency," Paper SPE 282, presented at SPE Production Research Symposium, Tulsa, Okla., April 1962.

Fay, C. H, and Prats, M.: "The Application of Numerical Methods to Cycling and Flooding Problems," Proceedings from Third World Petroleum Congress (1951), Section 11, 555-564.

Fitch, R. A, and Griffith, J. D.: "Experimental and Calculated Performance of Miscible Floods in Stratified Reservoirs," J. Pet. Tech. (Nov. 1964), 1289-1298.

Gelhar, L. W., and Collins. M. A.: "General Analysis of Longitudinal Dispersion in Nonuniform Flow," Water Res. Research (Dec. 1971), 7, No; 6, 5111-1521.

Gradshteyn, 1. S, and Ryzhik, I. M.: "Table of Integrals, Series, and Products," Accademic Press, Inc., New York (1980).

Guckert, G. L.: "Areal Sweepout Performance of Seven- and Nine-Spot Flood Patterns," M.S. Thesis, Pennsylvania State University, Pennsylvania (Jan. 1961).

Handy, L. L.: "An Evaluation of Diffusion Effects in Miscible Displacement," Trans. AIME (1959), 216, 382-384.

Halevy, E., and Nir, A.: "The Determination of Aquifer Parameters with the Aid of Radioactive Tracers," J. Geophys. Res. (June 1962), 67, No. 6, 2403-2409.

Harleman, R. F., and Rumer, R. R: "Longitudinal and Lateral Dispersion in an Isotropic Porous Medium," J. Fluid Mech. (1963), 3, No. 16, 385-394.

Hauber, W. C.: "Prediction of Waterflood Performance for Arbitrary Well Patterns and Mobility Ratios," J. Pet. Tech. (Jan. 1964), 95-103.

Hearn, C. L.: "Simulation of Stratified Waterflooding by Pseudo Relative Permeability Curves," J. Pet. Tech. (July 1971), 805-813.

Higgins, R. V., and Leighton, A. J.: "A Computer Method to Calculate Two-Phase Flow in Any Irregularly Bounded Porous Medium," J. Pet. Tech. (June 1962), 679-682.

Horne, R. N.: "Geothermal Reinjection Experience in Japan," Paper SPE 9925, presented at the 1981 California Regional Meeting of SPSE, Bakersfield, California, March 1981.

Horne, R. N., and Rodriguez, F.: "Dispersion in Tracer Flow in Fractured Geothermal Systems," Proceedings (1981), 7th Annual Stanford Geothermal Workshop.

Hutchinson, C. A., Jr.: "Reservoir Inhomogeneity Assessment and Control," Pet. Eng. (1959), 31, B19-B26.

Ivanovich, M., and Smith, D. B.: "Determination of Aquifer Parameters by a Two-Well Pulsed Method Using Radioactive Tracers," Jour. of Hydrology (1978), 36, 34-45.

Koch, H. A., Jr., and Slobod, R. L.: "Miscible Slug Process," Trans. AIME (1957), 210, 40.

Lau, L. K., Kaufman, W. J., and Todd, D. K.: "Dispersion of a Water Tracer in Radial Laminar Flow Through Homogeneous Porous Media," Progress Report No. 5, Sanitary Engineering Research Lab., U. of California at Berkeley, (1959).

Levorsen, A. I.: "Geology of Petroleum," W. H. Freeman and Company, San Francisco (1956).

Martin. W. L., Dew. J. N.. Powers, M. L., and Steves, H. B.: "Results of a Tertiary Hot Waterflood in a Thin Sand Reservoir," J. Pet. Tech. (July 1968), 739-750.

Mercado A, and Halevy, E: "Determining the Average Porosity and Permeability of a Stratified Aquifer with the Aid of Radioactive Tracers," Water Res. Research (1966), 2, No. 3, 525-531.

Morales, E. C: "A First Step to Obtain a Single Correlation Characterizing the Different Patterns in Waterflooding," MS. Thesis, Stanford University, Stanford, California (June 1975).

Morel-Seytoux, H. J: "Analytical-Numerical Method in Waterflooding Predictions," Soc. Pet. Eng. J. (Sept. 1965), 247-258.

Morel-Seytoux, H. J: "Unit Mobility Ratio Displacement Calculations for Pattern Floods in Homogeneous Medium," Soc. Pet. Eng. J. (Sept. 1966), 217-227.

Morgan, H. T: "A Single Correlation Characterizing Areal Sweep for the Different Patterns in Waterflooding after Breakthrough," MS. Thesis, Stanford University, Stanford, California (June 1977).

Muskat, M: "Physical Principles of Oil Production," McGraw-Hill Book Company, Inc., New York (1949).

Ogata, A.: "Dispersion in Porous Media," Ph.D. Thesis, Northwestern Univ., Evanston, Ill. (1958).

Ogata, A., and Banks, R. B: " A Solution of the Differential Equation of Longitudinal Dispersion in Porous Media," U. S. Geol. Surv. Prof. Pap. (1961), 411-A.

Prats, M: "The Breakthrough Sweep Effeciency of a Staggered Line Drive," Trans. AIME (1956), 207, 361-362.

Prats, M, Strickler, W. R., and Mathews, C. S: "Single-Fluid Five-Spot Floods in Dipping Reservoirs," Trans. AIME (1955), 204, 160-174.

Raimondi, P., Gardner, G. H. F., and Petrick, C. B: "Effect of Pore Structure and Molecular Diffusion on the Mixing of Miscible Liquids Flowing in Porous Media," Paper 43, AIChE-SPE joint Symposium, National AIChE Meeting, San Francisco, Dec. 6-9, 1959.

Sauty, J. P.: "Analysis of Hydrodispersive Transfer in Aquifers," Water Res. Research (Feb. 1980), 16, No 1, 145-158.

Smith, D. H, and Brigham, W.E: "Field Evaluation of Waterflood Tracers in a Five-Spot,'' Prod. Monthly (Aug. 1965), 8-12.

Spiegel, R. M: "Complex Variables," Schaum's Outline Series, McGraw-Hill Book Company (1964).

Sturm, P. W, and Jonhson, W. E: "Field Experiments with Chemical Tracers in Flood Waters," Prod. Monthly (1951), 15, No. 2, 11-18.

Taylor, G. I: "Dispersion of Soluble Matter in Solvent Flowing Slowly Through a Tube," Proc. Royal Soc. (1953), 186-203.

Tester, J. N, Bivins, R. L, and Potter, R. M: "Interwell Tracer Analysis of a Hydraulically Fractured Granitic Geothermal Reservoirs," Paper SPE 8270, presented at the SPE-AIME 54th Annual Fall Meeting, Las Vegas, Nevada, Sept. 1979.

von Rosenburg, D. U: "Mechanics of Steady-State Single-phase Fluid Displacement from Porous Media," AIChE Jour. (March 1956), 2, No. 1, 55

Wallick. G. C. and Jenkins, R: "Analysis of Short-Time Tracer Injection in Underground Formations," Jour. Applied Physics (Dec. 1954), 25, No. 12, 1491-1496.

Wagner, O. R: "The Use of Tracers in Diagnosing Interwell Reservoir Heterogeneities — Field Results," J. Pet. Tech. (Nov. 1977), 1410-1416.

Wu, C. H.: "Comparison of Five-Spot Areal Sweep Efficiency Calculation Procedure to Model Performance for Mobility Ratio Other than One," M.S. Thesis, Colorado School of Mines, Golden, Calorado (May 1964).

Yuen, D. L, Brigham, W. E, and Cinco-Ley, H.: "Analysis of Five-Spot Tracer Tests to Determine Reservoir Layering," DOE Report SAW 1265-8 (Feb. 1979), 60.

Zaghi, N: "Effect of Injection Production Doublets in Shielding Coastal Aquifers from Brine Intrusion," Ph.D. Dissertation, Stanford University, Stanford, California (May 1977).

Zeito, A. G: "Interbedding of Shale Breaks and Reservoir Heterogeneities," J. Pet. Tech. (Oct. 1965), 1223-1228.

APPENDICES

There are four appendices in this section, most consisting of several sub-appendices. The first set, Appendix A, provides derivations of the analytic equations for several pattern breakthrough curves at a mobility ratio of unity. An extension of the analysis to a developed five-spot pattern at an arbitrary mobility ratio is provided in Appendix B. The third set, Appendix C, illustrates evaluation of the line integral embodied in the equations of tracer concentration profiles. The computer program developed to analyze tracer breakthrough curves from stratified reservoirs is provided in Appendix D. Also given in Appendix D are the programs to compute pattern breakthrough curves of a developed, inverted seven-spot at unit mobility ratio and a developed five-spot at any mobility ratio.

Appendix A

DERIVATION OF EQUATIONS FOR PATTERN BREAKTHROUGH CURVES FOR MOBILITY RATIO OF ONE

This appendix consists of five sub-appendices. The first four present the development of mathematical equations to define pattern breakthrough curves of staggered line drive, five-spot, direct line drive and inverted seven-spot. All the patterns are bounded and the mobility ratio of displacement is equal to one. The last appendix of this section details derivation of some equations used in Appendices A.1 and A.3.

When formulating the equations for fluid flow in any pattern, potential equations or stream functions are required. A basic theory of potentials is briefly presented in the following paragraphs. Application of the theory to specific patterns is then illustrated in the pertinent sub-appendices.

From the theory of incompressible and irrotational fluid flow in two dimensions, it follows that:

$$\Omega(z) = \Phi(x,y) + i\,\psi(x,y) \qquad \text{(A-1)}$$

where,

$\Omega(z)$ = complex potential

$\Phi(x,y)$ = velocity potential equation

$\psi(x,y)$ = stream function

$z = x + iy$

Both $\Phi(x,y)$ and $\psi(x,y)$ are harmonic functions; therefore, they satisfy the Laplace equation. From the Cauchy–Riemann principle and Darcy's law, the velocity components of fluid at any point are related to the potential equation and the stream function as follows:

$$v_x(x,y) = \frac{k}{\mu}\frac{\partial\Phi}{\partial x} = \frac{k}{\mu}\frac{\partial\psi}{\partial y} \qquad \text{(A-2)}$$

and,

$$v_y(x,y) = \frac{k}{\mu}\frac{\partial\Phi}{\partial y} = -\frac{k}{\mu}\frac{\partial\psi}{\partial x} \qquad \text{(A-3)}$$

where, k is the permeability and μ is the fluid viscosity.

The complex potential for a line source (injection well) in an infinite medium under steady state condition is:

$$\Omega(z) = \upsilon \ln z \qquad \text{(A-4)}$$

where, υ is the strength of the source and z is the distance of a point from the origin of a coordinate system positioned on the source. If the source is located at a distance z_o from the origin of a specified coordinate system, $\Omega(z)$ is given by:

$$\Omega(z) = \upsilon \ln (z - z_o) \qquad \text{(A-5)}$$

The complex potential due to a sink (production well) is subsequently given by the negative of either Eq. A-4 or Eq. A-5.

Since the complex potential defined by Eq. A-1 satisfies the Laplace equation, the superposition principle can be used to obtain the complex potential for any combination of injectors and producers. For a system of n_1 injectors located at points a_i ($i = 1, \ldots, n_1$) and n_2 producers positioned at b_j ($j = 1, \ldots, n_2$), the overall complex potential at any point, z, is:

$$\Omega(z) = \sum_{i=1}^{n_1} \upsilon_{ai} \ln (z - a_i) - \sum_{j=1}^{n_2} \upsilon_{bj} \ln (z - b_j) \qquad \text{(A-6)}$$

The terms υ and υ_{bj} denote the strength of the injectors and producers, respectively? Equation A-6 can be used to derive $\Omega(z)$ for any well arrangement. However, for some particular well patterns, the use of conformal mapping greatly eases the determination of complex potentials. This is illustrated in Appendices A.1 and A.3.

Appendix A.1: STAGGERED LINE DRIVE

Consider a repeated staggered line drive pattern as shown in Fig. A-1:

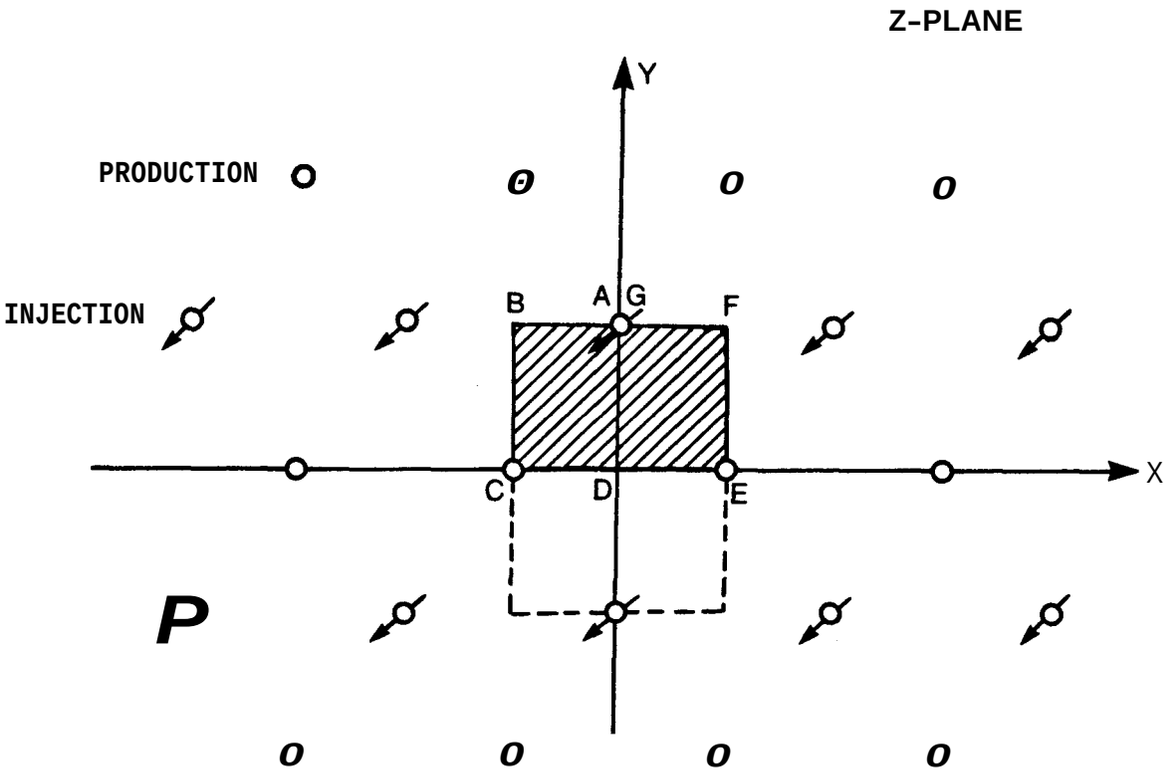

Fig. A-1: A DEVELOPED STAGGERED LINE DRIVE IN Z-PLANE

Using the following conformal transformation (Spiegel, 1964):

$$z = \int_0^w \frac{dt}{\sqrt{(1 - t^2)(1 - m\,t^2)}} \qquad 0 < m < 1 \qquad \text{(A-7)}$$

the shaded segment in Fig. A-1 is transformed into the upper half-plane of the w-plane as shown in Fig. A-2. The production wells are mapped at $w = 1$ and $w = -1$, the "corners" of the pattern (B and F) are mapped at $\pm \sqrt{1/m}$, and the injection well is mapped at infinity.

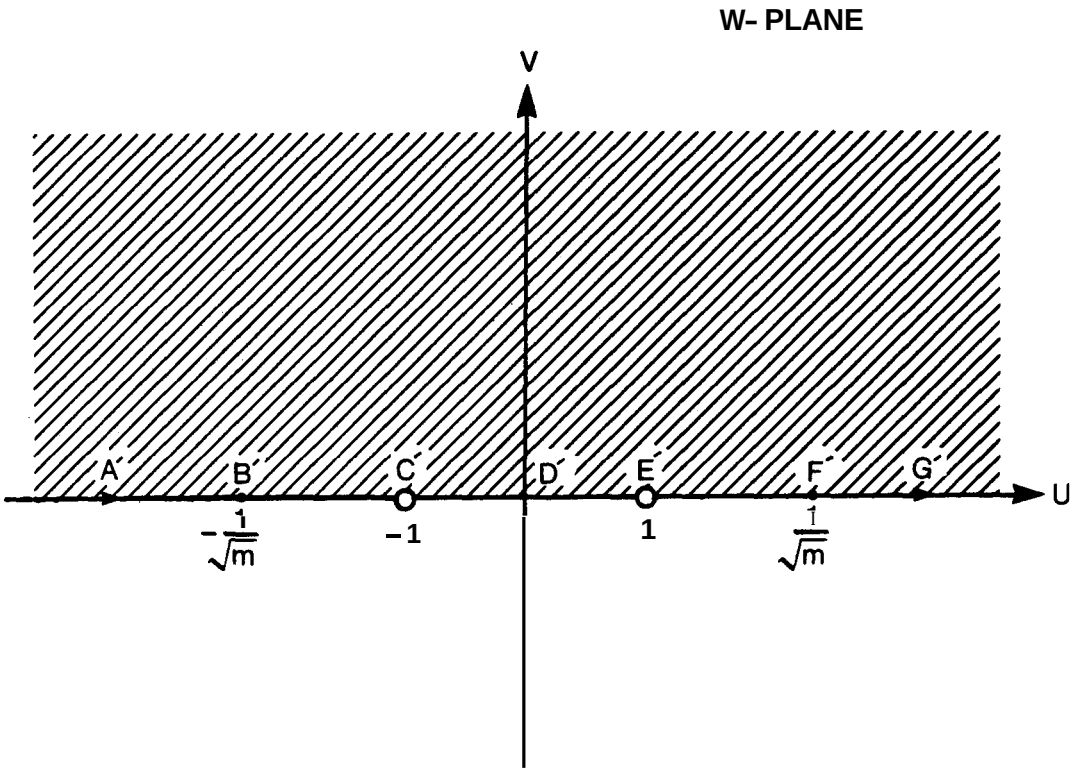

Fig. A-2: W-PLANE SHOWING THE TRANSFORMATION

The integral in Eq. A-7 is the inverse of the Jacobian elliptic function, $sn(z,m)$, as defined by Byrd and Friedman (1954). Therefore:

$$z = sn^{-1}(w,m) \tag{A-8}$$

Correspondingly:

$$w = sn(z,m) \tag{A-9}$$

Introducing a second transformation:

$$\bar{w} = i\,w \tag{A-10}$$

the upper half of the w-plane is mapped into the left half of the $\bar{w}$-plane as shown in Fig. A-3.

The production wells are now at $\bar{w} = i$ and $\bar{w} = -i$ and the injection well is again at infinity. The second transformation will only change the values of the streamlines. The $\bar{v}$ axis in Fig. A-3 is a no flow boundary, hence it can be mathematically removed by superimposing an image of the left half of the $\bar{w}$-plane into the right half of the $\bar{w}$-plane. In this way, the well system in the $\bar{w}$-plane becomes equivalent to two producers in an infinite medium. Since one quarter of a production well in the z-plane is mapped into one half of a well in the w or $\bar{w}$-plane, it is concluded that the strength of a well in the $\bar{w}$-plane is equal to one half of the strength of a corresponding well in the z-plane. For mathematical convenience, the strengths of the wells in the z-plane are assumed to be equal to one and the complex potential in the $\bar{w}$-plane subsequently is obtained from Eq. A-6 as follows:

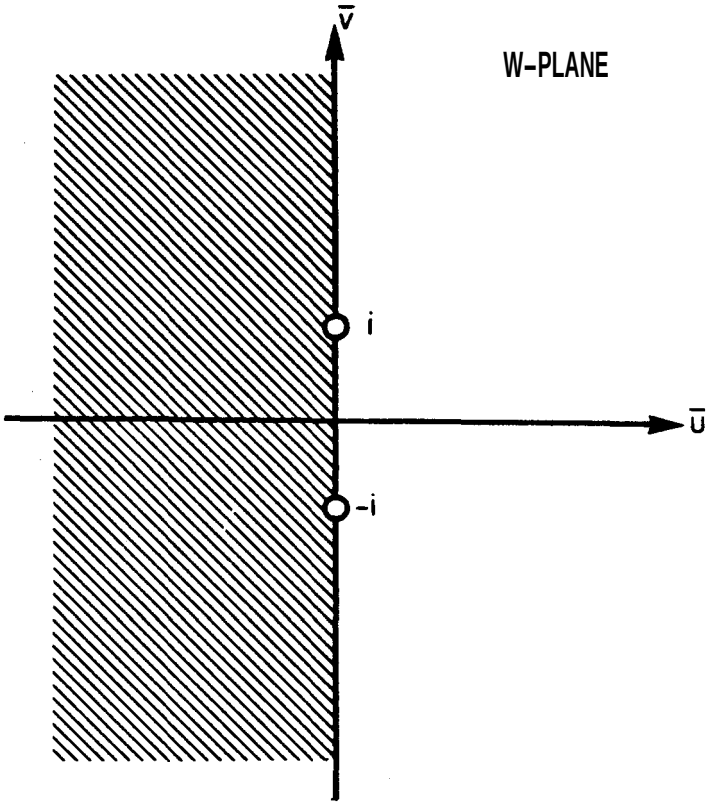

Fig. A.3: WELL LOCATIONS FOR A DEVELOPED STAGGERED LINE DRIVE IN $\bar{W}$-PLANE

$$\Omega(\bar{w}) = -\frac{1}{2}\ln(\bar{w} - i) - \frac{1}{2}\ln(\bar{w} + i) = -\ln\left(\sqrt{\bar{w}^2 + 1}\right) \qquad \text{(A-11)}$$

The wells at infinity do not contribute to the complex potential. From Eqs. A-0 and A-9:

$$\bar{w} = -i\,\mathrm{sn}(z,m) \qquad \text{(A-12)}$$

Substitute Eq. A-12 in Eq. A-11 and note that from the properties of Jacobian elliptic functions, $\mathrm{sn}^2(z,m) = 1 - cn^2(z,m)$:

$$\Omega(z) = -\ln\left[\mathrm{cn}(z,m)\right] \qquad \text{(A-13)}$$

Prats (1956) has reported the above expression (A-13) for the complex potential but with a positive sign because the injectors were assigned negative potential in his formulation. From Byrd and Friedman (1954):

$$cn(z,m) = cn(x + iy,m) = \frac{cn(x)\ cn(y) - i\ sn(x)\ dn(x)\ sn(y)\ dn(y)}{1 - sn^2(y)\ dn^2(x)} \tag{A-14}$$

where, $sn(x) = sn(x,m)$, $cn(x) = cn(x,m)$, $dn(x) = dn(x,m)$, $sn(y) = sn(y,m_1)$ and $cn(y) = cn(y,m_1)$ are various Jacobian elliptic functions with parameters m and m_1 where $m + m_1 = 1$. From complex variable theory:

$$\ln\ (x + iy) = \frac{1}{2}\ \ln\ (x^2 + y^2) + i\ \tan^{-1}\left(\frac{y}{x}\right) \tag{A-15}$$

Using Eqs. A-14 and A-15 in Eq. A-13, it is concluded that:

$$\Omega(z) = -\frac{1}{2}\ \ln\left(\frac{cn^2(x)\ cn^2(y) + sn^2(x)\ dn^2(x)\ sn^2(y)\ dn^2(y)}{[1 - sn^2(y)\ dn^2(x)]}\right)$$

$$+ i\ \tan^{-1}\left[\frac{sn(x)\ dn(x)\ sn(y)\ dn(y)}{cn(x)\ cn(y)}\right] \tag{A-16}$$

Comparing Eq. A-16 with Eq. A-1, it follows that:

$$\psi(x,y) = \tan^{-1}\ [f(x,m)\ f(y,m_1)] \tag{A-17}$$

$$f(x,m) = \frac{sn(x,m)\ dn(x,m)}{cn(x,m)} \tag{A-18}$$

Prats et al. (1955) had derived Eqs. A-17 and A-18 for the streamlines by applying Eq. A-6 to an infinite array of wells. Figure A-4 shows the coordinate system and the values of streamlines computed from Eqs. A-17 and A-18. The terms $K(m)$ and $K'(m)$ in this figure are complementary and incomplementary complete elliptic integrals defined by Eq. A-7 with $w = 1$ and $w = -1$, respectively. The relationship, $K'(m)/2K(m) = d/a$, relates the parameter m to the geometry of the system. The quadrant shown in Fig. A-4 is used in derivation of the equations for the pattern breakthrough curves.

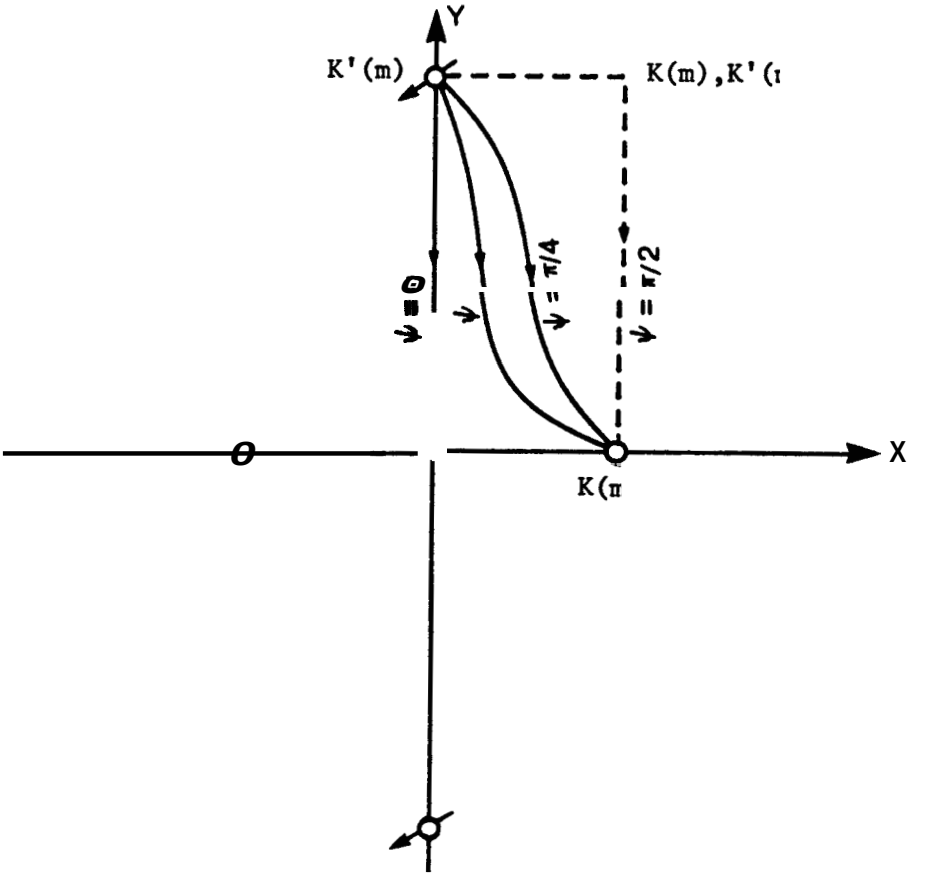

Fig. A-4: COORDINATE SYSTEM FOR A DEVELOPED STAGGERED LINE DRIVE

The breakthrough time, t_{bt}, of a particle on a streamline ψ is determined by a line integral along that streamline. This is:

$$t_{bt} = \int_0^{K(m)} \frac{dx}{v_x} \tag{A-19}$$

where v_x is the x component of the microscopic velocity. From Eq. A-2:

$$v_x = \frac{k}{\mu\phi} \frac{\partial\psi}{\partial y}\bigg|_{y = y(\psi,x)} \tag{A-20}$$

where ϕ is the porosity. From Eq. A-17 for the streamline ψ:

$$\frac{\partial\psi}{\partial y} = \frac{f(x,m)\ f'(y,m_1)}{1 + [f(x,m)\ f(y,m_1)]^2} \tag{A-21}$$

where,

$$f'(y,m_1) = \partial f(y,m_1)/\partial y \qquad \text{and,}$$

$$f(x,m)\ f(y,m_1) = \tan(\psi) \tag{A-22}$$

Therefore,

$$v_x = \frac{k}{\mu\phi} \cdot \frac{f(x,m)\ f'(y,m_1)}{1 + \tan^2\psi} \tag{A-23}$$

Substitute Eq. A-23 in Eq. A-19:

$$t_{bt} = \frac{\phi}{k/\mu}\,(1 + \tan^2\psi)\int_0^{K(m)} \frac{dx}{f(x,m)\ f'(y,m_1)} \tag{A-24}$$

The pore volume injected into the system at the time of breakthrough of streamline ψ is:

$$V_{pD} = \frac{t_{bt}\ q_t}{4\phi h\ K(m)\ K'(m)} \tag{A-25}$$

where q_t is the injection rate and h is the thickness of the pattern. The flow rate is given by:

$$q_t = \frac{kh}{\mu} \cdot \int d\psi \tag{A-26}$$

where the integral is taken around any closed surface in the flow regime. Because the flow in the vicinity of a wellbore is essentially radial, Eq. A-26, with the values of streamline shown in Fig. A-4, reduces *to:*

$$q_t = \frac{kh}{\mu}\ \Delta\psi = \frac{2nkh}{\mu} \tag{A-27}$$

Using this expressfon for q_t and Eq. A-24 for t_{bt}, Eq. A-25 simplifies to:

$$V_{pD} = \frac{\pi\ (1 + \eta)}{2K(m)\ K'(m)} \int_0^{K(m)} \frac{dx}{f(x,m)\ f'(y,m_1)} \tag{A-28}$$

where,

$$\eta = \tan^2\psi \tag{A-29}$$

and η is a constant for the streamline ψ.

Equations A–149 and A–150, derived later, relate the derivatives to the functions. The detailed derivation of these two relationships *is* presented in Appendix A.5.1. The equations **for** these derivatives are:

$$f'(x,m) = \sqrt{1 - 2\beta f^2(x,m) + f^4(x,m)} \tag{A–30}$$

and,

$$f'(y,m_1) = \sqrt{1 + 2\beta f^2(y,m_1) + f^4(y,m_1)} \tag{A–31}$$

where $\beta = m - m_1$. From **Eqs.** A–17 and A–29, the **y** terms can **be** expressed in terms of x terms as follows:

$$f^2(y,m_1) = \frac{\eta}{f^2(x,m)} \tag{A–32}$$

Utilizing Eqs. A–31 and A–32, Eq. A–28 becomes:

$$V_{pD} = \frac{\pi\ (1 + \eta)}{2K(m)\ K'(m)} \int_0^{K(m)} \frac{f(x,m)\ dx}{\sqrt{f^4(x,m) + 2\eta\beta f^2(x,m) + \eta^2}} \tag{A–33}$$

Introducing a change of variable $z = f^2(x,m)$ and using Eq. A–30 to substitute for $f'(x,m)$, the following equation **is** obtained:

$$V_{pD} = \frac{\pi\ (1 + \eta)}{4K(m)\ K'(m)} \cdot \int_0^{\infty} \frac{dz}{\sqrt{z^2 + 2\beta\eta z + \eta^2} \cdot \sqrt{z^2 - 2\beta z + 1}} \tag{A–34}$$

The integral term in Eq. A–34 is of the form of an incomplete elliptic integral of first order. The roots of the quadratic equations under the square roots all are complex. A closed–form solution for this integral **is** obtained from Byrd and Friedman (1954). The result is:

$$V_{pD} = \frac{\pi\ (1 + \eta)\ g}{4K(m)\ K'(m)} \left[F(\nu_2,\kappa) - F(\nu_1,\kappa)\right] \tag{A–35}$$

where $F(\nu_2,\kappa)$ and $F(\nu_1,\kappa)$ are incomplete elliptic integrals **of** the first kind with modulus κ and arguments ν_1 and ν_2 given **by:**

$$\nu_2 = \tan^{-1}\left(\frac{-\beta - a_1 g_1}{a_1 + \beta g_1}\right) \tag{A–36}$$

$$v_1 = \tan^{-1}\left(-\frac{1}{g_1}\right) \tag{A–37}$$

$$a_1^2 = 1 - \beta 2 \tag{A–38}$$

$$g_1^2 = \frac{4a_1^2 - (A - B)^2}{(A + B)^2 - 4a_1^2} \tag{A–39}$$

$$A = 1 + \eta \tag{A–40}$$

$$B = \sqrt{(1 - \eta)^2 + 4\eta\beta^2} \tag{A–41}$$

$$g = \frac{2}{A + B} \tag{A–42}$$

$$\kappa^2 = \frac{4AB}{(A + B)^2} \tag{A–43}$$

For a unit mobility ratio and a piston–like displacement, the displacing fluid cut in the producing stream at the production well, f_D, is the ratio of the angle at which the streamline ψ enters the well to the entire angle available for flow. From Fig. A–4, this is expressed by:

$$f_D = \frac{\frac{\pi}{4} - \psi}{\frac{\pi}{4}} = 1 - \frac{4\psi}{\pi} \tag{A–44}$$

Equations A–35 and A–44 jointly describe the pattern breakthrough curve of a developed staggered line drive system.

eakthrough Areal Sweep Efficien

The breakthrough streamline is $\psi = \pi/4$. ore at breakthrough, $f_D = 0$ and $\eta = 1$, and Eq. A–34 r to:

$$V_{pDbt} = \frac{\pi}{2\,K(m)\,K'(m)} \int_0^\infty \frac{dz}{\sqrt{(z^2 + 2\beta z + 1)(z^2 - 2\beta z + 1)}} \tag{A–45}$$

Due to symmetry of the breakthrough streamline around the point $\{K(m)/2, K'(m)/2\}$, Eq. A-45 can be written as:

$$V_{pDbt} = \frac{\pi}{K(m)\ K'(m)} \int_0^1 \frac{dz}{\sqrt{(z^2 + 2\beta z + 1)(z^2 - 2\beta z + 1)}} \qquad \text{(A-46)}$$

The upper limit of the integral is calculated from $z = f^2[\ K(m)/2\ , m] = 1$. The answer to this integral is obtained from the Byrd and Friedman handbook (1954):

$$V_{pDbt} = \frac{\pi}{2\ K(m)\ K'(m)}\ K[(1 - 2m)^2] \qquad \text{(A-47)}$$

Appendix A. 2: FIVE-SPOT PATTERN

The five-spot is a staggered line drive pattern with d/a = 1/2. For this special case:

$$m = m_1 = 0.5$$

$$\beta = m - m_1 = 0$$

$$K(m) = K'(m) = 1.8540747$$

Equation A-34 then reduces to:

$$V_{pD} = \frac{\pi\ (1 + \eta)}{4\ (1.8540747)^2} \int_0^\infty \frac{dz}{\sqrt{(z^2 + \eta^2)} \cdot \sqrt{(z^2 + 1)}} \qquad \text{(A-48)}$$

From a handbook of elliptic integrals (for example, Byrd and Friedman, 1954, or Abramowitz, 1972), the integral in this equation is equal to $K(1 - \eta^2)$, hence:

$$V_{pD} = 0.228473\ \ (1 + \eta)\ K(1 - \eta^2) \qquad \text{(A-49)}$$

where,

$$\eta = \tan^2 \psi \qquad \text{(A-50)}$$

$$\psi = \frac{\pi}{4}\ (1 - f_D) \qquad \text{(A-51)}$$

ugh Areal Sweep Efficiency

Breakthrough areal sweep efficiency is readily computed from Eq. A–49 with $\eta = 1$ for which $K(0) = \pi/2$:

$$V_{pDbt} = 0.71777$$

Appendix A.3: DIRECT LINE DRIVE

The complex potential for this pattern is obtained in a manner similar to that discussed in Appendix A.1. Equation A–7 is applied to transform the segment in Fig. A–5 into the upper half–plane of the w–plane. The production well is mapped at infinity and the injection well is mapped at the origin as was shown in Fig. A–2.

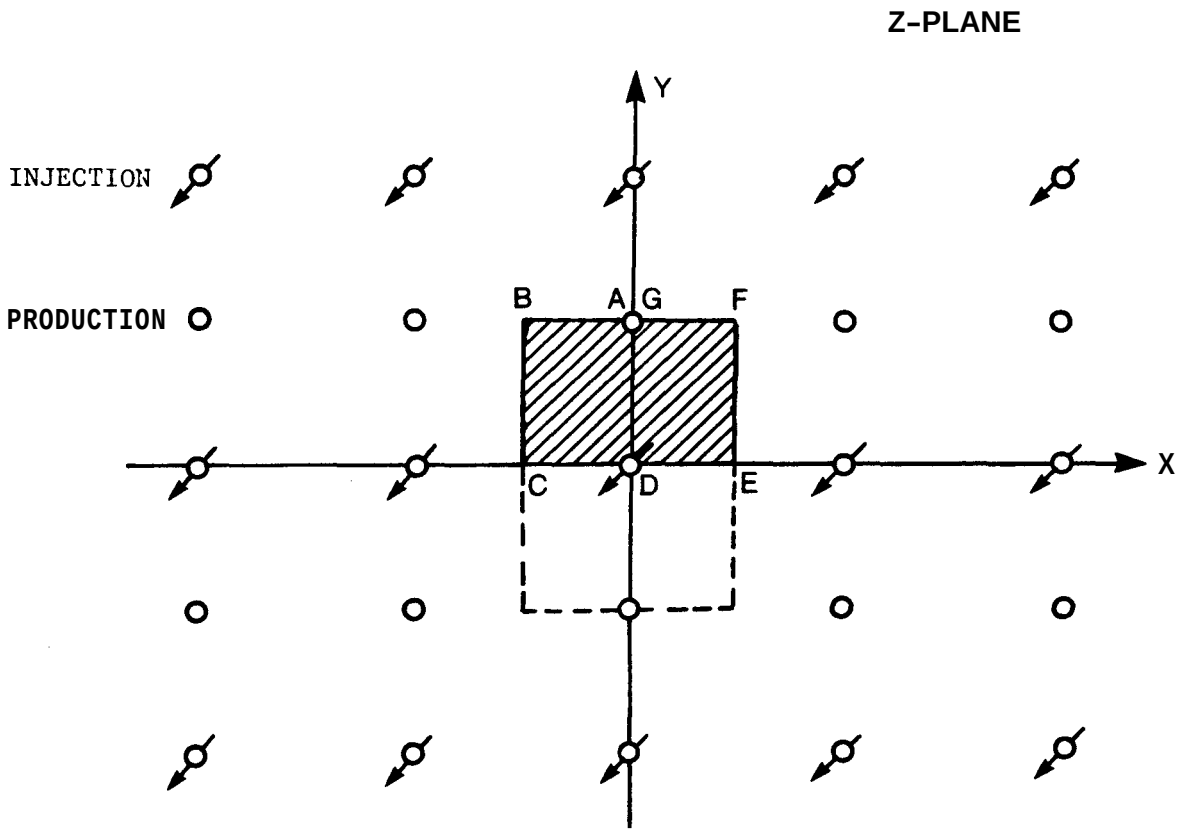

Fig. A–5: A DEVELOPED DIRECT LINE DRIVE IN Z-PLANE

The complex potential in the w-plane for this pattern is:

$$\Omega(w) = \ln w \tag{A-52}$$

Substitute for w from Eq. A-9:

$$\Omega(z) = \ln \left[sn(z,m)\right] \tag{A-53}$$

Equation A-1 can be used to obtain the stream functions. Hauber (1964) and Morel-Seytoux (1966) obtained the following equation for the streamlines:

$$\psi(x,y) = \tan^{-1} \left[f(x,m)\ g(y,m_1)\right] \tag{A-54}$$

where,

$$f(x,m) = \frac{cn(x,m)\ dn(x,m)}{sn(x,m)} \tag{A-55}$$

$$g(y,m_1) = \frac{sn(y,m_1)\ cn(y,m_1)}{dn(y,m_1)} \tag{A-56}$$

Figure A-6 shows the values of streamlines and the element considered in analyzing the direct line drive pattern.

The breakthrough time of a particle on a general streamline ψ is computed by using the y component; of the particle velocity as follows:

$$t_{bt} = \int_0^{K'(m)} \frac{dy}{v_y} \tag{A-57}$$

From Eq. A-3, the y component of microscopic velocity is:

$$v_y = - \frac{k/\mu}{\phi} \frac{\partial\psi}{\partial x}\bigg|_{x = x(\psi,y)} \tag{A-58}$$

From Eq. A-54 on the streamline Q:

$$\frac{\partial\psi}{\partial x} = \frac{f'(x,m)\ g(y,m_1)}{1 + \left[f(x,m)\ g(y,m_1)\right]^2} \tag{A-59}$$

and,

$$f(x,m)\ g(y,m_1) = \tan \psi \tag{A-60}$$

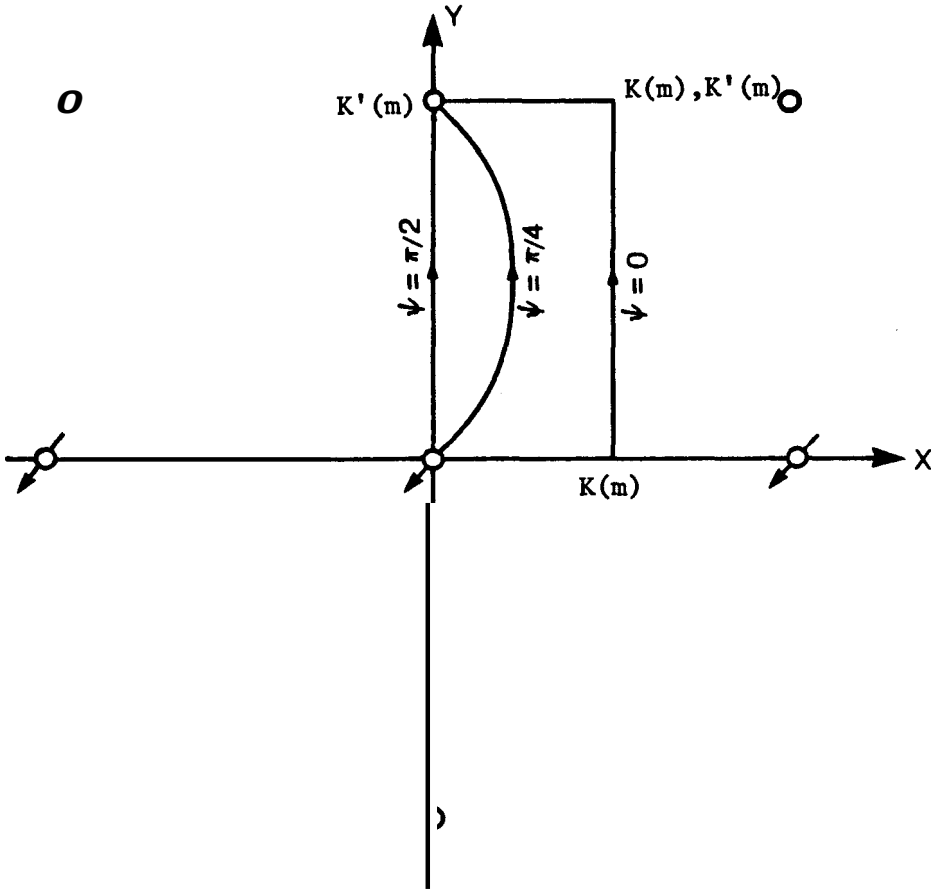

Fig. A-6: COORDINATE SYSTEM FOR A DEVELOPED DIRECT LINE DRIVE

Substituting Eq. A-58 in Eq. A-57 and using Eqs. A-59 and A-60:

$$t_{bt} = -\frac{\phi}{k/\mu}\,(1 + \tan^2\psi)\int_0^{K'(m)} \frac{dy}{g(y,m_1)\,f'(x,m)} \qquad \text{(A-61)}$$

Pore volume injected up to this breakthrough time is given by:

$$V_{pD} = \frac{t_{bt}\,q_t}{4\,\phi h\,K(m)\,K'(m)} \qquad \text{(A-62)}$$

Flow rate q_t is equal to $2\pi kh/\mu$ as was shown in Appendix A.1. Using this value for q_t and substituting for t_{bt} from Eq. A-61, Eq. A-62 reduces to:

$$V_{pD} = -\frac{\pi\,(1 + \tan^2\psi)}{2\,K(m)\,K'(m)}\int_0^{K'(m)} \frac{dy}{g(y,m_1)\,f'(x,m)} \qquad \text{(A-63)}$$

Since the streamlines are symmetric about $y = K'(m)/2$, the travel time from $y = 0$ to $y = K'(m)/2$ is equal to the travel time from $y = K'(m)/2$ to $y = K'(m)$. Therefore:

$$V_{pD} = -\frac{\pi\ (1 + \eta)}{K(m)\ K'(m)} \int_0^{\frac{K'(m)}{2}} \frac{dy}{g(y,m_1)\ f'(x,m)} \tag{A–64}$$

In this equation, $\eta = \tan^2\psi$ which is constant for a specified streamline.

Equations A–158 and A–166 in Appendix A.5.2 relate the derivatives to the functions as follows:

$$f'(x,m) = -\sqrt{\left[m_1 - f^2(x,m)\right]^2 + 4\ f^2(x,m)} \tag{A–65}$$

$$g'(y,m_1) = \sqrt{\left[1 + m_1\ g^2(y,m_1)\right]^2 - 4\ g^2(y,m_1)} \tag{A–66}$$

Using Eq. A–65 in conjunction with Eqs. A–29 and A–60 *to* eliminate $f(x,m)$, Eq. A–64 reduces to:

$$V_{pD} = \frac{\pi\ (1 + \eta)}{K(m)\ K'(m)} \int_0^{\frac{K'(m)}{2}} \frac{g(y,m_1)\ dy}{\sqrt{\left[m_1\ g^2(y,m_1) - \eta\right]^2 + 4\ \eta\ g^2(y,m_1)}} \tag{A–67}$$

Introduce a change of variable, $z = g^2(y,m_1)$ and use Eq. A–66 to replace the $g'(y,m_1)$ term, Eq. A–67 is simplified to:

$$V_{pD} = \frac{\pi\ (1 + \eta)}{2\ m_1^2\ K(m)\ K'(m)} \int_0^b \frac{dt}{\sqrt{(a - t)(b - t)(t - c)(t - d)}} \tag{A–68}$$

where,

$$a = \frac{1}{(1 - \sqrt{m})^2} \tag{A–69}$$

$$b = \frac{1}{(1 + \sqrt{m})^2} \tag{A–70}$$

$$c = \frac{-\eta}{(1 + \sqrt{m})^2} = -b\ \eta \tag{A–71}$$

$$d = \frac{-\eta}{(1-\sqrt{m})^2} = -a\eta \tag{A-72}$$

From Byrd and Friedman's (1954) table of elliptic integrals, an analytic expression for the integral in Eq. A-68 is obtained. This is:

$$V_{pD} = \frac{\pi}{m_1^2\ K(m)\ K'(m)} \cdot \frac{1+\eta}{\sqrt{(a+b\eta)(b+a\eta)}}\ F(\nu,\kappa) \tag{A-73}$$

where, $F(\nu,\kappa)$ is an incomplete elliptic integral of the first kind with argument v and modulus κ given by the following two expressions:

$$v = \text{Arcsin}\left(\sqrt{\frac{a+b\eta}{a+a\eta}}\right) \tag{A-74}$$

$$\kappa^2 = \frac{ab\ (1+\eta)^2}{(a+b\eta)(b+a\eta)} \tag{A-75}$$

The values of $F(\nu,\kappa)$ can either be obtained from a mathematical handbook or computed directly using Ascending Landen transformation successively (Abramowitz, 1972).

The displacing fluid cut, as before, is calculated from the angle at which the streamline enters the well. From Fig. A-6 it is:

$$f_D = 1 - \frac{2\psi}{\pi} \tag{A-76}$$

and thus, η is related to f_D as follows:

$$\eta = \tan^2\left[\frac{\pi}{2}(1-f_D)\right] \tag{A-77}$$

Equations A-73 and A-77 jointly describe the breakthrough curve of a developed direct line drive pattern.

Breakthrough Areal Sweep Efficiency

At breakthrough; $f_D = 0$, hence $\eta = \infty$, $\kappa^2 = 1$ and Eqs. A-73 through A-75 reduce to:

$$v = \text{Arcsin}\left(\sqrt{\frac{b}{a}}\right) \tag{A-78}$$

$$V_{pDbt} = \frac{\pi\ F(\nu,1)}{m_1^2\ K(m)\ K'(m)\sqrt{ab}} \tag{A-79}$$

However,

$$F(\nu,1) = \ln\ (\tan \nu + \sec \nu) \tag{A-80}$$

From Eq. A-78:

$$\sin v = \$ \tag{A-81}$$

Therefore, Eq. A-79 becomes:

$$V_{pDbt} = \frac{\pi}{m_1^2\ K(m)\ K'(m)\ \sqrt{ab}}\ \ln\left[\frac{\sqrt{a} + \sqrt{b}}{\sqrt{a - b}}\right] \tag{A-82}$$

Substitute for a and b from Eqs. A-69 and A-70 and simplify:

$$V_{pDbt} = \frac{-\pi\ \ln(m)}{4\ m_1\ K)m)\ K'(m)} \tag{A-83}$$

Appendix A.4: INVERTED SEVEN-SPOT

The complex potential for this pattern is given by Morel-Seytoux (1966) as follows:

$$\Omega(z) = \ln f(z) \tag{A-84}$$

where,

$$f(z) = \frac{[1 - cn^2(z,m)][a + b\ cn^2(z,m)]}{[1 + cn^2(z,m)][a - b\ cn^2(z,m)]} \tag{A-85}$$

$$a = 2 + \sqrt{3}$$

$$b = 2 - \sqrt{3}$$

$$m = (2 - \sqrt{3})/4$$

From Eq. A-14:

$$cn(z,m) = \frac{cn(x,m)\ cn(y,m_1)}{1 - sn^2(y,m_1)\ dn^2(x,m)} - i\ \frac{sn(x,m)\ dn(x,m)\ sn(y,m_1)\ dn(y,m_1)}{1 - sn^2(y,m_1)\ dn^2(x,m)}$$

Let:

$$h = \frac{cn(x,m)\ cn(y,m_1)}{1 - sn^2(y,m_1)\ dn^2(x,m)} \tag{A-86}$$

$$g = \frac{sn(x,m)\ dn(x,m)\ sn(y,m_1)\ dn(y,m_1)}{1 - sn^2(y,m_1)\ dn^2(x,m)} \tag{A-87}$$

Therefore:

$$cn(z,m) = h - ig \tag{A-88}$$

Substitute **Eq.** A-88 in **Eq.** A-85:

$$f(z) = \frac{[1 - (h^2 - g^2) + i\ 2hg][a + b(h^2 - g^2) - i\ 2bhg]}{[1 + (h^2 - g^2) - i\ 2hg][a - b(h^2 - g^2) + i\ 2bhg]} \tag{A-89}$$

Equation A-89 can be simplified ***to:***

$$f(z) = \frac{A + iB}{C - iD} = \frac{AC - BD}{C^2 + D^2} + i\,\frac{AD + BC}{C^2 + D^2} \tag{A-90}$$

where,

$$A = a + 4bu^2 - (a - b)\sqrt{t} - bt \tag{A-91}$$

$$B = 2u(a - b + 2b\sqrt{t}) \tag{A-92}$$

$$C = a + 4bu^2 + (a - b)\sqrt{t} - bt \tag{A-93}$$

$$D = 2u(a - b - 2b\sqrt{t}) \tag{A-94}$$

and,

$$t = (h^2 - g^2)^2 \tag{A-95}$$

$$u = hg \tag{A-96}$$

From Eqs. A-15, A-84 and A-90 the complex potential is:

$$\Omega(z) = \frac{1}{2} \ln \left[\frac{(AC - BD)^2 + (AD + BC)^2}{(C^2 + D^2)^2} \right] + i \tan^{-1} \left[\frac{AD + BC}{AC - BD} \right] \tag{A-97}$$

Comparing Eq. A-1 and A-97:

$$\psi(x,y) = \tan^{-1} \left(\frac{AD + BC}{AC - BD} \right) \tag{A-98}$$

Substitute for A, B, C, D from Eq. A-91 through A-94 in Eq. A-98 and rearrange:

$$\psi = \tan^{-1} \left\{ \frac{4u\left[(1 - b^2)(4u^2 + t) + a^2 - 1\right]}{8u^2(2b^2u^2 - 5 + b^2 t) + a^2 + b^2t^2 - 14t} \right\} \tag{A-99}$$

Streamlines given by this equation are shown in Fig. A-7.

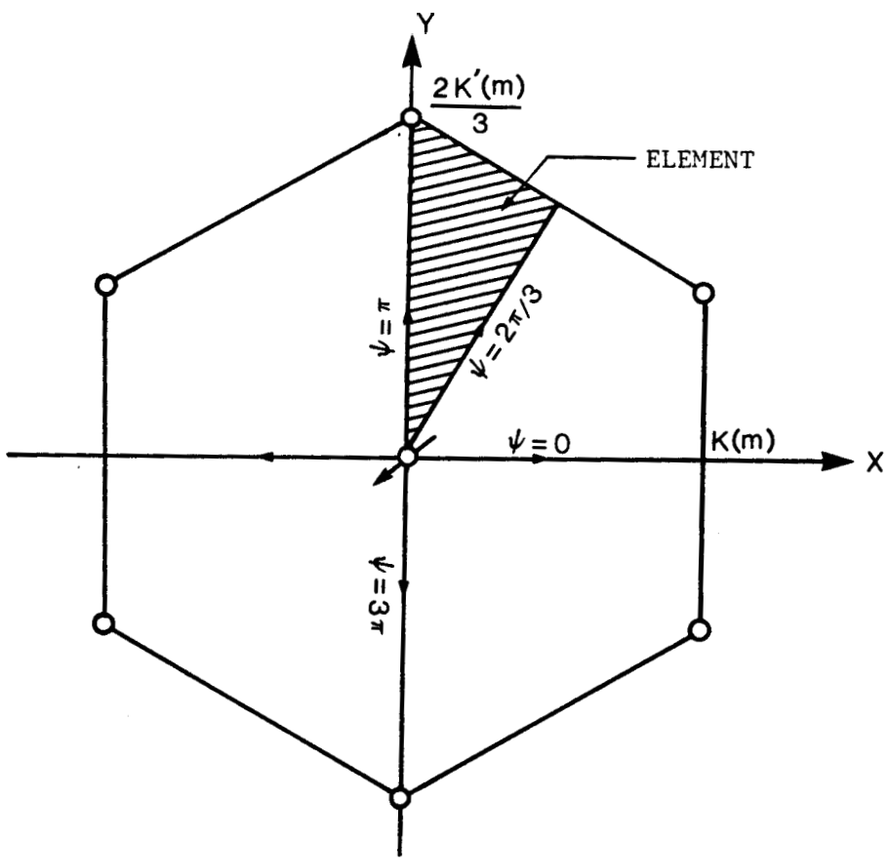

Fig. A-7: COORDINATE SYSTEM FOR AN INVERTED DEVELOPED SEVEN-SPOT

In the coordinate system of Fig. A–7, $K'(m) = \sqrt{3}K(m)$. The element chosen for the analysis is 1/12 of the pattern bounded between $\psi = 2\pi/3$ and $\psi = \pi$. Time to breakthrough of streamline ψ is:

$$t_{bt} = \int_0^{\frac{2K'(m)}{3}} \frac{dy}{v_Y} \tag{A–100}$$

and v_Y is given by Eq. A–58. Making the following substitutions for the terms in ψ equation (A–99):

$$r = (1 - b^2)(4u^2 + t) + a^2 - 1 \tag{A–101}$$

$$w = 8u^2(2b^2u^2 - 5 + b^2t) + a^2 + b^2t^2 - 14t \tag{A-102}$$

then:

$$\psi = \tan^{-1}\left(\frac{4ru}{w}\right) \tag{A-103}$$

Therefore, from Eqs. A–58 and A–103:

$$v_y = -\frac{k}{\mu\phi} \cdot \frac{4[w(ru' + r'u) - ruw']}{w^2[1 + \tan^2\psi]}\Bigg|_{x = x(\psi,y)} \tag{A-104}$$

Substitute Eq. A–104 in Eq. A–100 and rearrange:

$$t_{bt} = -\frac{\mu\phi}{k}\,\frac{(1 + \tan^2\psi)}{4}\int_0^{\frac{2K'(m)}{3}} \frac{w^2\,dy}{w(ru' + r'u) - ruw'} \tag{A–105}$$

Pore volumes injected:

$$V_{pD} = \frac{t_{bt}\,q_t}{\text{pattern pore volume}} \tag{A–106}$$

Flow rate around the wellbores from Eq. A–26:

$$q_t = \frac{k}{\mu}\,\Delta\psi = 4\pi\,\frac{k}{\mu} \tag{A–107}$$

and,

$$\text{pattern pore volume} = 2\sqrt{3}\,\phi\,K^2(m) \tag{A–108}$$

Using Eqs. A–105, A–107 and A–108, in the Eq. A–106, one obtains:

$$V_{pD} = \frac{-\pi(1 + \tan^2\psi)}{2\sqrt{3}\,K^2(m)} \int_0^{\frac{2K'(m)}{3}} \left. \frac{w^2 dy}{w(ru' + r'u) - ruw'} \right|_{x = x(\psi,y)} \tag{A–109}$$

From Eqs. A–95, A–96, A–101 and A–102, the derivatives of various terms in Eq. A–109 are:

$$u' = h'g - hg' \tag{A–110}$$

$$r' = (1 - b^2)(8uu' + t') \tag{A–111}$$

$$w' = 16uu'(4b^2u^2 - 5 + b^2t) + 2b^2(4u^2 + t)t' - 14t' \tag{A–112}$$

$$t' = 4(h^2 - g2)(hh' - gg') \tag{A–113}$$

From Eqs. A–86, A–87 and A–141 through A–143 the following expressions for $h' = \partial h/\partial x$ and $g' = \partial g/\partial x$ are obtained:

$$h' = -\,sn(x)dn(x)cn(y)\left[\frac{R + 2m\,cn^2(x)sn^2(y)}{R^2}\right] \tag{A–114}$$

$$g' = sn(y)dn(y)cn(x)\left\{\frac{R[dn^2(x) - m\,sn^2(x)] - 2m\,sn^2(y)dn^2(x)sn^2(x)}{R^2}\right\} \tag{A–115}$$

where:

$$R = 1 - sn^2(y)dn^2(x) \tag{A–116}$$

and,

$$sn(x) = sn(x,m)$$

$$sn(y) = sn(y,m_1)$$

In computing V_{pD} values from Eq. A–109, the x terms in the integral should be expressed as functions of y. Therefore, for a selected x value on a streamline $, the corresponding y value has to be evaluated. This was accomplished numerically by applying a root-finding routine to Eq. A–99 with a constant ψ value. The computed coordinate points on streamline ψ were then substituted into Eq. A–109 and the integral term in this equation was evaluated numerically. Equations A–110 through A–116 were used in evaluating the necessary terms in Eq. A–109, The computer program developed to generate the breakthrough curve of this pattern is given in Appendix D.2.

Displacing fluid cut at breakthrough of streamline ψ from Fig. A-7 is:

$$f_D = \frac{\pi - \psi}{\frac{\pi}{3}} = 3 - \frac{3\psi}{\pi} \tag{A-117}$$

where:

$$\frac{2\pi}{3} < \psi < \pi$$

Equations A-109 and A-117 describe the breakthrough curve of a repeated inverted seven spot pattern.

Breakthrough Areal Sweep Efficiency

The breakthrough streamline is $\psi = \pi$. On this streamline, $x = 0$; therefore, $cn(x,m) = 1$, $dn(x,m) = 1$, and $sn(x,m) = 0$. All the parameters defined before take simpler forms as follows:

$$h = \frac{1}{cn(y,m_1)} \tag{A-118}$$

$$g = 0 \tag{A-119}$$

$$h' = 0 \tag{A-120}$$

$$g' = \frac{sn(y,m_1)\ dn(y,m_1)}{cn^2(y,m_1)} \tag{A-121}$$

$$u = o \tag{A-122}$$

$$t = \frac{1}{cn^4(y,m_1)} \tag{A-123}$$

$$u' = \frac{sn(y,m_1)\ dn(y,m_1)}{cn^3(y,m_1)} \tag{A-124}$$

$$t' = 0 \tag{A-125}$$

$$r = \frac{(a^2 - 1)cn^4(y,m_1) + (1 - b^2)}{cn^4(y,m_1)} \tag{A-126}$$

$$w = \frac{a^2 cn^8(y,m_1) - 14cn^4(y,m_1) + b^2}{cn^8(y,m_1)} \tag{A-127}$$

$$r' = 0 \tag{A-128}$$

$$w' = 0 \tag{A-129}$$

Substitute Eqs. A-118 through A-129 into Eq. A-109 and rearrange:

$$V_{pDbt} = \frac{-\pi}{2\sqrt{3}\,(a^2 - 1)K^2(m)} \int_0^{\frac{2K'(m)}{3}} \frac{a^2 cn^8(y,m_1) - 14cn^4(y,m_1) + b^2}{sn(y,m_1)dn(y,m_1)cn(y,_1)[cn\,(y,m_1) + \frac{1 - b^2}{a^2 - 1}]}\, dy \tag{A-130}$$

To calculate the integral, let $p = cn^2(y,m_1)$, then:

$$dy = -\frac{dp}{2\,cn(y,m_1)\,sn(y,m_1)\,dn(y,m_1)}$$

$$= -\frac{cn(y,m_1)\,sn(y,m_1)\,dn(y,m_1)}{2\,cn^2(y,m_1)\,sn^2(y,m_1)\,dn^2(y,m_1)}\, dp$$

$$= -\frac{cn(y,m_1)\,sn(y,m_1)\,dn(y,m_1)}{2\,cn^2(y,m_1)[1 - cn^2(y,m_1)][m + m_1 cn^2(y,m_1)]}\, dp \tag{A-131}$$

At the limits:

$$p = cn^2(0,m_1) = 1$$

and,

$$p = cn^2\left[\frac{2K'(m)}{3}, m_1\right] = (2 - \sqrt{3})^2 = b^2$$

Hence, Eq. A-130 becomes:

$$V_{pDbt} = \frac{\pi}{4\sqrt{3}\,(a^2 - 1)K^2(m)} \int_1^b \frac{a^2 p^4 - 14p^2 + b^2}{p(1 - p)(m_1 p + m)(p + \frac{1 - b^2}{a^2 - 1})}\, dp \tag{A-132}$$

But :

$$m = (2 - \sqrt{3})/4$$

$$m_1 = 1 - m_1 = (2 + \sqrt{3})/4$$

$$\frac{m}{m_1} = \frac{2 - \sqrt{3}}{2 + \sqrt{3}} = \frac{b}{a} \qquad \text{(A-133)}$$

$$\frac{1 - b^2}{a^2 - 1} = \frac{2 - \sqrt{3}}{2 + \sqrt{3}} = \frac{b}{a} \qquad \text{(A-134)}$$

Using Eqs. A–133 and A–134, Eq. A–132 further simplifies *to:*

$$V_{pDbt} = \frac{\pi a^2}{4\sqrt{3}\, m_1 (a^2 - 1) K^2(m)} \int_1^{b^2} \frac{(p + 1)(p - \frac{b}{a})}{p(p^2 + \frac{b}{a})}\, dp \qquad \text{(A–135)}$$

The integral can now be calculated. This is:

$$\int_1^{b^2} \frac{(p + 1)(p - b}{p(p^2 + \frac{b}{a})}\, dp = \frac{1 - b^2}{b} \tan^{-1}(b) - \tan^{-1}(\frac{1}{b}) \qquad \text{(A–136)}$$

For :

$$a = 2 + \sqrt{3}$$

$$b = 2 - \sqrt{3}$$

$$m = (2 + \sqrt{3})/4$$

$$m_1 = (2 - \sqrt{3})/4$$

$$K(m) = 1.59842$$

The value of V_{pDbt} computed from Eq A–135 with the integral given by Eq. A–136 is:

$$V_{pDbt} = 0.743682$$

Appendix A.5: RELATING DERIVATIVES OF THE STREAM FUNCTIONS TO THE STREAM FUNCTIONS

This appendix is divided into two parts. The first part covers the staggered line drive pattern and the second part discusses the direct line drive pattern.

Appendix A.5.1: STAGGERED LINE DRIVE

From Eq. A-18:

$$f(y,m_1) = \frac{sn(y,m_1)\ dn(y,m_1)}{cn(y,m_1)} \tag{A–137}$$

From Abramowitz (1972) or Byrd and Friedman (1954):

$$\frac{\partial}{\partial y}\left[sn(y,m_1)\right] = cn(y,m_1)\ dn(y,m_1) \tag{A–138}$$

$$\frac{\partial}{\partial y}\left[dn(y,m_1)\right] = -\ m_1\ sn(y,m_1)\ cn(y,m_1) \tag{A–139}$$

$$\frac{\partial}{\partial y}\left[cn(y,m_1)\right] = -\ sn(y,m_1)\ dn(y,m_1) \tag{A–140}$$

And:

$$sn^2(y,m_1) = 1 - cn^2(y,m_1) \tag{A–141}$$

$$dn^2(y,m_1) = m_1\ cn^2(y,m_1) + m \tag{A–142}$$

$$dn^2(y,m_1) = 1 - m_1\ sn^2(y,m_1) \tag{A–143}$$

Therefore :

$$f'(y,m_1) = \frac{dn^2(y,m_1) - m_1\ sn^2(y,m_1)\ cn^2(y,m_1)}{cn^2(y,m_1)}$$

(A-144)

$$= \frac{m_1\ cn^4(y,m_1) + m}{cn^2(y,m_1)}$$

From Eq. A-137:

$$f^2(y,m_1) = \frac{sn^2(y,m_1)\ dn^2(y,m_1)}{cn^2(y,m_1)}$$

$$= \frac{-\ m_1\ cn^4(y,m_1) + (m_1 - m)cn^2(y,m_1) + m}{cn^2(y,m_1)}$$

Or:

$$m_1\ cn^4(y,m\ ) - [\ (m_1 - m) - f^2(y,m_1)\ ]cn^2(y,m_1) - m = 0 \qquad \text{(A-145)}$$

Let:

$$\gamma = m_1 - m - f^2(y,m_1) \qquad \text{(A-146)}$$

The solution for the quadratic equation in A-145 is:

$$cn^2(y,m_1) = \frac{\gamma \pm \sqrt{\gamma^2 + 4m_1m}}{2m_1} \qquad \text{(A-147)}$$

The negative sign is impossible, because m and m_1 both are positive numbers. Substitute Eq. A-147 in Eq. A-144 and simplify:

$$f'(y,m_1) = \sqrt{\gamma^2 + 4m_1m} \qquad \text{(A-148)}$$

Substitute back for γ from Eq. A-146:

$$f'(y,m_1) = \sqrt{1 + 2(m - m_1)\ f^2(y,m_1) + f^4(y,m_1)} \qquad \text{(A-149)}$$

Similarly:

$$f'(x,m) = \sqrt{1 + 2(m_1 - m)\ f^2(x,m) + f^4(x,m)} \qquad \text{(A-150)}$$

Appendix A.5.2: DIRECT LINE DRIVE

From Eq. A-55:

$$f(x,m) = \frac{cn(x,m)\ dn(x,m)}{sn(x,m)} \qquad \text{(A-151)}$$

Using the derivative of the Jacobian elliptic functions from Eqs. A-138 through A-143:

$$f'(x,m) = -\frac{dn^2(x,m) + m\ sn^2(x,m)\ cn^2(x,m)}{sn^2(x,m)}$$

$$= \frac{m^4 sn(x,m) - 1}{sn^2(x,m)} \qquad \text{(A-152)}$$

From Eq. A-151:

$$f^2(x,m) = \frac{cn^2(x,m)\ dn^2(x,m)}{sn^2(x,m)}$$

$$= \frac{m^4 sn(x,m) - (1 + m) sn^2(x,m) + 1}{sn^2(x,m)}$$

Or:

$$m\ sn^4(x,m) - \left[(1 + m) + f^2(x,m)\right] sn^2(x,m) + 1 = 0 \qquad \text{(A-153)}$$

Let:

$$\gamma_1 = 1 + m + f^2(x,m) \qquad \text{(A-154)}$$

The solution to Eq. A-153 is:

$$sn^2(x,m) = \frac{\gamma_1 \pm \sqrt{\gamma_1^2 - 4m}}{2m} \qquad \text{(A-155)}$$

Substitute Eq. A–155 in Eq. A–152 and simplify:

$$f'(x,m) = \pm \sqrt{\gamma_1^2 - 4m} \tag{A–156}$$

Because $m > 0$ and $-1 < sn(x,m) < 1$, from Eq. A–152 it is concluded that $f'(x,m) < 0$. Therefore:

$$f'(x,m) = - \sqrt{\gamma_1^2 - 4m} \tag{A–157}$$

Substitute for γ_1 from Eq. A–154 in Eq. A–157:

$$f'(x,m) = - \sqrt{[(m_1 - f^2(x,m)]^2 + 4f^2(x,m)} \tag{A–158}$$

The above approach can also be used to relate $g'(y,m_1)$ to $g(y,m_1)$. From Eq. A–56:

$$g(y,m\ ) = \frac{sn(y,m_1)\ cn(y,m_1)}{dn(y,m_1)} \tag{A–159}$$

The derivative of this function is:

$$g'(y,m_1) = \frac{dn^2(y,m_1)[cn^2(y,m_1) - sn^2(y,m_1)] + m_1\ sn^2(y,m_1)\ cn^2(y,m_1)}{dn^2(y,m_1)} \tag{A–160}$$

Using Eqs. A–141 through A–143 to express $sn(y,m_1)$ and $cn(y,m_1)$ in terms of $dn(y,m_1)$, Eq. A–160 reduces to:

$$g'(y,m_1) = \frac{dn^4(y,m_1) - m}{m_1\ dn^2(y,m_1)} \tag{A–161}$$

From Eq. A–159:

$$g^2(y,m_1) = \frac{sn^2(y,m_1)\ cn^2(y,m_1)}{dn^2(y,m_1)}$$

$$= \frac{-\ dn^4(y,m_1) + (1 + m)dn^2(y,m_1) - m}{m_1^2\ dn^4(y,m_1)}$$

Or:

$$dn^4(y,m_1) - [(1 + m) - m_1^2\, g^2(y,m_1)]dn^2(y,m_1) + m = 0 \qquad \text{(A-162)}$$

Let:

$$\gamma_2 = 1 + m - m_1^2\, g^2(y,m_1) \qquad \text{(A-163)}$$

The solution for $dn^2(y,m_1)$ from Eq. A-162 is:

$$dn^2(y,m_1) = \frac{\gamma_2 \pm \sqrt{\gamma_2^2 - 4m}}{2} \qquad \text{(A-164)}$$

Substitute Eq. A-164 in Eq. A-161 and simplify:

$$g'(y,m_1) = \pm \frac{1}{m_1} \sqrt{\gamma_2^2 - 4m} \qquad \text{(A-165)}$$

From Abramowitz (1972):

$$dn(0,m_1) = 1$$

$$dn\left[\frac{K'(m)}{2},m_1\right] = m^{1/4}$$

$$dn[K'(m),m_1)] = m^{1/2}$$

Therefore, From Eq. A-161 it is concluded that:

$$\begin{cases} g'(y,m_1) > 0 & \text{for} \quad 0 < y < \dfrac{K'(m)}{2} \\ g'(y,m_1) < 0 & \text{for} \quad \dfrac{K'(m)}{2} < y < K'(m) \end{cases}$$

Substitute for γ_2 from Eq. A-163 in A-165 and rearrange:

$$g'(y,m_1) = \begin{cases} +\sqrt{[\,1 + m_1 g^2(y,m_1)\,]^2 - 4g^2(y,m_1)} & 0 < y < \dfrac{K'(m)}{2} \\ -\sqrt{[\,1 + m_1 g^2(y,m_1)\,] - 4g^2(y,m_1)} & \dfrac{K'(m)}{2} < y < K'(m) \end{cases}$$

(A-166)

Appendix B

DERIVATION OF EQUATIONS FOR PATTERN RECOVERY CURVES AT VARIOUS MOBILITY RATIOS

The location of the displacement front plays a major role in the analysis of pattern performance when the mobility ratio is other than one. For such a displacement: 1) the streamlines in the regions behind and ahead of front deviate from those determined at mobility ratio of one; and 2) the total resistance to flow continually changes as the location of the front varies. This is in contrast to a unit mobility ratio displacement in which the resistance to flow is constant and independent of the interface position. In the following analysis, it is assumed that streamlines are the same for any mobility ratio while the overall resistance to flow varies during the displacement. Consequently, for a constant pressure drop between an injection well and a production well, the total flow rate in the pattern as well as the flow rates in the individual streamtubes will change as the front advances towards the production well. Furthermore, at any particular time, the flow rates in the individual streamtubes will differ from each other. This is due to establishment of different resistances in the streamtubes for the same total pressure drop across them.

Consider a piston-like displacement of two fluids in a developed five-spot pattern, as shown in Fig B-1.

Flow rate in a general streamtube $1 when the displacement front is at location $\bar{s}_{\psi 1}$ in the tube is:

$$q_{\psi 1}(\bar{s}) = \lambda_a A(s) \frac{\partial p_a}{\partial s} = \lambda_b A(s) \frac{\partial p_b}{\partial s} \qquad \text{(B-1)}$$

where :

$\lambda = \frac{k}{\mu}$ = fluid mobility

$A(s)$ = cross sectional area of streamtube at location s

a,b = subscripts for displacing and displaced fluids respectively

p = pressure

$q_{\psi 1}(\bar{s})$ = flow rate in the streamtube $1 as a function of front location

$\bar{s}$ = front location, same as $\bar{s}_{\psi 1}$

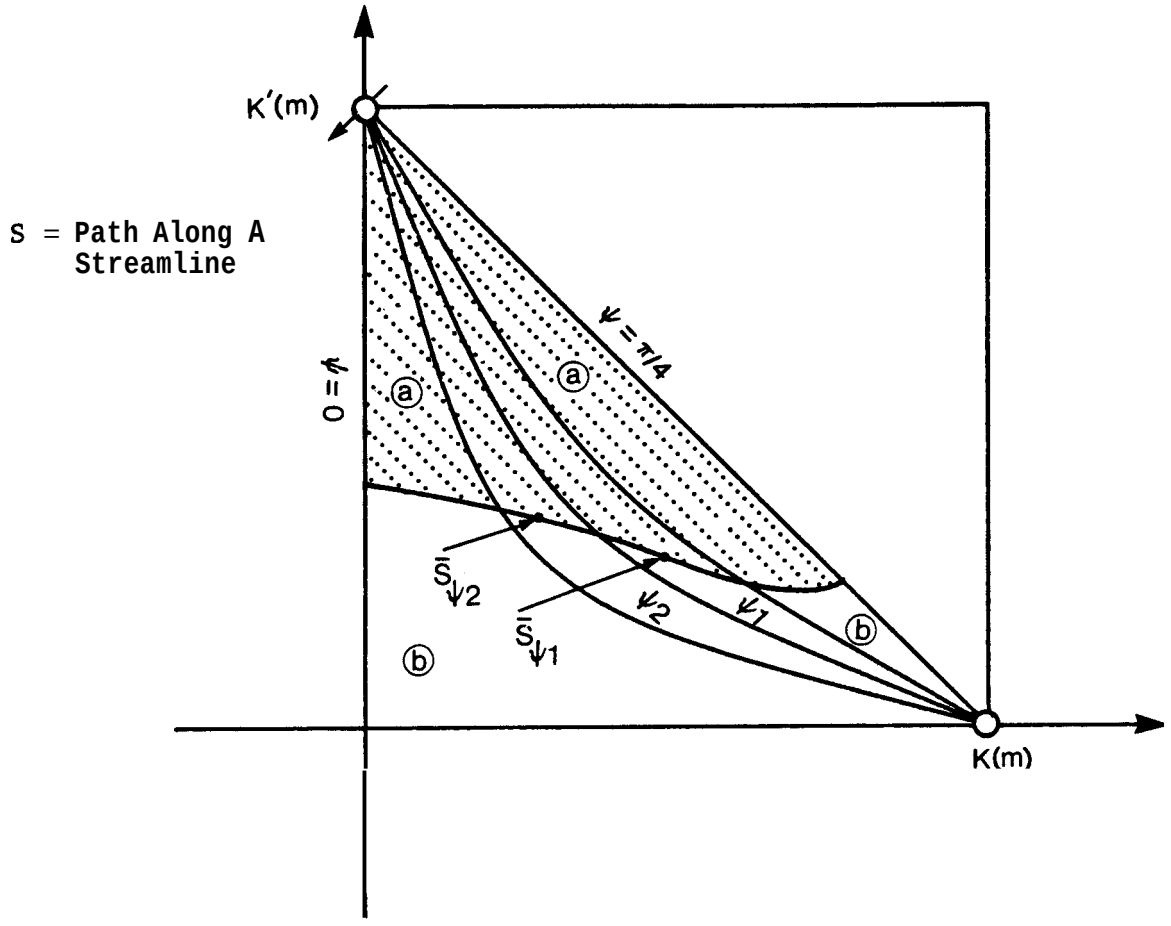

Fig. B-1: FRONT LOCATION IN A DEVELOPED FIVE-SPOT PATTERN AT AN ARBITRARY MOBILITY RATIO

Integrate Eq. B-1 to obtain the pressure drops in each zone:

$$\left(\Delta p_a\right)_{\psi 1} = \frac{q_{\psi 1}(\bar{s})}{d} \int_0^{\bar{s}_{\psi 1}} \frac{ds}{A(s)} \qquad \text{(B-2)}$$

and,

$$\left(\Delta p_b\right)_{\psi 1} = \frac{q_{\psi 1}(\bar{s})}{\lambda_b} \int_{\bar{s}_{\psi 1}}^{s_{\psi 1}} \frac{ds}{A(s)} \qquad \text{(B-3)}$$

where :

$s_{\psi 1}$ = total length of the streamtube $1

$\bar{s}_{\psi 1}$ = front location in the streamtube $1

The total pressure drop across the streamtube is the sum of pressure drops in the Lnvaded and the non-invaded zones. This total pressure drop is the same **for all** the tubes and will **be** assumed to **be** constant in this analysis. Add Eqe. **B-2** and B-3 and solve for $q_{\psi 1}(\bar{s})$:

$$q_{\psi 1}(\bar{s}) = \frac{\lambda_a \Delta p}{\int_0^{\bar{s}_{\psi 1}} \frac{ds}{A(s)} + M \int_{\bar{s}_{\psi 1}}^{s_{\psi 1}} \frac{ds}{A(s)}} \tag{B-4}$$

where Ap is the total pressure drop and M is the mobility ratio defined **as:**

$$M = \frac{\lambda_a}{\lambda_b} = \frac{k_a \mu_b}{k_b \mu_a} \tag{B-5}$$

The time required for the front in this streamtube to reach the production well is:

$$t_{\psi 1bt} = \int_0^{s_{\psi 1}} \frac{d\bar{s}}{v(\bar{s})} = \phi \int_0^{s_{\psi 1}} \frac{A(\bar{s})}{q(\bar{s})} d\bar{s} \tag{B-6}$$

Substitute for $q_{\psi 1}(\bar{s})$ from Eq. **B-4:**

$$t_{\psi 1bt} = \frac{\phi}{\lambda_a \Delta p} \int_{\bar{s}=0}^{s_{\psi 1}} \left[\int_0^{\bar{s}} \frac{ds}{A(s)} + M \int_{\bar{s}}^{s_{\psi 1}} \frac{ds}{A(s)} \right] A(\bar{s})\, d\bar{s} \tag{B-7}$$

At this time, the front location in the streamtube **$2** is at $\bar{s}_{\psi 2}$, which **is** given by:

$$t_{\psi 2bt} = \frac{\phi}{\lambda_a \Delta p} \int_{\bar{s}=0}^{\bar{s}_{\psi 2}} \left[\int_0^{\bar{s}} \frac{ds}{A(s)} + M \int_{\bar{s}}^{s_{\psi 2}} \frac{ds}{A(s)} \right] A(\bar{s})\, d\bar{s} \tag{B-8}$$

Equate Eqs. **B-7** and **B-8:**

$$\int_0^{\bar{s}_{\psi 2}} \left[\int_0^{\bar{s}} \frac{ds}{A(s)} + M \int_{\bar{s}}^{s_{\psi 2}} \frac{ds}{A(s)} \right] A(\bar{s})\, d\bar{s} = \int_0^{s_{\psi 1}} \left[\int_0^{\bar{s}} \frac{ds}{A(s)} + M \int_{\bar{s}}^{s_{\psi 1}} \frac{ds}{A(s)} \right] A(\bar{s})\, d\bar{s} \tag{B-9}$$

Equation B-9 provides the front location in the streamtube $2 at the time when the front in the streamtube $1 reaches the production well.

Areal sweep efficiency at the time of breakthrough in the streamtube $1 is the sum of two areas: 1) the total area of the streamtubes that are completely filled with the displacing fluid (broken-through streamtubes); and 2) the total swept area in the unbroken streamtubes. Mathematically, the areal sweep efficiency is given by:

$$E_A = \frac{\int_{\psi 1}^{\pi/4} \int_0^{s_\psi} A(s)\, ds\, d\psi + \int_0^{\psi 1} \int_0^{\bar{s}_\psi} A(s)\, ds\, d\psi}{(\text{pattern pore area})/8} \qquad \text{(B-10)}$$

For the developed five spot system in Fig. B-1, the pattern pore area can be calculated from the following equation:

$$\text{pattern pore area} = 4\phi K^2(0.5) = 4(1.8540746)^2\phi = 13.75036\ \phi$$

Therefore, Eq. B-10 becomes:

$$E_A = 0.5818\ \phi \int_{\psi 1}^{\pi/4} \int_0^{s_\psi} A(s)\, ds\, d\psi + \int_0^{\psi 1} \int_0^{\bar{s}_\psi} A(s)\, ds\, d\psi \qquad \text{(B-11)}$$

Pore volumes injected, V_{pD}, at the time of breakthrough in the streamtube $\psi 1$ are calculated from:

$$V_{pD} = E_A + (V_{pD})_a \qquad \text{(B-12)}$$

where, $(V_{pD})_a$ is the pore volumes of displacing fluid produced at that time. The term $(V_{pD})_a$ is equal to the sum of the cumulative volumes of the displacing fluid produced from each broken-through streamtube since the breakthrough time in each individual tube. Because only one fluid is flowing in the broken-through streamtubes, the flaw rates in such streamtubes are 'equal and remain constant after breakthrough of the displacing fluid from the pattern. Mathematically, the pore volumes of displacing fluid produced may be computed from:

$$(V_{pD})_a = \frac{q_a \int_{\psi 1bt}^{\pi/4} (t_{\psi 1bt} - t_{\psi bt})\, d\psi}{(\text{pattern pore volume})/8} \qquad \text{(B-13)}$$

In this equation, three terms must be defined. First, q represents the flow rate in the streamtubes that produce displacing fluid. #is term is the same for all the streamtubes that have already broken-through. It is given by:

$$q_a = \frac{\lambda_a \Delta p}{\int_0^{s_\psi} \frac{ds}{A(s)}} \tag{B-14}$$

The integral in the denominator of Eq. B-14 can be computed on any streamtube that is filled with the displacing fluid, a. The other two terms, $t_{\psi 1 bt}$ and $t_{\psi bt}$ represent the breakthrough time from the streamline $1 and a general streamline, ψ respectively. In analogy to Eq. B-7:

$$t_{\psi bt} = \frac{\phi}{\lambda_a \Delta p} \int_{\bar{s}=0}^{s_\psi} \left[\int_0^{\bar{s}} \frac{ds}{A(s)} + M \int_{\bar{s}}^{s_\psi} \frac{ds}{A(s)} \right] A(\bar{s})\, d\bar{s} \tag{B-15}$$

Substitute Eqs. B-7, B-14 and B-15 into Eq. B-13 and simplify:

$$(V_{pD})_a = \frac{0.5818}{\int_0^{s_{\pi/4}} \frac{ds}{A(s)}} \int_{\psi 1}^{\pi/4} \left\{ \int_0^{s_{\psi 1}} \left[\int_0^{\bar{s}} \frac{ds}{A(s)} + M \int_{\bar{s}}^{s_{\psi 1}} \frac{ds}{A(s)} \right] A(\bar{s})d\bar{s} - \int_0^{s_\psi} \left[\int_0^{\bar{s}} \frac{ds}{A(s)} + M \int_{\bar{s}}^{s_\psi} \frac{ds}{A(s)} \right] A(\bar{s})d\bar{s} \right\} d\psi \tag{B-16}$$

Displacing fluid cut, f_D, is the ratio of producing displacing fluid rate divided by the total production rate. This is given by:

$$f_D = \frac{q_a \int_{\psi 1}^{\pi/4} d\psi}{q_a \int_{\psi 1}^{\pi/4} d\psi + \int_0^{\psi 1} q_b(\psi)\, d\psi} \tag{B-17}$$

where, q_b is the flow rate in any streamtube that has not broken through. It varies with time and is different for different streamtubes, as it is within the integral sign.

Substitute for q_b from Eq. B-4 and for q_a from Eq. B-14:

$$f_D = \frac{1}{1 + \dfrac{\int_0^{\pi/4} \frac{ds}{A(s)}}{\frac{\pi}{4} - \psi 1} \cdot \int_{\psi=0}^{\psi 1} \dfrac{d\psi}{\int_0^{\bar{s}_\psi} \frac{ds}{A(s)} + M \int_{\bar{s}}^{s_\psi} \frac{ds}{A(s)}}} \tag{B-18}$$

Equations B-11, B-12, B-16 and B-18 are written in general forms. The rest of this appendix focusses on simplifing these equations.

Because of the assumption of no streamllne change with mobility ratio, the area terms in the preceding equations can be calculated from the streamlines determined at unit mobility ratio. That is:

$$A(s) = \frac{q_{M=1}}{\phi \left[v(s)\right]_{M=1}} \tag{B-19}$$

where,

$q_{M=1}$ = flow rate in the streamtube if the displacement was at M = 1

$\left[v(s)\right]_{M=1}$ = microscopic velocity at location s if the displacement was at M = 1

From Eqs. 3-42 and 3-50 with h = 1, it is concluded that:

$$q_{M=1} = \frac{k}{\mu} = \lambda \tag{B-20}$$

The term $\frac{ds}{A(s)}$ which appears frequently in the preceeding equations becomes:

$$\frac{ds}{A(s)} = \frac{\phi}{\lambda} ds \left[v(s)\right]_{M=1} \tag{B-21}$$

The following relationships facilitate evaluation of Eq. B-21:

$$ds = \sqrt{(dx)^2 + (dy)^2} = dx \sqrt{1 + (\frac{dy}{dx})^2} \tag{B-22}$$

$$\frac{dy}{dx} = \frac{\left(v_y\right)_{M=1}}{\left(v_x\right)_{M=1}} \tag{B-23}$$

$$\left[v(s)\right]_{M=1} = \sqrt{\left(v_x\right)^2_{M=1} + \left(v_y\right)^2_{M=1}} \tag{B-24}$$

Therefore:

$$\frac{ds}{A(s)} = \frac{\phi}{\lambda} \frac{\left(v_x\right)^2_{M=1} + \left(v_y\right)^2_{M=1}}{\left(v_x\right)_{M=1}} dx \tag{B-25}$$

From Eq. A-23:

$$\left(v_x\right)_{M=1} = \frac{\lambda}{\phi} \frac{f(x,m)\ f'(y,m_1)}{1 + \tan^2\psi} \tag{B-26}$$

and similarly:

$$\left(v_y\right)_{M=1} = -\frac{\lambda}{\phi} \frac{f'(x,m)\ f(y,m_1)}{1 + \tan^2\psi} \tag{B-27}$$

where, $f(x,m)$ and $f(y,m_1)$ are given by Eq. A-18. For a five-spot pattern, $m = m_1 = 0.5$, hence $\beta = m - m_1 = 0$. Equations A-30 and A-31 reduce to:

$$f'(x,m) = \sqrt{1 + f^4(x,m)} \tag{B-28}$$

$$f'(y,m_1) = \sqrt{1 + f^4(y,m_1)} \tag{B-29}$$

Substitute Eqs. B-26 through B-29 in B-25 and use Eq. A-32 *to* replace the $f(y,m_1)$ terms by $f(x,m)$ terms:

$$\frac{ds}{A(s)} = \frac{\eta + f^4(x,m)}{f(x,m)\ \sqrt{\eta^2 + f^4(x,m)}} dx \tag{B-30}$$

in which,

$$\eta = \tan^2\psi \tag{B-31}$$

Introducing the same change of variable, $z = f^2(x,m)$, as proposed in Appendix A.1:

$$\frac{ds}{A(s)} = \frac{(\eta + z^2)^2}{2\ z\sqrt{(1 + z^2)(\eta^2 + z^2)}} dz \tag{B-32}$$

From Gredshteyn and Ryzhik (1980):

$$\int \frac{ds}{A(s)} = \frac{1}{2} \int \frac{(\eta + z^2)\, dz}{z\sqrt{(1 + z^2)(\eta^2 + z^2)}} = \frac{1}{2} \ln \left| \frac{z\eta\sqrt{z^2 + 1} + \sqrt{z^2 + \eta^2}}{\eta\sqrt{z^2 + 1} + \sqrt{z^2 + \eta^2}} \right] \tag{B-33}$$

Let:

$$G(z,\eta) = \ln \left[\frac{z\eta\sqrt{z^2 + 1} + \sqrt{z^2 + \eta^2}}{\eta\sqrt{z^2 + 1} + \sqrt{z^2 + \eta^2}} \right] \tag{B-34}$$

At $z = 0$ and $z = \infty$, the term $G(z,\eta)$ approaches infinity. These points correspond to singularities at the injection and production wells. To avold the singularitles in the calculations, a radius equal to d/10000 is assigned to the wells, where d is the distance between an injector and a producer.

Another term that can be simplified is the integral defined in Eq. B-8 and in similar equations. Designate:

$$H_\psi = \int_{\bar{s}=0}^{\bar{s}_\psi} \left[\int_0^{\bar{s}} \frac{ds}{A(s)} + M \int_{\bar{s}}^{s_\psi} \frac{ds}{A(s)} \right] A(\bar{s})\, d\bar{s} \tag{B-35}$$

The $A(s)ds$ term in this equation can be reduced to the following by using Eqs. B-19, B-20, B-22, B-23 and B-24:

$$A(s)\, ds = \frac{\lambda\, dx}{\phi\left(v_x\right)_{M=1}} \tag{B-36}$$

Using Eqs. B-33, B-34 and B-36 and noting that wellbores have definite radii, the term in brackets in Eq. B-35 reduces *to:*

$$\int_0^{\bar{s}} \frac{ds}{A(s)} + M \int_{\bar{s}}^{s_\psi} \frac{ds}{A(s)} = \frac{1}{2} \left[M\, G(z_p,\eta) - G(z_i,\eta) + (1 - M)\, G(\bar{z},\eta) \right] \tag{B-37}$$

where,

$$z_p = f^2[(K - x_{wp}),m] \tag{B-38}$$

$$z_i = f^2(x_{wi},m) \tag{B-39}$$

$$\bar{z} = f(\bar{x}, m) \tag{B-40}$$

and,

$$x_{wi} = r_w \sin\psi \tag{B-41}$$

$$x_{wp} = r_w \cos\psi \tag{B-42}$$

$\bar{x}$ is the x component of front location, r_w is the wellbore radius and ψ is the value of a general streamline shown in Fig. B-1.

Define:

$$P(\eta) = M\, G(z_p, \eta) - G(z_i, \eta) \tag{B-43}$$

Using Eqs. B-36, B-37 and B-43, the H term defined in Eq. B-35 becomes:

$$H_\psi = \frac{P(\eta)}{2} \int_{x_{wi}}^{\bar{x}_\psi} \frac{d\bar{x}}{\left(\frac{v}{\bar{x}}\right)_{M=1}} + \frac{(1-M)}{2} \int_{x_{wi}}^{\bar{x}_\psi} G(\bar{z}, \eta) \frac{d\bar{x}}{\left(\frac{v}{\bar{x}}\right)_{M=1}} \tag{B-44}$$

where, $\bar{x}_\psi$ is the x coordinate of the front in the streamtube ψ. From Eqs. A-19, A-25, A-27 and A-34 with $\beta = 0$, it is concluded that:

$$\left(\frac{d\bar{x}}{v_{\bar{x}}}\right)_{M=1} = \frac{1+\eta}{2} \frac{d\bar{z}}{\sqrt{(\bar{z}^2 + \eta^2)(\bar{z}^2 + 1)}} \tag{B-45}$$

From Byrd and Friedman (1954):

$$\int_0^{\bar{z}} \frac{dz}{\sqrt{(z^2 + \eta^2)(z^2 + 1)}} = F(\nu, \kappa) \tag{B-46}$$

where,

$$\nu = \tan^{-1}\left(\frac{\bar{z}}{\eta}\right) \tag{B-47}$$

$$\kappa^2 = 1 - \eta^2 \tag{B-48}$$

with the property that,

$$F\left(\frac{\pi}{2}, \kappa\right) = K(\kappa) \tag{B-49}$$

Substitute Eq. B-45 and B-46 in Eq. B-44 and rearrange:

$$H_\psi = \frac{1+\eta}{4}\left[P(\eta)\,F(\nu,\kappa) + (1-M)\int_{z_i}^{\bar{z}} \frac{G(\bar{z},\eta)\,d\bar{z}}{\sqrt{(\bar{z}^2+\eta^2)(\bar{z}^2+1)}}\right] \qquad \text{(B-50)}$$

When the front in the streamtube $1 reaches the production well, $\bar{z}_{\psi 1} = z_p$. However, z is calculated at the production well and, hence, z_p approaches infinity (gee Eq. B-38). Therefore, the argument of $F(\nu,\kappa)$ becomes equal to $\pi/2$ and from Eq. B-49, $F(\pi/2,\kappa) = K(\kappa)$. Thus, the front in any streamtube, $2 defined by Eq. B-9, is reduced to:

$$\left\{(1+\eta)\left[P(\eta)\,F(\nu,\kappa) + (1-M)\int_{z_i}^{\bar{z}} \frac{G(\bar{z},\eta)\,d\bar{z}}{\sqrt{(\bar{z}^2+\eta^2)(\bar{z}^2+1)}}\right]\right\}_{\psi 2} =$$

$$\left\{(1+\eta)\left[P(\eta)\,K(\kappa) + (1-M)\int_{z_i}^{z_p} \frac{G(\bar{z},\eta)\,d\bar{z}}{\sqrt{(\bar{z}^2+\eta^2)(\bar{z}^2+1)}}\right]\right\}_{\psi 1_{bt}}$$

(B-51)

where, 1_{bt}$ represents $\psi 1$ at breakthrough. Note that in Eq. B-51, the left hand side is computed at $2 and the right side at $\psi 1_{bt}$.

At the breakthrough of $\psi 1$, substitution of Eq. B-36 in Eq. B-11 results in:

$$E_A = 0.5818\left[\int_{\psi 1_{bt}}^{\pi/4}\int_0^{K(m)} \frac{dx}{(v_x)_{M=1}}\,d\psi + \int_0^{\psi 1_{bt}}\int_0^{\bar{x}} \frac{dx}{(v_x)_{M=1}}\,d\psi\right] \qquad \text{(B-52)}$$

Applying Eqs. B-45, B-46 and B-47 to Eq. B-52 and noting that $z = \infty$ at the production well:

$$E_A = 0.2909\left[\int_{\psi 1_{bt}}^{\pi/4} (1+\eta)\,K(\kappa)\,d\psi + \int_0^{\psi 1_{bt}} (1+\eta)\,F(\nu,\kappa)\,d\psi\right] \qquad \text{(B-53)}$$

where, ν and κ are defined by Eqs. B-47 and B-48. Values of $\bar{z}$ are obtained from the solution of Eq. B-51.

The pore volumes of displaclng fluid produced at breakthrough of the stream-line ψl_{bt} are computed from Eqs. B-16, B-33, B-34, B-35 and B-50. The result is:

$$\left(V_{pD}\right)_a = 1.1636 \int_{\psi l_{bt}}^{\pi/4} \frac{H_{\psi l_{bt}} - H_{\psi_{bt}}}{G(z_p,\eta) - G(z_i,\eta)} \, d\psi \qquad \text{(B-54)}$$

where, $H_{\psi_{bt}}$ represents a streamline at breakthrough and is given by:

$$H_{\psi_{bt}} = \frac{1+\eta}{4} \left[P(\eta)\, K(\eta) + (1 - M) \int_{z_i}^{z_p} \frac{G(\bar{z},\eta)\, d\bar{z}}{\sqrt{(\bar{z}^2 + \eta^2)(\bar{z}^2 + 1)}} \right] \qquad \text{(B-55)}$$

Displacing fluid cut is computed from Eqs. B-18, B-33, B-34, B-37, and B-43 as follows:

$$f_D = \frac{\frac{\pi}{4} - \psi l_{bt}}{\frac{\pi}{4} - \psi l_{bt} + \left[G(z_p,1) - G(z_i,1)\right] \int_0^{\psi l_{bt}} \frac{d\psi}{P(\eta) + (1 - M)\, G(\bar{z},\eta)}} \qquad \text{(B-56)}$$

The computer program given in Appendix D.3 utilizes Eqs. B-12, B-53, B-54 and B-56 to evaluate areal sweep efficiency and displacing fluid cut for various mobility ratios.

Appendix C

EVALUATION OF THE LINE INTEGRAL IN MIXING EQUATIONS

In this appendix, evaluation of the line integral in the mixing equations is illustrated for developed staggered line drive, five-spot, and direct line drive patterns. The appendix consists of three sub-appendices, each corresponding to one of the above patterns.

Appendix C.1: STAGGERED LINE DRIVE

Consider a staggered line drive pattern with the dimensions shown in *Fig.* C-1.

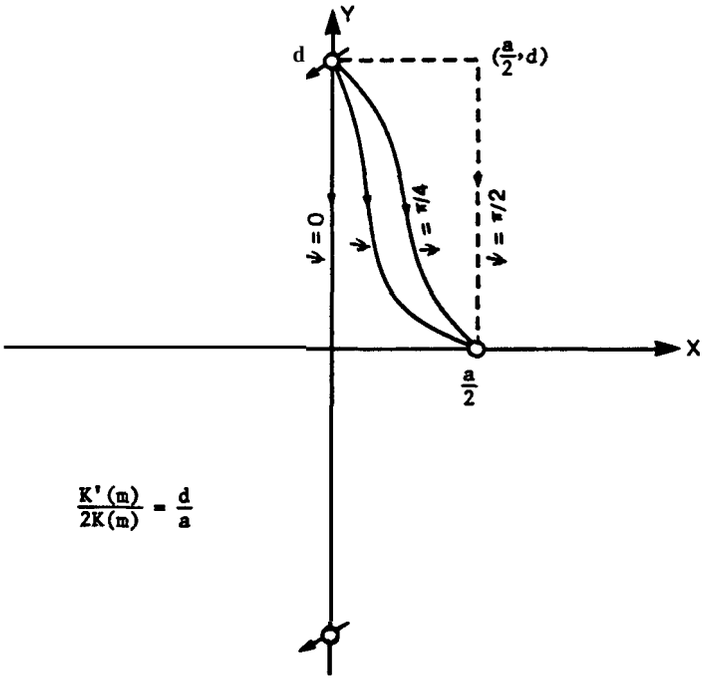

Fig. C-1: DIMENSIONS FOR A STAGGERED LINE DRIVE CONSIDERED IN ME ANALYSIS OF MIXING LINE INTEGRAL

The stream functions for this system are given by analogy to Eqs. A-17 and A-18 as follows:

$$\psi(x,y) = \tan^{-1}\left[f(w,m)\ f(z,m_1)\right] \tag{C-1}$$

$$f(w,m) = \frac{sn(w,m)\ dn(w,m)}{cn(w,m)} \tag{C-2}$$

$$w = \frac{2K(m)}{a} x \tag{C-3}$$

$$z = \frac{K'(m)}{d} y \tag{C-4}$$

$$\frac{K'(m)}{2K(m)} = \frac{d}{a} \tag{C-5}$$

Using Eqs. B-22, B-23 and B-24, the line integral, $I = \int_0^{\bar{s}} \frac{ds}{v^2(s)}$ is reduced to:

$$I = \int_0^{\bar{x}} \frac{dx}{v_x \sqrt{v_x^2 + v_y^2}} \tag{C-6}$$

If initial water saturation in the reservoir is S from Eqs. A-2 and A-3 the components of microscopic velocity are given by:

$$v_x = \frac{k}{\mu \phi S_w} \frac{\partial \psi}{\partial y} \Bigg|_{y = y(\psi, x)} \tag{C-7}$$

$$v_y = -\frac{k}{\mu \phi S_w} \frac{\partial \psi}{\partial x} \Bigg|_{x = x(\psi, y)} \tag{C-8}$$

Differentiating Eq. C-1 with respect to y and x, the velocity equations become:

$$v_x = \frac{k}{\mu \phi S_w} \frac{K'(m)}{d} \frac{f(w,m)\, f'(z,m_1)}{1 + [f(w,m)\, f(z,m_1)]^2} \tag{C-9}$$

$$v_y = -\frac{k}{\mu \phi S_w} \frac{2K(m)}{a} \frac{f'(w,m)\, f(z,m_1)}{1 + [f(w,m)\, f(z,m_1)]^2} \tag{C-10}$$

On a general streamline, ψ is a constant and Eq. C-1 yields:

$$f(w,m)\, f(z,m_1) = \sqrt{\eta} \tag{C-11}$$

where,

$$\eta = \tan^2 \psi = \text{constant} \tag{C-12}$$

Utilizing Eqs. C-3, C-5, C-9, C-10 and C-11, the following expression for the line integral is obtained:

$$I = \left(\frac{\mu\phi S_w}{k}\right)^2 (1+\eta)^2 \frac{ad^2}{2K(m)K'^2(m)} \int_0^{\bar{w}} \frac{dw}{f(w,m)\, f'(z,m_1)\sqrt{R_1}} \tag{C-13}$$

where,

$$R_1 = [f(w,m)\, f'(z,m_1)]^2 + [f'(w,m)\, f(z,m_1)]^2 \tag{C-14}$$

Equations A-149 and A-150 relate the derivatives to the functions. These are:

$$f'(z,m_1) = \sqrt{1 + f^4(z,m_1) + 2\beta f^2(z,m_1)} \tag{C-15}$$

$$f'(w,m) = \sqrt{1 + f^4(w,m) - 2\beta f^2(w,m)} \tag{C-16}$$

where ,

$$\beta = m - m_1 \tag{C-17}$$

Substitute for the derivatives in Eq. C-13 and C-14 from Eqs. C-15 and C-16, and eliminate $f(z,m_1)$ by Eq. C-11; then Eq. C-13 simplifies to:

$$I = \left(\frac{\mu\phi S_w}{k}\right)^2 (1+\eta)^{\frac{3}{2}} \frac{ad^2}{2K(m)K'^2(m)}$$

$$\cdot \int_0^{\bar{w}} \frac{f^2(w,m)\, dw}{\sqrt{[f^4(w,m)+\eta][f^4(w,m) + 2\beta\eta f^2(w,m) + \eta^2]}} \tag{C-18}$$

Introducing a variable change of $f^2(w,m) = t$, and using Eq. C-16 to replace the $f'(w,m)$ terms, Eq. C-18 becomes:

$$I = \left(\frac{\mu\phi S_w}{k}\right)^2 \frac{ad^2}{4K(m)K'^2(m)}\, Y \tag{C-19}$$

where,

$$Y = (1+\eta)^3 \int_0^{f^2(\bar{w},m)} \frac{\sqrt{t}\, dt}{\sqrt{(t^2 - 2\beta t + 1)(t^2 + 2\beta\eta t + \eta^2)(t^2 + \eta)}} \tag{C-20}$$

A plot of Y versus $\bar{w}/K(m)$ or $2\bar{x}/a$ for different streamlines (various η) is illustrated in Fig. C-2. This figure shows that Y asymptotically approaches constant values at the production well. Consequently, for $\bar{w}$ close to the production well, the exact location of $\bar{w}$ in the streamtube does not affect the values of Y significantly. On the other hand, since the tracer slug is small,

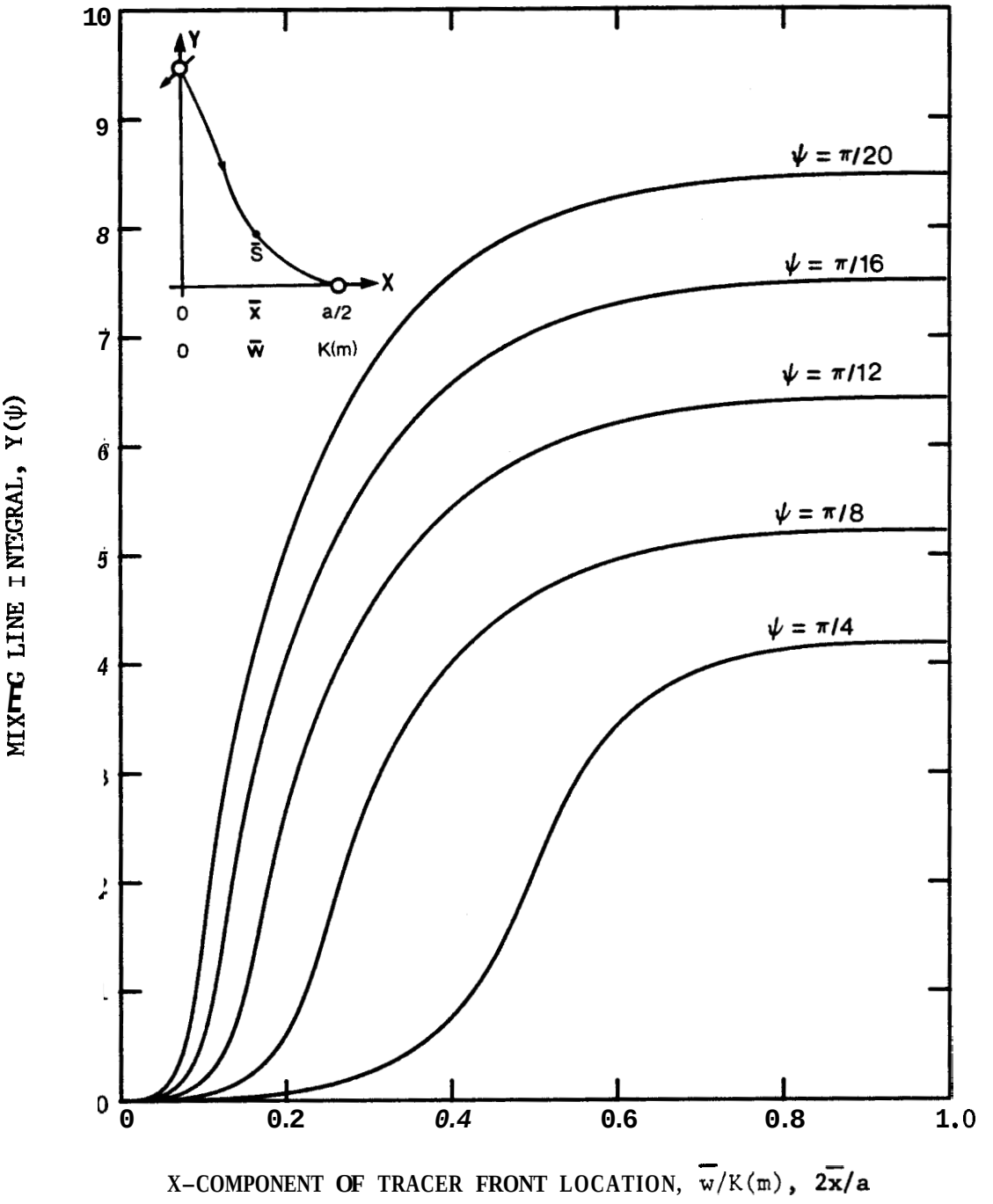

Fig. C-2: VARIATION OF MIXING LINE INTEGRAL WITH TRACER FRONT LOCATION FOR VARIOUS STREAMLINES OF A STAGGERED LINE DRIVE, d/a = 1

the amount of tracer flow to the well is insignificant unless the tracer front is close to the production well. Therefore, for all practical purposes, the upper limit of the integral in Eq. C-20 can always be computed at the production well. For this case, $f^2[K(m),m] = \infty$ and Y is:

$$Y = (1+\eta)^{\frac{3}{2}} \int_0^{\infty} \frac{\sqrt{t}\, dt}{\sqrt{(t^2 - 2\beta t + 1)(t^2 + 2\beta\eta t + \eta^2)(t^2 + \eta)}} \qquad \text{(C-21)}$$

All the roots of the quadratic equations in Eq. C-21 are complex. Therefore, there is no singularity in the range of integration. However, for $d/a > 2$, $m \to 0$, $\beta \to -1$; hence, one of the roots approaches η. For this case, precautions should be taken in the numerical integration around the point $t = \eta$.

Appendix C.2: FIVE SPOT

For a five-spot system:

$$\frac{d}{a} = \frac{1}{2}$$

$$\beta = m - m_1 = 0$$

$$K(m) = K'(m) = 1.854074$$

Equations C-19 and C-21 reduce to:

$$I = \left(\frac{\mu\phi S_w}{k}\right)^2 \frac{a^3}{101.97678} Y \qquad \text{(C-22)}$$

where,

$$Y = (1+\eta)^{\frac{3}{2}} \int_0^{\infty} \frac{\sqrt{t}\, dt}{\sqrt{(t^2 + 1)(t^2 + \eta^2)(t^2 + \eta)}} \qquad \text{(C-23)}$$

Appendix C.3: DIRECT LINE DRIVE

Figure C-3 shows the coordinate system with the dimensions for this pattern:

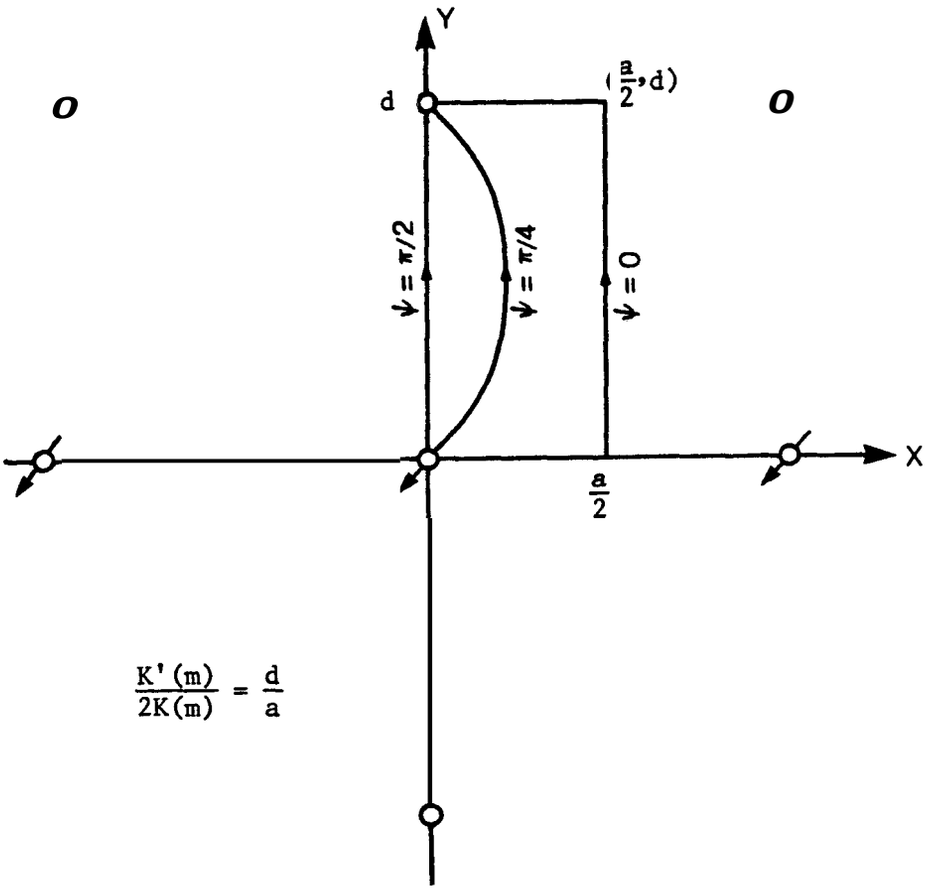

Fig. C-3: DIMENSIONS OF A DEVELOPED DIRECT LINE DRIVE CONSIDERED IN 'ME ANALYSIS OF MIXING LINE INTEGRAL

The stream functions for the above coordinate system are obtained by analogy to Eqs. A-54, A-55 and A-56 as follows:

$$\psi(x,y) = \tan^{-1}\left[f(w,m)\ g(z,m_1)\right] \tag{C-24}$$

$$f(w,m) = \frac{cn(w,m)\ dn(w,m)}{sn(w,m)} \tag{C-25}$$

$$g(z,m_1) = \frac{sn(z,m_1)\ cn(z,m_1)}{dn(z,m_1)} \tag{C-26}$$

$$w = \frac{2K(m)}{a} x \tag{C-27}$$

$$z = \frac{K'(m)}{d} y \tag{C-28}$$

$$\frac{K'(m)}{2K(m)} = \frac{d}{a} \tag{C-29}$$

The following equations facilitate evaluation of $I = \int_0^{\bar{s}} \frac{ds}{v^2(s)}$:

$$ds = \sqrt{(dx)^2 + (dy)^2} = dy \sqrt{\left(\frac{dx}{dy}\right)^2 + 1} \tag{C-30}$$

$$v^2 = v_x^2 + v_y^2 \tag{C-31}$$

$$\frac{dx}{dy} = \frac{v_x}{v_y} \tag{C-32}$$

Using these equations, the I integral becomes:

$$I = \int_0^{\bar{y}} \frac{dy}{v_y \sqrt{v_x^2 + v_y^2}} \tag{C-33}$$

The velocity components are related to stream functions by Eqs. C-7 and C-8. Performing the partial differention on $\psi(x,y)$, the expressions for the velocities become:

$$v_x = \frac{k}{\mu\phi S_w} \frac{K'(m)}{d} \frac{f(w,m)\, g'(z,m_1)}{1 + [f(w,m)\, g(z,m_1)]^2} \tag{C-34}$$

$$v_y = -\frac{k}{\mu\phi S_w} \frac{2K(m)}{a} \frac{f'(w,m)\, g(z,m_1)}{1 + [f(w,m)\, g(z,m_1)]^2} \tag{C-35}$$

For a general streamline, ψ is constant and Eq. C-24 results in:

$$f(w,m)\, g(z,m_1) = \sqrt{\eta} \tag{C-36}$$

where, η is given by Eq. C-12.

Utilizing Eq. C-28 and Eqs. C-33 through C-36, the following expression for the line integral, I, is obtained:

$$I = -\left(\frac{\mu\phi S_w}{k}\right)^2 (1+\eta)^2 \frac{ad^2}{2K(m)K'^2(m)} \int_0^{\bar{z}} \frac{dz}{f'(w,m)\, g(z,m_1)\sqrt{R_1}} \tag{C-37}$$

where,

$$R_1 = [f(w,m)\, g'(z,m_1)]^2 + [f'(w,m)\, g(z,m_1)]^2 \tag{C-38}$$

Equations A-158 and A-166 relate the derivatives to the functions:

$$f'(w,m) = -\sqrt{[m_1 - f^2(w,m)]^2 + 4f^2(w,m)} \tag{C-39}$$

and,

$$g'(z,m_1) = \begin{cases} +\sqrt{[1 + m_1\, g^2(z,m_1)]^2 - 4g^2(z,m_1)} & 0 < z < \frac{K'(m)}{2} \\ -\sqrt{[1 + m_1\, g^2(z,m_1)]^2 - 4g^2(z,m_1)} & \frac{K'(m)}{2} < z < K'(m) \end{cases} \tag{C-40}$$

Substitute for the derivatives from Eqs. C-39 and C-40 in Eq. C-37 and eliminate the f(w,m) term by using Eq. C-36:

$$I = \left(\frac{\mu\phi S_w}{k}\right)^2 (1+\eta)^{\frac{3}{2}} \frac{ad^2}{2K(m)K'^2(m)} \int_0^{\bar{z}} \frac{g^2(z,m_1)}{\sqrt{R_2}}\, dz \tag{C-41}$$

$$R_2 = [m_1^2\, g^4(z,m_1) + 2\eta(2 - m_1)g^2(z,m_1) + \eta^2][m_1^2\, g^4(z,m_1) + \eta] \tag{C-42}$$

Introducing a change of variable, $t = g^2(z,m_1)$:

$$dz = \frac{dt}{2g(z,m_1)\, g'(z,m_1)} = \frac{dt}{\pm\, 2g(z,m_1)\sqrt{[1 + m_1 g^2(z,m_1)]^2 - 4g^2(z,m_1)}} \tag{C-43}$$

Substitute this new variable and Eq. C-43 into Eq. C-41 and utilize the ranges given in Eq. C-40, the result of Eq. C-41 is:

$$I = \left(\frac{\mu\phi S_w}{k}\right)^2 \frac{ad^2}{4K(m)K'^2(m)} Y \qquad (c\text{-}44)$$

with:

$$Y = (1+\eta)^{\frac{3}{2}} \int_0^{g^2(\bar{z},m_1)} \frac{\sqrt{t}\,dt}{\sqrt{\Theta}} \qquad (C\text{-}45)$$

if $0 < \bar{z} < \frac{K'(m)}{2}$, or equivalently, $0 < g^2(\bar{z},m_1) < \frac{1}{(1+\sqrt{m})^2}$

and,

$$Y = (1+\eta)^{\frac{3}{2}} \left[\int_0^{1/(1+\sqrt{m})^2} \frac{\sqrt{t}\,dt}{\sqrt{\Theta}} - \int_{1/(1+\sqrt{m})^2}^{g^2(\bar{z},m_1)} \frac{\sqrt{t}\,dt}{\sqrt{\Theta}} \right] \qquad (C\text{-}46)$$

if $\frac{K'(m)}{2} < \bar{z} < K'(m)$ or equivalently, $\frac{1}{(1+\sqrt{m})^2} > g^2(\bar{z},m_1) > 0$

where,

$$\Theta = [m_1^2t^2 - 2(2-m_1)t + 1][m_1^2t^2 + 2\eta(2-m_1) + \eta^2][m_1^2t^2 + \eta] \qquad (C\text{-}47)$$

At the production well, $\bar{z} = K'(m)$, and $g^2[K'(m),m_1] = 0$; therefore, from Eq. c-45:

$$Y = 2(1+\eta)^{\frac{3}{2}} \int_0^{1/(1+\sqrt{m})^2} \frac{\sqrt{t}\,dt}{\sqrt{\Theta}} \qquad (C\text{-}48)$$

The roots of the quadratic equations in the expression for Θ in Eq. C-46 are:

$$m_1^2t^2 - 2(2-m_1)t + 1 = m_1^2(t-a)(t-b) \qquad (C\text{-}49)$$

$$m_1^2t^2 + 2\eta(2-m_1)t + \eta^2 = m_1^2(t-c)(t-d) \qquad (C\text{-}50)$$

$$m_1^2t^2 + \eta = m_1^2(t \pm e) \qquad (C\text{-}51)$$

where :

$$a = \frac{1}{(1 - \sqrt{m})^2} \qquad (C-52)$$

$$b = \frac{1}{(1 + \sqrt{m})^2} \qquad (c-53)$$

$$c = \left[- \eta \ (2 - m_1) + 2\eta\sqrt{m} \right] \ / \ m_1^2 \qquad (C-54)$$

$$d = \left[- \eta (2 - m_1) - 2\eta\sqrt{m} \right] \ / \ m_1^2 \qquad (C-55)$$

$$e = i \frac{\eta}{m_1} = \text{complex} \qquad (C-56)$$

Since $\eta > 0$, $0 < m_1 < 1$, and $0 < m < 1$; then, $a > b$, $c < 0$ and $d < 0$. Therefore, the integrand contains a singularity at point $t = b$ which corresponds to the upper limit of the integral in Eq. *C-48.* To remove this singularity, let:

$$b - t = \xi^2 \qquad (C-57)$$

Then :

$$Y = \frac{4}{m_1} (1 + \eta)^{\frac{3}{2}} \int_0^{\sqrt{b}} \sqrt{\frac{b - \xi^2}{T_1 T_2 T_3}} \, d\xi \qquad (C-58)$$

where :

$$T_1 = m_1^2 \xi^4 - 2(b m_1^2 + 2\eta - \eta m_1)\xi^2 + b^2 m_1^2 + 2b\eta(2 - m_1) + \eta^2 \qquad (c-59)$$

$$T_2 = a - b + \xi^2 \qquad (C-60)$$

$$T_3 = m_1^2 \xi^4 - 2b m_1^2 \xi^2 + b^2 m_1^2 + \eta \qquad (C-61)$$

Appendix D

COMPUTER PROGRAMS

This appendix consists of three sub-appendices, each containing a computer program. The first appendix provides a program to analyze tracer breakthrough curves from stratified reservoirs. The second appendix gives an algorithm to compute the pattern breakthrough curve of a developed inverted seven-spot for mobility ratio of one. A program to calculate the pattern breakthrough curve of a developed five-spot at any mobility ratio is the content of the last appendix.

Appendix D.1: PROGRAM TO ANALYZE A TRACER ELUTION CURVE

The algorithm provided in this section decomposes a tracer breathrough profile from a stratified formation into several layer responses. From the constructed layer responses, the parameters of the layers are evaluated. The decomposition process is carried out internally through a non-linear least-squares routine (subroutine VARPRO). Since an inverse problem is being solved, the number of layers should be determined by trial-and-error, each time observing the improvement of the generated match with an increase in number of layers. However, this program can be modified to perform this iterative process internally and generate an optimum match in one run,

```
// JOB (JE.MAD,104),'MAGSUD'
// EXEC WATFIV
//GO.SYSIN DD *
C
C     ************************************************************
C     *                                                          *
C     * THIS PROGRAM ANALYZES A TRACER BREAKTHROUGTH CURVE FROM A *
C     * STRATIFIED RESERVOIR FOR A GIVEN TYPE OF FLOODING PATTERN. *
C     * THE PROGRAM GENERATES POROSITY THICKNESS PRODUCT, (PHI*H), *
C     * AND FRACTIONAL PERMEABILITY THICKNESS PRODUCT, (KH/SUM(KH),*
C     * FOR EACH LAYER AS WELL AS A MATCH TO THE INPUT TRACER     *
C     * BREAKTHROUGH PROFILE FOR A SPECIFIED NUMBER OF LAYERS.    *
C     * THE PROGRAM CAN CURRENTLY HANDLE FIFTEEN LAYERS.          *
C
C     ************************************************************
C
C                          PREPARED BY
C
C                  MAGHSOOD ABBASZADEH-DEHGHANI
C                      STANFORD UNIVERSITY
C                            JULY 1982
C
C     NOMENCLATURE:
C
C       AALFAP = PECLET NUMBER FOR THE PATTERN
C       AALFA5 = PECLET NUMBER FOR AN EQUIVALENT FIVE-SPOT
C         AREA = DRAINAGE AREA OF A WELL WHOSE TRACER RESPONSE CURVE
C                IS BEING ANALYZED, FT SQUARE
C       CPHIHJ = TRACER COKCENTRATION FROM LAYER J, C/C0
C        CSTAR = TRACER CONCENTRATIONS IN THE FIELD TRACER ELUTION
C                CURVE, PPM.  AN ARRAY CONTAINING NDATA POINTS
C       CONCEN = TRACER CONCENTRATION IN THE GENERATED MATCH, PPM
C        EABTP = BREAKTHROUGH AREAL SWEEP EFFICIENCY OF A DEVELOPED
C                PATTERN
C        EABT5 = BREAKTHROUGH AREAL SWEEP EFFICIENCY OF A DEVELOPED
C                FIVE-SPOT
C       FACTOR = A CONVERSION FACTOR TO CONVERT TRACER CONCENTRATION
C                (FROM USUALLY PPM) TO WEIGHT FRACTION
C           FM = CORRECTION FACTOR ON TRACER PEAK CONCENTRATION
C           FP = CORRECTION FACTOR ON PECLET NUMBER
C         FRAC = RATIO OF THE RATE OF FLUID FLOWING FROM THE INJECTOR
C                OF THE PATTERN TOWARDS THE WELL, DIVIDED BY THE TOTAL
C                PRODUCTION RATE FROM THE WELL.  FOR EXAMPLE, IN A
C                DEVELOPED FIVE-SPOT WHEN TRACER IS INJECTED INTO ONE
C                OF THE WELLS ONLY, FRAC = 0.25
C        K, KP = COMPLEMENTARY AND INCOMPLEMENTARY COMPLETE ELLIPTIC
C                INTEGRALS OF THE FIRST KIND
C          KHJ = FRACTIONAL CONDUCTANCE OF LAYER J, (KH)J/SUM(KH)
C        NDATA = NUMBER OF DATA POINTS INPUTED FROM A FIELD TRACER
C                RESPONSE CURVE
C       NLAYER = NUMBER OF LAYERS IN THE STRATIFIED MODEL
C       NOTPUT = NUMBER OF POINTS DESIRED TO BE CALCULATED ON THE
C                MATCH CURVE
C        PHIHJ = POROSITY THICKNESS PRODUCT OF LAYER J
C       PVDMX5 = CORRELATING DIMENSIONLESS PORE VOLUME FOR A DEVE-
C                LOPED FIVE-SPOT.
C           SW = INITIAL WATER SATURATION IN THE RESERVOIR
C            T = VOLUMES CORRESPONDING TO SELECTED "CSTAR" VALUES
C                IN THE FIELD DATA, BBLS
C           TR = TOTAL VOLUME OF TRACER SOLUTION INJECTED INTO A
```

```
C                 PATTERN, FT3.
C          VCAL = CALCULATED PEAK VOLUMES OF THE LAYERS, IF THE
C                 SYSTEM WAS DEVELOPED AND THE WELL WAS RECEIVING
C                 TRACER FROM ALL THE INJECTORS SURRONDING IT, BDLS
C        VMXCAL = CALCULATED PEAK VOLUMES OF THE LAYERS IN THE MATCH
C                 CURVE TO THE FIELD DATA, BBLS
C        VOBSRV = VOLUMES IN THE MATCH CURVE (X-AXIS), BBLS
C         VPDBT = X-COORDINATE OF THE PATTERN BREAKTHROUGH CURVE OF A
C                 DEVELOPED FIVE-SPOT (DISPLACING FLUID CUT VS PORE
C                 VOLUMES), DIMENSIONLESS
C        VPDMXP = PORE VOLUMES CORRESPONDING TO THE PEAK CONCENTRATION
C                 IN A TRACER BREAKTHROUGH CURVE FROM A HOMOGENEOUS
C                 PATTERN, DIMENSIONLESS
C         VTMAX = UPPER VALUE OF THE RANGE AT WHICH A MATCH TO THE
C                 FIELD TRACER ELUTION CURVE IS SOUGHT, BBLS
C         VTMIN = LOWER VALUE OF THE RANGE, BBLS
C        VTMAXP = VOLUMES CORRESPONDING TO THE PEAK CONCENTRATIONS IN
C                 THE FIELD TRACER RESPONSE CURVE, BBLS.  THESE WILL BE
C                 USED AS INITIAL ESTIMATES IN THE OPTIMIZATION ROUTINE
C         YSIGH = "Y" VALUE IN THE MIXING LINE INTEGRAL, FUNCTION OF
C                 STREAMLINE
C          Y(J) = J TH NONLINEAR PARAMETER IN THE OPTIMIZATION ROUTINE
C               - KJ/(PHI*SUM(KH))
C         XY(J) = J TH LINEAR PARAMETER IN THE OPTIMIZATION ROUTINE
C               - KJ/(PHI*SUM(KH))*KHJ/SUM(KH)
C
C
C
      IMPLICIT REAL*8 (A-ti,O-Z)
      REAL*8 K,KP,M,M1,KHJ,KETA
      DIMENSION VPDBT(110),YSIGH(110),T(50,1),CSTAR(50)
      DIMENSION W(50),AA(50,32),Y(15),XY(15),CPHIH(15),VTMAXP(15)
      EXTERNAL ADA
      COMMON /PAR/YSIGH,VPDBT
      COMMON /PARK/K,KP,VTMAXP,VPDMXP,EABT5,EABTP,FM,FP
      COMMON /FORM/AREA,SW,AALFA5,TR,N,NM,H1,H2
C
C     INPUT PARAMETERS:
C
      READ,FRAC,FACTOR,NDATA,NLAYER
      READ,SW,AREA,AALFAP,TR
      READ,EABTP,FM,FP
      READ,VTMIN,VTMAX,NOTPUT
      DO 10 J=1,NLAYER
      READ,VTMAXP(J)
10    VTMAXP(J)=VTMAXP(J)*FRAC
      DO 20 I=1,NDATA
      READ,T(I,1),CSTAR(I)
      T(I,1)=T(I,1)*FRAC
20    CSTAR(I)=CSTAR(I)/FRAC*FACTOR
C
C     IN THE ABOVE, VALUES OF VTMAXP, T, AND CSTAR WERE CONVERETED TO
C     THOSE CORRESPONDING TO A DEVELOPED PATTERN
C
C
      EABT5=.7177783
C
C     AN EQUIVALENT FIVE-SPOT IS DETERMINED
C
      AALFA5=AALFAP/FP
```

```
C
C     DIMENSIONLESS CORRELATING PORE VOLUME IS COMPUTED FROM THE
C     EQUATION OF THE FIVE-SPOT LINE IN FIG. 3.24
C
        PVDMX5=2.5032*AALFA5**(-0.464)
C
C     PORE VOLUME CORRESPONDING TO A PEAK FROM A HOMOGENEOUS
C     PATTERN IS COMPUTED
C
        VPDMXP=EABTP+(1.-EABTP)*PVDMX5
        PI=4.*DATAN(1.D0)
        K=1.8540746773D0
        KP=K
        M=0.5D0
        M1=M
C
C
C     PATTERN BREAKTHROUGH CURVE, "VPBD", AND MIXING LINE INTEGRAL,
C     "Y(SIGH)" FOR A DEVELOPED FIVE-SPOT ARE COMPUTED.  IN THE
C     FOLLOWING, THE STREAMLINES BETWEEN ZERO AND 10 DEGREES ARE
C     DIVIDED INTO "N=50" STREAMTUBES AND THOSE BETWEEN 10 DEGRRES
C     AND 45 DEGREES ARE ALSO DIVIDED INTO "N=50" TUBES.  THIS IS
C     DONE TO OBTAIN HIGHER ACCURACY FOR THE EXTREME STREAMTUBES
C
C
        UPPER=1.D+4
        TET1=0.D0
        TETL=PI*10.0/180.
        N=50
        NN=N+1
        NNN=2*NN-1
        NM=2*N
        H2=(PI/4.-TETL)/N
        H1=TETL/N
        DO 50 I=2,NNN
        IF (I.LE.NN)GO TO 30
        TET=TETL+H2*(I-N-1)
        GO TO 40
30      TET=H1*(I-1)
40      ETA=DTAN(TET)**2
        C=PI/4.*(1+ETA)/K/KP
        ZZ=1.-ETA**2
        CALL KVALUE(ZZ,KETA)
        VPDBT(I-1)=C*KETA
        CALL GAUSS(UPPER,ETA,SIGMA)
50      YSIGH(I-1)=SIGMA
C
C     "IPRINT" CONTROLS THE TYPE OF THE OUTPUT FROM THE OPTIMIZATION
C     ROUTINE.  SEE SUBROUTINE "VARPRO" FOR INFORMATION
C
        IPRINT=1
C
C     THE WEGHTING FACTORS FOR THE FUNCTION NEEDED IN "VARPRO" ARE
C     EVALUATED
C
        DO 60 LMK=1,NDATA
60      W(LMK)=1.
        LENGTH=2*NLAYER+2
        CALL VARPRO(NLAYER,NLAYER,NDATA,NDATA,LENGTH,1,T,CSTAR,W,
     &  ADA,AA,IPRINT,Y,XY,IERR)
```

```
      WRITE(6,70)
70    FORMAT('1',2X,'LAYER NO.',7X,'POROSITY.THICKNESS',12X,
     % 'KH/SUM(KH)',/)
C
C     CALCULATE THE PARAMETRES OF THE LAYERS FROM THE COMPUTED LINEAR
C     AND NON-LINEAR PARAMETERS
C
      DO 90 IOPT=1,NLAYER
      KHJ  =XY(IOPT)/Y(IOPT)
      PHIHJ=XY(IOPT)/Y(IOPT)/Y(IOPT)
      WRITE(6,80 )IOPT,PHIHJ,KHJ
      IF (PHIHJ.LT.0.)GO TO 204
80    FORMAT(6X,I2,14X,F10.6,16X,F10.6)
90    CONTINUE
      WRITE(6,100)
100   FORMAT('1',1X,'VOLUME PRODUCED, BBLS', 9X,'CONCENTR TION, PPM',/
C
C     A MATCH TO THE FIELD DATA WITHIN THE SPECIFIED RANGE OF VOLUMES
C     AND DESIRED NUMBER OF POINTS IS GENERATED
C
      DELTAP=(VTMAX-VTMIN)/NOTPUT
      NOTPT=NOTPUT+1
      DO 180 IK=1,NOTPT
      VOBSRV=(IK-1)*DELTAP+VTMIN
      VPATT=VOBSRV*FRAC
      CALL FUNC(Y,VPATT ,CPHIH,NLAYER)
      SUMC=0.
      DO 110 ML=1,NLAYER
110   SUMC=SUMC+XY(ML)*CPHIH(ML)
      CONCEN=FEAC/FACTOR*SUMC
      WRITE(6,120)VOBSRV,CONCEN
120   FORMAT(5X,F9.2,20X,F10.6)
183   CONTINUE
C
C     "NLAYER" VOLUMES CORRESPONDING TO THE PEAK VOLUNES FROM THE
C     COKSTITUTING LAYERS ARE COMPUTED.  THE DIFFERENCE BETWEEN THE
C     INPUTED PEAK VOLUMES AND THE COMPUTED PEAK VOLUMES IS THE
C     AMOUNT OF SHIFT GENERATED UPON ADDING THE LAYER RESPONSES TO
C     FRODUCE AN OVERAL TRACER BREAKTHROUGH CURVE
C
      WRITE(6,200)
200   FORMAT(//,1X,'SELECTED PEAK VOLUME',5X,'COMPUTED PEAK VOLUME',/)
      DO 201 IJI=1,NLAYER
      VTMAXP(IJI)=VTMAXP(IJI)/FRAC
      VCAL=AREA*SW*VPDMXP /5.615/Y(IJI)
      VMXCAL=VCAL/FRAC
201   WRITE (6,202)VTMAXP(IJI),VMXCAL
202   FORMAT(7X,F7.1,18X,F7.1)
      GO TO 300
204   WRITE(6,205)
205   FORMAT(//,2X,'A LAYER PARAMETER IS NEGATIVE,',/,2X,'PROBABLY THE
     & SELECTED PEAK VOLUMES ARE NOT GOOD',//)
300   STOP
      END
C
C
C
      SUBROUTINE FUNC(VARBLE,VT,GAMA,NLAYER)
C
C     THIS SUBROUTINE COMPUTES THE GAMA(J,I) FOR A GIVEN TOTAL VOLUME
```

```
C     INJECTED. WHERE, GAMMA CORRESPOND TO THE PHI(J,I) FUNCTION IN
C     SUBROUTINE "VARPRO".  THE ROUTINE USES THE EQUATIONS OF TACER
C     BREAKTHROUGH CURVE FROM A DEVELOPED FIVE-SPOT IN CONJUCTION
C     WITH THE CQRRECTION FACTORS TO EVALUATE THE TRACER BREAKTHROUGH
C     FROM A PATTERN.
C
C     INPUT:  VARBLE = KJ/(PHI)J*SUM(KH), THE NON-LINEAR PARAMETERS
C                 VT = TOTAL PORE VOLUMES INJECTED INTO THE PATTERN
C                      AT WHICH GAMA WILL BE CALCULATED
C             NLAYER = NUMDER OF LAYERS
C     OUTPUT:   GAMA = VALUE OF GAMA AT VT.  IF THIS VALUE IS MULTI-
C                      PLIED BY THE J TH NON-LINEAR PARAMETER, TRACER
C                      CONCENTRATION FOR LAYER J AT TOTAL VOLUME OF
C                      VT, IS OBTAINED.
C
C
C
      IMPLICIT REAL*8 (A-H,O-Z)
      REAL*8 K,KP
      DIMENSION YSIGH(110),VPDBT(110),VARBLE(NLAYER),GAMA(15)
      DIMENSION FS(101),VTMAXP(15)
      COMMON /PAR/YSIGH,VPDBT
      COMMON /PARK/K,KP,VTMAXP,VPDMXP,EABT5,EABTP,FM,FP
      COMMON /FOEM/AREA,SW,AALFA5,TR,N,NM,H1,H2
      PI=4.*DATAN(1.D0)
      DO 55 IJ=1,NLAYER
      VPDPAT=5.615*VT*VARBLE(IJ)/(AREA*SW)
C
C     PORE VOLUMES INJECTED INTO AN EQUIVALENT FIVE-SPOT ARE CALCULATED
C     FROM THE PORE VOLUMES INJECTED INTO A PATTERN
C
      VPD5=(VPDPAT-EABTP)/(1-EABTP)*(1-EABT5)+EABT5
C
C     DIMENSIONLESS TRACER CONCENTRATIONS, CD, FROM A DEVELOPED
C     HOMOGENEOUS FIVE-SPOT ARE COMPUTED
C
      FS(1)=0.
      DO 80 J=1,N
      PVDIFF=(VPDBT(J)-VPD5)**2
      EX=-K*KP*KP*AALFA5*PVDIFF/(PI*PI*YSIGH(J))
      IF(EX.LT.-170.D0)GO TO 40
      FS(J+1)=DEXP(EX)/DSQRT(YSIGH(J))
      GO TO 80
40    FS(J+1)=0.D0
80    CONTINUE
      CALL INTGRL(N,H1,FS,VOL1)
      DO 90 J=N,NM
      PVDIFF=(VPDBT(J)-VPD5)**2
      EX=-K*KP*KP*AALFA5*PVDIFF/(PI*PI*YSIGH(J))
      IF(EX.LT.-170.D0)GO TO 50
      FS(J+1-N)=DEXP(EX)/DSQRT(YSIGH(J))
      GO TO 90
50    FS(J+1-N)=0.D0
90    CONTINUE
      CALL INTGRL(N,H2,FS,VOL2)
      VOL=VOL1+VOL2
      IF(VOL.GT.1.D-70)GO TO 115
      GAMA(IJ)=0.D0
      GO TO 55
C
```

```
C     VALUES OF "GAMA" FOR A FIVE-SPOT AXE EVALUATED
C
115     FR=DSQRT(AALFA5)*TR/(AREA*SW)
        GAMA(IJ)=4.*KP*DSQRT(K/PI)*VOL/(PI*PI)*FR
C
C     THE COMPUTED "GAMA" VALUES FOR THE FIVE-SPOT ARE CONVERTED
C     TO THOSE CORRESPONDING TO A PATTERN BY USING THE CORRECTION
C     FACTORS, FM AND FP.
C
        GAMA(IJ)=GAMA(IJ)*FM*DSQRT(FP)
55      CONTINUE
        RETURN
        END
C
C
C
        SUBROUTINE DFUNC(VARBLE,VT,DGAMA,NLAYER)
C
C     THIS SUBROUTINE COMPUTES DERIVATIVE OF THE GAMA FUNCTION WITH
C     RESPECT TO NON-LINEAR PARAKETERS FOR EACH LAYER.
C
C     INPUT:  VARBLE = KJ/(PHI)J*SUM(KH), THE NON-LINEAR PARAMETERS
C                 VT = TOTAL PORE VOLUMES INJECTED INTO THE PATTERN
C                      AT WHICH GAMA WILL BE CALCULATED
C             NLAYER = KUMBER OF LAYERS
C     OUTPUT : DGAMA = DERIVATIVE OF THE GAMA FUNCTION WITH RESPECT
C                      TO THE NON-LINER PARAMETER COMPUTED AT TOTAL
C                      VOLUME INJECTED, VT.
C
C
C
        IMPLICIT REAL*8 (A-H,O-Z)
        REAL*8 K,KP
        DIMENSION YSIGH(110),VPDBT(110),VARBLE(NLAYER),DGAMA(15)
        DIMENSION FS(101),VTMAXP(15)
        COMMON /PAR/YSIGH,VPDBT
        COMMON /PARK/K,KP,VTMAXP,VPDMXP,EABT5,EABTP,FM,FP
        COMMON /FORM/AREA,SW,AALFA5,TR,N,NM,H1,H2
        PI=4.*DATAN(1.D0)
        DO 55 IJ=1,NLAYER
        VPDPAT=5.615*VT*VARBLE(IJ)/(AREA*SW)
C
C     PORE VOLUMES INJECTED INTO A PATTERN ARE CONVERTED INTO THOSE
C     FROM AN EQUIVALENT DEVELOPED FIVE-SPOT
C
        VPD5=(VPDPAT-EABTP)/(1-EABTP)*(1-EABT5)+EABT5
C
C     DEIVATIVES OF DIMENSIOKLESS TRACER BREAKTHROUGH CURVE FROM A
C     HOMOGENEOUS FIVE-SPOT ARE COMPUTED
C
        FS(1)=0.
        DO 80 J=1,N
        PVDIFF=(VPDBT(J)-VPD5)**2
        EX=-K*KP*KP*AALFA5*PVDIFF/(PI*PI*YSIGH(J))
        IF(EX.LT.-150.D0)GO TO 40
        FS(J+1)=DEXP(EX)/DSQRT(YSIGH(J))*(VPDBT(J)-VPD5)/YSIGH(J)
        GO TO 80
40      FS(J+1)=0.D0
80      CONTINUE
        CALL INTGRL(N,H1,FS,VOL1)
```

```
      DO 90 J=N,NM
      PVDIFF=(VPDBT(J)-VPD5)**2
      EX=-K*KP*KP*AALFA5*PVDIFF/(PI*PI*YSIGH(J))
      IF(EX.LT.-150.D0)GO TO 50
      FS(J+1-N)=DEXP(EX)/DSQRT(YSIGH(J))*(VPDBT(J)-VPD5)/YSIGH(J)
      GO TO 90
50    FS(J+1-N)=0.D0
90    CONTINUE
      CALL INTGRL(N,H2,FS,VOL2)
      VOL=VOL1+VOL2
      IF(DABS(VOL).GT.1.D-70)GO TO 115
      DGAMA(IJ)=0.D0
      GO TO 55
C
C     DERIVATIVES OF GAMA FUNCTION FOR A DEVELOPED FIVE-SPOT ARE
C     CALCULATED
C
115   FR=DSQRT(AALFA5)*TR/(AREA*SW)
      DGAMA(IJ)=4.*KP*DSQRT(K/PI)*VOL/(PI*PI)*FR
      DGAMA(IJ)=DGAMA(IJ)*2*K*KP**2*AALFA5*5.615*VT/PI/PI/AREA/SW
C
C     DERIVATIVES OF GAMA FUNCTION ARE CONVERTED TO THOSE CORRESPONDING
C     TO THE PATTERN
C
      DGAMA(IJ)=DGAMA(IJ)*(1-EABT5)/(1-EABTP)*FM*DSQRT(FP)
55    CONTINUE
      RETURN
      END
C
C
C
      SUBROUTINE ADA(LP,NLAYER,NMAXA,NDATA,LENGTH,IP1,A,INC,T,ALF
     &  ,ISEL)
C
C     THIS SUBROUTINE SUPPLIES THE REQUIRED PARAMETRES FOR SUBROUTINE
C     "VARPRO"
C
C
      IMPLICIT REAL*8 (A-H,O-Z)
      REAL*8 K,KP
      DINENSION YSIGH(110),VPDBT(110),INC(15,16),T(NDATA,1)
      DIMENSION A(NDATA,LENGTH),VTMAXP(15),C(15),DC(15),ALF(NLAYER)
      COMMON /PAR/YSIGH,VPDBT
      COMMON /PARK/ K,KP,VTMAXP,VPDMXP,EABT5,EABTP,FM,FP
      COMMON /FORM/AREA,SW,AALFA5,TR,N,NM,H1,H2
C
      IF(ISEL.EQ.1)GO TO 10
      IF(ISEL.EQ.2)GO TO 20
      DO 30 I=1,NDATA
      VT=T(I,1)
      CALL DFUNC(ALF,VT,DC,NLAYER)
      DO 30 J=1,NLAYER
30    A(I,NLAYER+1+J)=DC(J)
      GO TO 100
10    DO 6 I=1,NLAYER
6     INC(I,I)=1
      DO 7 I=1,NLAYER
7     ALF(I)=AREA*SW*VPDMXP/5.615/VTMAXP(I)
      DO 9 I=1,NDATA
      VT=T(I,1)
```

```
      CALL FUNC(ALF,VT,C,NLAYER)
      CALL DFUNC(ALF,VT,DC,NLAYER)
      DO 9 J=1,NLAYER
      A(I,J)=C(J)
9     A(I,NLAYER+1+J)=DC(J)
      GO TO 100
20    DO 12 I=1,NDATA
      VT=T(I,1)
      CALL FUNC(ALF,VT,C,NLAYER)
      DO 12 J=1,NLAYER
12    A(I,J)=C(J)
100   RETURN
      END
C
C
      SUBROUTINE INTGRL(N,H,F,VOL)
C
C     THIS SUBROUTINE COMPUTES VALUE OF AN INTEGRAL USING SIMPSON'S
C     RULE OF INTEGRATION.
C     INPUT:  N = NUMBER OF INTERVALS, AN EVEN INTEGER NUMBER
C             H = INTERVAL SIZE
C             F = VALUES OF FUNCTIONS CCMPUTED AT INTERVALS, AN ARRAY
C     OUTPUT: VOL = VALUE OF THE INTEGRAL
C
      IMPLICIT REAL*8 (A-H,O-Z)
      DIMENSION F(91)
      SUN1=0
      SUM2=0
      N1=N/2-1
      DO 50 I=1,N1
      SUN1=SUM1+F(2*I)
50    SUM2=SUM2 +F(2*I+1)
      SUM1=SUM1+F(N)
      VOL=H/3*(F(1)tF(Nt1)t4.*SUM1+2.*SUM2)
      RETURN
      END
C
C
C
      SUBROUTINE GAUSS(UPPER,E,SIGMA)
C
C     THIS SUBROUTINE COMPUTES THE "Y" TERM IN THE MIXING LINE
C     INTEGRAL.  THE ROUTINE UTILIZES 8-POINT GAUSSIAN QUDRATURE METHOD
C     APPLIED SUCCESSIVELY TO A SERIES OF BROKEN INTERVALS.
C
C        INPUT: UPPER  = UPPER LIMIT OF THE INTEGRAL
C                    E = PARAPIETERS OF THE INTEGRAL = TAN(SIGH)**2
C        OUTPUT: SIGMA = VALUE OF THE INTEGRAL WHICH CORRESPONDS TO
C                        Y(SIGH)
C
C
      IMPLICIT REAL*8 (A-H,O-Z)
      DIMENSION W(15),X(15)
      F(Y)=DSQRT(Y/((Y*Y+1.)*(Y*Y+E2)*(Y*Y+E)))
      E2=E*E
      N=8
      X(1)=.183434642495650D0
      X(2)=.525532409916329D0
      X(3)=.796664774136272D0
      X(4)=.960289856497536D0
```

```
      X(5)=-X(1)
      X(6)=-X(2)
      X(7)=-X(3)
      X(8)=-X(4)
      W(1)=.362683783378362D0
      W(2)=.313706645877887D0
      W(3)=.222381034453374D0
      W(4)=.101228536290376D0
      W(5)=W(1)
      W(6)=W(2)
      W(7)=W(3)
      W(8)=W(4)
      AINT=0.D0
C
C     FOR VERY SMALL VALUES OF "E" (THE EXTREME STRRAMTUBES),
C     T=0 APPROACHES A SINGULARITY.  THEREFORE, SMALL INTERVAL
C     SIZES ARE CHOSEN AROUND THE LOWER LIMIT OF THE INTEGRAL.
C
      A=0.D0
      B=.01*E
20    IF(UPPER.LE.B) B=UPPER
      SUM=0.D0
      DO 10 I=1,N
      Y=.5D0*((B+A)+(B-A)*X(I))
10    SUM=SUM+W(I)*F(Y)
      VALUE=.5D0*(B-A)*SUM
      AINT=AINT+VALUE
      IF(UPPER.EQ.B)GO TO 30
      A=B
      IF(B.GT.1.0)  GO TO 50
      B=2.0D0*B
      GO TO 20
50    B=5.D0*B
      GO TO 20
30    SIGMA=(1.D0+E)**1.5*AINT
      RETURN
      END
C
C
      SUBROUTINE KVALUE(M,KM)
C
C     THIS SUBROUTINE COMPUTES THE VALUES OF K(M)
C     K(M)=COMPLEMENTARY COMPLETE ELLIPTIC INTEGRAL OF FIRST KIND
C     M=INPUT     ,KM=OUTPUT
C
      IMPLICIT REAL*8 (A-H,O-Z)
      REAL*8 M,M1,KM
      M1=1.D0-M
      A0=1.38629436112D0
      A1=.09666344259D0
      A2=.03590092383D0
      A3=.03742563713D0
      A4=.01451196212D0
      B0=.5D0
      B1=.12498593597D0
      B2=.06880248576D0
      B3=.03328355346D0
      B4=.00441787012D0
      X=A0+A1*M1+A2*M1**2+A3*M1**3+A4*M1**4
      Y=B0+B1*M1+B2*M1**2+B3*M1**3+B4*M1**4
```

```
      KM=X+Y*DLOG(1./M1)
      RETURN
      END
C
C
      SUBROUTINE ELLEP(Y,Z,A)
C
C     THIS SUBROUTINE COMPUTES INCOMPLETE ELLIPTIC INTEGRALN F(PHI,k)
C     PHI IS THE ARGUMENT AND k IS THE MODULUS.  THE MODULUS IS EQUAL
C     TO THE, SQUARE ROOT OF THE PARAMETER.
C     INPUT:  Y = ARGUMENT OF THE ELLIPTIC FUNCTION
C             Z = PARAMETER OF THE ELLIPTIC INTEGRAL
C             A = VALUE OF THE ELLIPTIC INTEGRAL
C     THE ROUTINE USES LANDENS DECENDING TRANSFORMATION.  FOR REFERENCE
C     SEE ABRAMOWITZ, PAGE
C
C
      IMPLICIT REAL*8 (A-H,O-Z)
      REAL*8  K,K1,KP
      TOL=1.D-4
      PI=4.*DATAN(1.D0)
      W=1.D0
      X=Y
      K=DSQRT(Z)
15    K1=2.*DSQRT(K)/(1+K)
      X=.5*(X+DARSIN(K*DSIN(X)))
      QE=DARSIN(K1)
      QE=QE*180./PI
      W=2.*W/(1+K)
      IF((90.-QE).LE.TOL)GO TO 30
      K=K1
      GO TO 15
30    A=W*DLOG(DTAN(PI/4+X/2))
      RETURN
      END
C
      SUEROUTINE VARPRO (L, NL, N, NMAX, LPP2, IV, T, Y, W, ADA, A,
     X IPRINT, ALF, BETA, IERR)
C
C          GIVEN A SET OF N OBSERVATIONS, CONSISTING OF VALUES Y(1),
C       Y(2), ..., Y(N) OF A DEPENDENT VARIABLE Y, WHERE Y(I)
C       CORRESPONDS TO THE IV INDEPENDENT VARIABLE(S) T(I,1), T(I,2),
C       ..., T(I,IV), VARPEO ATTEMPTS TO COMPUTE A WEIGHTED LEAST
C       SQUARES FIT TO A FUNCTION ETA (THE 'MODEL')  WHICH IS A LINEAR
C       COMBINATION
C                                L
C      ETA(ALF, BETA; T)  =  SUM  BETA   * PHI (ALF; T) + PHI   (ALF; T)
C                            J=1      J      J              L+1
C
C       OF NONLINEAR FUNCTIONS PHI(J) (E.G., A SUN OF EXPONENTIALS AND/
C       OR GAUSSIANS).  THAT IS, DETERMINE THE LINEAR PARAMETERS
C       BETA(J) AND THE VECTOR OF NONLINEAR PARAMETERS ALF BY MINIMIZ-
C       ING
C
C                          2     N                                  2
C          NORM(RESIDUAL)  =  SUN  W  * (Y  - ETA(ALF, BETA; T ))  .
C                             I=1   I     I                    I
C
C       THE (L+1)-ST TERN IS OPTIONAL, AND IS USED WHEN IT IS DESIRED
C       TO FIX ONE OR MORE OF THE BETA'S  (RATHER THAN LET THEM BE
```

```
C        DETERMINED).   VARPRO REQUIRES FIRST DERIVATIVES OF THE PHI'S.
C
C                                  NOTES:
C
C        A)  THE ABOVE PROBLEM IS ALSO REFERRED TO AS 'MULTIPLE
C        NONLINEAR REGRESSION'.   FOR USE IN STATISTICAL ESTIMATION,
C        VARPRO RETURNS THE RESIDUALS, THE COVARIANCE MATRIX OF THE
C        LINEAR AND NONLINFAR PARAPIETERS, AND THE ESTIMATED VARIANCE OF
C        THE OBSERVATIONS.
C
C        B) 'AN ETA OF THE ABOVE FORM IS CALLED 'SEPARABLE'.   THE
C        CASE OF A NONSEPARABLE ETA CAN BE HANDLED BY SETTING L = 0
C        AND USING PHI(L+1).
C
C        C) VARPRO MAY ALSO BE USED TO SOLVE LINEAR LEAST SQUARES
C        PROBLEMS (IN THAT CASE NO ITERATIONS ARE PERFORMED).   SET
C        NL = 0.
C
C        D)  THE MAIN ADVANTAGE OF VARPRO OVER OTHER LEAST SQUARES
C        PROGRAMS IS THAT NO INITIAL GUESSES ARE NEEDED FOR THE LINEAR
C        PARAMETERS.   NOT ONLY DOES THIS MAKE IT EASIER TO USE, BUT IT
C        OFTEN LEADS TO FASTER CONVERGENCE.
C
C
C     DESCRIPTION OF PARAMETERS
C
C        L        NUMBER OF LINEAR PARAMETERS BETA (MUST BE .GE. 0).
C        NL       NUMBER OF NONLINEAR PARAMETERS ALF (MUST BE .GE. 0).
C        N        NUMBER OF OBSERVATIONS.   N MUST BE GREATER THAN L + NL
C                 (I.E., THE NUMBER OF OBSERVATIONS MUST EXCEED THE
C                 NUMBER OF PARAPIETERS) .
C        IV       NUMBER OF INDEPENDENT VARIABLES T.
C        T        REAL N BY IV MATRIX OF INDEPENDENT VARIABLES.   T(I, J)
C                 CONTAINS THE VALUE OF THE I-TH OBSERVATION OF THE J-TH
C                 INDEPENDENT VARIABLE.
C        Y        N-VECTOR OF OBSERVATIONS, ONE FOR EACH ROW OF T.
C        W        N-VECTOR OF NONNEGATIVE WEIGHTS.   SHOULD BE SET TO 1'S
C                 IF WEIGHTS ARE NOT DESIRED.   IF VAEIANCES OF THE
C                 INDIVIDUAL OBSERVATIONS ARE KNOWN, W(I) SHOULD BE SET
C                 TO 1./VARIANCE(I).
C        INC      NL X (L+1) INTEGER INCIDENCE MATRIX.   INC(K, J) = 1 IF
C                 NON-LINEAR PARAMETER ALF(K) APPEARS IN THE J-TH
C                 FUNCTION PHI(J).   (THE PROGRAM SETS ALL OTHER INC(K, J)
C                 TO ZERO.)   IF PHI(L+1) IS INCLUDED IN THE MODEL,
C                 THE APPROPRIATE ELEMENTS OF THE (L+1)-ST COLUMN SHOULD
C                 BE SET TO 1'S.   INC IS NOT NEEDED WHEN L = 0 OR NL = 0.
C                 CAUTION:   THE DECLARED ROW DIMENSION OF INC (IN ADA)
C                 MUST CURRENTLY BE SET TO 12.   SEE 'RESTRICTIONS'  BELOW.
C        HMAX     THE DECLARED ROW DIMENSION OF THE MATRICES A AND T.
C                 IT MUST BE AT LEAST MAX(N, 2*NL+3).
C        LPP2     L+P+2, WHERE P IS THE NUMBER OF ONES IN THE MATRIX INC.
C                 THE DECLARED COLUMN DIMENSION OF A MUST BE AT LEAST
C                 LPP2.   (IF L = 0, SET LPP2 = NL+2. IF NL = 0, SET LPPZ
C                 L+2.)
C        A        REAL MATRIX OF SIZE MAX(N, 2*NL+3) BY L+P+2.   ON INPUT
C                 IT CONTAINS THE PHI(J)'S AND THEIR DERIVATIVES (SEE
C                 BELOW).   ON OUTPUT, THE FIRST L+NL ROWS AND COLUMNS OF
C                 A WILL CONTAIN AN APPROXIMATION TO THE (WEIGHTED)
C                 COVARIANCE MATRIX AT THE SOLUTION (THE FIRST L ROWS
C                 CORRESPOND TO THE LINEAR PARAMETERS,  THE LAST NL TO THE
```

```
C               NONLINEAR ONES),  COLUMN L+NL+1 WILL CONTAIN THE
C               WEIGHTED RESIDUALS (Y - ETA),  A(1, L+NL+2) WILL CONTAIN
C               THE (EUCLIDEAN) NORM OF THE WEIGHTED RESIDUAL,  AND
C               A(2, L+NL+2) WILL CONTAIN AN ESTIMATE OF THE (WEIGHTED)
C               VARIANCE OF THE OBSERVATIONS,  NORM(RESIDUAL)**2/
C               (N - L - NL).
C       IPRINT  INPUT INTEGER CONTROLLING PRINTED OUTPUT.  IF IPRINT IS
C               POSITIVE,  THE NONLINEAR PARAMETERS,  THE NORM OF THE
C               RESIDUAL,  AND THE MARQUARDT PARAMETER WILL BE OUTPUT
C               EVERY IPRINT-TH ITERATION (AND INITIALLY,  AND AT THE
C               FINAL ITERATION).  THE LINEAR PARAMETERS WILL BE
C               PRINTED AT THE FINAL ITERATION.  ANY ERROR MESSAGES
C               WILL ALSO BE PRINTED.  (IPRINT = 1 IS RECOMMENDED AT
C               FIRST.)  IF IPRINT = 0,  ONLY THE FINAL QUANTITIES WILL
C               BE PRINTED,  AS WELL AS ANY ERROR MESSAGES.  IF IPRINT =
C               - 1,  NO PRINTING WILL BE DONE.  THE USER IS THEN
C               RESPONSIBLE FOR CHECKING THE PARAMETER IERR FOR ERRORS.
C       ALF     NL-VECTOR OF ESTIMATES OF NONLINEAR PARAMETERS
C               (INPUT).  ON OUTFUT IT WILL CONTAIN OPTIMAL VALUES OF
C               THE NONLINEAR PARAMETERS.
C       BETA    L-VECTOR OF LINEAR PARAMETERS (OUTPUT ONLY).
C       IERR    INTEGER ERROR FLAG (OUTPUT):
C               .GT. 0 - SUCCESSFUL CONVERGENCE,  IERR IS THE NUMBER OF
C                   ITERATIOKS TAKEN.
C               - 1  TERMINATED FOR TOO MANY ITERATIONS.
C               - 2  TERMINATED FOX ILL-CONDITIONING (MARQUARDT
C                   PARAMETER TOO LARGE.)  ALSO SEE IERR = -8 BELOW.
C               -4  INPUT ERROR IN PARAMETER N,  L,  NL,  LPP2,  OR NMAX.
C               -5  INC MATRIX IMPROPERLY SPECIFIED,  OR P DISAGREES
C                   WITH LPP2.
C               -6  A WEIGHT WAS NEGATIVE.
C               -7  'CONSTANT' COLUMN WAS COMPUTED MORE THAN ONCE.
C               -8  CATASTROPHIC FAILURE - A COLUMN OF THE A MATRIX HAS
C                   BECOME ZERO.  SEE 'CONVERGENCE FAILURES' BELOW.
C
C               (IF IERR .LE. -4,  THE LINEAR PARAMETERS,  COVARIANCE
C               MATRIX,  ETC.  ARE NOT RETURNED.)
C
C     SUBROUTINES REQUIRED
C
C          NINE SUBROUTINES,  DPA,  ORFAC1,  ORFAC2,  BACSUB,  POSTPR,  COV,
C       XNORM,  INIT,  AND VARERR ARE PROVIDED.  IN ADDITION,  THE USER
C       MUST PROVIDE A SUBROUTINE (CORRESPONDING TO THE ARGUMENT ADA)
C       WHICH,  GIVEN ALF,  WILL EVALUATE THE FUNCTIONS PHI(J) AND THEIR
C       PARTIAL DERIVATIVES D PHI(J)/D ALF(K),  AT THE SAMPLE POINTS
C       T(I).  THIS ROUTINE MUST BE DECLARED 'EXTERNAL'  IN THE CALLING
C       PROGRAM.  ITS CALLING SEQUENCE IS
C
C       SUBROUTINE ADA (L+1,  NL,  N,  NMAX,  LPP2,  IV,  A,  INC,  T,  ALF,
C       ISEL)
C
C          THE USER SHOULD MODIFY THE EXAMPLE SUBROUTINE 'ADA'  (GIVEN
C       ELSEWHERE) FOR HIS OWN FUNCTIONS.
C
C          THE VECTOR SAMPLED FUNCTIONS PHI(J) SHOULD BE STORED IN THE
C       FIRST N ROWS AND FIRST L+1 COLUMNS OF THE MATRIX A,  I.E.,
C       A(I,  J) SHOULD COKTAIN PHI(J,  ALF;  T(I,1),  T(I,2),  ...,
C       T(I,IV)),  I = 1,  ...,  N;  J = 1,  ...,  L (OR L+1).  THE (L+1)-ST
C       COLUMN OF A CONTAINS PHI(L+1) IF PHI(L+1) IS IN THE MODEL,
C       OTHERLJISE IT IS RESERVED FOR WORKSPACE.  THE 'CONSTANT'  FUNC-
```

```
C       TIONS (THESE ARE FUNCTIONS PHI(J) WHICH DO NOT DEPEND UPON ANY
C       NONLINEAR PARAMETERS ALF, E.G., T(I)**J) (IF ANY) MUST APPEAR
C       FIRST, STARTING IN COLUMN 1.  THE COLUMN N-VECTORS OF NONZERO
C       PARTIAL DERIVATIVES D PHI(J) / D ALF(K) SHOULD BE STORED
C       SEQUENTIALLY IN THE MATRIX A IN COLUMNS L+2 THROUGH L+P+1.
C       THE ORDER IS
C
C         D PHI(1)  D PHI(2)        D PHI(L)  D PHI(L+1)  D PHI(1)
C         --------, --------, ...,  --------, ----------, --------,
C         D ALF(1)  D ALF(1)        D ALF(1)   D ALF(1)   D ALF(2)
C
C         D PHI(2)       D PHI(L+1)       D PHI(1)        D PHI(L+1)
C         --------, ..., ----------, ..., ---------, ...,  ----------,
C         D ALF(2)        D ALF(2)        D ALF(NL)       D ALF(NL)
C
C       OMITTING COLUMNS OF DERIVATIVES WHICH ARE ZERO, AND OMITTING
C       PHI(L+1) COLUMNS IF PHI(L+1) IS NOT IN THE MODEL.  NOTE THAT
C       THE LINEAR PARAMETERS BETA ARE NOT USED IN THE MATRIX A.
C       COLUMN L+P+2 IS RESERVED FOR WORKSPACE.
C
C       THE CODING OF ADA SHOULD BE ARRANGED SO THAT:
C
C       ISEL = 1  (WHICH OCCURS THE FIRST TIME ADA IS CALLED) MEANS:
C                 A.  FILL IN THE INCIDENCE MATRIX INC
C                 B.  STORE ANY CONSTANT PHI'S IN A.
C                 C.  COMPUTE NONCONSTANT PHI'S AND PARTIAL DERIVA-
C                     TIVES.
C            = 2  MEANS COMPUTE ONLY THE NONCONSTANT FUNCTIONS PHI
C            = 3  MEANS COMPUTE ONLY TtiE DERIVATIVES
C
C       (WHEN THE PROBLEM IS LINEAR (NL = 0) ONLY ISEL = 1 IS USED, AND
C       DERIVATIVES ARE NOT NEEDED.)
C
C     RESTRICT1ONS
C
C          THE SUBROUTINES DPA, INIT (AND ADA) CONTAIN THE LOCALLY
C       DIMENSIONED MATRIX INC, WHOSE DIMENSIONS ARE CURRENTLY SET FOE
C       MAXIMA OF LtI =16, NL = 15.  THEY MUST BE CHANGED FOR LARGER
C       PROBLEMS.  DATA PLACED IN ARRAY A IS OVERWRITTEN ('DESTROYED').
C       DATA PLACED IN ARRAYS T, Y AND INC IS LEFT INTACT.  THE PROGRAM
C       RUNS IN WATFIV, EXCEPT WHEN L = 0 OR NL = 0.
C
C          IT IS ASSUMED THAT THE MATRIX PHI(J, ALF; T(I)) HAS FULL
C       COLUMN RANK.  THIS MEANS THAT THE FIRST L COLUMNS OF THE MATRIX
C       A MUST BE LINEARLY INDEPENDENT.
C
C          OPTIONAL NOTE:  AS WILL BE NOTED FROM THE SAMPLE SUBPROGRAM
C       ADA, THE DERIVATIVES D PHI(J)/D ALF(K) (ISEL = 3) MUST BE
C       COMPUTED INDEPENDENTLY OF THE FUNCTIONS PHI(J) (ISEL = 2),
C       SINCE THE FUNCTION VALUES ARE OVERWRITTEN AFTER ADA IS CALLED
C       WITH ISEL = 2.  THIS IS DONE TO MINIMIZE STORAGE, AT THE POS-
C       SIBLE EXPENSE OF SOME RECOMPUTATION (SINCE THE FUNCTIONS AND
C       DER■VAT■VES FREQUENTLY HAVE SOME COMMON SUBEXPRESSIONS).  TO
C       REDUCE THE AMOUNT OF COMPUTATION AT THE EXPENSE OF SOME
C       STORAGE, CREATE A MATRIX B OF DIMENSION NMAX BY L+1 IN ADA, AND
C       AFTER THE COMPUTATION OF THE PHI'S (ISEL = 2), COPY THE VALUES
C       INTO B.  THESE VALUES CAN THEN BE USED TO CALCULATE THE DERIV-
C       ATIVES (ISEL = 3).  (THIS MAKES USE OF THE FACT THAT WHEN A
C       CALL TO ADA WITH ISEL = 3 FOLLOWS A CALL WITH ISEL = 2, THE
C       ALFS ARE THE SAME.)
```

```
C
C          TO CONVERT TO OTHER MACHINES, CHANGE THE OUTPUT UNIT IN THE
C       DATA STATEMENTS IN VARPRO, DPA, POSTPR, AND VARERR.  THE
C       PROGRAM HAS BEEN CHECKED FOR PORTABILITY BY THE BELL LABS PFORT
C       VERIFIER.  FOR MACHINES WITHOUT DOUBLE PRECISION HARDWARE, IT
C       MAY BE DESIRABLE TO CONVERT TO SINGLE PRECISION.  THIS CAN DE
C       DONE BY CHANGING (A) THE DECLARATIONS 'DOUBLE PRECISION' TO
C       'REAL', (B) THE PATTERN '.D' TO '.E' IN THE 'DATA' STATEMENT IN
C       VARPRO, (C) DSIGN, DSQRT AND DABS TO SIGN, SQRT AND ABS,
C       RESPECTIVELY, AND (D) DEXP TO EXP IN THE SAMPLE PROGRAMS ONLY.
C
C     NOTE ON INTERPRETATION OF COVARIANCE MATRIX
C
C          FOR USE IN STATISTICAL ESTIMATION (MULTIPLE NONLINEAR
C       REGRESSION) VARPRO RETURNS THE COVARIANCE MATRIX OF THE LINEAR
C       AND NONLINEAR PARAMETERS.  THIS MATRIX WILL BE USEFUL ONLY IF
C       THE USUAL STATISTICAL ASSUMPTIONS HOLD:  AFTER WEIGHTING, THE
C       ERRORS IN THE OBSERVATIONS ARE INDEPENDENT AND NORMALLY DISTRI-
C       BUTED, WITH MEAN ZERO AND THE SAME VARIANCE.  IF THE ERRORS DO
C       NOT HAVE MEAN ZERO (OR ARE UNKNOWN), THE PROGRAM WILL ISSUE A
C       WARNING MESSAGE (UNLESS IPRINT .LT. 0) AND THE COVARIANCE
C       MATRIX WILL NOT BE VALID.  IN THAT CASE, THE MODEL SHOULD BE
C       ALTERED TO INCLUDE A CONSTANT TERM (SET PHI(1) = 1.).
C
C          NOTE ALSO THAT, IN ORDER FOR TtiE USUAL ASSUMPTIONS TO HOLD,
C       THE OBSERVATIONS MUST ALL BE OF APPROXIMATELY THE SAME
C       MAGNITUDE (IN THE ABSENCE OF INFORMATION ABOUT THE ERROR OF
C       EACH OBSERVATION) , OTHERWISE TIIE VARIANCES WILL NOT BE THE
C       SAME.  IF THE OBSERVATIONS ARE NOT THE SAME SIZE, THIS CAN BE
C       CURED BY WEIGHTING.
C
C          IF TtiE USUAL ASSUMFTIONS HOLD, THE SQUARE ROOTS OF THE
C       DIAGONALS OF THE COVARIANCE MATRIX A GIVE THE STANDARD ERROR
C       S(I) OF EACH PARAMETER.  DIVIDING A(I,J) BY S(I)*S(J) YIELDS
C       THE CORRELATION MATRIX OF THE PARAMETERS.  PRINCIPAL AXES AND
C       CONFIDENCE ELLIPSOIDS CAN BE OBTAINED BY PERFORMING AN EIGEN-
C       VALUE/EIGENVECTOR ANALYSIS ON A.  ONE SHOULD CALL THE EISPACK
C       PROGRAM TRED2, FOLLOWED BY TQL2 (OR USE THE EISPAC CONTROL
C       PROGRAM).
C
C     CONVERGENCE FAILURES
C
C          IF CONVERGENCE FAILURES OCCUR, FIRST CHECK FOR INCORRECT
C       CODING OF THE SUBROUTINE ADA.  CHECK ESPECIALLY THE ACTION OF
C       ISEL, AND THE COMPUTATION OF THE PARTIAL DERIVATIVES.  IF THESE
C       ARE CORRECT, TRY SEVERAL STARTING GUESSES FOR ALF.  IF ADA
C       IS CODED CORRECTLY, AND IF ERROR RETURNS IERR = -2 OR -8
C       PERSISTENTLY OCCUR, THIS IS A SIGN OF ILL-CONDITIONING, WHICH
C       MAY BE CAUSED BY SEVERAL THINGS.  ONE IS POOR SCALING OF THE
C       PARAMETERS; ANOTHER IS AN UNFORTUNATE INITIAL GUESS FOR THE
C       PARAMETERS, STILL ANOTHER IS A POOR CHOICE OF THE MODEL.
C
C     ALGORITHM
C
C          THE RESIDUAL R IS MODIFIED TO INCORPORATE, FOR ANY FIXED
C       ALF, THE OPTIMAL LINEAR PARAMETERS FOR THAT ALF.  IT IS THEN
C       POSSIBLE TO MINIMIZE ONLY ON THE NONLINEAR PARAMETERS.  AFTER
C       THE OPTIMAL VALUES OF THE NONLINEAR PARAMETERS HAVE BEEN DETER-
C       MINED, THE LINEAR PARAMETERS CAN BE RECOVERED BY LINEAR LEAST
C       SQUARES TECHNIQUES (SEE REF. 1).
```

```
C
C          TtiE MINIMIZATION IS BY A MODIFICATION OF OSBORNE'S (REF. 3)
C       MODIFICATION OF THE LEVENBERG-MARQUARDT ALGORITHM.  INSTEAD OF
C       SOLVING THE NORMAL EQUATIONS WITH MATRIX
C
C                T      2
C             (J J + NU  * D),      WHERE  J = D(ETA)/D(ALF),
C
C       STABLE ORTHOGONAL (HOUSEHOLDER) REFLECTIONS ARE USED ON A
C       MODIFICATION OF THE MATRIX
C                                  (   J   )
C                                  (------) ,
C                                  ( NU*D )
C
C       WHERE D IS A DIAGONAL MATRIX CONSISTING OF THE LENGTHS OF THE
C       COLUMNS OF J.  THIS MARQUARDT STABILIZATION ALLOWS THE ROUTINE
C       TO RECOVER FROM SOME RANK DEFICIENCIES IN THE JACOBIAN.
C       OSBORNE'S EMPIRICAL STRATEGY FOR CHOOSING THE MARQUARDT PARAM-
C       ETER HAS PROVEN REASONABLY SUCCESSFUL IN PRACTICE.  (GAUSS-
C       NEWTON WITH STEP CONTROL CAN BE OBTAINED BY MAKING THE CHANGE
C       INDICATED BEFORE THE INSTRUCTION LABELED 5).  A DESCRIPTION CAN
C       BE FOUND IN REF. (3), AND A FLOW CHART IN (2), P. 22.
C
C       FOR REFERENCE, SEE
C
C       1.  GENE H. GOLUB AND V. PEREYRA, 'THE DIFFERENTIATION OF
C           PSEUDO-INVERSES AND NONLINEAR LEAST SQUARES PROBLEMS WHOSE
C           VARIABLES SEPARATE,'  SIAM J. NUMER. ANAL. 10, 413-432
C           (1973).
C       2.  ------, SAME TITLE, STANFORD C.S. REPORT 72-261, FEB. 1972.
C       3.  OSBORNE, MICHAEL R., 'SOME ASFECTS OF RON-LINEAE LEAST
C           SQUARES CALCULATIONS,'  IN LOOTSMA, ED., 'NUMERICAL METHODS
C           FOE Noli-LINEAR OPTIMIZATION,' ACADEMIC PRESS, LONDON, 1972.
C       4.  KROGH, FRED, 'EFFICIENT IMPLEMENTATION OF A VARIABLE FRO-
C           JECTION ALGORITHM FOR NONLINEAR LEAST SQUARES PROBLEMS,'
C           COMM. ACM 17, PP. 167-169 (MARCH, 1974).
C       5.  KAUFMAN, LINDA, 'A VARIABLE PROJECTION METHOD FOR SOLVING
C           SEPARABLE NONLINEAR LEAST SQUARES PROBLEMS', B.I.T. 15,
C           49-57 (1975).
C       6.  DRAPER, N., AND SMITH, H., APPLIED REGRESSION ANALYSIS,
C           WILEY, N.Y., 1966 (FOR STATISTICAL INFORMATION ONLY).
C       7.  C. LAWSON AND R. HANSON, SOLVING LEAST SQUARES PROBLEMS,
C           PRENTICE-HALL, ENGLEWOOD CLIFFS, N. J., 1974.
C
C                     JOHN BOLSTAD
C                     COXPUTER SCIENCE DEPT., SERRA HOUSE
C                     STANFORD UNIVERSITY
C                     JANUARY, 1977
C
C     ..............................................................
C
      DOUBLE PRECISION A(NMAX, LPP2), BETA(L), ALF(NL), T(NMAX, IV),
     2 W(N), Y(N), ACUM, EPS1, GNSTEP, NU, PRJRES, R, RNEW, XNORM
      INTEGER B1, OUTPUT
      LOGICAL SKIP
      EXTERNAL ADA
      DATA EPSI /1.D-6/, ITMAX /28/, OUTPUT /6/
C
C          THE FOLLOWING TWO PARAMETERS ARE USED IN THE CONVERGENCE
C          TEST:  EPSI IS AN ABSOLUTE AND RELATIVE TOLERANCE FOR THE
```

```
C           NORM OF THE PROJECTION OF THE RESIDUAL ONTO THE RANGE OF THE
C           JACOBIAN OF THE VARIABLE PROJECTION FUNCTIONAL.
C           ITMAX IS THE MAXIMUM NUMBER OF FUNCTION AND DERIVATIVE
C           EVALUATIONS ALLOWED.  CAUTION:  EPSI MUST NOT BE
C           SET SMALLER THAN 10 TIMES THE UNIT ROUND-OFF OF THE MACHINE.
C
C-----------------------------------------------------------------
CALL LIB MONITOR FROM VARPRO, MAINTENANCE NUMBER 509, DATE 77178
C***PLEASE DON'T REMOVE OR CHANGE THE ABOVE CALL. IT IS YOUR ONLY
C***PROTECTION AGAINST YOUR USING AN OUT-OF-DATE OR INCORRECT
C***VERSION OF THE ROUTINE. THE LIBRARY MONITOR REMOVES THIS CALL,
C***SO IT ONLY OCCURS ONCE, ON THE FIRST ENTRY TO THIS ROUTINE.
C-----------------------------------------------------------------
      IERR = 1
      ITER = 0
      LP1 = L + 1
      B1 = L + 2
      LNL2 = L + NL + 2
      NLP1 = NL + 1
      SKIP = .FALSE.
      MODIT = IPRINT
      IF (IPRINT .LE. 0) MODIT = ITMAX + 2
      NU = 0.
C               IF GAUSS-NEWTON IS DESIRED REMOVE THE NEXT STATEMENT.
      NU = 1.
C
C               BEGIN OUTER ITERATION LOOP TO UPDATE ALF.
C               CALCULATE THE NORM OF THE RESIDUAL AND THE DERIVATIVE OF
C               THE MODIFIED RESIDUAL THE FIRST TIME, BUT ONLY THE
C               DERIVATIVE IN SUBSEQUENT ITERATIONS.
C
    5 CALL DPA (L, NL, N, NMAX, LPP2, IV, T, Y, W, ALF, ADA, IERR,
     X IPRINT, A, BETA, A(1, LP1), R)
      GNSTEP = 1.0
      ITERIN = 0
      IF (ITER .GT. 0) GO TO 10
         IF (NL .EQ. 0) GO TO 90
         IF (IERR .NE. 1) GO TO 99
C
         IF (IPRINT .LE. 0) GO TO 10
         WRITE (OUTPUT, 207) ITERIN, R
         WRITE (OUTPUT, 200) NU
C                                BEGIN TWO-STAGE ORTHOGONAL FACTORIZATION
   10 CALL ORFAC1(NLP1, NMAX, N, L, IPRINT, A(1, B1), PRJRES, IERR)
      IF (IERR .LT. 0) GO TO 99
      IERR = 2
      IF (NU .EQ. 0.) GO TO 30
C
C               BEGIN INNER ITERATION LOOP FOR GENERATING NEW ALF AND
C               TESTING IT FOR ACCEPTANCE.
C
   25    CALL ORFAC2(NLP1, NMAX, NU, A(1, B1))
C
C               SOLVE A NL X NL UFPER TRIANGULAR SYSTEM FOR DELTA-ALF.
C               THE TRANSFORMED RESIDUAL (IN COL. LNLP DF A) IS OVER-
C               WRITTEN BY THE RESULT DELTA-ALF.
C
   30    CALL BACSUB (NMAX, NL, A(1, B1), A(1, LNL2))
         DO 35 K = 1, NL
   35       A(K, B1)  = ALF(K) + A(K, LNL2)
```

```
C           NEW ALF(K) = ALF(K) + DELTA ALF(K)
C
C              STEP TO THE NEW POINT NEW ALF, AND COMPUTE THE NEW
C              NORM OF RESIDUAL.  NEW ALF IS STORED IN COLUMN B1 OF A.
C
   40     CALL DPA (L, NL, N, NMAX, LPP2, IV, T, Y, W, A(1, B1), ADA,
     X    IERR, IPRINT, A, BETA, A(1, LP1), RNEW)
          IF (IERR .NE. 2) GO TO 99
          ITER = ITER + 1
          ITERIN = ITERIN + 1
          SKIP = MOD(ITER, MODIT) .NE. 0
          IF (SKIP) GO TO 45
             WRITE (OUTPUT, 203) ITER
             WRITE (OUTPUT, 216) (A(K, B1), K = 1, NL)
             WRITE (OUTPUT, 207) ITERIN, RNEW
C
   45     IF (ITER .LT. ITMAX) GO TO 50
             IERR = -1
             CALL VARERR (IPRINT, IERR, 1)
             GO TO 95
   50     IF (RNEW - R .LT. EPS1*(R + 1.D0)) GO TO 75
C
C              RETRACT THE STEP JUST TAKEN
C
             IF (NU .NE. 0.) GO TO 60
C                                                GAUSS-NEWTON OPTION ONLY
             GNSTEP = 0.5*GNSTEP
             IF (GNSTEP .LT. EPS1) GO TO 95
             DO 55 K = 1, NL
   55           A(K, B1) = ALF(K) + GNSTEP*A(K, LNL2)
             GO TO 40
C                                          ENLARGE THE MARQUARDT PARAMETER
   60        NU = 1.5*NU
             IF (.NOT. SKIP) WRITE (OUTPUT, 206) NU
             IF (NU .LE. 100.) GO TO 65
                IERR = -2
                CALL VARERR (IPRINT, IERR, 1)
                GO TO 95
C                                          RETRIEVE UPPER TRIANGULAR FORM
C                                          AND RESIDUAL OF FIRST STAGE.
   65     DO 70 K = 1, NL
             KSUB = LP1 + K
             DO 70 J = K, NLPI
                JSUB = LP1 + J
                JSUB = NLPI + J
   70           A(K, JSUB) = A(ISUB, KSUB)
          GO TO 25
C                                          END OF INNER ITERATION LOOP
C            ACCEPT THE STEP JUST TAKEN
C
   75 R = RNEW
      DO 80 K = 1, NL
   80    ALF(K) = A(K, B1)
C                                          CALC. NORM(DELTA ALF)/NORM(ALF)
      ACUM = GNSTEP*XNORM(NL, A(1, LNL2))/XNORM(NL, ALF)
C
C            IF ITERIN IS GREATER THAN 1, A STEP WAS RETRACTED DURING
C            THIS OUTER ITERATION.
C
      IF (ITERIN .EQ. 1) NU = 0.5*NU
```

```
      IF (SKIP) GO TO 85
         WRITE (OUTPUT, 200) NU
         WRITE (OUTPUT, 208) ACUM
   85 IERR = 3
      IF (PRJRES .GT. EPS1*(R + 1.D0)) GO TO 5
C           END OF OUTER ITERATION LOOP
C
C           CALCULATE FINAL QUANTITIES -- LINEAR PARAMETERS, RESIDUALS,
C           COVARIANCE MATRIX, ETC.
C
   90 IERR = ITER
   95 IF (NL .GT. 0) CALL DPA(L, NL, N, NMAX, LPP2, IV, T, Y, W, ALF,
     X ADA, 4, IPRINT, A, BETA, A(1, LP1), R)
      CALL POSTPR(L, NL, N, NMAX, LNL2, EPS1, R, IPRINT, ALF, W, A,
     X A(1, LP1), BETA, IERR)
   99 RETURN
C
  200 FORMAT (9H     NU =, E15.7)
  203 FORMAT (12H0  ITERATION, I4, 24H    NONLINEAR PARAMETERS)
  206 FORMAT (25H     STEP RETRACTED, NU =, E15.7)
  207 FORMAT (1H0, I5, 20H  NORM OF RESIDUAL =, E15.7)
  208 FORMAT (34H     NORMCDELTA-ALF) / NORM(ALF) =, E12.3)
  216 FORMAT (1H0, 7E15.7)
      END
C
      SUBROUTINE ORFAC1(NLP1, NMAX, N, L, IPRINT, B, PRJRES, IERR)
C
C           STAGE 1:  HOUSEHOLDER REDUCTION OF
C
C                 (          )      ( DE'.  R3 )    NL
C                 ( DR  . R2 )  TO  (----. -- ),
C                 (          )      (  0  . R4 )  N-L-NL
C
C                   NL     1           NL    1
C
C         WHERE DR = -D(Q2)*Y IS THE DERIVATIVE OF THE MCDIFIED RESIDUAL
C         PRODUCED BY DPA, R2 IS THE TRANSFORMED RESIDUAL FROM DPA, AND
C         DR' IS IN UPPER TRIANGULAR FORM (AS IN REF. (2), P. 18).
C         DR IS STORED IN ROWS L+1 TO N AND COLUMNS L+2 TO L + NL + 1 OF
C         THE MATRIX A (I.E., COLUMNS 1 TO NL OF THE MATRIX B).  R2 IS
C         STORED IN COLUMN L + NL + 2 OF THE MATRIX A (COLUMN NL + 1 OF
C         B).  FOR K = 1, 2, ..., NL, FIND REFLECTION I - U * U' / BETA
C         WHICH ZEROES B(I, K), I = L+K+1, ..., N.
C
C     ..............................................................
C
      DOUBLE PRECISION ACUM, ALPHA, B(NMAX, NLP1), BETA, DSIGN, PRJRES,
     X U, XNORM
C
      NL = NLPl - 1
      NL23 = 2*NL + 3
      LP1 = L + 1
C
      DO 30 K = 1, NL
         LPK = L + K
         ALPHA = DSIGN(XNORM(N+1-LPK, B(LPK, K)), B(LPK, K))
         U = B(LPK, K) + ALPHA
         B(LPK, K) = U
         BETA = ALPHA * U
         IF (ALPHA .NE. 0.0) GO TO 13
```

```
C                                                       COLUMN WAS ZERO
         IERR = -8
         CALL VARERR (IPRINT, IERR, LP1 + K)
         GO TO 99
C                                  APPLY REFLECTIONS TO REMAINING COLUMNS
C                                  OF B AND TO RESIDUAL VECTOR.
   13    KP1 = K + 1
         DO 25 J = KP1, NLP1
            ACUM = 0.0
            DO 20 I = LPK, N
   20          ACUM = ACUM + B(I, K) * B(I, J)
            ACUM = ACUM / BETA
            DO 25 I = LPK, N
   25          B(I, J) = B(I, J) - B(I, K) * ACUM
   30    B(LPK, K) = -ALPHA
C
      PRJRES = XNORM(NL, B(LP1, NLP1))
C
C           SAVE UPPER TRIANGULAR FORM AND TRANSFORMED RESIDUAL, FOR USE
C           IN CASE A STEP IS RETRACTED.  ALSO COMPUTE COLUMN LENGTHS.
C
      IF (IERR .EQ. 4) GO TO 99
      DO 50 K = 1, NL
         LPK = L + K
         DO 40 J = K, NLPI
            JSUB = NLPI + J
            B(K, J) = B(LPK, J)
   40       B(JSUB, K) = B(LPK, J)
   50    B(NL23, K) = XNORM(K, B(LP1, K))
C
   99 RETURN
      END
C
      SUBROUTINE ORFAC2(NLP1, NMAX, NU, B)
C
C        STAGE 2:  SPECIAL HOUSEHOLDER REDUCTIOH OF
C
C                     NL     ( DR' . R3 )      (DR'' . R5 )
C                            (-----. -- )      (-----. -- )
C                  N-L-NL    (  0  . R4 )  TO  (  0  . R4 )
C                            (-----. -- I      (-----. -- )
C                     NL     (NU*D . 0  )      (  0  . R6 )
C
C                                NL    1           NL    1
C
C        WHERE DR', R3, AND R4 ARE AS IN ORFAC1, NU IS THE MARQUARDT
C        PARAMETER, D IS A DIAGONAL MATRIX CONSISTING OF THE LENGTHS OF
C        THE COLUMNS OF DR', AND DR'' IS IN UPPER TRIANGULAR FORM.
C        DETAILS IN (1), PP. 423-424.  NOTE THAT THE (N-L-NL) BAND OF
C        ZEROES, AND R4, ARE OMITTED IN STORAGE.
C
C     ..................................................................
C
      DOUBLE PRECISION ACUM, ALPHA, B(NMAX, NLP1), BETA, DSIGN, NU, U,
     X XNORM
C
      NL = NLPI - 1
      NL2 = 2*NL
      NL23 = NL2 + 3
      DO 30 K = 1, NL
```

```
      KP1 = K + 1
      NLPK = NL + K
      NLPKM1 = NLPK - 1
      B(NLPK, K) = NU * B(NL23, K)
      B(NL, K) = B(K, K)
      ALPHA = DSIGN(XNORM(K+1, B(NL, K)), B(K, K))
      U = B(K, K) + ALPHA
      BETA = ALPHA * U
      B(K, K) = -ALPHA
C                     THE K-TH REFLECTION MODIFIES ONLY ROWS K,
C                     NL+1, NL+2, ..., NL+K, AND COLUMNS K TO NL+1.
      DO 30 J = KP1, NLP1
         B(NLPK, J) = 0.
         ACUM = U * B(K,J)
         DO 20 I = NLP1, NLPKM1
   20       ACUM = ACUM + B(I,K) * B(I,J)
         ACUM = ACUM / BETA
         B(K,J) = B(K,J) - U * ACUM
         DO 30 I = NLP1, NLPK
   30       B(I,J) = B(I,J) - B(I,K) * ACUM
C
    RETURN
    END
C
    SUBROUTINE DPA (L, NL, N, NMAX, LPP2, IV, T, Y, W, ALF, ADA, ISEL,
   X IPRINT, A, U, R, RNORM)
C
C      COMPUTE THE NORM OF THE RESIDUAL (IF ISEL = 1 OR 2), OR THE
C      (N-L) X NL DERIVATIVE OF THE MODIFIED RESIDUAL (N-L) VECTOR
C      Q2*Y (IF ISEL = 1 OR 3).  HERE Q * PHI = S, I.E.,
C
C       L     ( Q1 ) (     .   .        )   ( S   . R1 .  F1  )
C             (----) ( PHI . Y . D(PHI) ) = (--- . -- . ---- )
C       N-L   ( Q2 ) (     .   .        )   ( 0   . R2 .  F2  )
C
C                N       L    1      P          L     1     P
C
C      WHERE Q IS N X N ORTHOGONAL, AND S IS L X L UPPER TRIANGULAR.
C      THE NORM OF THE RESIDUAL = NORM(R2), AND THE DESIRED DERIVATIVE
C      ACCORDING TO REF. (5), IS
C                                                  - 1
C                  D(Q2 * Y) = -Q2 * D(PHI)* S  * Q1* Y.
C
C     ..............................................................
C
    DOUBLE PRECISION A(NMAX, LPP2), ALF(NL), T(NMAX, IV), W(N), Y(N),
   X ACUM, ALPHA, BETA, RNORM, DSIGN, DSQRT, SAVE, R(N), U(L), XNORM
    INTEGER FIRSTC, FIRSTR, INC(15,16)
    LOGICAL NOWATE, PHILP1
    EXTERNAL ADA
C
    IF (ISEL .NE. 1) GO TO 3
      LP1 = L + 1
      LNL2 = L + 2 + NL
      LP2 = L + 2
      LPP1 = LPPZ - 1
      FIRSTC = 1
      LASTC = LPP1
      FIRSTR = LP1
      CALL INIT(L, NL, N, NMAX, LPP2, IV, T, W, ALF, ADA, ISEL,
```

```
     X   IPRINT, A, INC, NCON, NCONP1, PHILP1, NOWATE)
         IF (ISEL .NE. 1) GO TO 99
         GO TO 30
C
    3 CALL ADA (LP1, NL, N, NMAX, LPP2, IV, A, INC, T, ALF, MIN0(ISEL,
     X 3))
      IF (ISEL .EQ. 21 GO TO 6
C                                                    ISEL = 3 OR 4
      FIRSTC = LP2
      LASTC = LPPI
      FIRSTR = (4 - ISEL)*L + 1
      GO TO 50
C                                                    ISEL = 2
    6 FIRSTC = NCONPI
      LASTC = LP1
      IF (NCON .EQ. 01 GO TO 30
      IF (A(1, NCON) .EQ. SAVE) GO TO 30
         ISEL = -7
         CALL VARERR (IPRINT, ISEL, NCON)
         GO TO 99
C                                                     ISEL = 1 OR 2
   30 IF (PHILP1) GO TO 40
         DO 35 I = 1, N
   35       R(I) = Y(I)
         GO TO 50
   40    DO 45 I = 1, N
   45       R(I) = Y(I) - R(I)
C                                              WEIGHT APPROPRIATE COLUMNS
   50 IF (NOWATE) GO TO 58
      DO 55 I = 1, N
         ACUM = W(I)
         DO 55 J = FIRSTC, LASTC
   55       A(I, J) = A(I, J) * ACUM
C
C           COMPUTE ORTHOGONAL FACTORIZATIONS BY HOUSEHOLDER
C           REFLECTIONS.  IF ISEL = 1 OR 2, REDUCE PHI (STORED IN THE
C           FIRST L COLUMNS OF THE MATRIX A) TO UPPER TRIANGULAR FORM,
C           (Q*PHI = S), AND TRANSFDRM Y (STORED IN COLUMN L+1), GETTING
C           Q*Y = R.  IF ISEL = 1, ALSO TRANSFORM J = D PHI (STORED IN
C           COLUMNS L+2 THROUGH L+P+1 OF THE MATRIX AI, GETTING Q*J = F.
C           IF ISEL = 3 OR 4, PHI HAS ALREADY BEEN REDUCED, TRANSFORM
C           ONLY J.  S, R, AND F OVERWRITE PHI, Y, AND J, RESPECTIVELY,
C           AND A FACTORED FORM OF Q IS SAVED IN U AND THE LOLJER
C           TRIANGLE OF PHI.
C
   58 IF (L .EQ. 01 GO TO 75
      DO 70 K = 1, L
         KP1 = K + 1
         IF (ISEL .GE. 3 .OR. (ISEL .EQ. 2 .AND. K .LT.NCONP1)) GO TO 66
         ALPHA = DSIGN(XNORM(N+1-K, A(K, K)), A(K, K))
         U(K) = A(K, K) + ALPHA
         A(K, K) = -ALPHA
         FIRSTC = KP1
         IF (ALPHA .NE. 0.0) GO TO 66
         ISEL = -8
         CALL VARERR (IPRINT, ISEL, K)
         GO TO 99
C                                        APPLY REFLECTIONS TO COLUMNS
C                                        FIRSTC TO LASTC.
   66    BETA = -A(K, K) * U(K)
```

```
         DO 70 J = FIRSTC, LASTC
            ACUM = U(K)*A(K, J)
            DO 68 I = KP1, N
        IF(DABS(A(I,K)).LT.1.D-30.OR.DABS(A(I,J)).LT.1.D-30)GO TO 68
               ACUM = ACUM + A(I, K)*A(I, J)
68      CONTINUE
            ACUM = ACUM / BETA
            A(K,J) = A(K,J) - U(K)*ACUM
            DO 70 I = KP1, N
   70          A(I, J) = A(I, J) - A(I, K)*ACUM
C
   75 IF (ISEL .GE. 3) GO TO 85
      RNORM = XNORM(N-L, R(LP1))
      IF (ISEL .EQ. 2) GO TO 99
      IF (NCON .GT. 0) SAVE = A(1, NCON)
C
C           F2 IS NOW CONTAINED IN ROWS L+l TO N AND COLUMNS L+2 TO
C           L+P+1 OF THE MATRIX A.  NOW SOLVE THE L X L UPPER TRIANGULAR
C           SYSTEM S*BETA = R1 FOR THE LINEAR PARAMETERS BETA.  BETA
C           OVERWRITES R1.
C
   85 IF (L .GT. 0) CALL BACSUB (NMAX, L, A, R)
C
C           MAJOR PART OF KAUFMAN'S SIMPLIFICATION OCCURS HERE.  COMPUTE
C           THE DERIVATIVE OF ETA WITH RESPECT TO THE NONLINEAR
C           PARAMETERS
C
C   T   D ETA        T    L          D PHI(J)    D PHI(L+1)
C  Q * -------- =  Q * (SUM BETA(J) --------  + ----------)  =  F2*BETA
C      D ALF(K)          J=1         D ALF(K)     D ALF(K)
C
C           AND STORE THE RESULT IN COLUMNS L+2 TO L+NL+1.  IF ISEL NOT
C           = 4, THE FIRST L ROWS ARE OMITTED.  THIS IS -D(Q2)*Y.  IF
C           ISEL NOT = 4 THE RESIDUAL R2 = Q2*Y (IN COL. L+1) IS COPIED
C           TO COLUMN L+NL+2.  OTHERWISE ALL OF COLUMN L+l IS COPIED.
C
      DO 95 I = FIRSTR, N
         IF (L .EQ. NCON) GO TO 95
         M = LP1
         DO 90 K = 1, NL
            ACUM = 0.
            DO 88 J = NCONPl, L
               IF (INC(K, J) .EQ. 0) GO TO 88
               M = M + 1
               ACUM = ACUM t A(I, M) * R(J)
   88          CONTINUE
            KSUB = LP1 + K
            IF (INC(K, LP1) .EQ. 0) GO TO 90
            M = M + 1
            ACUM = ACUM + A(I, M)
   90       A(I, KSUB) = ACUM
   95    A(I, LNL2) = R(I)
C
   99 RETURN
      END
C
      SUBROUTINE INIT(L, NL, N, NMAX, LPP2, IV, T, W, ALF, ADA, ISEL,
     X IPRINT, A, INC, NCON, NCONP1, PHILP1, NOWATE)
C
C        CHECK VALIDITY OF INPUT PARAMETERS, AND DETERMINE NUMBER OF
```

```
C        CONSTANT FUNCTIONS.
C
C     ..............................................................
C
      DOUBLE PRECISION A(NMAX, LPP2), ALF(NL), T(NMAX, IV), W(N),
     X DSQRT
      INTEGER OUTPUT, P, INC(15,16)
      LOGICAL NOWATE, PHILP1
      DATA OUTPUT /6/
C
      LP1 = L + 1
      LNL2 = L + 2 + NL
C                                          CHECK FOR VALID INPUT
      IF (L .GE. 0 .AND. NL .GE. 0 .AND. L+NL .LT. N .AND. LNL2 .LE.
     X LPP2 .AND. 2*NL + 3 .LE. NMAX .AND. N .LE. NMAX .AND.
     X IV .GT. 0 .AND. .NOT. (NL .EQ. 0 .AND. L .EQ. 0)) GO TO 1
         ISEL = -4
         CALL VARERR (IPRINT, ISEL, 1)
         GO TO 99
C
    1 IF (L .EQ. 0 .OR. NL .EQ. 0) GO TO 3
         DO 2 J = 1, LP1
            DO 2 K = 1, NL
    2          INC(K, J) = 0
C
    3 CALL ADA (LP1, NL, N, NMAX, LPP2, IV, A, INC, T, ALF, ISEL)
C
      NOWATE = .TRUE.
      DO 9 I = 1, N
         NOWATE = NOWATE .AND. (W(I) .EQ. 1.0)
         IF (W(I) .GE. 0.) GO TO 9
C                                                ERROR IN WEIGHTS
         ISEL = -6
         CALL VARERR (IPRINT, ISEL, I)
         GO TO 99
    9    W(I) = DSQRT(W(I))
C
      NCON = L
      NCONPI = LP1
      PHILPI = L .EQ. 0
      IF (PHILP1 .OR. NL .EQ. 0) GO TO 99
C                                  CHECK INC MATRIX FOR VALID INPUT AND
C                                  DETERMINE NUMBER OF CONSTANT FCNS.
      P = 0
      DO 11 J = 1, LP1
         IF (P .EQ. 0) NCONPI = J
         DO 11 K = 1, NL
            INCKJ = INC(K, J)
            IF (INCKJ .NE. 0 .AND. INCKJ .NE. 1) GO TO 15
            IF (INCKJ .EQ. 1) P = P + 1
   11       CONTINUE
C
      NCON = NCONP1 - 1
      IF (IPRINT .GE. 0) WRITE (OUTPUT, 210) NCON
      IF (L+P+2 .EQ. LPP2) GO TO 20
C                                              INPUT ERROR IN INC MATRIX
   15 ISEL = -5
      CALL VARERR (IPRINT, ISEL, 1)
      GO TO 99
C                                 DETERMINE IF PHI(L+1) IS IN THE MODEL.
```

```
   20 DO 25 K = 1, NL
   25    IF (INC(K, LP1) .EQ. 1) PHILP1 = .TRUE.
C
   99 RETURN
  210 FORMAT (33H0  NUMBER OF CONSTANT FUNCTIONS =, I4 /)
      END
      SUBROUTINE BACSUB (NMAX, N, A, X)
C
C        BACKSOLVE THE N X N UPPER TRIANGULAR SYSTEM A*X = B.
C        THE SOLUTION X OVERWRITES THE RIGHT SIDE B.
C
      DOUBLE PRECISION A(NMAX, N), X(N), ACUM
C
      X(N) = X(N) / A(N, N)
      IF (N .EQ. 1) GO TO 30
      NP1 = N t 1
      DO 20 IBACK = 2, N
         I = NP1 - IBACK
C           I = N-1, N-2, ..., 2, 1
         IP1 = I + 1
         ACUM = X(I)
         DO 10 J = IP1, N
   10       ACUM = ACUM - A(I,J)*X(J)
   20    X(I) = ACUM / A(I,I)
C
   30 RETURN
      END
      SUBROUTINE POSTPR(L, NL, N, NMAX, LNL2, EPS, RNORM, IPRINT, ALF,
     X W, A, R, U, IERR)
C
C        CALCULATE RESIDUALS, SAMPLE VARIANCE, AND COVARIANCE MATRIX.
C        ON INPUT, U CONTAINS INFORMATION ABOUT HOUSEHOLDER REFLECTIONS
C        FROM DPA.  ON OUTPUT, IT CONTAINS THE LINEAR PARAMETERS.
C
      DOUBLE FRECISION A(NMAX, LNL2), ALF(NL), R(N), U(L), W(N), ACUM,
     X EPS, PRJRES, RNORM, SAVE, DADS
      INTEGER OUTPUT
      DATA OUTPUT /6/
C
      LP1 = L + 1
      LPNL = LNL2 - 2
      LNL1 = LPNL + 1
      DO 10 I = 1, N
   10    W(I) = W(I)**2
C
C              UNWIND HOUSEHOLDER TRANSFORMATIONS TO GET RESIDUALS,
C              AND MOVE THE LINEAR PARAMETERS FROM R TO U.
C
      IF (L .EQ. 0) GO TO 30
      DO 25 KBACK = 1, L
         K = LP1 - KBACK
         KP1 = K + 1
         ACUM = 0.
         DO 20 I = KP1, N
   20       ACUM = ACUM + A(I, K) * R(I)
         SAVE = R(K)
         R(K) =  ACUM / A(K, K)
         ACUM = -ACUM / (U(K) * A(K, K))
         U(K) = SAVE
         DO 25 I = KP1, N
```

```
   25       R(I) = R(I) - A(I, K)*ACUM
C                                                    COMPUTE MEAN ERROR
   30 ACUM = 0.
      DO 35 I = 1, N
   35    ACUM = ACUM + R(I)
      SAVE = ACUM / N
C
C              THE FIRST L COLUMNS OF THE MATRIX HAVE BEEN REDUCED TO
C              UPPER TRIANGULAR FORM IN DPA.  FINISH BY REDUCING ROWS
C              L+1 TO N AND COLUMNS L+2 THROUGH L+NL+1 TO TRIANGULAR
C              FORM.  THEN SHIFT COLUMNS OF DERIVATIVE MATRIX OVER ONE
C              TO THE LEFT TO BE ADJACENT TO THE FIRST L COLUMNS.
C
      IF (NL .EQ. 0) GO TO 45
      CALL ORFAC1(NL+1, NMAX, N, L, IPRINT, A(1, L+2), PRJRES, 4)
      DO 40 I = 1, N
         A(I, LNL2) = R(I)
         DO 40 K = LP1, LNL1
   40       A(I, K) = A(I, K+1)
C                                                    COMPUTE COVARIANCE MATRIX
   45 A(1, LNL2) = RNORM
      ACUM = RNORM*RNORM/(N - L - NL)
      A(2, LNL2) = ACUM
      CALL COV(NMAX, LPNL, ACUM, A)
C
      IF (IPRINT .LT. 0) GO TO 99
      WRITE (OUTPUT, 209)
      IF (L .GT. 0) WRITE (OUTPUT, 210) (U(J), J = 1, L)
      IF (NL .GT. 0) WRITE (OUTPUT, 211) (ALF(K), K = 1, NL)
      WRITE (OUTPUT, 214) RNORM, SAVE, ACUM
      IF (DABS(SAVE) .GT. EPS) WRITE (OUTPUT, 215)
      WRITE (OUTPUT, 209)
   99 RETURN
C
  209 FORMAT (1H0, 50(1H'))
  210 FORMAT (20H0  LINEAR PARAMETERS // (7E15.7))
  211 FORMAT (23H0  NONLINEAR PARAMETERS // (7E15.7))
  214 FORMAT (21H0  NORM OF RESIDUAL =, E15.7, 33H EXPECTED ERROR OF OBS
     XERVATIONS =, E15.7, / 39H   ESTIMATED VARIANCE OF OBSERVATIONS =,
     X E15.7 )
  215 FORMAT (95H  WARNING -- EXPECTED ERROR OF OBSERVATIONS IS NOT ZERO
     X.  COVARIANCE MATRIX MAY BE MEANINGLESS. /)
      END
      SUBROUTINE COV(NMAX, N, SIGMA2, A)
C
C          COMPUTE THE SCALED COVARIANCE MATRIX OF THE L + NL
C       PARAMETERS.  THIS INVOLVES COMPUTING
C
C                                 2      -1     -T
C                            SIGMA  *  T    *  T
C
C       WHERE THE (L+NL) X (L+NL) UPPER TRIANGULAR MATRIX T IS
C       DESCRIBED IN SUBROUTINE POSTPR.  THE RESULT OVERWRITES THE
C       FIRST L+NL ROWS AND COLUMNS OF THE MATRIX A.  THE RESULTING
C       MATRIX IS SYMMETRIC.  SEE REF. 7, PP. 67-70, 281.
C
C     ..............................................................
C
      DOUBLE PRECISION A(NMAX, N), SUM, SIGMA2
C
```

```
      DO 10 J = 1, N
   10    A(J, J) = 1./A(J, J)
C
C                 INVERT T UPON ITSELF
C
      IF (N .EQ. 1) GO TO 70
      NM1 = N - 1
      DO 60 I = 1, NM1
         IP1 = I + 1
         DO 60 J = IP1, N
            JM1 = J - 1
            SUM = 0.
            DO 50 M = I, JM1
   50          SUM = SUM + A(I, M) * A(M, J)
   60       A(I, J) = -SUM * A(J, J)
C
C                 NOW FORM THE MATRIX PRODUCT
C
   70 DO 90 I = 1, N
         DO 90 J = I, N
            SUM = 0.
            DO 80 M = J, N
   80          SUM = SUM + A(I, M) * A(J, M)
            SUM = SUM * SIGMA2
            A(I, J) = SUM
   90       A(J, I) = SUM
C
      RETURN
      END
      SUBROUTINE VARERR (IPRINT, IERR, K)
C
C        PRINT ERROR MESSAGES
C
      INTEGER ERRNO, OUTPUT
      DATA OUTPUT /6/
C
      IF (IPRINT .LT. 0) GO TO 99
      ERRNO = IABS(IERR)
      GO TO (1, 2, 99, 4, 5, 6, 7, 8), ERRNO
C
    1 WRITE (OUTPUT, 101)
      GO TO 99
    2 WRITE (OUTPUT, 102)
      GO TO 99
    4 WRITE (OUTPUT, 104)
      GO TO 99
    5 WRITE (OUTPUT, 105)
      GO TO 99
    6 WRITE (OUTPUT, 106) K
      GO TO 99
    7 WRITE (OUTPUT, 107) K
      GO TO 99
    8 WRITE (OUTPUT, 108) K
C
   99 RETURN
  101 FORMAT (46H0  PROBLEM TERMINATED FOR EXCESSIVE ITERATIONS //)
  102 FORMAT (49H0  PROBLEM TERMINATED BECAUSE OF ILL-CONDITIONING //)
  104 FORMAT (/ 50H INPUT ERROR IN PARAMETER L, NL, N, LPP2, OR NMAX. /)
  105 FORMAT (68H0  ERROR -- INC MATRIX IMPROPERLY SPECIFIED, OR DISAGRE
     XES WITH LPP2. /)
```

```
  106 FORMAT (19H0  ERROR -- WEIGHT(, I4, 14H) IS NEGATIVE. /)
  107 FORMAT (28H0  ERROR -- CONSTANT COLUMN , I3, 37H MUST BE COMPUTED
     XONLY WHEN ISEL = 1.  /)
  108 FORMAT (33H0  CATASTROPHIC FAILURE -- COLUMN , I4, 28H IS ZERO,  SE
     XE DOCUMENTATION. /)
      END
      DOUBLE PRECISION FUNCTION XNORM(N, X)
C
C        COMPUTE THE L2 (EUCLIDEAN) NORM OF A VECTOR,  MAKING SURE TO
C        AVOID UNNECESSARY UNDERFLOWS.   NO ATTEMPT IS MADE TO SUPPRESS
C        OVERFLOWS.
C
      DOUBLE PRECISION X(N), RMAX, SUM,  TERM,  DABS,  DSQRT
C
C            FIND LARGEST (IN ABSOLUTE VALUE)  ELEMENT
      RMAX = 0.
      DO 10 I = 1, N
         IF (DABS(X(I)) .GT. RMAX) RMAX = DABS(X(I))
   10    CONTINUE
C
      SUM = 0.
      IF (RMAX .EQ. 0.) GO TO 30
      DO 20 I = 1, N
         TERM = 0.
         IF (RMAX + DABS(X(I)) .NE.  RMAX) TERM = X(I)/RMAX
   20    SUM = SUM + TERM*TERM
C
   30 XNORM = RMAX*DSQRT(SUM)
   99 RETURN
      END
$DATA
.8541676,1.D-6,34,7
.55,27225.,6600.,1.093753
.7177783,1.,1.
2000.,4000.,15
2200.
2390.
2610.
2930.
3050.
3270.
3640.
2040.,1.5
2070. ,.8
2200. ,4.5
2280.r4.75
2340.,8.
2400.,10.
2500.,20.
2540.,21.5
2600.,31.
2660.,27.6
2700.,29.2
2800.,25.
2870.,28.
3000.,28.
3040. ,30.
3070.,28.25
3120.,28.
3160.,26.
```

```
3200.132.
3260.132.
3360.,26.
3400.,25.9
3460.125.
3520.,25.
3580.,28.
3620.,28.
3700.124.
3720.,25.6
3800.,20.
3860.,21.5
3900.121 .75
3925.,19.25
3960.119.5
4000.,12.
/*
```

] FROM ROGRAM

```
NUMBER OF CONSTANT FUNCTIONS =   0

  0  NORM OF RESIDUAL =  0.1442714D-04
  NU =  0.1000000D 01
ITERATION   1    NONLINEAR PARAMETERS
0.1042649D 01  0.9485506D 00  0.8722263D 00  0.78373878 00  0.74415011) 00  0.695689'
  1  NORM OF RESIDUAL =  0.1334315D-04
  NU =  0.5000000D 00
  NORMCDELTA-ALF) / NORMCALF) =   0.500D-02
ITERATION   2    NONLINEAR PARAMETERS
0.1046405D 01  0.94177720 00  0.8712702D 00  0.7916243D 00  0.7472037D 00  0.694535
  1  NORM OF RESIDUAL =  0.1252686D-04
  NU =  0.2500000D 00
  NORMCDELTA-ALF) / NORMCALF) =   0.528D-02
ITERATION   3    NONLINEAR PARAMETERS
0.1046952D 01  0.9342167D 00  0.8697866D 00  0.7954584D 00  0.7468173D 00  0.6944111
  1  NORM OF RESIDUAL =  0.1207254D-04
  NU =  0.1250000D 00
  NORM(DELTA-ALF) / NORMCALF) =   0.394D-02
ITERATION   4    NONLINEAR PARAMETERS
0.1046302D 01  0.9272034D 00  0.8671941D 00  0.7954597D 00  0.7468120D 00  0.6944090
  1  NORM OF RESIDUAL =  0.1174424D-04
  NU =  0.6250000D-01
  NORM(DELTA-ALF) / NORM(ALF) =   0.344D-02
ITERATION   5    NONLINEAR PARAMETERS
0.1045457D 01  0.9239122D 00  0.8648639D 00  0.7940712D 00  0.7464616D 00  0.6943551
  1  NORM OF RESIDUAL =  0.1162343D-04
  NU =  0.3125000D-01
  NORMCDELTA-ALF) / NORMCALF) =   0.200D-02
ITERATION   6    NONLINEAR PARAMETERS
0.1044500D 01  0.9230081D 00  0.8640470D 00  0.7932118D 00  0.7462077D 00  0.6943202
  1  NORM OF RESIDUAL =  0.1160925D-04
  NU =  0.1562500D-01
  NORMCDELTA-ALF) / NORMCALF) =   0.821D-03
''''''''''''''''''''''''''''''''''''''''''''''''''''
LINEAR PARAMETERS

0.1705885D-01  0.40428030-01  0.6303247D-01  0.3332297D-01  0.3242721D-01  0.4207849D
NONLINEAR PARAMETERS

0.1044500D 01  0.9230081D 00  0.864047013 00  0.79321183) 00  0.7462077D 00  0.69432029
NORM OF RESIDUAL =  0.1160925D-04 EXPECTED ERROR OF OBSERVATIONS =  0.1398237D-06
ESTIMATED VARIANCE OF OBSERVATIONS =  0.6738738D-11
''''''''''''''''''''''''''''''''''''''''''''''''''''
```

LAYER NO.	POROSITY.THICKNESS	KH/SUM(KH)
1	0.015636	0.016332
2	0.047454	0.043800
3	0.084429	0.072950
4	0.052962	0.0420 10
5	0.058236	0.043456
6	0.087285	0.060604
7	0.087129	0.054508

VOLUME PRODUCED, BBLS	CONCENTRATION, PPM
2000.00	0.037696
2133.33	4.600 928
2266.67	4.167477
2400.00	11.495150
2533.33	21.593647
2666.67	29.679569
2800.00	25.71 1356
2933.33	27.380659
3066.67	28.569303
3200.00	30.307478
3333.33	29.44766 1
3466.67	23.823376
3600.00	28.6 22558
3733.33	24.487 164
3866.67	18.975435
4000.00	15.983867

SELECTED PEAK VOLUME	COMPUTED PEAK VOLUME
2200.0	2181.1
2390.0	2468.2
2610.0	2636.7
2930.0	2872.1
3050.0	3053.0
3270.0	3281.2
3640.0	3641.6

```
STATEMENTS EXECUTED= 2576626
CORE USAGE       OBJECT CODE=   42368 BYTES,ARRAY AREA=   19416 BYTES,TOTAL AREA AVAIL
DIAGNOSTICS        NUMBER OF ERRORS=       0, NUMBER OF WARNINGS=       0, NUMBER OF E
COMPILE TIME=     0.37 SEC,EXECUTION TIME=    27.20 SEC,     16.00.30     MONDAY
        CSSTOP
```

Appendix D.2: PROGRAM TO COMPUTE PATTERN BREAKTHROUGH CURVE OF A DEVELOPED INVESTED SEVEN-SPOT FOR UNIT MOBILITY RATIO

This program calculates the curve of displacing fluid cut versus displaceable pore volume Injected for a developed inverted seven-spot at unit mobility ratio. As was mentioned in the text, for every selected y coordinate of a point on a general streamline, a corresponding value for the x coordinate of the point must be evaluated. Subroutine "ROOT" performs this evaluation. The routine uses the "bisection method." However, a more efficient root-finding method can reduce the computation time.

```
// JOB (JE.MAD,104,2),'MAGSUD'
// EXEC WATFIV
//GO.SYSIN DD *
C
C
C     ***************************************************************
C     *                                                             *
C     * THIS PROGRAM COMPUTES PATTERN BRRAKTHROUGH CURVE (DISPLACING *
C     * FLUID CUT VS DISPLACEAULE FORE VOLUMES INJECTED) FOR A DEVEL- *
C     * LOPED INVERTED SEVEN-SPOT AT MOBILITY RATIO OF ONE.          *
C     *                                                             *
C     ***************************************************************
C
C
C     OUTFUTS FROM THE PROGRAM ARE:
C     FW    = DISPLACING FLUID CUT AT THE PRODUCIND STREAM
C     PV(I) = CISPLACEADLE PORE VOLUMES INJECTED CORRESPONDING TO FW
C     DPV   = DIMENSIONLESS PORE VOLUME USED IN THE CORRELATION
C
C
      IMPLICIT REAL*8 (A-lit O-2)
      DIMENSION F(200),PV(30)
      REAL*8 M,M1,K
      COMMON AA,BB,M,M1,P
      PI=4.*DATAN(1.DO)
      AA=DSQRT(3.D0)
      BB=1./AA
      M=(2.-AA)/4.D0
      M1=1.-M
      N=50
      NN=N+1
      FW=.5D-1
      00 35 L=1,9
      SIGH=PI*(1.-FW/3)
      P=DTAN(SIGH)
      CALL KM(AA,Z,K)
      Y2=2.*K*BB
      H=Y2/N
      F(1)=0.000
      DO 10 I=2,NN
      Y=(I-1)*H
C
C     FOR A Y-CODRDINATE OF A POINT ON A GENERAL STREAMLINE, A
C     COORESPOEDXNG VALUE FOE THE X-COORDINATE IS COMPUTED.
C
      CALL ROOT(Y,X)
C
C     THE IHTEGRANE IN EQ. A-109 IS EVALUATED
C
      CALL VALUE(X,Y,U,UP,R,RP,W,WP)
      F(I)=W*W/(W*(R*UP+RP*U)-R*U*WP)
10    CONTINUE
C
C     POKE VOLUMES INJECTED ARE COMPUTED
C
      CALL INTGRL(N,H,F,SUM)
      C=-PI*(1+P*P)/(2.*AA*K*K)
      PV(L)=C*SUM
      DPV=(PV(L)-.743682)/(1.-.743682)
      WRITE(6,200) FW,PV(L),DPV
```

```
200   FORMAT(1X,3(F15.5))
35    FW=FW+.10
      STOP
      END
C
C
C
      SUBROUTINE VALUE(X,Y,U,UP,R,RP,W,WP)
C
C
C     THIS SUBROUTINE COMPUTES THE FOLLOLJING FUNCTIONS THAT ARE
C     NEEDED FOR THE PROGRAM.  THE FUNCTIONS ARE:
C     H, G, U, U', T, T', R, R', W, W'
C     THESE FUNCTIONS HAVE BEEN ASSIGNED THE SAME NOTATIONS AS IN
C     APPENDIX A-4.
C     INFUT:  X,Y = COORDINATES OF A POINT ON A STREAMLINE
C     OUTPUT: FUNCTIONS U, U', R, R', W, W'
C
      IMPLICIT REAL*8 (A-H,O-Z)
      REAL*8 M,M1
      COMMON AA,BB,M,M1,P
      A2=(2.+AA)**2
      B2=(2.-AA)**2
      CALL JACOB(X,M,AA,SNX,CNX,DNX)
      CALL JACOB(Y,M1,BB,SNY,CNY,DNY)
      DENUM=1.-SNY*SNY*DNX*DNX
      H=CNX*CNY/DENUM
      G=SNX*DNX*SNY*DNY/DENUM
      HP=-(DENUM+2*M*SNY*SNY*CNX*CNX)*SNX*DNX*CNY/(DENUM*DENUM)
      GP=SNY*DNY*CNX*((DNX**2-M*SNX**2)*DENUM-2*M*(SNX*DNX*SNY)**2)/
     $(DENUM*DENUM)
      U=H*G
      T=(H*H-G*G)**2
      UP=HP*G+GP*H
      TP=4.*(H*HP-G*GP)*(H*H-G*G)
      UU=U*U
      R=(1-B2)*(4*UU+T)+A2-1.
      W=8*UU*(2*B2*UU-5.+B2*T)+A2+B2*T*T-14*T
      RP=(1-B2)*(8*U*UP+TP)
      WP=16*U*UP*(4.*B2*UU-5.+B2*T)+2*B2*TP*(4*UU+T)-14*TP
      RETURN
      END
C
C
C
      SUEROUTINE ROOT(Y,Z)
C
C
C     THIS SUBROUTINE CALCULATES THE ROOT OF F(X,Y) = 0 FOR A GIVEN Y.
C     THE FUNCTION F(X,Y) IS SUPPLIED BY EQ. A-103 IN APPENDIX A-4.
C     THE SUBCOUTINE USES THE  "BISECTION" METHOD.
C     INFUT:  Y = Y-COORDINATE OF A POINT ON STREAMLINE, SIGH
C     OUTFUT: Z = X-COORDINATE CORRESPONDING TO Y
C
C
      IMPLICIT REAL*8 (A-H,O-Z)
      REAL*8 M,M1
      COMMON AA ,BB ,M,M1,P
      TOL=5.D-4
      D=P/4.DO
```

```
      X1=1.D-5
      X2=.5D-3
      CALL VALUE(X1,Y,U,UP,R,RP,W,WP)
      F1=R*U/W-D
10    CALL VALUE(X2,Y,U,UP,R,RP,W,WP)
      F2=R*U/W-D
      IF(F1*F2.LT.0.)GO TO 20
      x2=1.5*X2
      GO TO 10
20    I=1
30    Z=(X1+X2)/2.D0
      CALL VALUE(Z,Y,U,UP,R,RP,W,WP)
      FZ=R*U/W-D
      IF(F1*FZ.LT.0.) GO TO 40
      X1=Z
      IF(DABS(X2-Z).LT.TOL)RETURN
      I=I+1
      GO TO 30
40    X2=Z
      IF(DABS(X1-Z).LT.TOL)RETURN
      I=I+1
      GO TO 30
      END
C
C
C
      SUBROUTINE JACOB(U,M,KPOK,SN,CN,DN)
C
C
C     THIS SUBROUTINE EVALUATES THE ELLIPTIC FUNCTIONS OF
C     SN(X,M), CN(X,M), DN(X,M), SN(Y,M1), CN(Y,M1), DN(Y,M1)
C     THE ROUTINE USES THE FOURIER EXPANSION OF THE ELLIPTIC FUCTION
C     SN(U), COMBINED WITH RELATIONSHIPS BETWEEN THE FUNCTIONS.
C     KPOK IN THIS SUBROUTINE IS K'(M)/K(M) WHEN THE PARAMETER IS M,
C     AND IS EQUAL TO K(M)/K'(M) = K'(M1)/K(M1) WHEN THE PARAMETER
C     IS M1
C
C
      IMPLICIT REAL*8 (A-H,O-Z)
      REAL*8 K,M,KPOK
      PI=4.*DATAN(1.D0)
      CALL KM(KPOK,Q,K)
      V=PI*U/(2.*K)
      SUM1=0.
      DO 10 I=1,8
      A=(I-1)+.5
      B=2.*(I-1)+1.
10    SUM1=SUM1+Q**A/(1.-Q**B)*DSIN(B*V)
      SN=2.*PI*SUM1/(K*DSQRT(M))
      CN=DSQRT(DABS(1.-SN**2))
      DN=DSQRT(DABS(1.-M*SN**2))
      RETURN
      END
C
C
C
      SUBROUTINE KM(KPOK,Q,K)
C
C     THIS SUBROUTINE COMPUTES COMPLEMENTARY OR INCOMPLEMENTARY COMPLETE
C     ELLIPTIC INTEGRAL FUNCION K(M) OR K(M1)=K'(M).  THE ROUTHINE
```

```
C     UTILIZES THE EXFANSION PRESEKTED IN ABRAMOWITZ (1972) .
C
      IMPLICIT REAL*8 (A-H,O-Z)
      REAL*8 K,M,KPOK
      PI=4.*DATAN(1.D0)
      Q=DEXP(-PI*KPOK)
      SUM=0.
      DO 30 I=1,10
30    SUM=SUM+Q**I/(1.+Q**(2.*I))
      K=PI/2.*(1.+4.*SUM)
      RETURN
      END
C
C
C
      SUBROUTINE INTGRL(N,H,F,VOL)
C
C     THIS SUBROUTINE COMPUTES VALUE OF AN INTEGRAL USING SIMPSON'S
C     RULE OF INTEGRATION.
C     INPUT:  N = NUMBER OF INTERVALS, AN EVEN INTEGER NUMBER
C             H = INTERVAL SIZE
C             F = VALUES OF FUNCTIONS COMPUTED AT INTERVALS, AN ARRAY
C     OUTFUT: VOL = VALUE OF THE INTEGRAL
C
      IMPLICIT REAL*8 (A-H,O-Z)
      DIMENSION F(91)
      SUM1=0
      SUM2=0
      N1=N/2-1
      DO 50 I=1,N1
      SUM1=SUP11+F(2*I)
50    SUM2=SUM2 +F(2*I+1)
      SUM1=SUM1+F(N)
      VOL=H/3*(F(1)+F(N+1)+4.*SUM1+2.*SUP12)
      RETURN
      END
SDATA
```

Appendix D.3: PROGRAM TO COMPUTE PATTERN BREAKTHROUGH CURVE OF A DEVELOPED FIVE-SPOT AT AN ARBITRARY MOBILITY RATIO

This program computes both the displacing fluid cut and areal sweep efficiency curves of a developed five-spot pattern for any mobility ratio. The assumption made in the derivation of the equations is that the streamlines are independent of mobility ratio; hence, they can be calculated from single-phase fluid flow (mobility ratio equal to one).

```
// JOB (JE.MAD,104),'MAGHSOOD'
// EXEC WATFIV
//GO.SYSIN DD *
C
C
C     ***************************************************************
C     * THIS PROGRAM COMPUTES PATTERN BREAKTHROUGH CURVES (DISPLACING  *
C     * FLUID CUT VS DISPLACEADLE PORE VOLUME) AND AREAL SWEEP EFFICI- *
C     * ENCY CURVES (FRACTIONAL AREA SWEPT VS DISPLACEABLE PORE VOLUME *
C     * INJECTED) FOR A DEVELOPED FIVE-SPOT PATTERN AT VARIOUS MOBILITY*
C     * RATIOS. THE PROGRAM ASSUMES THAT THE STREAMLINES DO NOT CHANGE *
C     * WITH MOBILITY RATIO.
C     ***************************************************************
C
C
C     THE LOCATION OF THE FRONT IN THE SYSTEM IS CONTINUOUSLY
C     COMPUTED AS THE STREAMLINES BREAKTHROUGH.
C     THE INPUT AND OUTPUT FROM THE PROGRAM ARE AS FOLLOLJS:
C     INPUT:  MOBLTY = MOBILITY RATIO
C     OUTPUT: PV = DISPLACEABLE FORE VOLUMES INJECTED
C             SWEEP = AREAL SWEEP EFFICIENCY, FRACTION
C             FA, DISPLACING FLUID CUT IN THE PRODUCING STREAM, FRACTION
C
C
      IMPLICIT REAL *8(A-H,O-Z)
      REAL*8 MOBLTY,LEFT,FF(91),GG(91),FSWEP(91)
      G1(Z)=DSQRT(Z*Z+1)
      G2(Z,ETA)=DSQRT(Z*Z+ETA*ETA)
      G(Z,ETA)=DLOG((Z*ETA*(G1(Z)+G2(Z,ETA)))/(ETA*G1(Z)+G2(Z,ETA)))
      READ,MO3LTY
      PI=4.*DATAN(1.00)
      AK=1.854074677301372D0
      RW=AK*DSQRT(2.D0)/10000.
C
C     ONE EIGHTH OF A FIVE-SPOT IS DIVIDED INTO "NP" STREAMTUBES.
C     THESE NP STREAMTUBES BREAKTHROUGH ONE BY ONE.
C
      NP=10
      H=PI/4./NP
      DO 1 J=1,NP
C
C     IN THE FOLLOWING, TETUT = STREAMLINE THAT IS CONSIDERED TO
C     BREAKTHROUGH. RIGHT HAND SIDE OF EQ. B-51 IS COMPUTED FOR THIS
C     STREAMLINE AND IS STORED IN "RIGHT".
C
      TETBT=H*(NP+1-J)
      E1=DTAN(TETBT)**2
      XWIBT=RW*DSIN(TETBT)
      XWPBT=AK-RW*DCOS(TETRT)
      CALL FUNCT(1,F2PBT,XWPBT)
      CALL FUNCT(1,F2IBT,XWIBT)
      CALL GAUSS(1,F2IBT,FZFBT,EI,VAL)
      P1E1=MOBLTY*G(F2PBT,E1)-G(F2IBT,E1)
      EP=1-E1*E1
      PP=PI/2.
      CALL ELLEP(PP,EP,AKE1)
      RIGHT=(1+E1)*(F1E1*AKE1+(1.-MOBLTY)*VAL)
C
C     STREAMLINES BETWEEN ZERO AND BROKENTHROUGH (TETBT) ARE DIVIDED
C     INTO "N" STREAMTUBES AND THE FRONT LOCATION IN EACH OF THEM
```

```
C     IS CALCULATED BY EQ. B-51.  FIRST A LOWER AND AN UPPER VALUE FOR
C     Z BAR IN THIS EQUATION ARE COMPUTED IN SUCH A WAY THAT THE EXACT
C     Z PAR VALUE LIES BETWEEN THEM.  THEN, A ROOT FINDING ROUTINE IS
C     UTILIZED TO DETERMINE THE EXACT VALUE OF THE Z FAR.
C
      N=90
      NN=N-1
      STEP=TETBT/N
      DO 10 I=1,NN
      TET=STEP*I
      XW =RW*DSIN(TET)
      XWP=RW*DCOS(TET)
      E=DTAN(TET)**2
      ZZ=1.-E*E
      X1=AK-XWP
      CALL FUNCT(1,F2P,X1)
      CALL FUNCT(1,F2I,XWI)
      P1E=MOBLTY*G(F2P,E)-G(F2I,E)
      A=F2I
      B=5.*F2I
      AINT=0.0
20    CALL GAUSS(2,AtBtEtVALUE)
      AINT=AINT+VALUE
      PHI=DATAN(B/E)
      CALL ELLEP(PHI,ZZ,T1)
      LEFT=(1.+E)*(P1E*T1+(1.-MOBLTY)*AINT)
      IF(LEFT.GT.RIGHT)GO 10 15
      A=B
      B=5.*A
      SAVE1=LEFT
      GO TO 20
15    POLD=AINT-VALUE
      SAVE2=LEFT
      CALL ROOT(A,B,SAVE1,SAVE2,POLD,RIGHT,MOBLTY,E,ZZ,P1E,T,X)
C
C     AFTER DETERMINING THE FRONT LOCATIONS FROM THE SUBROUTINE ROOT,
C     CALCULATION DISPLACING FLUID CUT STARTS:
C
      GG(I+1)=2./(P1E+(1-MOBLTY)*G(X,E1))
      IF(I.EQ.1)FF(1)=T
      FF(I+1)=(1.+E)*T
10    CONTINUE
      GG(1)=GG(2)
      FF(N+1)=(1+E1)*AKE1
      GG(N+1)=2./(G(F2PBT,E1)-G(F2IBT,E1))
C
C     QA = PRODUCING FLOLJ RATE OF DISPLACING FLUID
C     QB = PRODUCING FLOW RATE OF DISPLACED FLUID
C     FA = DISPLACING FLUID CUT IN THE PRODUCTION STREAM
C
      CALL INTGRL(N,STEP,GG,QB)
      QA=GG(N+1)*(PI/4-TETBT)
      FA=QA/(QA+QB)
C
C     CALCULATION OF AREAL SWEEP EFFICIENCY AND INJECTED DISPLACEADLE
C     PORE VOLUMES START.  FIRST, THE PORE VOLUMES OF WATER PRODUCED
C     ARE COMPUTED.  THIS IS STORED IN "VP".
C
      HTETBT=RIGHT/4.
      HBT=(PI/4.-TETBT)/N
```

```
      N1=N+1
      DO 11 L=1,N1
      TET=TETBT+HBT*(L-1)
      ET=DTAN(TET)**2
      PP=PI/2.
      Z=1-ET*ET
      CALL ELLEP(PP,Z,EK)
      FSWEP(L)=(1+ET)*EK
      XWI=RW*DSIN(TET)
      XWP=AK-RW*DCOS(TET)
      CALL FUNCT(1,ZP,XWP)
      CALL FUNCT(1,ZI,XWI)
      PE=MOBLTY*G(ZP,ET)-G(ZI,ET)
      CALL GAUSS(1,ZI,ZP,ET,VAL)
      HTETA=(1+ET)/4*(PE*EK+(1-MOBLTY)*VAL)
      GG(L)=(HTETBT-HTETA)/(G(ZP,ET)-G(ZI,ET))
11    CONTINUE
C
C
      CALL INTGRL(N,HBT,GG,VP)
C
C     IN THE FOLLOWING CALCULATIONS OF AREAL SWEEP EFFICIENCY AND
C     PORE VOLUMES INJECTED, THE TWO SYMBOLS S1 AND S2 ARE USED TO
C     DESIGNATE:
C     S1 = AREA ENCOMPASED BETWEEN THE BROKEN-THROUGH STREAMLINE (TETBT)
C          AND THE STREAMLINE PI/4
C     S2 = SWEPT AREA ENCOMPASED BETWEEN STREAMLINE, TETDT, AND
C          STREAMLINE ZERO.
C
      CALL INTGRL(N,STEP,FF,S1)
      CALL INTGRL(N,HBT,FSWEP,S2)
      SWEEP=(S1+S2)/AK/AK
      PV=SWEEP+4.*VP/AK/AK
      WRITE(6,100)PV,SWEEP,FA
100   FORMAT(1X,'PORE VOLUME=',F8.5,4X,'EABT=',F8.5,3X,'CUT=',F6.4)
1     CONTINUE
      STOP
      END
C
C
C
      SUBROUTINE SN(X,SNX)
C
C     THIS SUBROUTINE CALCULATES THE JACOBIAN ELLIPTIC FUNCTION SN(X,0.5)
C     THE ROUTINE USES FOURIER SERIES EXPANSION OF SN(X,0.5).
C     INPUT:  X, ARGUMENT OF THE JACOBIAN ELLIPTIC FUNCTION
C     OUTPUT: SNX, VALUE OF THE JACOBIAN ELLIPTIC FUNCTION
C
      IMPLICIT REAL*8 (A-H,O-Z)
      AK=1.854074677301372D0
      AM=.5
      PI=4.*DATAN(1.D0)
      Q=DEXP(-PI)
      SUM=0.D0
      V=PI*X/2./AK
      DO 10 I=1,9
      II=I-1
      C1=II+.5
      C2=2.*II+1
10    SUM=SUM+Q**C1*DSIN(C2*V)/(1.-Q**C2)
```

```
      SNX=2.*PI*SUM/AK/DSQRT(AM)
      RETURN
      END
C
C
C
      SUBROUTINE FUNCT(INDIC,F2,X)
C
C     THIS SUBROUTINE CONFUTES F2 FOR A GIVEN X OR COMPUTES X FOR A
C     GIVEN F2.
C     F2=F*F AND F IS TItE EQUATION FOR THE DEFINITION OF STREAMLINE
C     WHICH IS GIVEN BY EQ. A-18 WITH m = 0.5.
C
C
C     INDIC=1, COMPUTE F2 FOR GIVEN X
C     INDIC=2, CONFUTE X FOR GIVEN F2
C
      IMPLICIT REAL*8 (A-H,O-Z)
      IF(INDIC.EQ.1)GO TO 10
      SNX=DSQRT(1.+F2-DSQRT(1.+F2*F2))
      ANGLE=DARSIN(SNX)
      Z=.5
      CALL ELLEP(ANGLE,Z,X)
      GO TO 20
10    CALL SN(X,SNX)
      SN2X=SNX*SNX
      F2=SN2X*(1.-.5*SN2X)/(1.-SN2X)
20    RETURN
      END
C
C
C
      SUBROUTINE ELLEP(Y,Z,A)
C
C     THIS SUEROUTINE COMPUTES INCOMPLETE ELLIPTIC INTEGRALN F(PHI,k)
C     PHI IS THE ARGUMENT AND k IS THE MODULUS.  TIIE MODULUS IS EQUAL
C     TO THE SQUARE ROOT OF TItE PARAMETER.
C     INPUT:  Y = ARGUMENT OF THE ELLIPTIC FUNCTION
C             Z = PARAMETER OF THE ELLIPTIC INTEGRAL
C             A = VALUE OF TIIE ELLIPTIC INTEGRAL
C     THE ROUTINE USES LANDENS DECENDING TRANSFORMATION.  FOR REFERENCE
C     SEE ABRAMOWITZ, PAGE
C
C
      IMPLICIT REAL*8 (A-H,O-Z)
      REAL*8  K,K1,KP
      TOL=1.D-4
      PI=4.*DATAN(1.D0)
      W=1.D0
      X=Y
      K=DSQRT(Z)
15    K1=2.*DSQRT(K)/(1+K)
      X=.5*(X+DARSIN(K*DSIN(X)))
      QE=DARSIN(K1)
      QE=QE*180./PI
      W=2.*W/(1+K)
      IF((90.-QE).LE.TOL)GO TO 30
      K=K1
      GO TO 15
30    A=W*DLOG(DTAN(PI/4+X/2))
```

```
      RETURN
      END
C
C
C
      SUBROUTINE GAUSS(L,ALOWER,UPPER,E,VALUE)
C
C     THIS SUPROUTINE CONFUTES VALUE OF AN INTEGRAL USING EIGHT POINT
C     GAUSSIAN QUDRATURE METHOD.
C     INPUT:  ALOWER = LOWER LIMIT OF THE INTEGRAL
C             UPPER = UPPER LIMIT OF THE INTEGRAL
C             IF L = 1, PROGRAM COMPUTES THE INTEGRAL BY DIVIDING THE
C             INTERVAL INTO SEVERAL SEGMENTS ON A LOGARITHMIC SCALE
C             (BASE 10)
C             IF L # 1, THE PROGRAM USES ONLY ONE INTERVAL
C             E = ETA TERM DEFINED BY EQ. 9-31
C     OUTPUT: VALUE = VALUE OF THE INTEGRAL
C
      IMPLICIT REAL*8 (A-H,O-Z)
      DIMENSION W(10),X(10)
      F1(Y)=DSQRT(1.+Y*Y)
      F2(Y)=DSQRT(E*E+Y*Y)
      F(Y)=DLOG(E*Y*(F1(Y)+F2(Y))/(E*F1(Y)+F2(Y)))/(F1(Y)*F2(Y )
      N=8
      X(1)=.183434642495650D0
      X(2)=.525532409916329D0
      X(3)=.796664774136272D0
      X(4)=.960289856497536D0
      X(5)=-X(1)
      X(6)=-X(2)
      X(7)=-X(3)
      X(8)=-X(4)
      W(1)=.362683783378362D0
      W(2)=.313706645877887D0
      W(3)=.222381034453374D0
      W(4)=.101228536290376D0
      W(5)=W(1)
      W(6)=W(2)
      W(7)=W(3)
      W(8)=W(4)
      A=ALOWER
      IF(L.EQ.1)GO TO 15
      B=UPPER
      SUM=0.D0
      DO 10 I=1,N
      Y=.5D0*((B+A)+(B-A)*X(I))
10    SUM=SUM+W(I)*F(Y)
      VALUE=.5D0*(B-A)*SUM
      GO TO 100
15    VALUE=0.
17    B=10.*A
      IF(B.GE.UPPER)B=UPPER
      SUM=0.D0
      DO 12 I=1,N
      Y=.5D0*((B+A)+(B-A)*X(I))
12    SUM=SUM+W(I)*F(Y)
      VAL=.5D0*(B-A)*SUM
      IF(VAL.EQ.0)GOTO 100
      VALUE=VALUE+VAL
      A=B
```

```
      GO TO 17
100   RETURN
      END
C
C
C
      SUBROUTINE ROOT(X1,X2,F1,F2,P1,RIGHT,AM,E,Z,P1E,T,X)
C
C     THIS SUBROUTINE COMPUTES THE ROOTS OF EQ. D-51
C     THE INPUT TO THE ROUTINE ARE:
C     X1 = VALUE OF Z BAR AT WHICH THE LEFT SIDE IN EQ. 1)-51 IS
C          SMALLER THAN THE RIGHT SIDE
C     X2 = VALUE OF Z BAR AT WHICH THE RIGHT SIDE OF EQ. B-51 IS
C          LARGER THAN THE RIGHT SIDE
C     F1 = VALUE OF THE LEFT SIDE COMPUTED AT X1
C     F2 = VALUE OF THE LEFT SIDE COMPUTED AT X2
C     P1 = VALUE OF THE INTEGRAL IN THE LEFT SIDE OF EQ. B-51 COMPUTED
C          AT X1
C     AM = MOBILITY RATIO
C     E  = VALUE OF ETA DEFINED BY EQ. 0-31
C     Z  = ARGUMENT OF ELLIPTIC INTEGRAL F(n,k)
C     P1E = THE P TERM IN LEFT SIDE OF EQ. 6-51
C     RIGHT = VALUE OF THE RIGHT HAND SIDE OF EQ. D-51 COMPUTED AT
C             A BREAKENTHROUGH STREAMLINE, TETBT
C     THE OUTPUT FROM THE ROUTINE ARE:
C     X = EXACT VALUE OF Z FAR (SOLUTION TO EQ. B-51)
C     T = VALUE OF THE INTEGRAL IN THE LEFT SIDE OF EQ. B-51 COMPUTED
C         AT X1
C
      IMPLICIT REAL*8 (A-H,O-Z)
      TOL=1.D-4
      F1=F1-RIGHT
      F2=F2-RIGHT
5     X=(X1+X2)/2.
      CALL GAUSS(2,X1,X,E,V)
      AINT=V+P1
      PHI=DATAN(X/E)
      CALL ELLEP(PHI,Z,T)
      ALEFT=(1.+E)*(P1E*T+(1.-AM)*AINT)
      FX=ALEFT-RIGHT
      IF(F1*FX.LT.0.D0)GO TO 10
      X1=X
      F1=FX
      P1=AINT
      IF(DABS(X2-X).LT.DABS(TOL*X))GO TO 20
      GO TO 5
10    X2=X
      IF(DABS(X1-X).LT.DABS(TOL*X))GO TO 20
      GO TO 5
20    RETURN
      END
C
C
      SUBROUTINE INTGRL(N,H,F,VOL)
C
C     THIS SUBROUTINE COMPUTES VALUE OF AN INTEGRAL USING SIMPSON'S
C     RULE OF INTEGRATION.
C     INPUT:  N = NUMBER OF INIERVALS, AN EVEN INTEGER NUMBER
C             H = INTERVAL SIZE
C             F = VALUES OF FUNCTIONS COMPUTED AT INTERVALS, AN ARRAY
```

```
C      OUTPUT: VOL = VALUE OF THE INTEGRAL
C
       IMPLICIT REAL*8 (A-H,O-Z)
       DIMENSION F(91)
       SUM1=0
       SUM2=0
       N1=N/2-1
       CO 50 I=1,N1
       SUM1=SUM1+F(2*I)
50     SUM2=SUM2 +F(2*I+1)
       SUM1=SUM1+F(N)
       VOL=H/3*(F(1)+F(N+1)+4.*SUM1+2.*SUM2)
       RETURN
       END
SDATA
0.5D0
```

Table 1

ASSUMED AND COMPUTED PARAMETERS OF THE LAYERS
FOR EXAMPLE 1

LAYER	ASSUMED PARAMETERS		COMPUTED PARAMETERS USING EQUATIONS FOR STAGGERED LINE DRIVE, d/a = 1		COMPUTED PARAMETERS USING EQUATIONS OF EQUIVALENT 5-SPOT SYSTEM	
	ϕh	$\frac{kh}{\Sigma kh}$	ϕh	$\frac{kh}{\Sigma kh}$	ϕh	$\frac{kh}{\Sigma kh}$
1	0.2850	0.2	0.2800	0.19750	0.27830	0 1363[illegible]
2	1 0[illegible]34	0 4	1 00601	0 398[illegible]4	1 001[illegible]	0 3[illegible]664
3	1 14[illegible]3	[illegible] 3	1 133[illegible]6	0 2[illegible]92[illegible]	1 1[illegible]944	0 3[illegible]0[illegible]1
4	0.5068	0.1	0.51094	0.10113	0.52816	0.10454
SUM	2.9455	1.0	2.93071	0.99608	2.94787	0.99819

Table 2

ASSUMED AND COMPUTED VALUES OF LAYER PARAMETERS FOR EXAMPLE 2*

LAYER	ASSUMED PARAMETERS				COMPUTED PARAMETERS USING OPTIMIZATION TECHNIQUE			
	ϕh	$\frac{kh}{\Sigma kh}$	h, ft	k, md	ϕh	$\frac{kh}{\Sigma kh}$	h, ft	k, md
1	0.315	0.15	1.26	119.05	0.314996	0.143998	1.26	119.05
2	1.000	0.40	4.00	100.00	0.933357	0.333384	0.40	100.00
3	0.6875	0.25	2.75	90.31	0.687447	0.243383	2.75	90.31
4	0.6000	0.20	2.4	83.33	0.600065	0.200024	2.40	83.33
SUM	2.6025	1.00			2.602466	0.999989		

*The k and h values in this table have been computed for ϕ = .25 and Σkh = 1000 md-ft.

Table 3

COMPUTED VALUES OF LAYER PARAMETERS USING OPTIMIZATION TECHNIQUE WITH VARIOUS NUMBER OF LAYERS*

LAYER	COMPUTED PARAMETERS WITH THREE LAYERS				COMPUTED PARAMETERS WITH FIVE LAYERS			
	ϕh	$\frac{kh}{\Sigma kh}$	h, ft	k, md	ϕh	$\frac{kh}{\Sigma kh}$	h, ft	k, md
1	0.33817	[illegible]	1.35	118.76	0.31499	[illegible]	1 26	119.05
2	[illegible]	[illegible]	[illegible]	[illegible]	[illegible]	[illegible]	[illegible]	[illegible]
[illegible]	[illegible]	[illegible]	[illegible]	[illegible]	[illegible]	[illegible]	[illegible]	[illegible]
4					[illegible]	[illegible]	[illegible]	[illegible]
5					0.60014	0.20005	2.40	83.33
SUM	1.45202	0.95404			2.60243	0.99998		

*The k and h values in this table have been computed for ϕ = .25 and Σkh = 1000 md-ft.

Table 4

COMPUTED LAYER PARAMETERS FOR FIELD TEST USING THE OPTIMIZATION ROUTINE WITH DIFFERENT NUMBER OF LAYERS

LAYER	FIVE LAYERS		SEVEN LAYERS		NINE LAYERS		TEN LAYERS	
	ϕh	$\frac{kh}{\Sigma kh}$	ϕh	$\frac{kh}{\Sigma kh}$	ϕh	$\frac{kh}{\Sigma kh}$	ϕh	$\frac{kh}{\Sigma kh}$
1	0.035 12	0.033734	0.015658	0.016360	0.011562	0.012167	0.011410	0.012009
2	0 10652[illegible]	0 0[illegible]2838	0 04741[illegible]	0 043[illegible]6[illegible]	0 0155[illegible]5	0 015031	0 013[illegible]82	0 013344
3	0 1061[illegible]8	0 0821[illegible]5	0 084410	0 07[illegible]63	0 041[illegible]26	0 0[illegible]813[illegible]	0 034880	0 031[illegible]38
4	0 0[illegible]4516	0 0660[illegible]	0 052[illegible]45	0 041[illegible]8	0 0[illegible]8[illegible]8[illegible]	0 068042	0 0[illegible]0605	0 061395
5	0 0886[illegible]3	0 055505	0 058256	0 0434 1	0 0524[illegible]2	0 041585	0 02672[illegible]	0 022284
6			0 08[illegible]285	0 060604	0 05[illegible]068	0 042590	0 04[illegible]820	0 0[illegible]617
7			0 08[illegible]4[illegible]2	0 054503	0 08486[illegible]	0 058[illegible]0	0 053306	0 0[illegible]56
8					0 0[illegible]5888	0 04[illegible]84	0 0[illegible]4643	0 058[illegible]40
9					0 0[illegible]10[illegible]6	0 012465	0 0[illegible]5661	0 04[illegible]6[illegible]2
10							0.021079	0.012466
SUM	0.431180	0.330280	0.433100	0.333670	0.439450	0.337060	0.439920	0.337290

Table 5

COMPUTED PERMEABILITIES AND THICKNESSES OF LAYERS
FOR FIELD TEST WITH DIFFERENT NUMBER OF LAYERS*

LAYER	FIVE LAYERS		SEVEN LAYERS		NINE LAYERS		TEN LAYERS	
	h	k	h	k	h	k	h	k
1	0.1358	4471	0.0602	4890	0.0445	4925	0.0439	4926
2	0.4097	4078	0.1824	4320	0.0599	4516	0.0530	4531
3	0.6085	3622	0.3248	4044	0.1613	4257	0.1342	4285
4	0.3635	3267	0.2036	3712	0.3038	4032	0.2716	4070
5	0.3409	2931	0.2036	3843	0.2019	3708	0.1028	3902
6			0.3357	3249	0.2195	3493	0.1839	3682
7			0.3351	2928	0.3264	3253	0.2050	3490
8					0.2919	1967	0.3256	3253
9					0.0811	2767	0.1620	2947
10							0.0810	2768

*The k and h values in this table have been computed for ϕ = .26 and Σkh = 18000 md-ft.

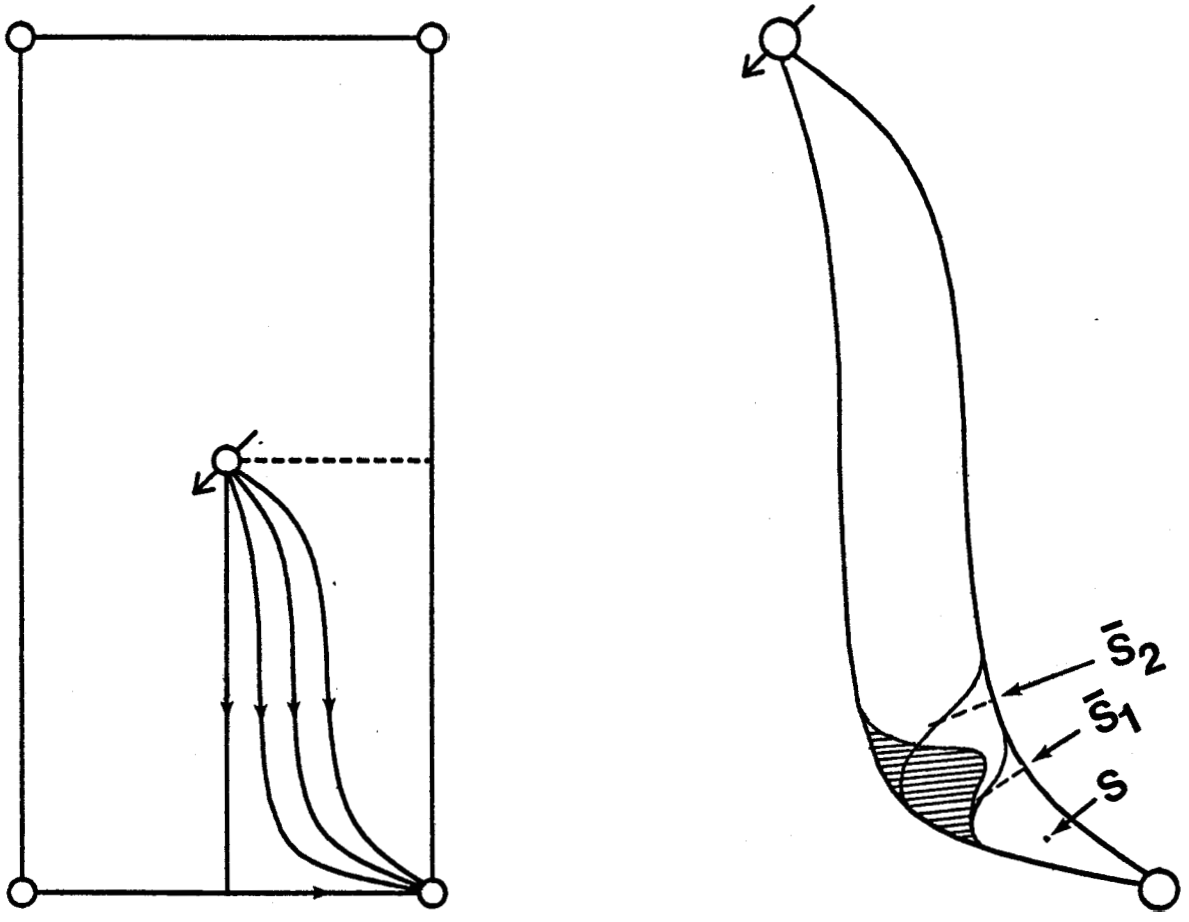

Fig. 1: A STAGGERED-LINE-DRIVE WITH TRACER PROFILE IN A STREAMTUBE

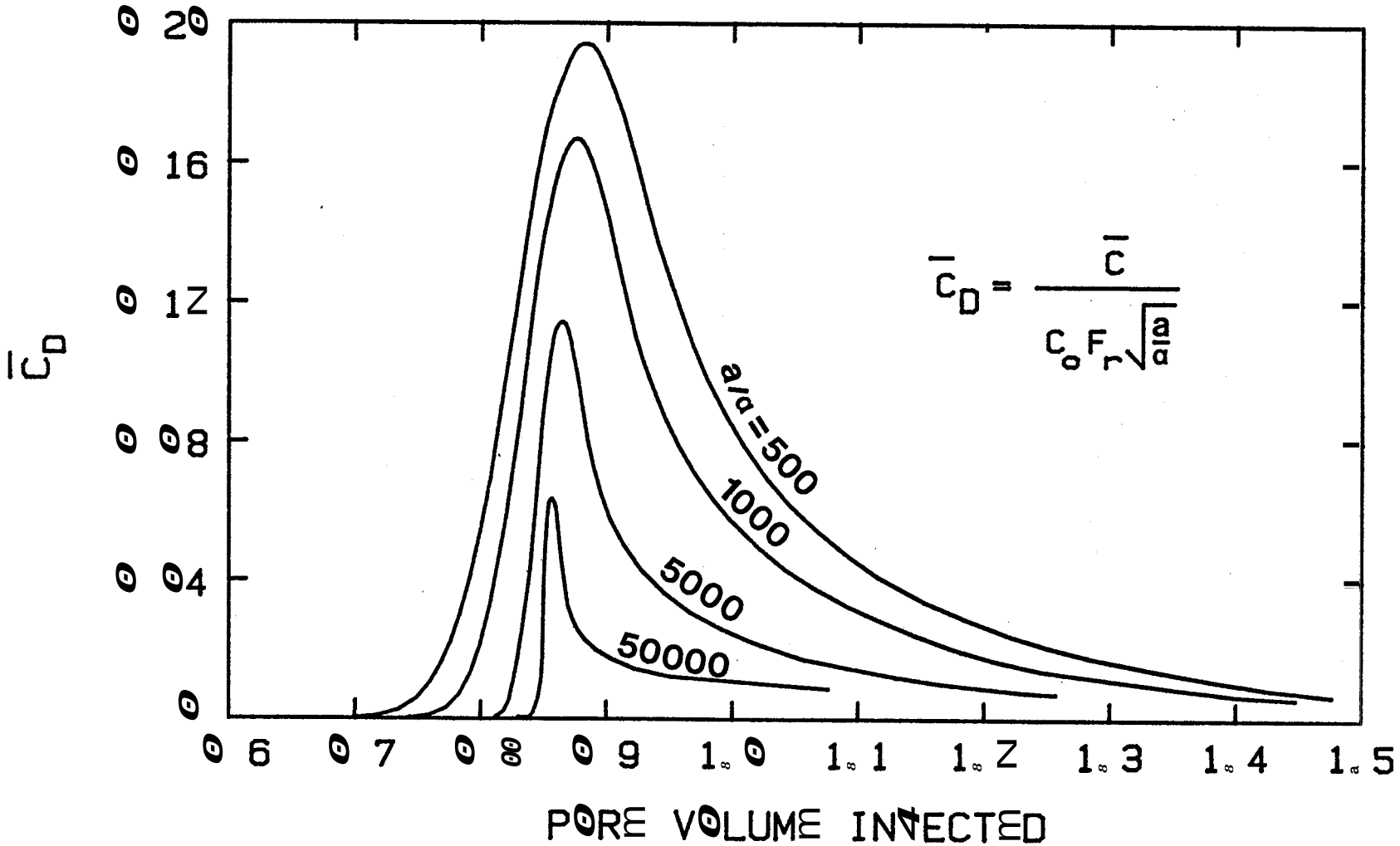

Fig. 2: TRACER BREAKTHROUGH CURVES FOR HOMOGENEOUS STAGGERED-LINE-DRIVE, d/a = 1.5

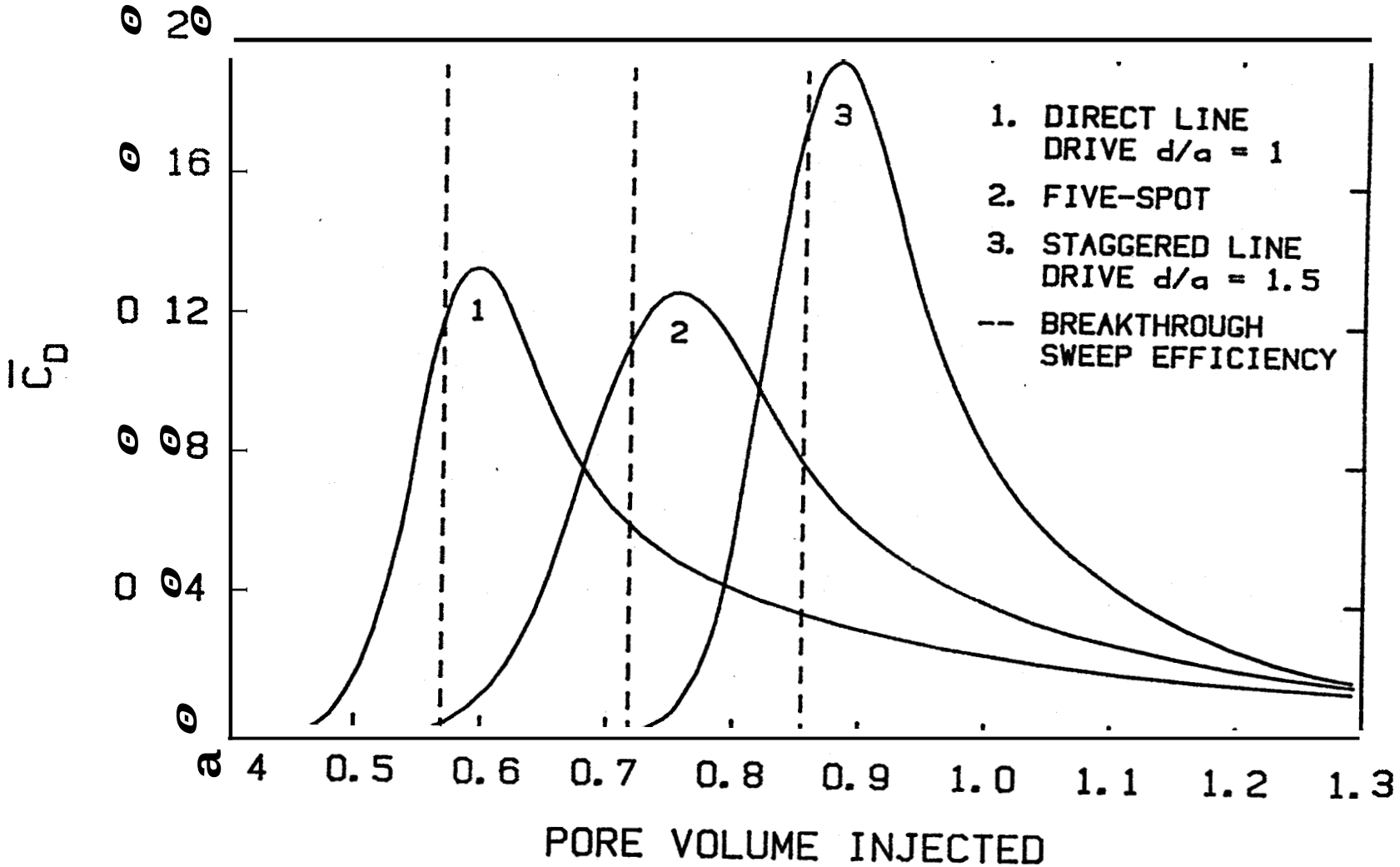

Fig. 3: TRACER BREAKTHROUGH CURVES FOR DIFFERENT PATTERNS, $a/\alpha = 500$

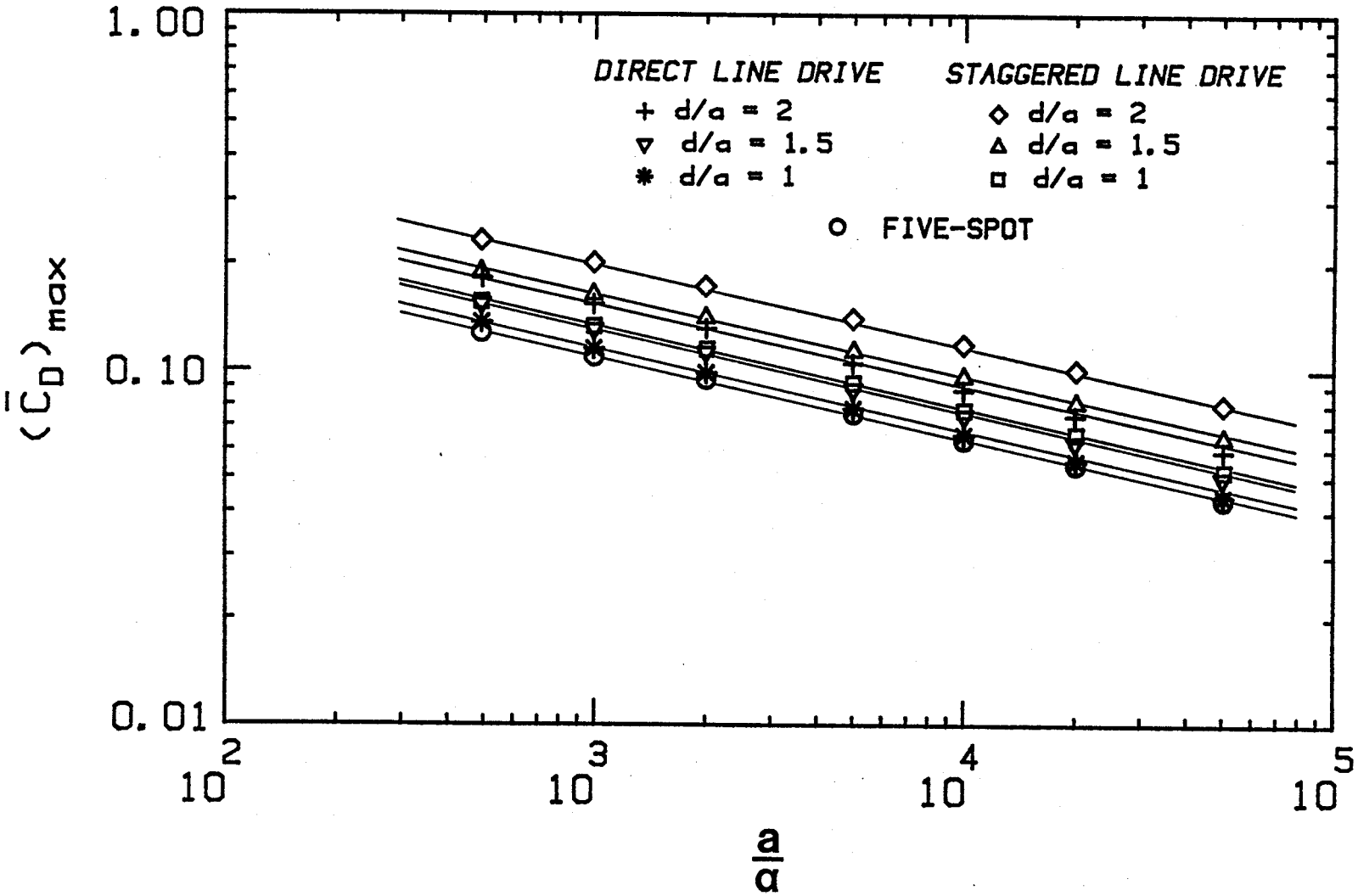

Fig. 6: DIMENSIONLESS PEAK TRACER CONCENTRATIONS

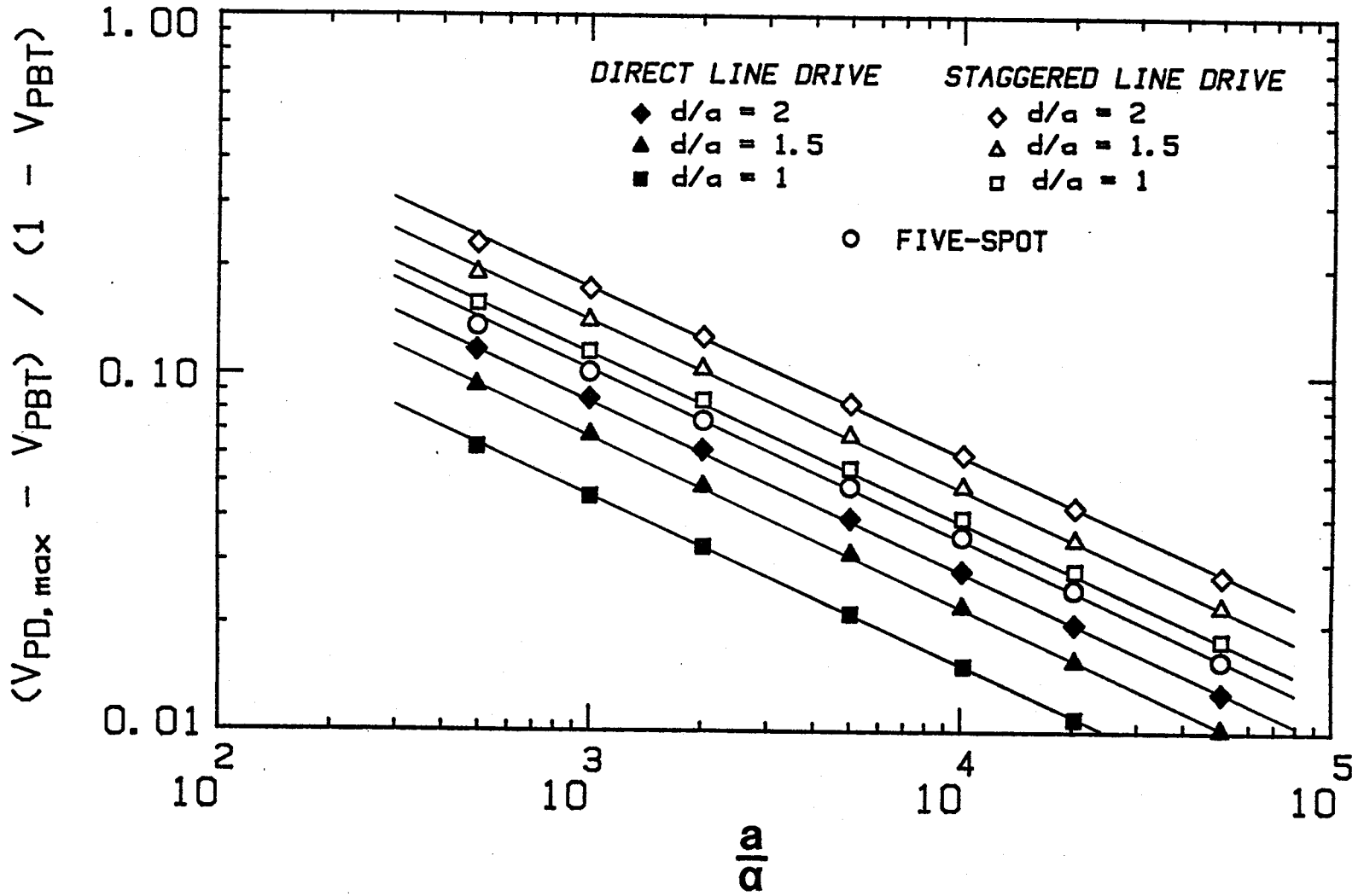

Fig. 7: DIMENSIONLESS PLUG PORE VOLUME LOCATIONS

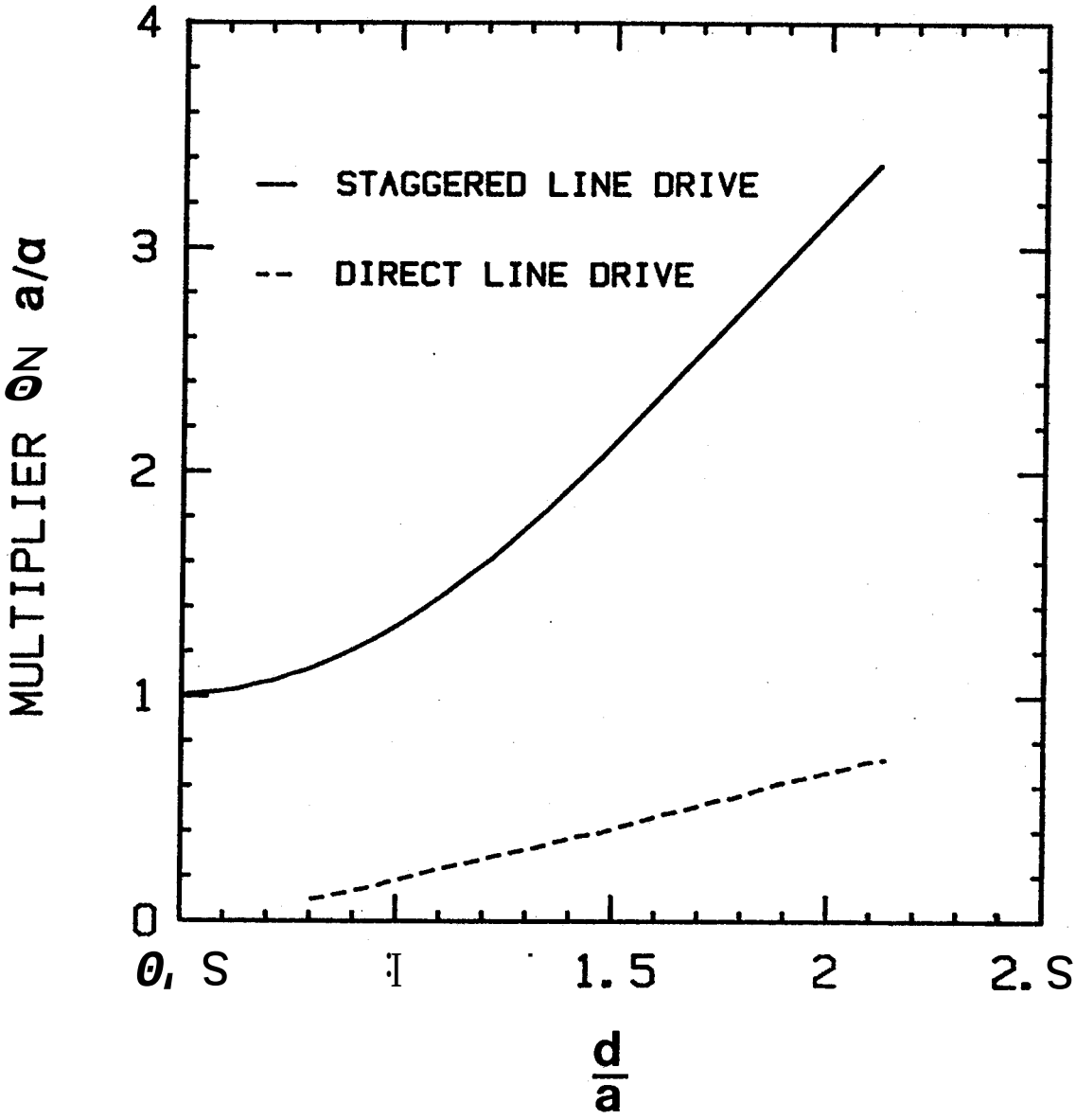

Fig. 8: CORRECTION FACTORS ON PEAK CONCENTRATIONS

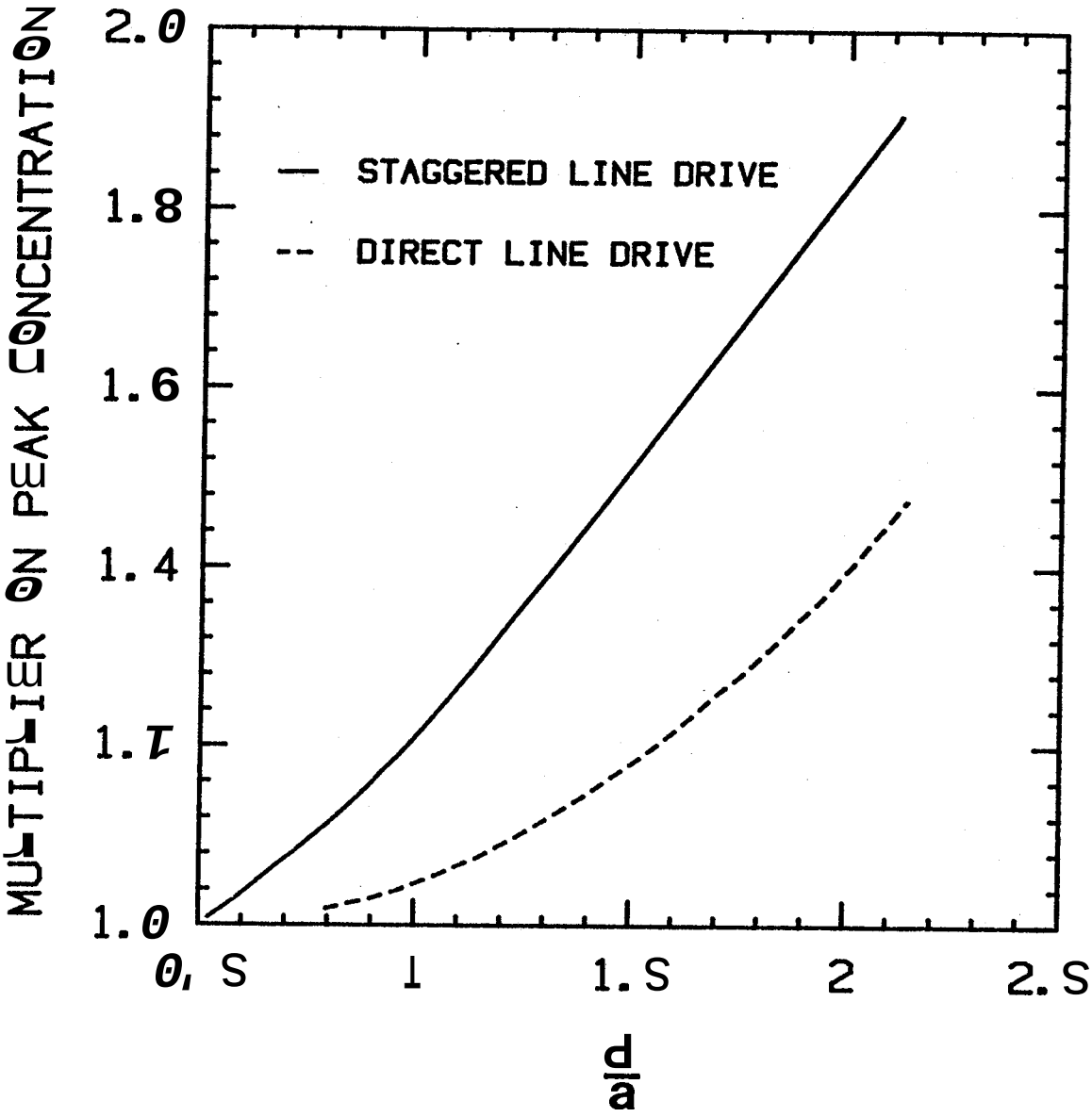

Fig. 9: CORRECTION FACTORS ON a/α TO CALCULATE PEAK LOCATIONS

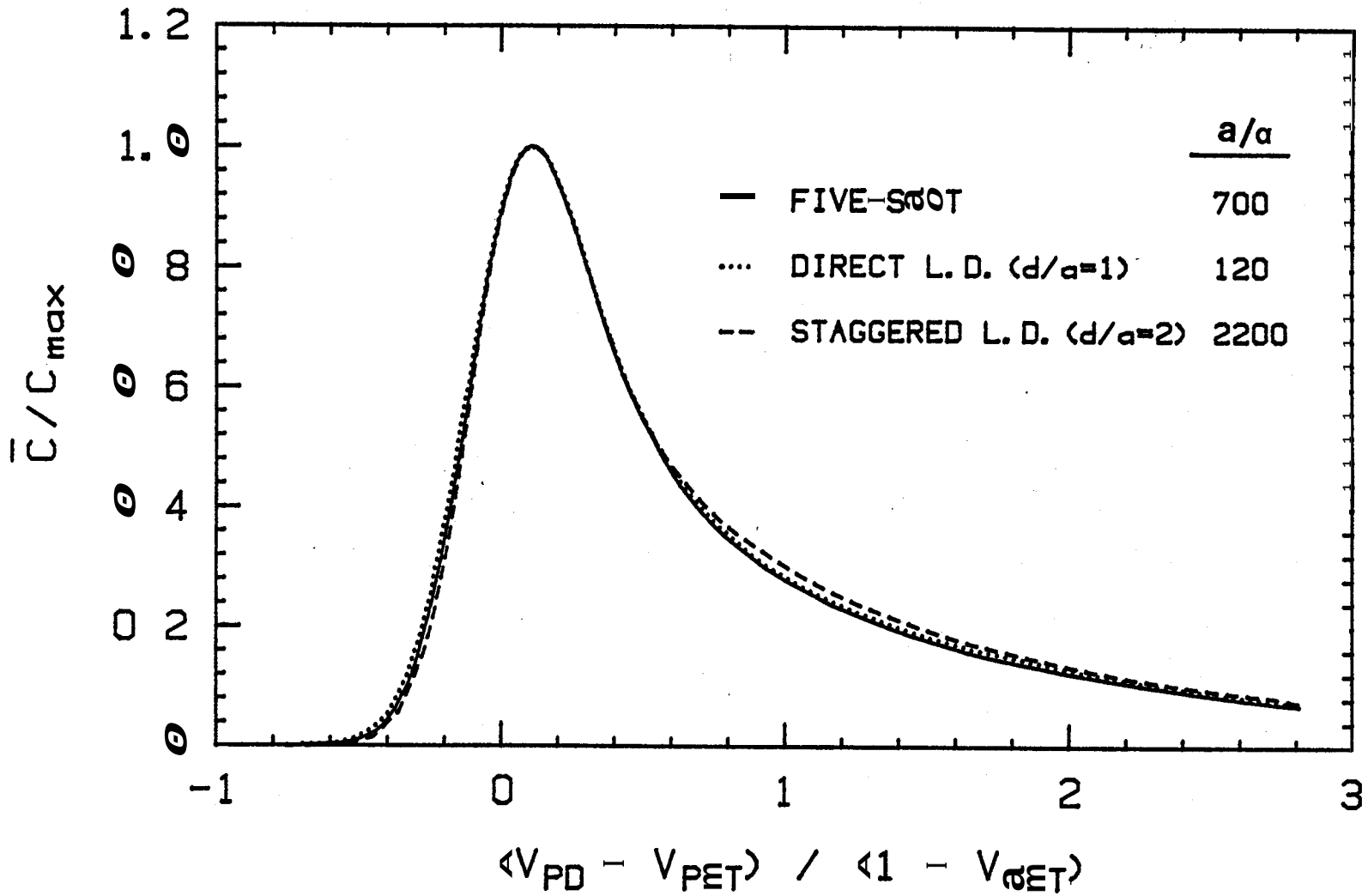

Fig. 10: CORRELATION OF TRACER BREAKTHROUGH CURVES FOR HOMOGENEOUS PATTERNS

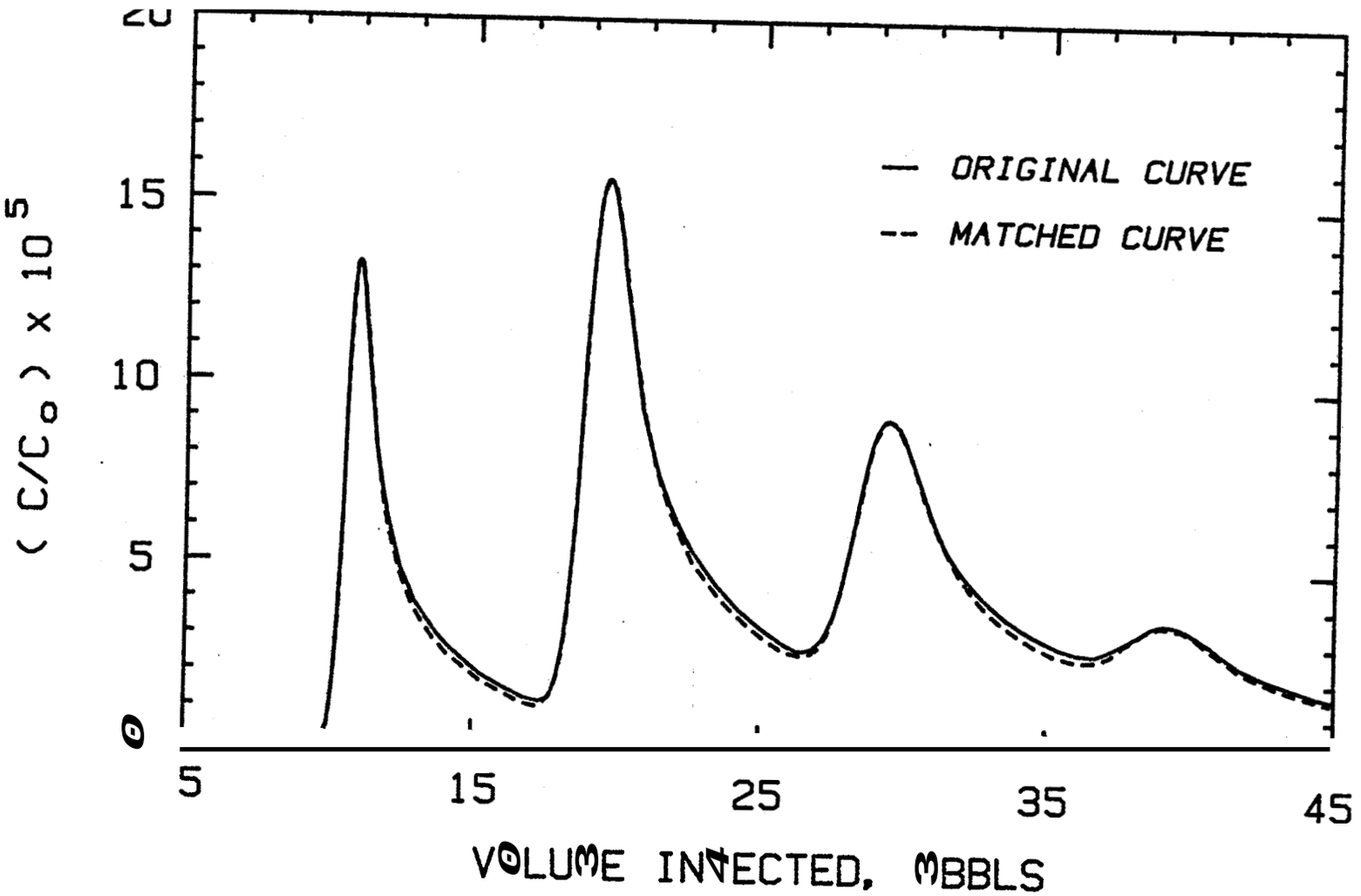

Fig. 11: TRACER RESPONSE AND MATCH FOR A 4-LAYERED STAGGERED-LINE-DRIVE, d/a = 1

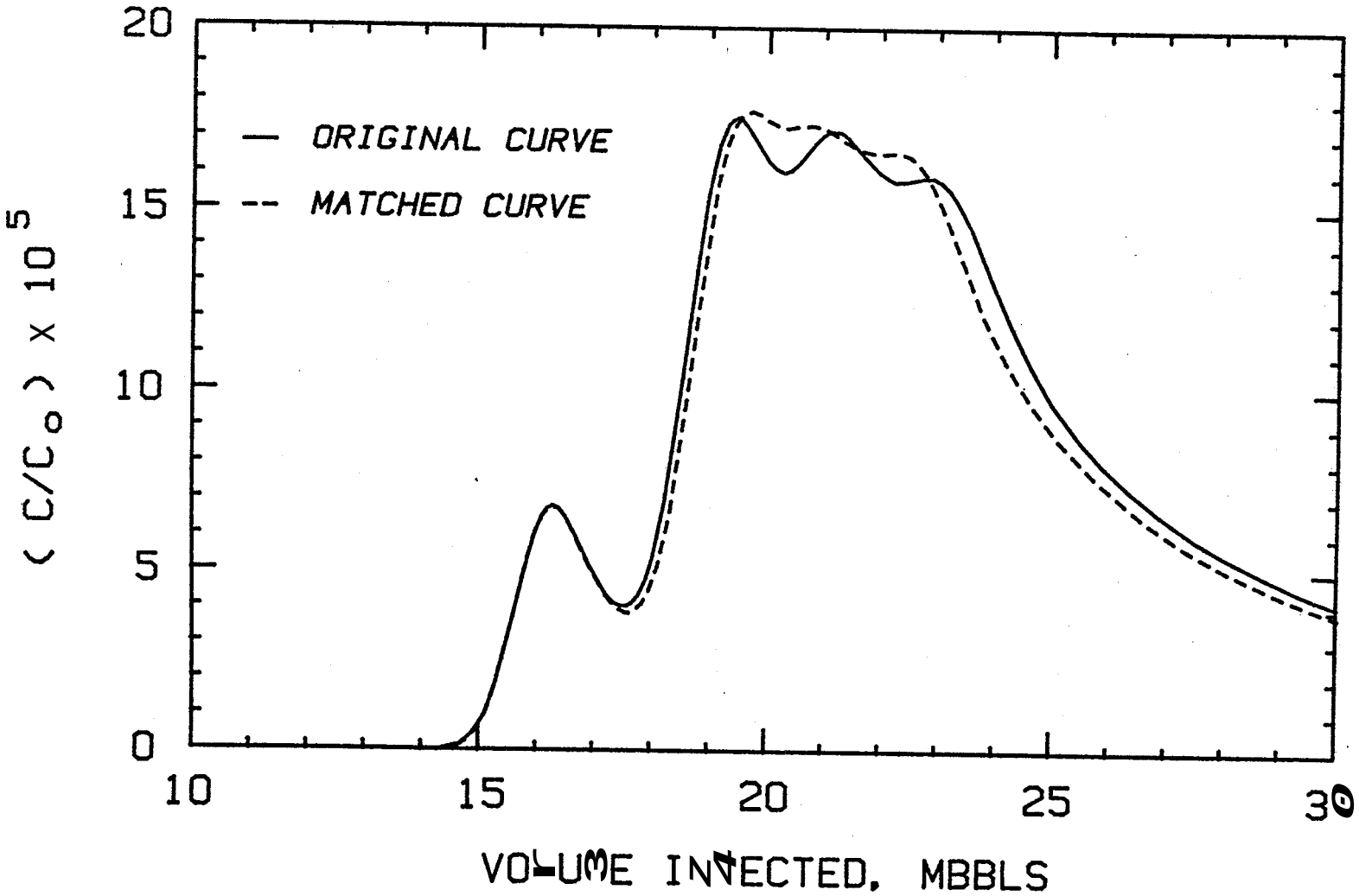

Fig. 12: TRACER RESPONSE AND MATCH FOR ANOTHER 4-LAYERED STAGGERED-LINE-DRIVE, d/a = 1

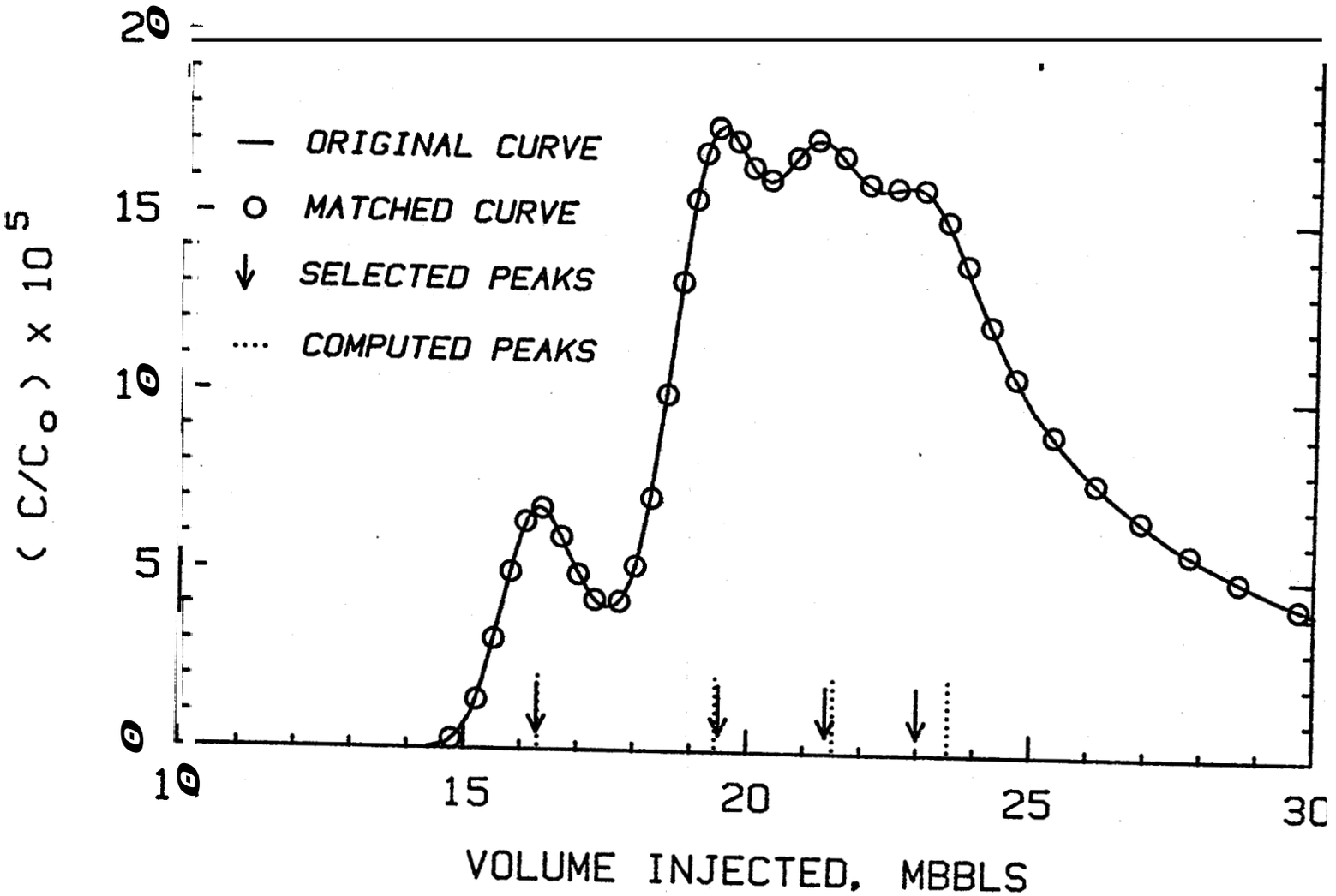

Fig. 13: MATCH USING OPTIMIZATION TECHNIQUE WITH 4 LAYERS

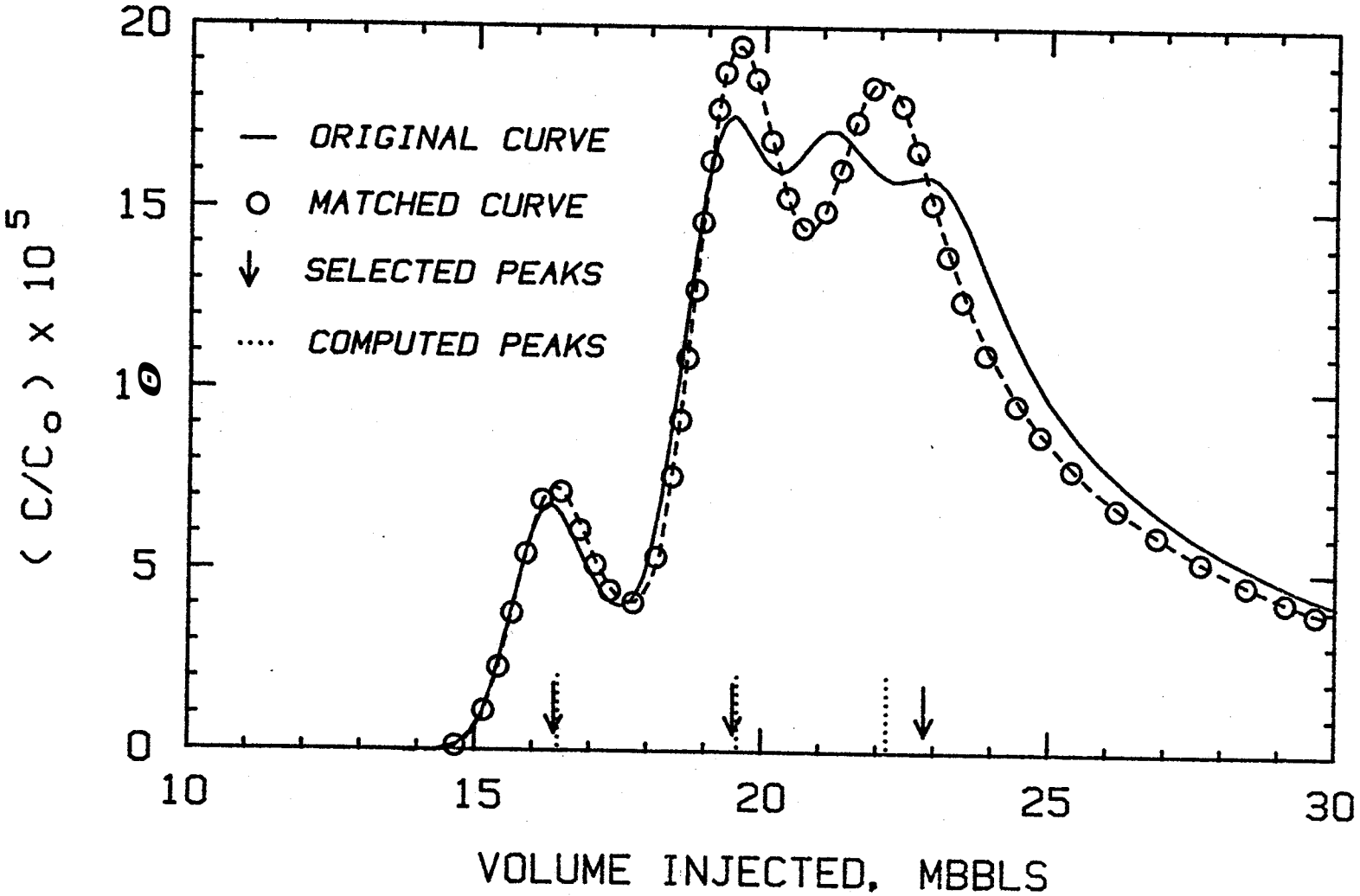

Fig 14: MATCH USING OPTIMIZATION TECHNIQUE WITH 3 LAYERS

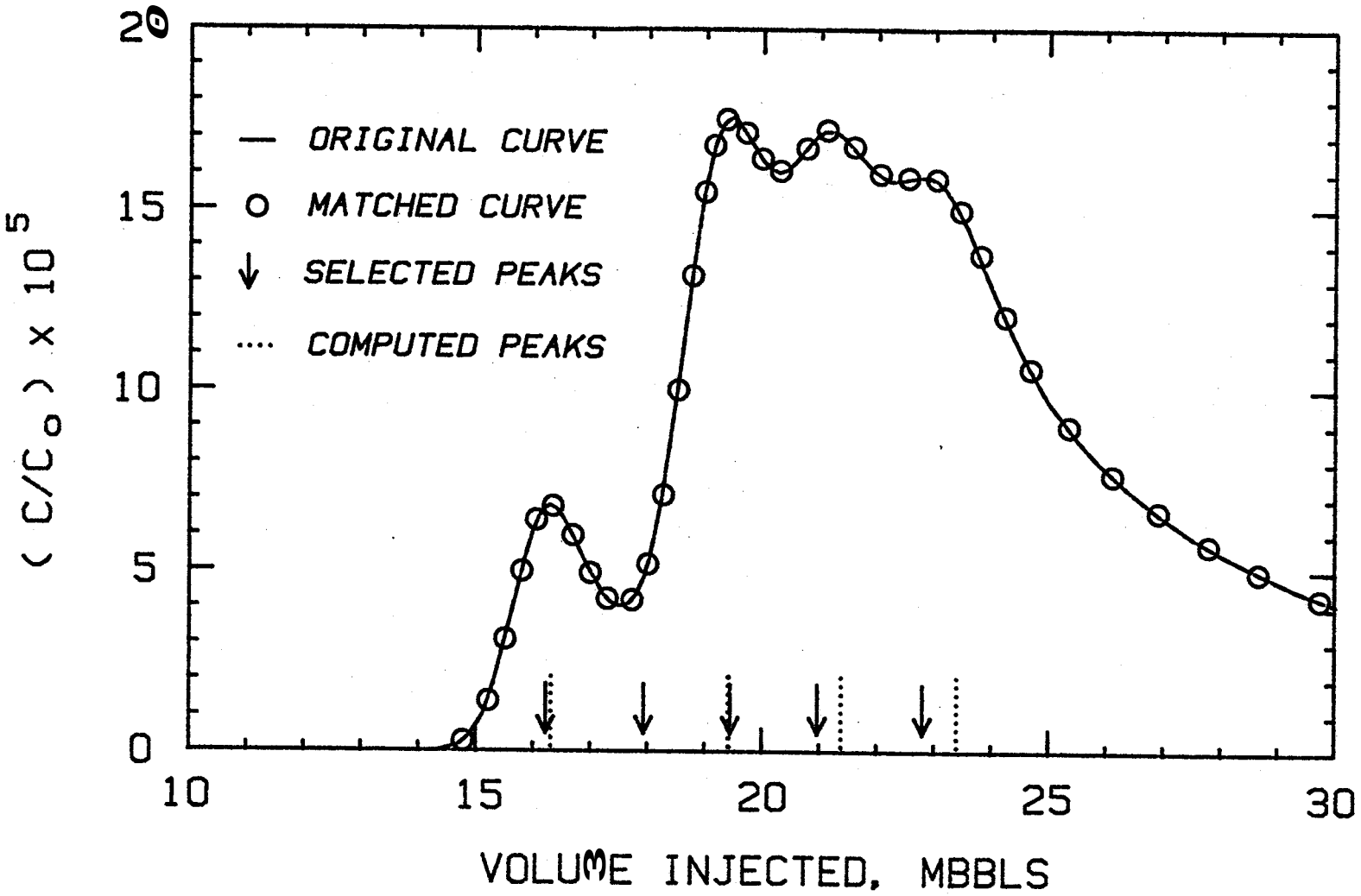

Fig. 15: MATCH USING OPTIMIZATION TECHNIQUE WITH 5 LAYERS

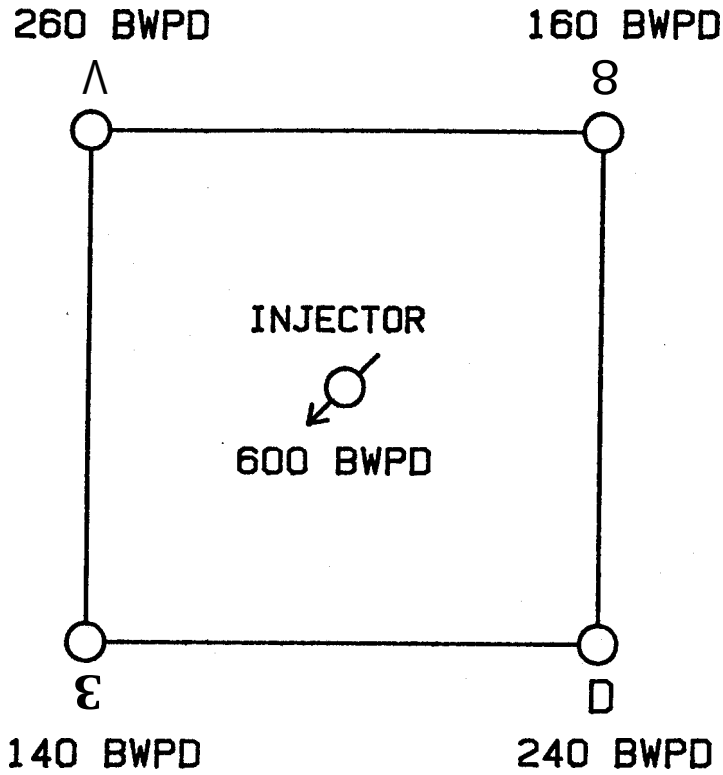

PATTERN AREA	= 2.5 acres
TOTAL TRACER INJECTED	= 200 lbs
NET PAY THICKNESS	= 12 ft
AVERAGE PERMEABILITY	= 1500 md
AVERAGE POROSITY	= 0.26
AVERAGE WATER SATURATION	= 0.55
MIXING CONSTANT, α	= 0.05 ft

Fig. 16: WELL CONFIGURATION AND RESERVOIR DATA FOR THE FIELD TEST

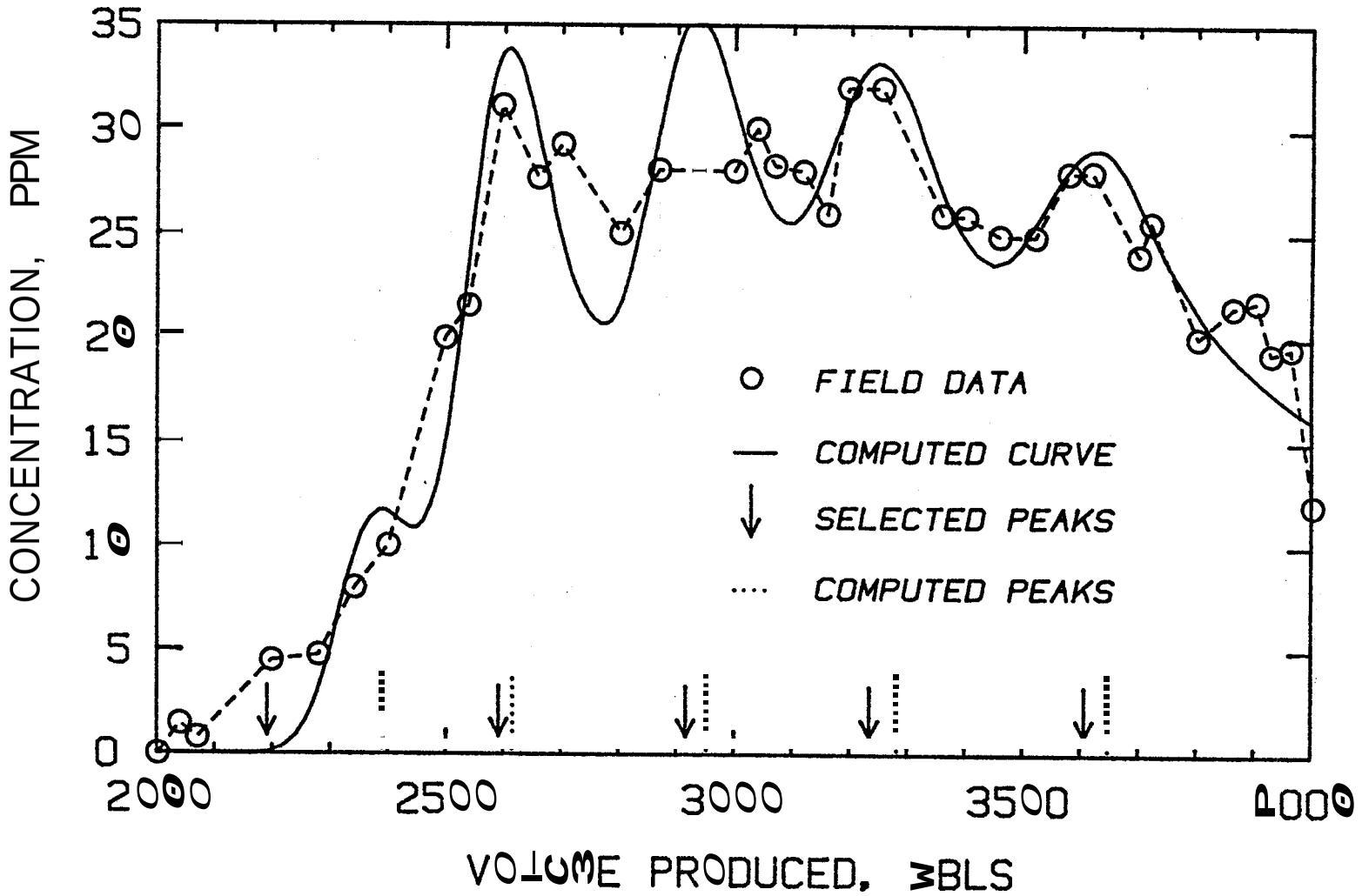

Fig. 17: ANALYSIS WITH 5 LAYERS

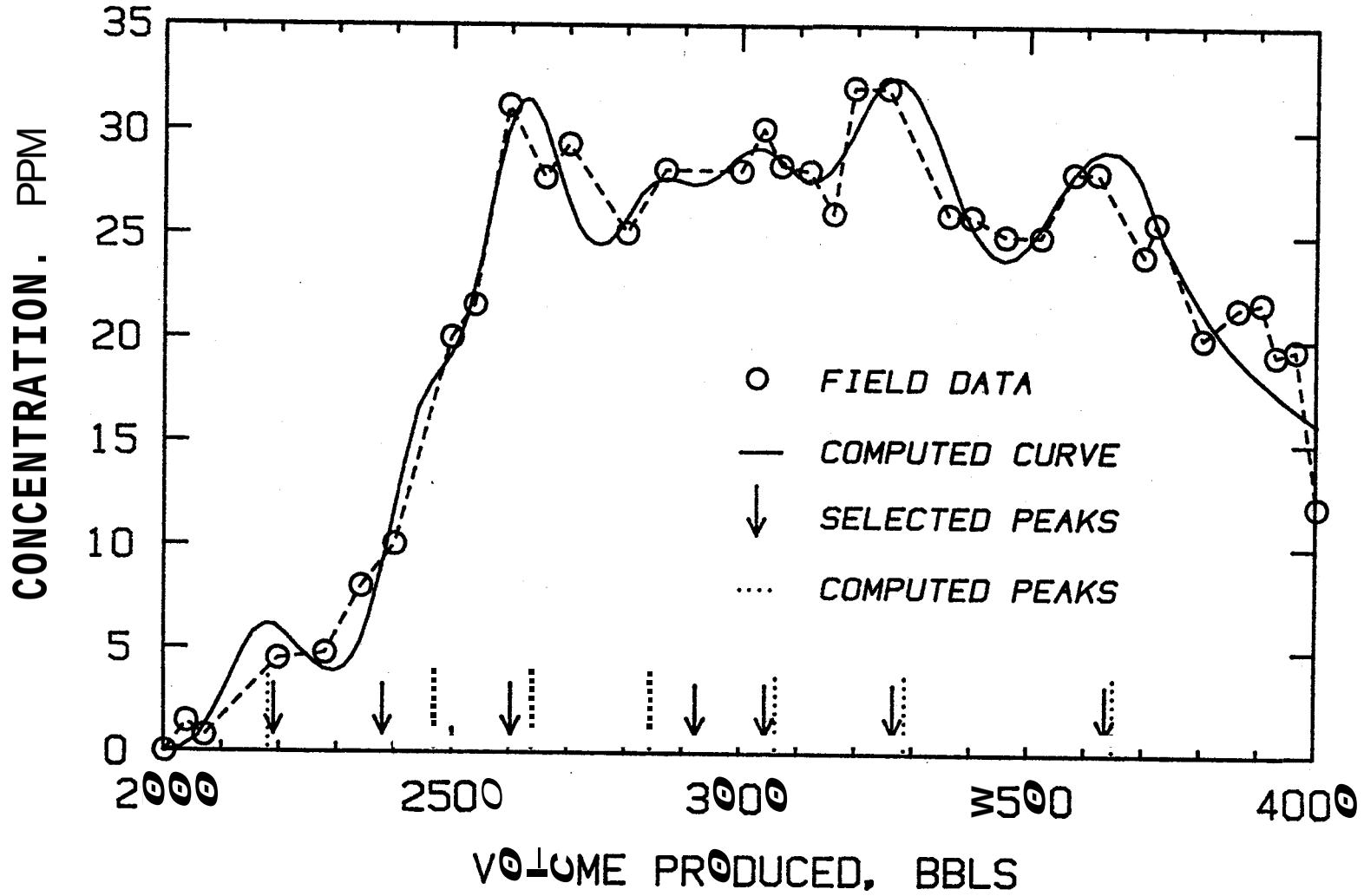

Fig. 18: ANALYSIS WITH 7 LAYERS

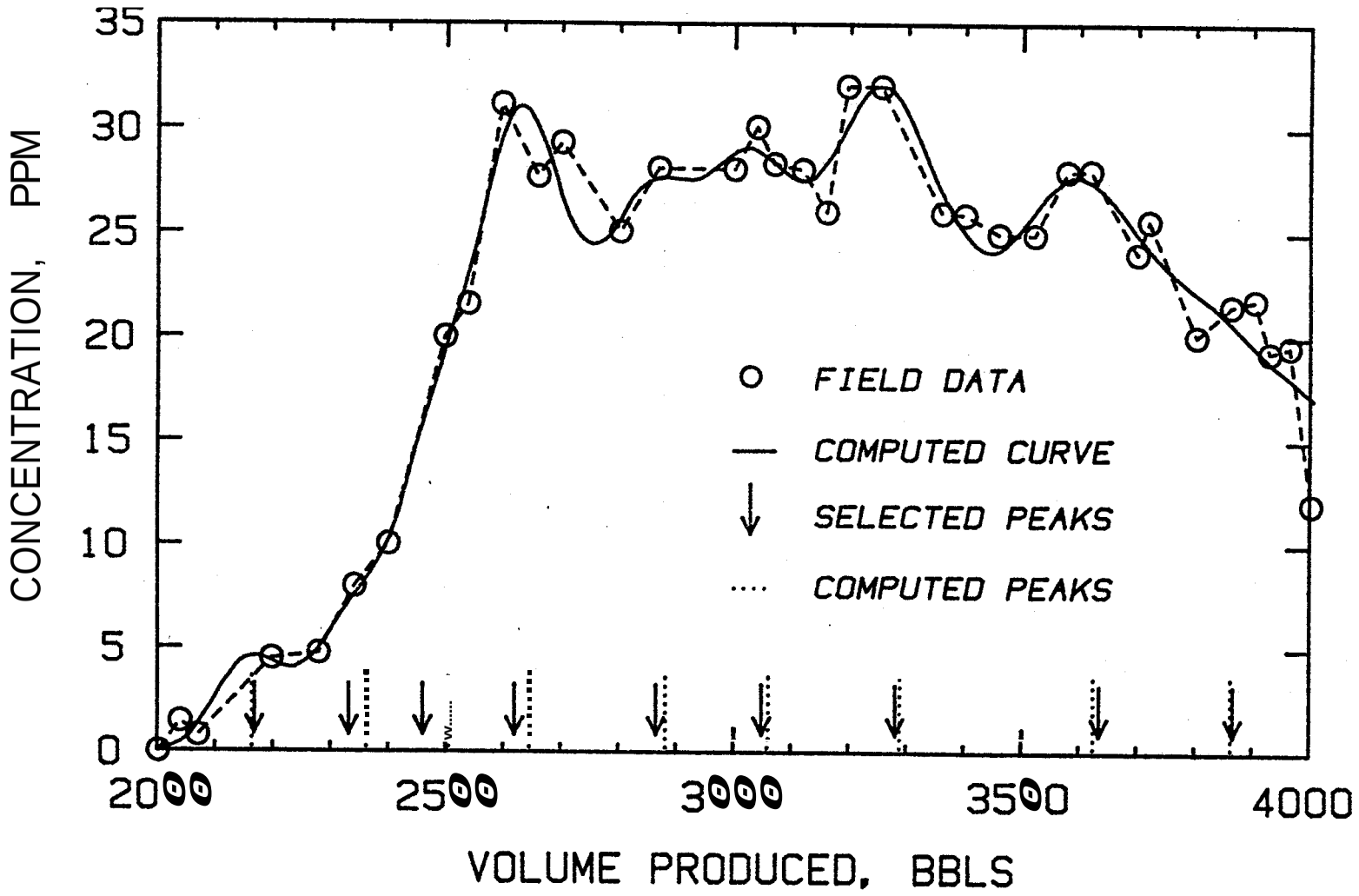

Fig. 19: ANALYSIS WITH 9 LAYERS

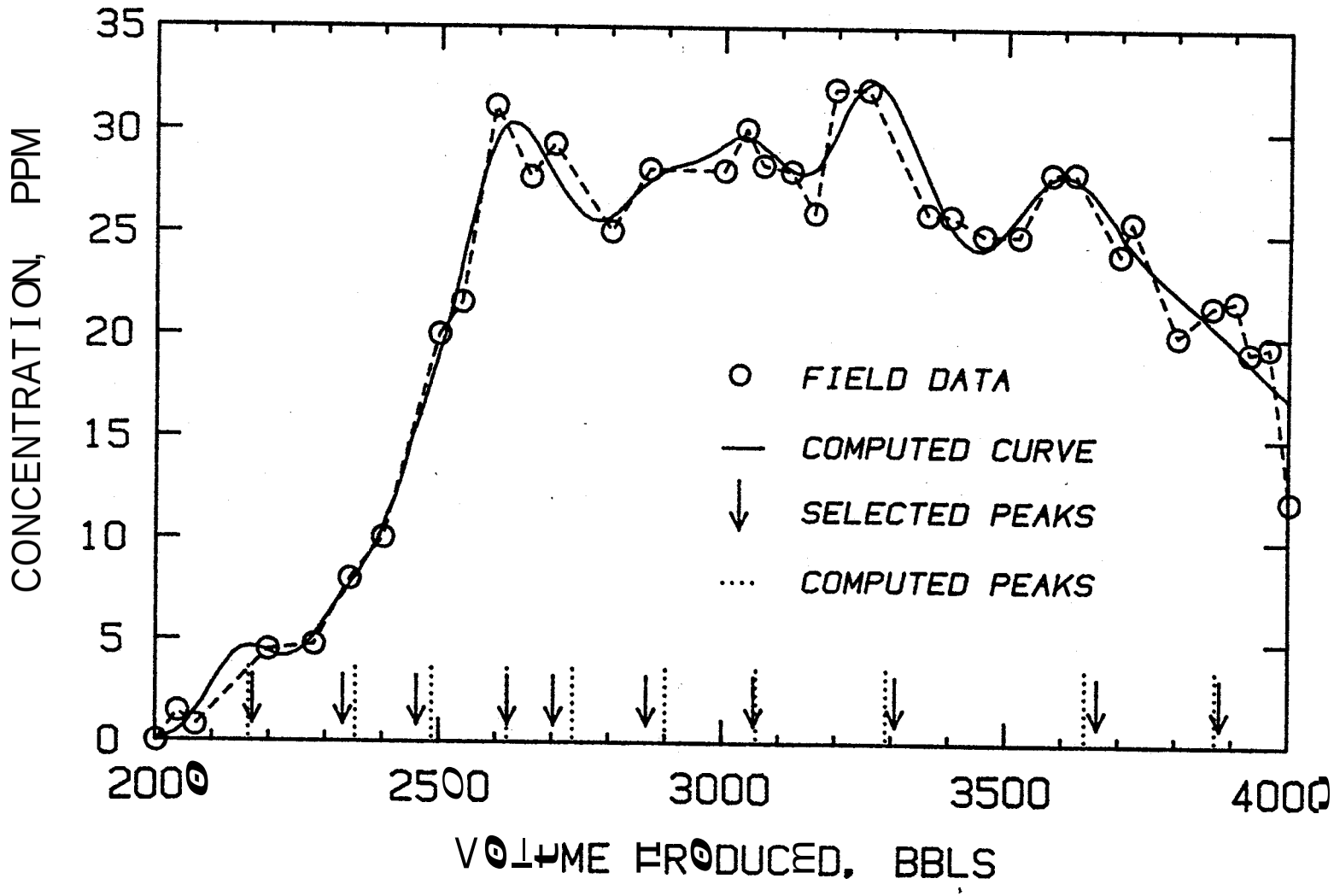

Fig. 10: ANALYSIS WITH 10 LAYERS

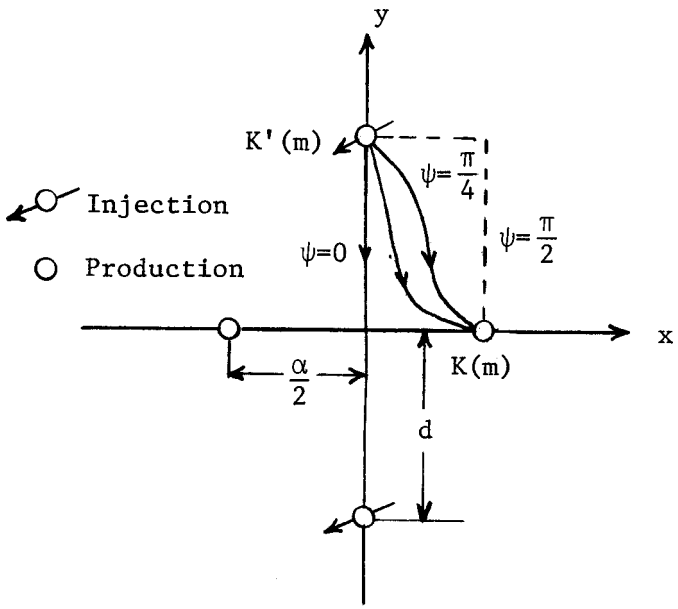
y
K'(m)
Injection
Production
ψ=0
ψ=π/4
ψ=π/2
x
α/2
K(m)
d

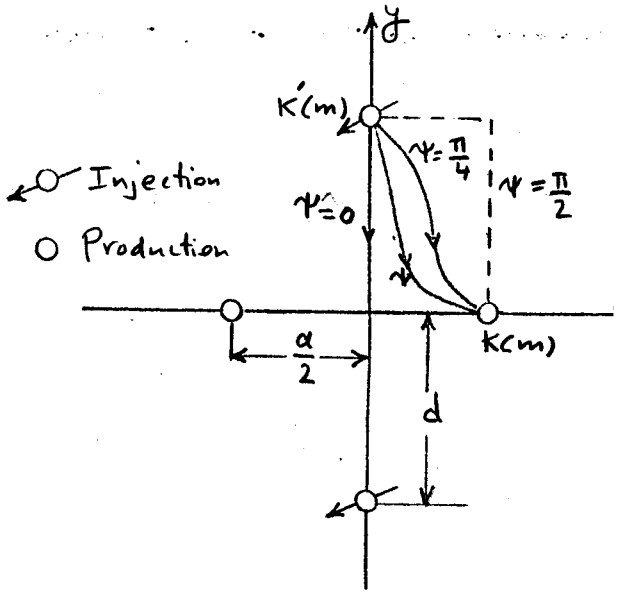
y
K'(m)
Injection
Production
ψ = π/4
ψ = π/2
ψ' = 0
ψ
K(m)
a/2
d

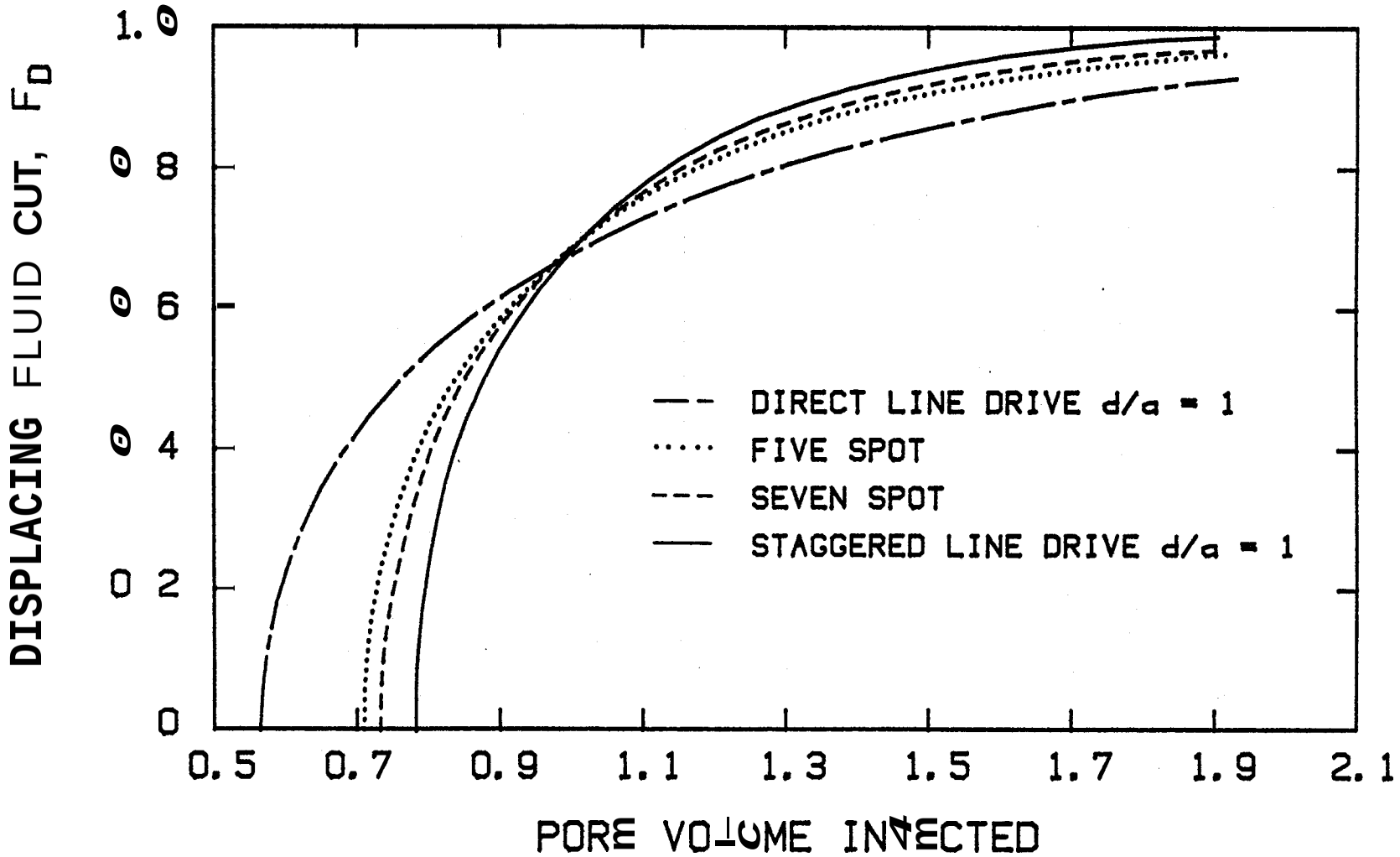

Fig. 4: PATERN BREAKTHROUGH CURVES, MOBILITY RATIO = 1

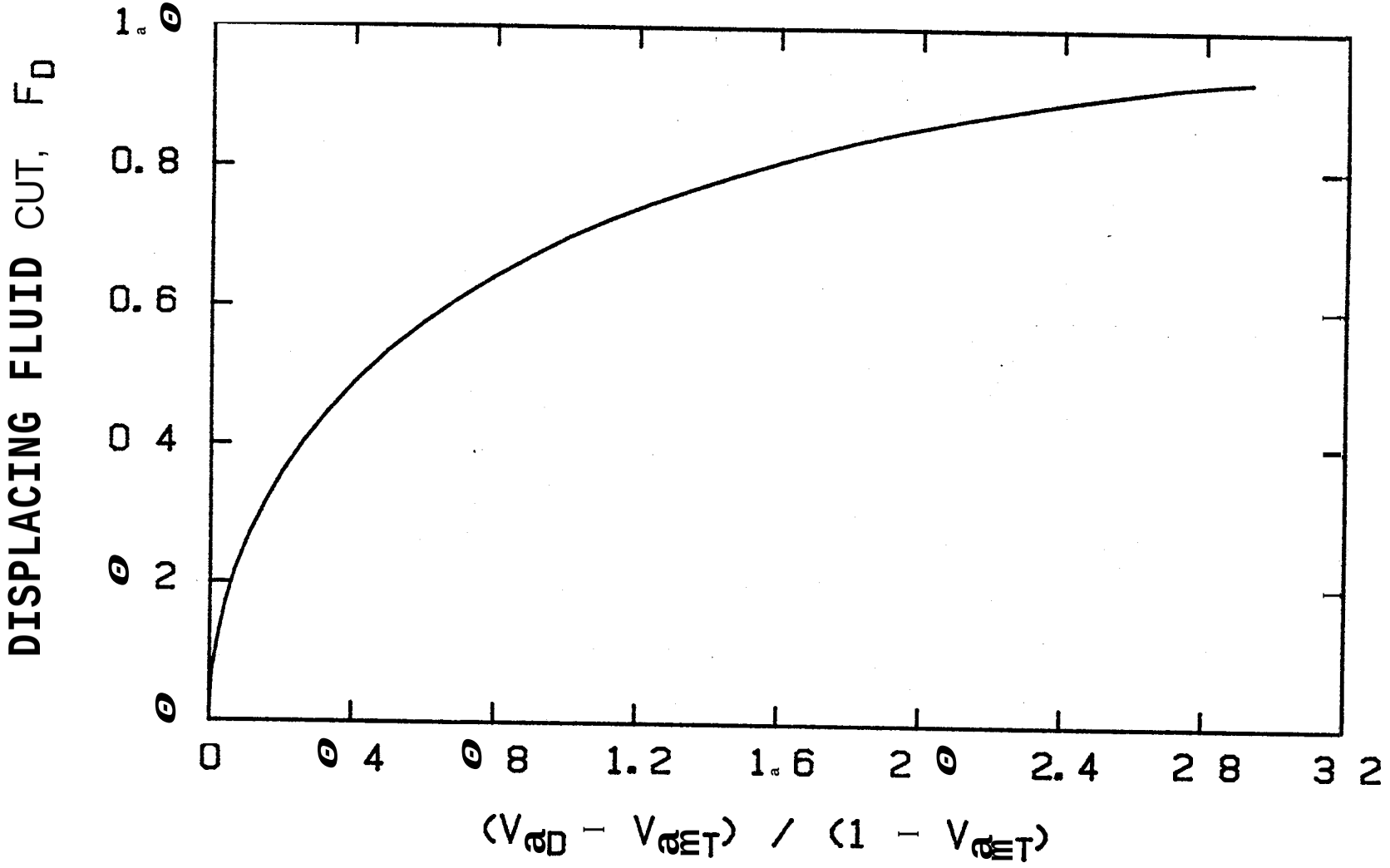

Fig. 5: CORRELATED PATTERN BREAKTHROUGH CURVE, MOBILITY RATIO = 1